

# The fruticose genera in the Ramalinaceae (Ascomycota, Lecanoromycetes): their diversity and evolutionary history

Richard Spjut<sup>1</sup>, Antoine Simon<sup>2</sup>, Martin Guissard<sup>2</sup>,  
Nicolas Magain<sup>2</sup>, Emmanuël Sérusiaux<sup>2</sup>

**1** World Botanical Associates, PO Box 81145, Bakersfield, California 93380, USA **2** Evolution and Conservation Biology Unit, Sart Tilman B22, Quartier Vallée 1, chemin de la vallée 4, B-4000 Liège, Belgium

Corresponding author: Emmanuël Sérusiaux (e.serusiaux@uliege.be)

---

Academic editor: T. Lumbsch | Received 13 October 2019 | Accepted 19 July 2020 | Published 11 September 2020

**Citation:** Spjut R, Simon A, Guissard M, Magain N, Sérusiaux E (2020) The fruticose genera in the Ramalinaceae (Ascomycota, Lecanoromycetes): their diversity and evolutionary history. MycoKeys 73: 1–68. <https://doi.org/10.3897/mycokeys.73.47287>

---

## Abstract

We present phylogenetic analyses of the fruticose Ramalinaceae based on extensive collections from many parts of the world, with a special focus on the Vizcaíno deserts in north-western Mexico and the coastal desert in Namibia. We generate a four-locus DNA sequence dataset for accessions of *Ramalina* and two additional loci for *Niebla* and *Vermilacinia*. Four genera are strongly supported: the subcosmopolitan *Ramalina*, the new genus *Namibialina* endemic to SW Africa, and a duo formed by *Niebla* and *Vermilacinia*, endemic to the New World except the sorediate *V. zebrina* that disjunctly occurs in Namibia. The latter three genera are restricted to coastal desert and chaparral where vegetation depends on moisture from ocean fog. *Ramalina* is subcosmopolitan and much more diverse in its ecology.

We show that *Ramalina* and its sister genus *Namibialina* diverged from each other at c. 48 Myrs, whereas *Vermilacinia* and *Niebla* split at c. 30 Myrs. The phylogeny of the fruticose genera remains unresolved to their ancestral crustose genera.

Species delimitation within *Namibialina* and *Ramalina* is rather straightforward. The phylogeny and taxonomy of *Vermilacinia* are fully resolved, except for the two youngest clades of corticolous taxa, and support current taxonomy, including four new taxa described here. Secondary metabolite variation in *Niebla* generally coincides with major clades which are comprised of species complexes with still unresolved phylogenetic relationships. A micro-endemism pattern of allopatric species is strongly suspected for both genera, except for the corticolous taxa within *Vermilacinia*. Both *Niebla* and saxicolous *Vermilacinia* have chemotypes unique to species clades that are largely endemic to the Vizcaíno deserts.

The following new taxa are described: *Namibialina* **gen. nov.** with *N. melanothrix* (**comb. nov.**) as type species, a single new species of *Ramalina* (*R. krogiae*) and four new species of *Vermilacinia* (*V. breviloba*, *V. lacunosa*, *V. pustulata* and *V. reticulata*). The new combination *V. granulans* is introduced. Two epithets are re-introduced for European *Ramalina* species: *R. crispans* (= *R. peruviana* auct. eur.) and *R. rosacea* (= *R. bourgeana* auct. p.p). A lectotype is designated for *Vermilacinia procera*. A key to saxicolous species of *Vermilacinia* is presented.

## Keywords

Atacama, Baja California, Namib, *Namibialina*, *Niebla*, *Ramalina*, taxonomy, *Vermilacinia*, Vizcaíno deserts

## Introduction

The genus *Ramalina* Ach. is one of the best known lichen genera, easily recognized and widely studied by scientists in various fields of research, including biomonitoring of environmental changes (Agnan et al. 2016; López Berdonces et al. 2016), evaluation of impacts of industrial activities to the environment (Domínguez-Morueco et al. 2015), biotoxicity (Anar et al. 2015), use in cancer therapy (Lee et al. 2016; Suh et al. 2017) and other human diseases (Kim et al. 2018; Furmanek et al. 2019), biotechnologies (Biosca et al. 2016), decontamination (Candan et al. 2017), and even in ethnological studies of rural human populations (Devkota et al. 2017).

Furthermore, the genus is at the cutting edge of research about the very nature of lichenization as several species [mostly *R. farinacea* (L.) Ach.] have been shown to host and use several strains or even species of their green algal partners within the same thallus (Casano et al. 2015; Catalá et al. 2016; Moya et al. 2017). It is also a model for physiological studies of the lichen as a distinct entity (Sanders and Tokamov 2015; Sanders and de los Ríos 2019) and of the physiological dimension of symbiosis (Guéra et al. 2016).

As the genus *Ramalina* is subcosmopolitan and easily detected, it is almost always included in any floristic account, usually with ecological and biogeographical data, of any area in the world (Gasparyan and Sipman 2016; Diederich et al. 2017; Paukov et al. 2017); several include conservation assessment (McMullin 2015; Sparrius et al. 2017). Species new to science continue to be described, including those from unexpected ecological niches, such as riverside rocks submitted to a continuous water spray (Gumboski et al. 2018).

Yet the evolutionary history of the genus is poorly known, with a positioning within the Lecanorales, suborder Sphaerophorinae in the Lecanoromycetes (Miadlikowska et al. 2014). The genus *Ramalina* is included in the well-supported Ramalinaceae s.l. together with well-known genera such as *Bacidia* De Not., *Bacidina* Vězda, *Biatora* Fr.: Fr., *Bilimbia* De Not., *Lecania* A. Massal., *Phyllopsora* Müll. Arg. and *Toninia* A. Massal. The Ramalinaceae s. str. (Sérusiaux et al. 2012) excludes *Bacidia*, *Bacidina*, *Byssolecania* Vain., the *Lecania chlorotiza* group and *Toninia* that are assigned to the Bacidiaceae. The remaining genera form a highly variable assemblage, a basal and poorly supported clade including *Megalalaria grossa* (Pers. ex Nyl.) Haffellner and *Lopezaria versicolor*

(Flot.) Kalb and Haffelner as sister to a much stronger supported clade, including *Cliostomum griffithii* (Sm.) Coppins and *Vermilacinia cephalota* (Tuck.) Spjut and Hale as sister to four accessions of *Ramalina* (Miadlikowska et al. 2014).

Bowler (1981) studied cortical anatomy features of the subfruticose or typically fruticose Ramalinaceae, relating his findings to chemical, chorological and ecological data. He empirically recognized seven genera: *Cenozosia* A. Massal. [type: *C. inanis* (Mont.) A. Massal.], *Dievernina* Choisy [type: *D. ramulicola* M. Choisy], *Fistulariella* Bowler and Rundel [type: *F. inflata* (Hook. F. and Taylor) Bowler and Rundel], *Niebla* Rundel and Bowler [type: *N. homalea* (Ach.) Rundel and Bowler], *Ramalina* Ach. [type: *R. fraxinea* (L.) Ach.], *Ramalinopsis* (Zahlbr.) Follm. and Huneck [type: *R. manii* (Zahlbr.) Follmann and Huneck] and *Trichoramalina* Rundel and Bowler [type: *T. crinita* (Tuck.) Rundel and Bowler]. Spjut (1995a) segregated the new genus *Vermilacinia* Spjut and Hale [type species: *V. combeoides* (Nyl.) Spjut and Hale] from *Niebla*.

Sérusiaux et al. (2010) provided the first assessment of the North American *Niebla* (sensu Rundel and Bowler 1978; Bowler and Marsh 2004) within an evolutionary context using molecular sequence data; however, sampling was limited to relatively few accessions of *Vermilacinia*, while the *Ramalina bourgeana* group in the Mediterranean and Macaronesian regions in Europe (Krog and Østhagen 1980; Bowler and Marsh 2004; Aptroot and Schumm 2008) were shown to be nested within *Ramalina*. Additionally, accessions representative of two other genera, *Dievernina* and *Fistulariella* (Bowler and Rundel 1977; Bowler 1981) were also resolved within *Ramalina* s.l.

More recently, using a 5-locus dataset, Kistenich et al. (2018) produced a comprehensive phylogeny of the family, including a larger set of tropical taxa (formerly assigned to *Crocynia* (Ach.) Massal., *Eschatogonia* Trev., *Krogia* Timdal, *Phyllopsora*, *Physcidia* Tuck. and others). They included accessions of the monotypic *Cenozosia* Massal. (endemic to the Atacama Desert in South America) and *Ramalinopsis* (Zahlbr.) Follm. and Huneck (endemic to the Hawaii archipelago), as well as both species assigned to *Trichoramalina* (*T. crinita*, endemic to the Pacific coast of California, USA and Baja California, Mexico and *T. melanothrix*, endemic to the coastal desert of Namibia and South Africa). They resolved *T. crinita* within *Ramalina* s.l. and *T. melanothrix* as sister to a strongly supported clade of “*Niebla homalea*” (= *Vermilacinia laevigata*) and “*Niebla combeoides*” (= *V. combeoides*), based on Bowler and Marsh (2004), which included *Vermilacinia*, exhibiting “extreme plasticity in morphological appearance”. Further, they showed that *Cenozosia* is the sister group to all fruticose genera and, finally, that *Ramalinopsis* and *Trichoramalina* can be reduced into synonymy with *Ramalina*.

## Objectives of this study

In this study, our first objective was to revisit the delimitation of the “fruticose” genera within the Ramalinaceae, their phylogenetical relationships and biogeography, with a special focus on *Niebla* and *Vermilacinia* sensu Spjut (1996), endemic to the coastal deserts along the Pacific coasts of the New World and the enigmatic species *Ramalina angulosa* and *R. melanothrix*, endemic to coastal deserts in SW Africa.

The second objective was to evaluate the diversity within *Niebla* and *Vermilacinia* with molecular data and statistical inferences in a phylogenetic context. We wish to compare the taxonomical treatment of both genera proposed by Spjut (1996) with our DNA sequence data. The rationale of this work was to give taxonomic weight to chemical characters and to delimit species within each “chemical group” by morphological patterns. Chemical characters have phylogeographical significance; for example,  $\beta$ -depsidones-producing thalli in *Niebla* are almost all endemic to the Northern Vizcaíno Desert (NVD) and often terricolous, in contrast to depside-producing terricolous thalli occurring on San Nicolas Island. As a result, 42 species were recognized in *Niebla* and 18 in *Vermilacinia* (Spjut 1996). This taxonomical treatment was denied by Bowler and March (2004) in the “Lichen Flora of the Greater Sonoran Desert Region”, without detailed evaluation and under the presumption that all morphological characters are highly plastic and unworthy of consideration in a taxonomical treatment.

Our third and last objective was to evaluate the phylogenetic variation within the genus *Ramalina* s. str., with an expanded sampling compared to the current available data (Sérusiaux et al. 2010) and with several species that are quite variable and that may unveil cryptic taxa. Such species include *R. breviuscula* Nyl., *R. fastigiata* (Pers.) Ach., *R. requienii* (De Not.) Jatta, *R. subfarinacea* (Nyl. ex Cromb.) Nyl. and *R. tingitana* Salzm. Indeed, two recent studies unveiled an impressive and unexpected phylogenetic variation: the well-known epiphytic species of the western coasts of North America *R. menziesii* strongly structured in well-delimited lineages (Sork and Werth 2014) and the puzzling *R. pollinaria* shown to be a three species complex (Gasparyan et al. 2017).

As indicated above, three geographical areas play a special role in the evolutionary history and the present range of the fruticose genera of the Ramalinaceae: (I) the coasts of California/USA and Baja California/Mexico; (II) the Atacama and Sechura deserts along the western coasts of South America and (III) the coasts of Namibia and the South-West of South Africa. These areas are briefly presented in Suppl. material 1, focusing on their biodiversity, especially for lichenized fungi and their recent climatic history. The botanical significance of each of these is briefly discussed. Suppl. material 1 further includes updates (with Spjut 1996 as the seminal reference) on the ecogeographical data and evolutionary interpretation for the genera *Niebla* and *Vermilacinia* in Baja California.

## Material and methods

### Sampling and identification of collections

Almost all collections used for this study were gathered by the authors during several field trips, especially to Mexico/Baja California and Baja California Sur (Figs 1, 3), USA/California and Namibia/coastal desert (Fig. 3). Material was further collected in France, including Corsica, Italy/Sardinia (Fig. 2), the Canary Islands, Madeira, including Porto Santo, the Azores, Armenia, Norway, Rwanda, Switzerland and Taiwan. We

further added samples collected by other workers, *inter alia*, P. van den Boom in the Cabo Verde archipelago and T. Raus and H. Sipman in Greece.

During the field trip to Baja California and Baja California Sur, fruticose Ramalinaceae were sampled from 31 localities, treated as 11 broader collection areas (Suppl. material 6: Table S6), along the Pacific coast of North America, starting at Cabo Colonet, south of Ensenada (Mexico/Baja California: 31°04'24"N, 116°12'28"W) to Guerrero Negro, then southwest to Bahía Asunción (Mexico/Baja California Sur: 27°08'18"N, 114°17'45"W) and northwest to Punta Eugenia (Figs 1, 5). Each locality was carefully sampled and, for all material collected, the ITS region has been sequenced. A set of recent collections from the coasts of California (USA) assembled in 2017 was also included. However, no recent collections of *Niebla* from the islands off the coasts of California and Baja California were available; three endemic species occur on these islands, two on San Nicolas Island (*N. dactylifera* and *N. ramosissima*) and a third (*N. soreliata*) on Isla Guadalupe and San Clemente Island (type locality); *N. dilatata* and *N. isidiosa*, previously reported endemic to Isla Guadalupe, have since been discovered on the Baja peninsula. For *Vermilacinia*, the same protocol was adopted, except for the *V. leopardina* group (here referred to as “black-banded species group” that includes *V. howei*, *V. nylanderii*, *V. tigrina* and *V. zebrina*) whose variation needs further study. An accession of the soreliate *V. zebrina* from the Atlantic coast of Namibia has been included (Wirth 2010a, b).

Unfortunately, we were unable to include material of *Vermilacinia* from South America. Several species of *Vermilacinia* occur in the Atacama desert (Peru and Chile): the terricolous *V. ceruchis*, which is related to North American saxicolous species and corticolous *V. flaccescens*, “*Niebla*” *granulans* (Sipman 2011), *V. leonis*, *V. leopardina*, “*Niebla*” *nashii* (Sipman 2011) and *V. tigrina* (also terricolous). *Vermilacinia cephalota* was reported by Sipman (2011), but we consider this to be possibly *V. leonis*. However, Spjut (BRY loan) identified *V. aff. acicularis*, *V. aff. robusta*, *V. procera* and *V. varicosa*, reportedly collected in the Atacama Desert, May 2017; these specimens were not included in the molecular sampling.

During the field trip to Namibia, we sampled *Ramalina* s.l. from the coastal desert, between Swakopmund (22°20.389'S, 014°26.446'E) and Cape Cross (21°39.319'S, 013°59.550E) where the so-called “lichen fields” are well-developed and partly protected. The sampling was extensive, but restricted to a short portion (ca. 120 km long) of the coast enjoying fog and thus providing appropriate ecological conditions for lichen communities, that spread from southern Angola down to the Cape of Good Hope in South Africa.

We included most accessions used by Sérusiaux et al. (2010), including material from USA/California and Mexico/Baja California. We added accessions of species expected to be resolved at the base of the *Ramalina* s. str. Tree [e.g. *R. fraxinea*, *R. hoehneliana*, *R. polymorpha* and *R. sinensis* (Fig. 4)]. For the latter species, assumed to be subcosmopolitan that consistently resolved at the base of all other accessions of *Ramalina*, we added accessions from Asia, Europe and North America. Both species of “*Trichoramalina*” (*T. crinita* and *T. melanothrix*; Fig. 3) were included along with the sequences provided by Kistenich et al. (2018). We assessed several variable species of *Ramalina* from different geographical areas: *R. breviscula* (including from type local-

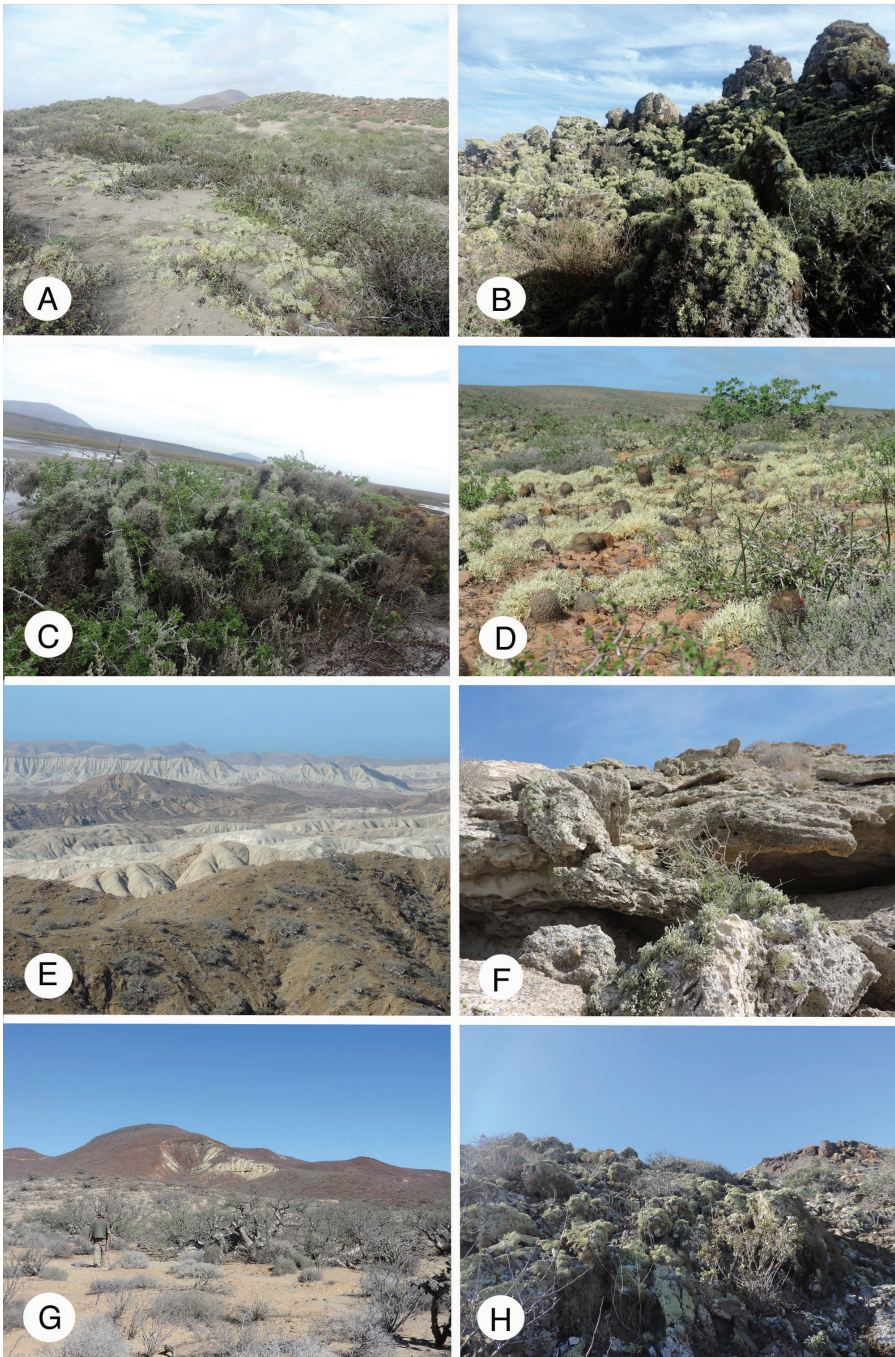


**Figure 1.** Landscapes of Baja California and Baja California Sur. **A** Arenicolous species of *Niebla* in sand dunes at San Quintín BC **B** saxicolous species of *Niebla* over dark volcanic rocks at San Quintín BC **C** twigs of *Lycium* covered with fruticose *Roccella* and *Vermilacinia* at San Quintín BC **D** Free-living species of *Niebla* on “red” rocky slopes at Punta Baja BC **E** landscapes of the peninsula de Vizcaíno **F** gypsicolous rocks near the sea at Bahía Ascension BCS with *Niebla lobulata* **G** chaparral near Bahía Tortugas BCS **H** outcrops subjected to intermittent fog near Bahía Tortugas BCS. Photographs by E. Sérusiaux and R. Spjut.

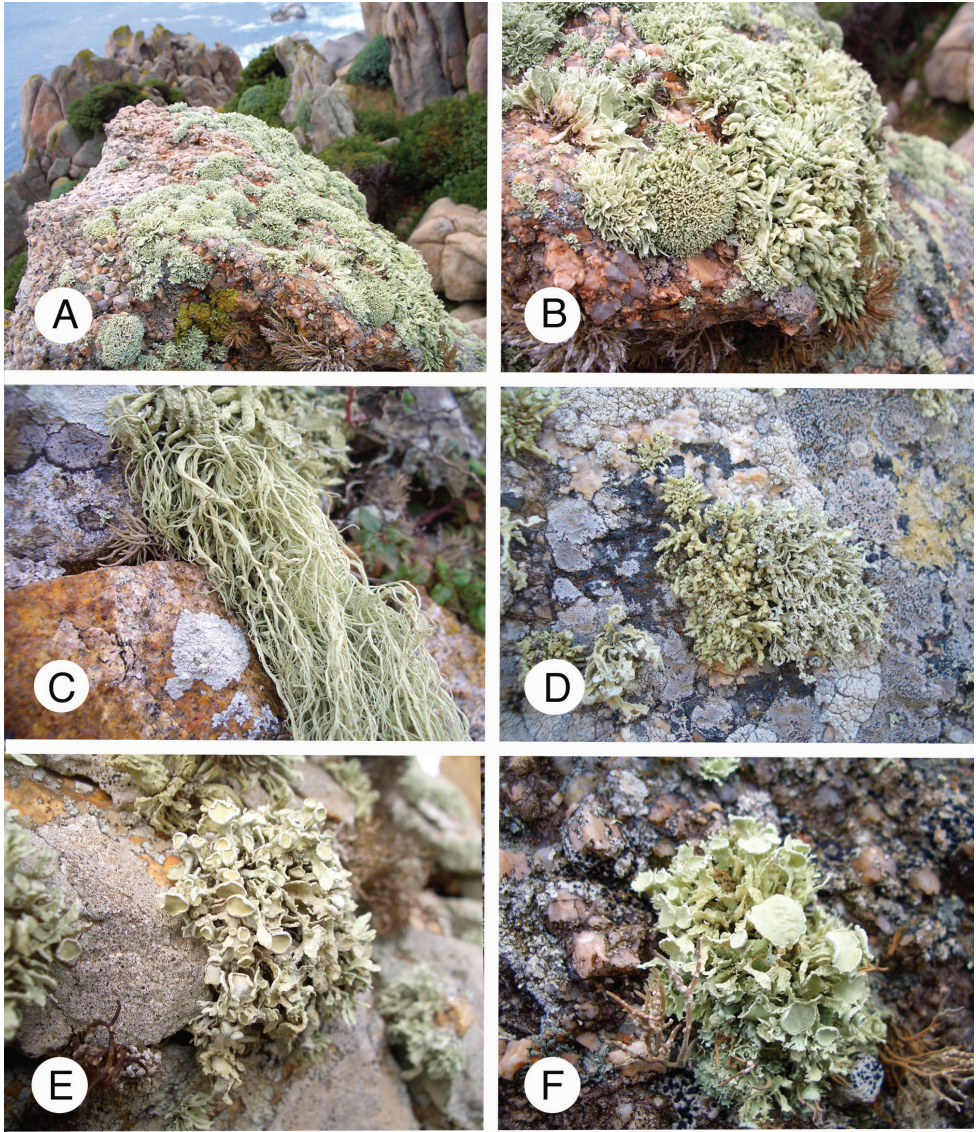


**Figure 2.** Species of *Ramalina* on rocky seashores in Italy/Sardinia **A** general view of species and habitat **B** from left to right: *R. tingitana*, *R. breviuscula* and *R. cribrosa* **C** *R. implexa* **D** from left to right: *R. clementeana* and *R. requienii* **E** *R. tingitana* **F** *R. inaequalis*. Photographs by M. Guissard and E. Sérusiaux.

ity), *R. fastigiata*, *R. requienii*, *R. subfarinacea* and *R. tingitana*. We further focused on saxicolous species thriving along sea-shores of islands in the Western Mediterranean region [Italy: Sardinia, France: Corsica (Fig. 2) and Spain: Cabo del Gata].

Finally, we added two accessions retrieved from GenBank, *R. complanata* and *Vermilacinia cephalota* (both collected in the USA) for which the four targeted loci were available; they were included in the phylogenetic synthetic analysis of the Lecanoromycetes by Miadlikowska et al. (2014) and are here used as references to check consistency.

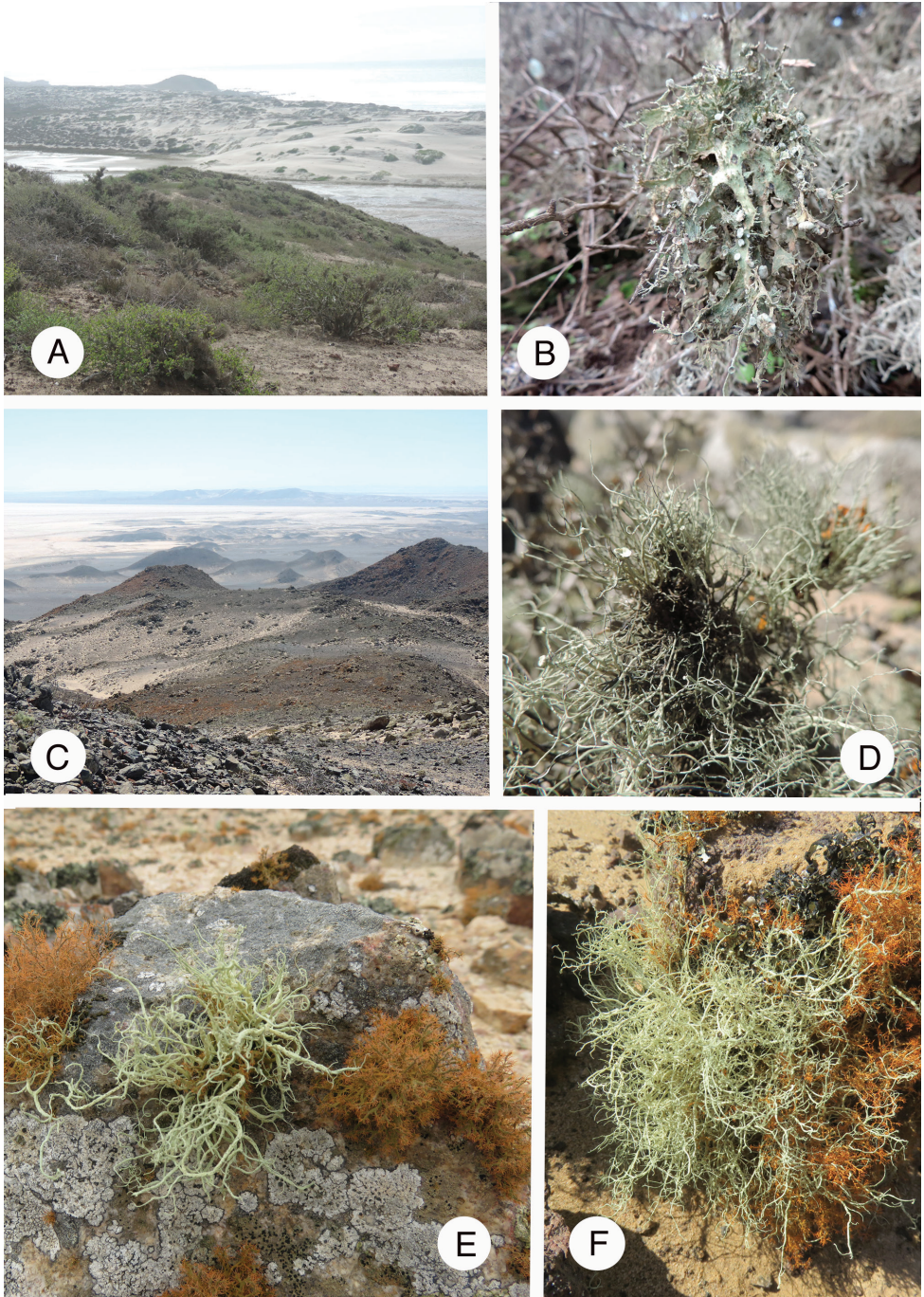


**Figure 3.** **A** Landscape in Baja California, San Quintín where *Ramalina crinita* thrives **B** *R. crinita*; **C** Landscape of the Skeleton Coast Park in Namibia where *Namibialina "angulosa"* and *N. melanothrix* thrive **D** *N. melanothrix* **E–F** *N. "angulosa" 1* (**E**) and *N. "angulosa" 2* (**F**). Photographs by E. Sérusiaux.

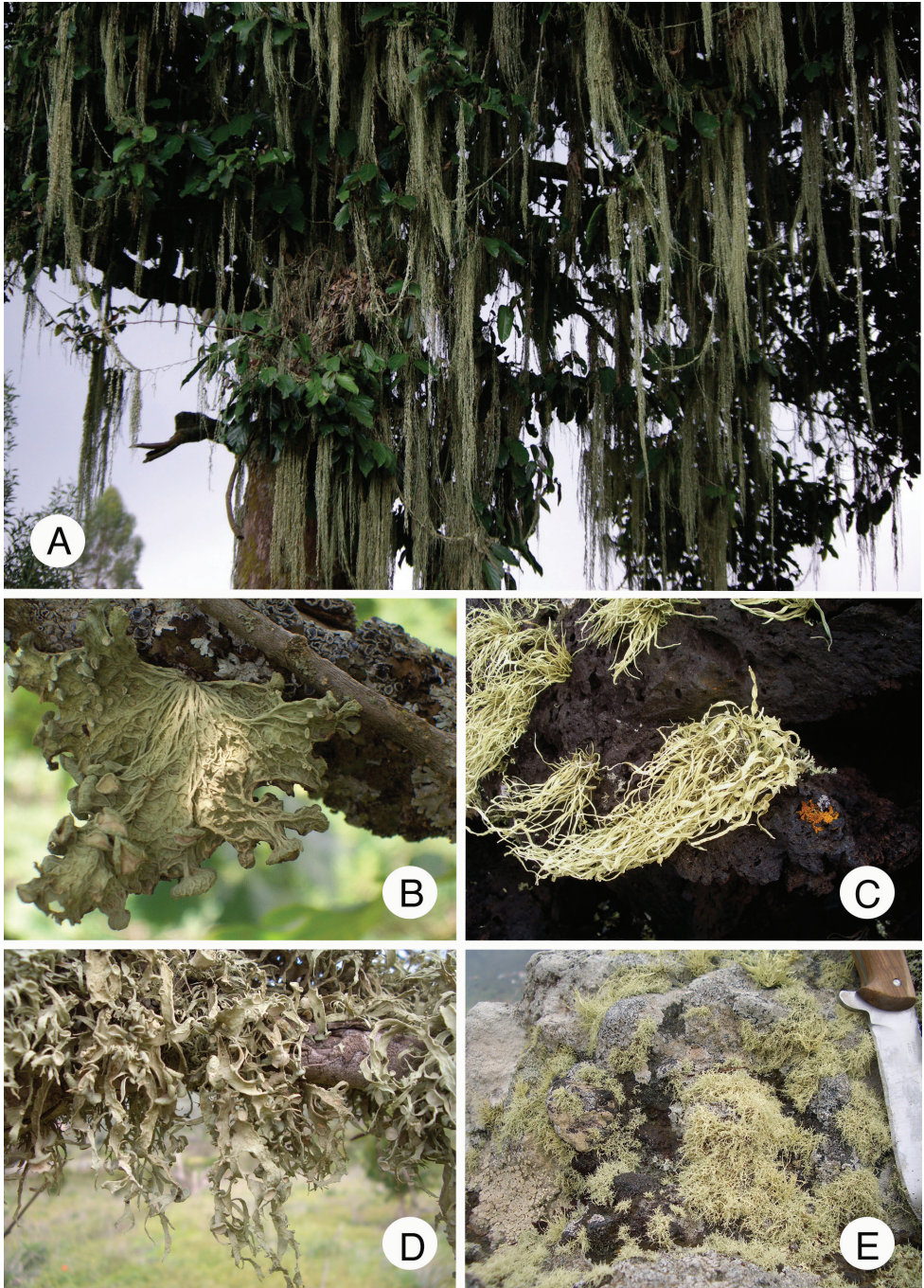


**Figure 4.** Several species of *Ramalina* **A** *R. hoehneliana*, hanging down the branches of a large *Strombosia scheffleri* in Gishwati forest (Rwanda) **B** *R. sinensis* (Armenia) **C** *R. azorica* (Azores, Pico) **D** *R. huei* (Canary Is., Tenerife) **E** *R. nodosa* (Canary Is., Tenerife). Photographs by E. Sérusiaux.

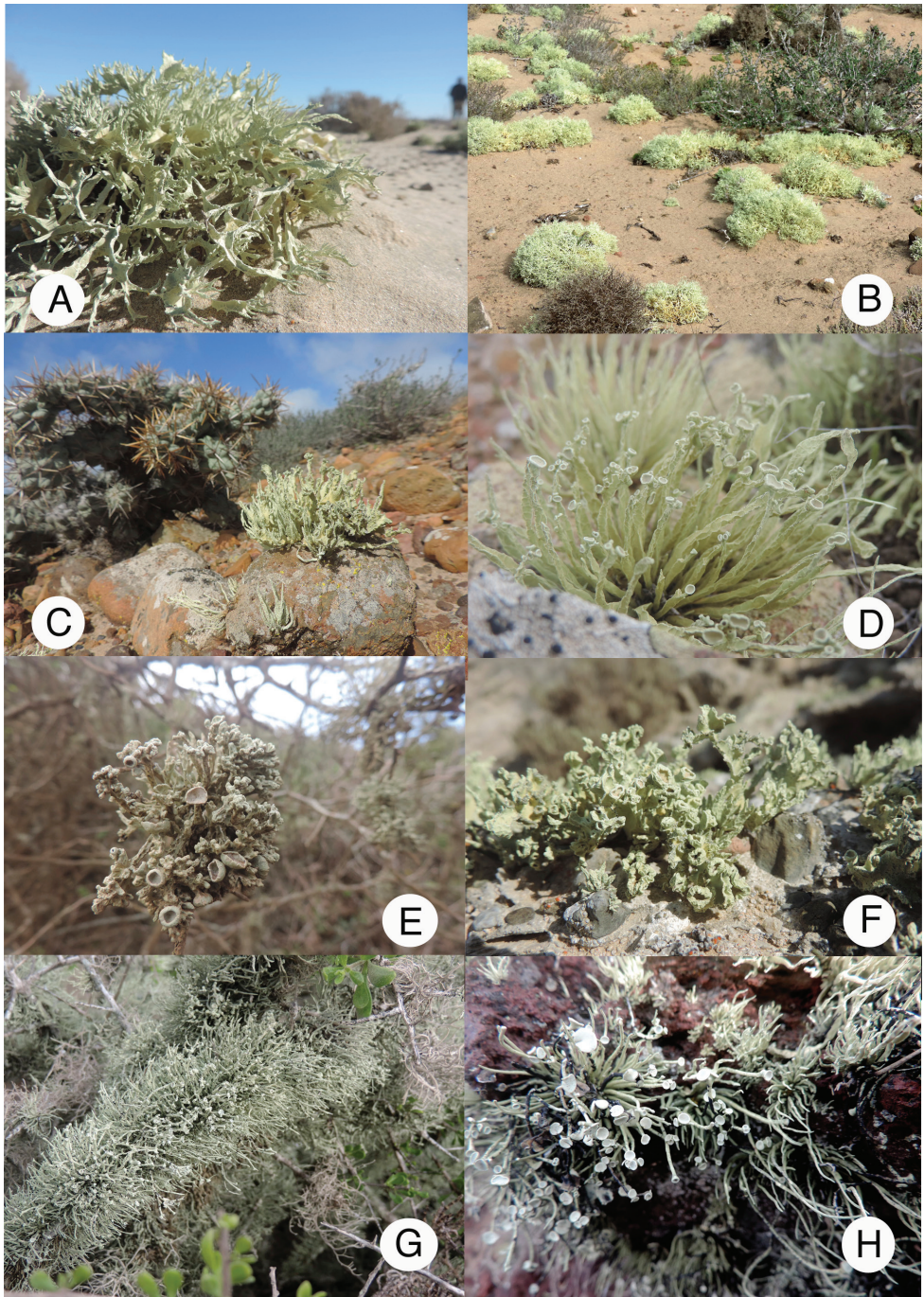


**Figure 5.** Several species of *Niebla* and *Vermilacinia*. Identifications based on Spjut (1996) **A** *Niebla limicola* on sand dunes at Guerrero Negro BCS **B** *N. marinii* at Santo Domingo BC **C** *N. podetiaforma* at Punta Baja BC **D** *N. siphonoloba* at San Antonio BC **E** *Vermilacinia cerebrata* at San Antonio BC **F** *Niebla lobulata* at Bahía de Tortugas BCS **G** *Vermilacinia leopardina* on branches at San Quintín BC **H** *V. procerata* on rocks at San Quintín BC. Photographs by E. Sérusiaux and R. Spjut.

Identification of collections was performed with the following support: Spjut (1996) for the collections of *Niebla* and *Vermilacinia* from USA and Mexico; the accession of *Vermilacinia* from Africa/Namibia was also assessed following Wirth (2010a, b); Krog and Østhagen (1980) and Aproot and Schumm (2008) for the material gathered in Macaronesia (archipelagos of the Canary Islands, Madeira, Porto Santo and the Azores), Krog and James (1977) and the French translation of the *Ramalina* chapter of Clauzade and Roux (1985) provided by G. Duclaux for material from continental Europe and Armenia; and Swinscow and Krog (1988) for collections from Rwanda (Africa).

In order to assess validly published epithets appropriate for several species, type collections and related material were examined at the Natural History Museum in London (BM), the “Museum National d’Histoire Naturelle” in Paris (PC), the “Institut Botànic de Barcelona” (BC) and the Herbarium of the University of Barcelona (BCN).

Specimens at the University of Liège (Liège, Belgium) were studied using standard microscopic techniques. Morphological descriptions are based on observations using a Leica S4E dissecting microscope (Leica Microsystems GmbH, Wetzlar, Germany) and a Nikon Eclipse 80i compound microscope (Nikon Corporation, Tokyo, Japan). Thin-layer chromatography (TLC) was carried out following Orange et al. (2010) using solvents B (*Niebla*), C and G. Specimens were deposited at LG; specimens gathered in Mexico/Baja California and Baja California Sur in 2016 were deposited in BCMEX, LG and the private herbarium of World Botanical Associates (WBA); those sampled in USA/California were deposited in LG and WBA.

## DNA extraction and loci amplification

For the overall analysis of the generic delimitation of the target genera (*Niebla*, *Ramalina* s.l. and *Vermilacinia*), we included two representatives of the Psoraceae (*Protoblastenia calva* and *Psora rubiformis*) and one representative of the Tephromelataceae (*Tephromela atra*) as outgroups, following Miadlikowska et al. (2014) and Kistenich et al. (2018). We further included representatives of the Bacidiaceae (*Bacidia schweinitzii*, “*B. soredata*”, *Bacidina arnoldiana*, *Biatora vernalis* and *Thalloidema sedifolia*), as well as *Lopezaria versicolor* and *Megalaria grossa*. Finally, we included selected representatives of *Phyllospora* s.l. in order to include all lineages featuring this thallus type in the dataset (*Eschatagonia prolifera*, *Parallospora leucophyllina*, *Phyllospora breviscula*, *P. gossypina*, *P. chlorophaea* and “*P. borbonica*”) following the results of Kistenich et al. (2018). These provide calibration points for the time calibration of our phylogenetic tree.

Two datasets were analyzed independently for this study:

- Matrix 1: a four-locus dataset (ITS-LSU-RPB1-RPB2) comprising a selection of accessions for *Niebla* (37 out of 101) and *Vermilacinia* (19 out of 46) and all representatives (9) of *Ramalina angulosa* and *R. melanothrix* (these two species are assigned to the new genus *Namibialina*) and *Ramalina*, except for one accession of *R. rosacea* and all accessions of *R. sarahae* (102 out of 112). Accessions included in Matrix 1 are marked with X in the first column of Suppl. material 3: Table S3.

- Matrix 2: a six-locus dataset (ITS-LSU-RPB1-RPB2-GDP-EF-1 $\alpha$ ) comprising all representatives of *Niebla* and *Vermilacinia* (147 specimens), with *R. farinacea* and *R. tingitana* as outgroup.

For further information regarding the sequences generated and used in this study, see Suppl. material 3: Table S3.

## Molecular phylogenetic analyses

Multiple sequence alignments were performed with MAFFT using the auto option (Kato et al. 2002; Kato et al. 2009) as implemented in Geneious 10.0.7 (Biomatters Ltd., Auckland, New Zealand) and were carefully checked by eye and manually adjusted. For each dataset, ambiguous alignment sites in the ITS, LSU, and EF-1 $\alpha$  markers were excluded using the GBLOCKS server 0.91b [http://molevol.cmima.csic.es/castresana/Gblocks\\_server.html](http://molevol.cmima.csic.es/castresana/Gblocks_server.html), with settings allowed to produce the least stringent selection (Castresana 2000). Intronic regions within RPB1 and RPB2 were manually removed when present. The GAPDH locus was analyzed with all sites included. Prior to concatenation and for each dataset, single-locus phylogenetic trees were produced for each marker via RAxML-HPC2 8.2.3 (Stamatakis 2006; Stamatakis et al. 2008) on the CIPRES portal (Miller et al. 2010; <http://www.phylo.org>) using the rapid hill-climbing algorithm and bootstrapping with 1000 pseudo-replicates under a GTR+G model of evolution. Inspection of gene tree incongruence was performed using *compat.py* (Kauff and Lutzoni 2002). Significant conflict was detected only within *Ramalina* pointing to a variable position of two lineages (*R. clementeana* and the *R. fastigiata* gr.). The matrices were nevertheless concatenated and the phylogenetic analysis applied to these data, because the phylogenetic placement of these two groups was not the focal point of this study.

PartitionFinder 2 (Lanfear 2016) was used to determine the best partitioning schemes and nucleotide substitution models for the subsequent analyses. For Matrix 1, eight initial subsets were considered (ITS; LSU; RPB1 1<sup>st</sup>, 2<sup>nd</sup>, 3<sup>rd</sup> codon positions; RPB2 1<sup>st</sup>, 2<sup>nd</sup>, 3<sup>rd</sup> codon positions). Seven additional subsets were considered for Matrix 2 (GAPDH 1<sup>st</sup>, 2<sup>nd</sup>, 3<sup>rd</sup> codon positions; EF-1 $\alpha$  1<sup>st</sup>, 2<sup>nd</sup>, 3<sup>rd</sup> codon positions and introns). PartitionFinder 2 was run with the default configuration settings (branch-lengths = linked, model\_selection = BIC, search = greedy); for the ML analyses, the GTR+G model was the only one allowed.

## Evolutionary tree for all fruticose Ramalinaceae and age calibration

We ran an analysis on Matrix 1 running BEAST2 v.2.6.1 (Bouckaert et al. 2014) as implemented on the CIPRES portal. We unlinked substitution models but linked clocks and trees across loci. Models of sequence evolution for each subset were determined by the Bayesian Information Criterion (BIC; Schwarz 1978) in jModel-Test 2.1.6 (Darriba et al. 2012) on the CIPRES Science Gateway (ITS: TrNef+I+G;

LSU: TrN+I+G; RPB1: K80+I+G; RPB2: TrNef+I+G). A lognormal relaxed clock was implemented. Two fossil priors with lognormal prior distributions were set to calibrate the tree: one on the monophyly of *Phyllopsora* with an age of [(5% quantile –) median (–95% quantile)] (16.4–17.8(–19.3) Myrs following Rikkinen and Poinar (2008) and the other on the monophyly of Ramalinaceae with an age of (116–)126(–137) Myrs following Rivas Plata (2011). The tree was generated with a Yule model. Trees were sampled every 1000<sup>th</sup> generation. Convergence was assessed using Tracer v.1.7.1 (Rambaut et al. 2018). The run was initially set up to 500 million generations, but since all ESS values were superior to 200 and stationarity appeared to be reached, the analysis was stopped after 399 600 000 generations. The first 129 600 000 generations were discarded as burn-in, then one tree every 20 000<sup>th</sup> generation was selected, resulting in a sample of 13 500 trees which was used to generate a final consensus tree with TreeAnnotator.

### Evolutionary tree for the genera *Niebla* and *Vermilacinia*

A maximum likelihood analysis was performed on Matrix 2 with RAxML 8.2.3 on the CIPRES portal using the rapid hill-climbing algorithm and bootstrapping with 1000 pseudoreplicates under a GTR+G model of evolution for each partitioned subset. We provide the bootstrap results obtained with the method recently developed by Lemoine et al. (2018). Indeed, phylogenies, based on hundreds of taxa, tend to have low supports with Felsenstein's method (Felsenstein 1985), based on resampling and replications; the new version of the phylogenetic bootstrap introduced by Lemoine et al. (2018) is designed to address this matter without inducing falsely supported branches. The results of the ML analyses were visualized with the R package ggtree (Yu et al. 2012).

### Species delimitation analyses within *Niebla* and *Vermilacinia*

Species delimitation was inferred from molecular data following four methods: ABGD (Puillandre et al. 2012), PTP (Zhang et al. 2013), BPP (Rannala and Yang 2003) and STACEY (Jones 2015). Each genus (*Niebla* and *Vermilacinia*) was treated individually (these lineages were isolated into separate input files) and without outgroups, except for the STACEY analysis. For BPP, the genus *Niebla* was further divided into two subgroups [Clades “depsides” and “ $\beta$ -depsidones”] in order to make the analysis less computationally-intensive.

A first species delimitation was performed using the ITS dataset only (extracted from Matrix 2), following the ABGD method (Puillandre et al. 2012). This method uses short DNA sequences to assign organisms into species. The automatic procedure is based on the barcode gap, which can be observed whenever the divergence amongst organisms belonging to the same species is smaller than divergence amongst organisms from different species. Based on the input data, the method uses a range of priors to infer from the data a model-based one-sided confidence limit for intraspecific divergence, then detects the barcode gap

as the first significant gap beyond this limit and uses it to partition the data. Inference of the limit and gap detection are then recursively applied to previously obtained groups to get finer partitions until there is no further partitioning. The ABGD analyses were carried out on the two genera separately (*Niebla* and *Vermilacinia*) on the ABGD website (<https://bioinfo.mnhn.fr/abi/public/abgd/abgdweb.html>). Default parameters were chosen using Kimura (K80) genetic distances for each analysis and testing for different relative gap width values ( $X = 0.1, 0.5, 1.0, 1.5$ ). Ultimately, the following partitions were selected: 17 groups of *Niebla* ( $P = 2.78e-03; X = 0.1$ ) and 16 groups of *Vermilacinia* ( $P = 2.78e-03; X = 0.5$ ).

The second method uses the so-called Poisson tree processes model (PTP; Zhang et al. 2013). It is a coalescent-based species delimitation method, which utilizes the number of substitutions to infer putative species boundaries on the trees built via RAxML (Matrix 2). While this method is usually intended for delimiting species in single-locus phylogenies, this programme may also be used on concatenated gene trees when there are no strong conflicts between gene trees (Luo et al. 2018; Bustamante et al. 2019). We chose to use it here on our concatenated tree obtained from Matrix 2 in order to objectively assign each specimen into input candidate species for the subsequent BPP (Bayesian Posterior Probability) analysis. Additionally, PTP was run on the corresponding single-locus ITS trees and the obtained results are included in Fig. 7. All analyses were run on the PTP web server (<https://species.h-its.org/ptp/>) using the default parameters and 500,000 MCMC (Markov Chain Monte Carlo) generations.

The third method uses a Bayesian MCMC implementation of the MultiSpecies Coalescent model, which allows both species delimitation and species tree inference (Rannala and Yang 2003; Yang and Rannala 2010, 2014, 2017). This method is known as BPP and the analyses were run for a total of 500,000 MCMC generations, thinning set to 100. The delimitation followed the result of the ML solution. The multi-locus coalescent-based BPP v. 3.3 analysis was performed using the above mentioned ML trees as guide trees (i.e. analysis A10). The divergence time parameter tau ( $\tau$ ) was estimated using the root height of the guide trees and was set to  $G(2, 60)$  (corresponding to distribution mean of 0.03). The population size parameter theta ( $\theta$ ) gamma prior was tested for different values:  $G(4, 1000)$ ,  $G(8, 1000)$  and  $G(12, 1000)$ . The matrix was analyzed using the reversible-jump Markov Chain Monte Carlo (rjMCMC) algorithms implemented in the programme BPP, sampling every generation for a total of 5,000,000 generations, with a burn-in period of 500,000. We used the posterior mean ( $P = 0.5$ ) as the probability threshold above which input groups are considered heterospecific. Each BPP analysis was carried out twice to confirm the consistency between runs.

The fourth method is the STACEY package, implemented in BEAST2 (Bouckaert et al. 2014; Jones 2015): it does not require a priori assignment of each individual accession to a putative species and, further, is a Bayesian method. Indeed, although it is sensitive to the choice of priors, it can explore the entire space of species trees including evolutionary processes causing discordance, such as ILS (Incomplete Lineage Sorting). The STACEY approach has been successfully applied to species delimitation in several lichen groups (Boluda et al. 2019; Gerlach et al. 2019; Mark et al. 2019; Lutsak et al. 2020) and seems to avoid the overestimation of the number of potential species usually encountered with BPP (Edwards et al. 2016).

We ran a \*BEAST analysis as implemented in BEAST2 v. 2.6.1 with the STACEY module enabled. Substitution models were determined using jModeltest as above. Substitution models were TN93+G for EF and TN93+I+G for GDP. Exponential relaxed clocks were used. The analysis was run for 500 million generations, sampling every 10 000<sup>th</sup> generation. We discarded the first 9 960 000 generations as burn-in and kept a tree every 25 000<sup>th</sup> generation, resulting in a sample of 19 600 trees which was used to generate a consensus species tree with TreeAnnotator. The graphical display of the STACEY matrix was generated using R version 3.2.1 (R core team 2015). Visual display of trees with categorical columns was generated using R package ggtree (Yu et al. 2017).

### Evolutionary tree for *Ramalina* s.l.

This tree encompasses all accessions of *Ramalina* (except for one accession of *R. rosacea* and all accessions of *R. sarahae*) and those assigned to the new genus *Namibialina* and is based on accessions included in Matrix 1. Therefore, the tree is a subset of the analysis performed on Matrix 1; all calibrations and parameters are identical.

## Results

Altogether, we generated DNA sequence data for a total of 283 specimens of the Ramalinaceae sensu lato (Suppl. material 3: Table S3). The concatenated Matrices 1 and 2 consisted of 3,312 positions (ITS: 410 bp; LSU: 1063 bp; RPB1: 1011 bp; RPB2: 828 bp) and 4,466 positions (ITS: 457 bp; LSU: 1,262 bp; RPB1: 1,011 bp; RPB2: 828 bp; GAPDH: 531 bp; EF-1 $\alpha$ : 377 bp), respectively.

### Evolutionary tree for all fruticose Ramalinaceae and age calibration (Fig. 6)

A single strongly supported branch sustains all accessions of fruticose taxa in the Ramalinaceae. Strong support is detected for the delimitation of two lineages for the fruticose genera: (1) *Ramalina* as sister to a strongly delimited group endemic to the coastal desert in SW Africa assigned to the new genus *Namibialina*, the relationship between the two genera being strongly supported; (2) two genera (*Niebla* and *Vermilacinia*), endemic to coastal deserts along the Pacific coast in the New World, strongly supported together and, further, sister to three species of *Cliostomum*, including the type species (*C. corrugatum*), but with weak support. Both accessions of the crustose *Cliostomum griffithii* form a lineage sister to the strongly supported clade, including all other lineages studied: *Cliostomum* s. str., *Namibialina*, *Niebla*, *Ramalina* and *Vermilacinia*. Therefore, the genus *Cliostomum*, as delimited by Ekman (1997), is polyphyletic; and emergence of fruticose taxa within the Ramalinaceae is not a unique event.

The time calibration, based on a fossil of *Phyllopsora*, yielded results (Suppl. material 4: Table S4) consistent with several studies for the time calibration of the

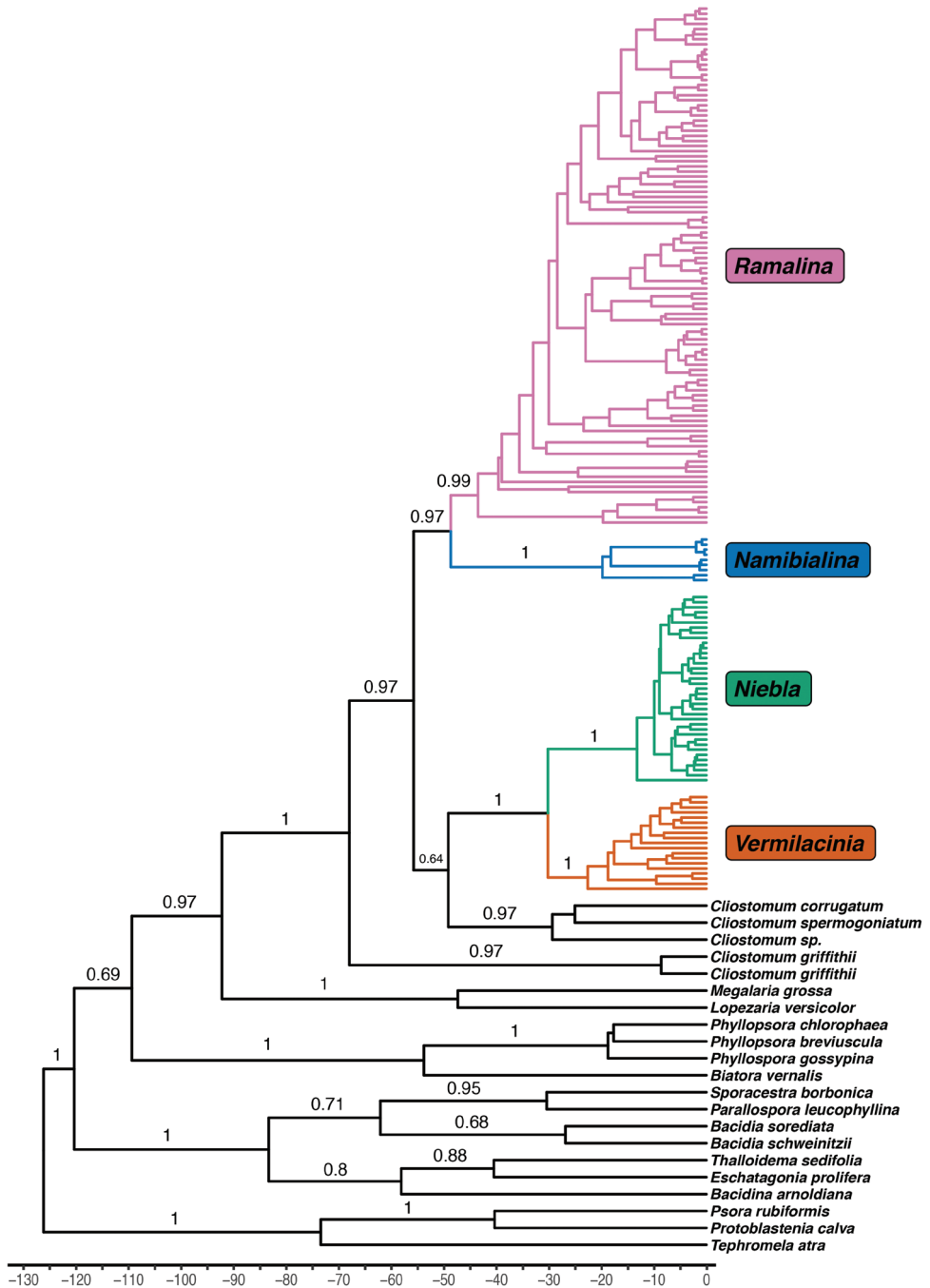


**Figure 6.** Time-calibrated phylogenetic tree generated by the BEAST2 analysis on four loci (Matrix 1), for the four genera of fruticose Ramalinaceae studied and their crustose sister genus *Cllostomum*: *Namibialina*, *Niebla*, *Ramalina* and *Vermilacinia*. Values above branches represent the posterior probabilities of support.

Lecanoromycetes, closest to the *Lecanora* crown (sensu Prieto and Wedin 2013: table 3; Beimforde et al. 2014; Samarakoon et al. 2016; Huang et al. 2019).

The mean divergence time of the clade including all accessions of the fruticose Ramalinaceae plus their crustose sister taxon (*Cliostomum* s. str., including the genus type *C. corrugatum*) is 55.53 Myrs [95% highest posterior density (HPD) interval: 40.23–72.29] at the boundary between the Paleocene and the Eocene.

The emergence of the duo *Ramalina* + *Namibialina* is dated at 48.45 Myrs (HDP: 35.13–63.66) at the middle of Eocene. The duo *Niebla* + *Vermilacinia* diverged from one another at 30.05 Myrs (HDP: 17.27–43.11) during the Oligocene period; this date is almost identical to the diversification within *Cliostomum* s. str. Interestingly, *Vermilacinia* diversified starting at the beginning of the Miocene, 22.47 Myrs (HDP: 3.44–32.06), whereas *Niebla* began later, mid-Miocene, at 13.14 Myrs (HDP: 7.05–21.05). *Namibialina* diversified at 19.71 Myrs (HDP: 8.47–32.75) almost at the same time as the diversification within the basal species of *Ramalina*, *R. sinensis*.

### Evolutionary tree for the genera *Niebla* and *Vermilacinia* and species delimitation

Results of the species delimitation methods are summarized in Fig. 7 and in Suppl. material 3: Table S3.

The two genera *Niebla* and *Vermilacinia*, as circumscribed by Spjut (1995a, 1996), are strongly supported. *Vermilacinia* is divided into two strongly supported groups (Fig. 7): (1) all saxicolous or terricolous species, except for two, *V. laevigata* and *V. combeoides* and (2) the sister clade includes these two saxicolous species that form a supported group, sister to a widely distributed corticolous group in the New World and Namibia.

The genus *Niebla* is divided into two clades (Fig. 7). One is strongly supported by the absence of triterpenes and defined by the presence of medullary  $\beta$ -depsidones; the other of depside species with triterpenes is less clearly defined and can be interpreted as one polytomy of at least five strongly supported clades (BS > 90%), four producing divaricatic acid and a fifth with basal species producing the same acid with a terminal, strongly supported node of sekikaic acid species with or without divaricatic acid.

The branching within the “ $\beta$ -depsidones” clade does not discriminate amongst the three secondary medullary metabolites (protocetraric, salazinic and hypoprotocetraric acids).

Following Spjut’s identification key (1996), nine  $\beta$ -depsidone species were identified by secondary metabolites followed by morphology. None is supported even though 9 putative species are recognized by the BPP analysis. Other delimitation methods recognized fewer putative species: STACEY five species, PTP four species and the ABGD three species.

The “depsides” clades are also very diverse with little match between the identification following Spjut (1996) and the phylogeny-based statistical species delimitation methods. Within these “depsides” clades, the BPP method recognized 24 putative species, the ABGD method 22, PTP 16 and STACEY 13.

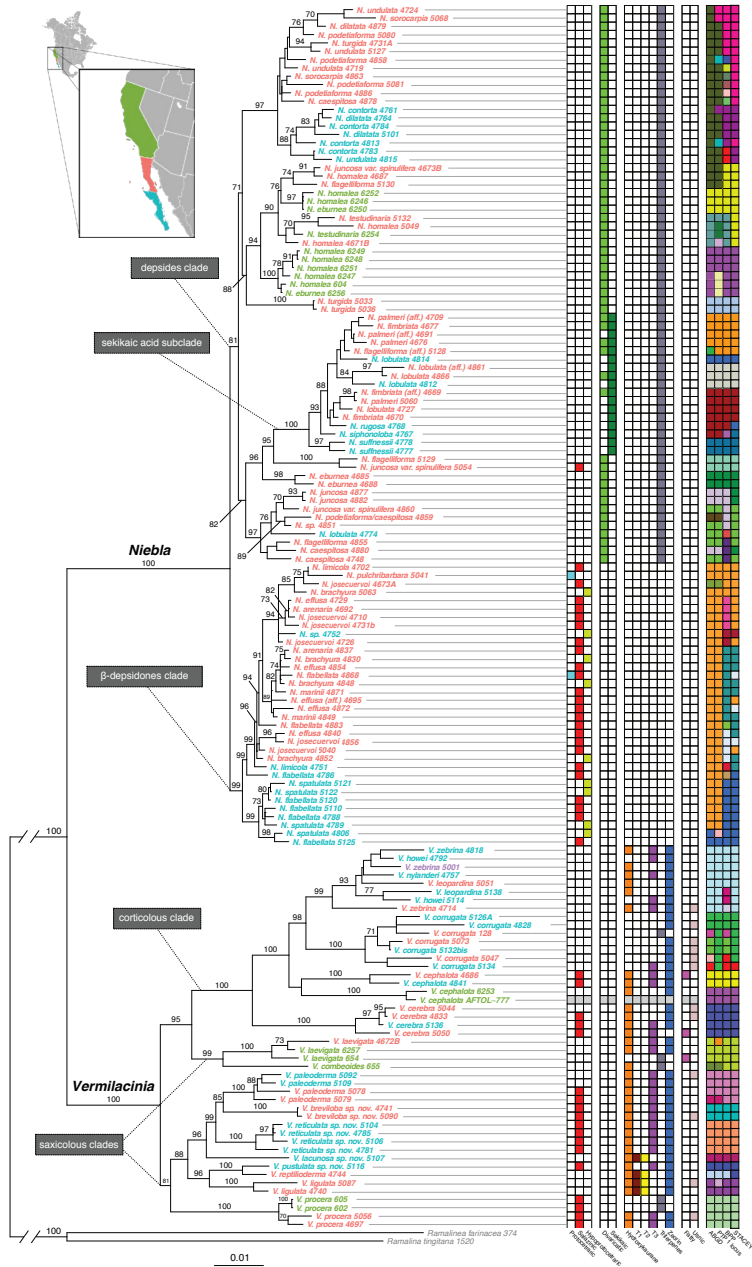


**Figure 7.** Evolutionary tree for the genera *Niebla* and *Vermilacinia*, produced with the 6-locus matrix (Matrix 2) and using RAxML. Support value for branches follow Lemoine et al. (2018). Epithets in colour following insert: green = collected in USA/California; pink = collected in Mexico/Baja California; blue = collected in Mexico/Baja California Sur. Table on right side provides further information for all accessions: column 1-3:  $\beta$ -depsidones (protocetraric acid, salazinic acid, hypprotocetraric acid); column 4-5: depsides (divaricatic acid, sekkikaic acid); column 6-11: [-]-16 $\alpha$ -hydroxykaurane, triterpenes T1, T2, T3, unidentified triterpenes, zeorin; column 12-13: fatty acid, usnic acid; greyish colour through columns 1-13 for one accession (*V. cephalota*) means that no data are available; column 14–17: results of species delimitation methods: 14 = ABGD; 15 = PTP on 1 locus; 16 = BPP; 17 = STACEY.

In order to evaluate the evolutionary scenario that might be hidden under such discrepancies, we built three data tables for accessions of *Niebla* (Suppl. material 5: Table S5, Suppl. material 6: Table S6, and Suppl. material 7: Table S7): the first one compares the number of accessions in the dataset with the number of species delimited by BPP and STACEY; the other two with the number of species as recognized by BPP and STACEY within each locality. These data demonstrate: (a) no inclusive pattern can be detected with the first dataset (Suppl. material 5: Table S5), as the data spread from a complete match between the classical identification and the BPP and STACEY methods (as shown with the unique example *N. turgida*: two accessions are identified as a single species by the three methods) to the complete reverse (as shown by *N. lobulata*, where four accessions, recognized as that single species by the classical method, are recognized as four different taxa by the BPP and STACEY methods); Spjut (1996) reported differences in spore length and metabolites for *N. lobulata* collections in the Southern Vizcaíno Desert (SVD) and in the Northern Vizcaíno Desert (NVD); (b) the number of species as recognized by BPP (33 in our dataset) and STACEY (18) confirm a highly diverse genus as shown by Spjut (1996), but the number of species per locality ranges (Suppl. material 6: Table S6) from one to eight. The number of localities where a species is found is very low: with BPP data, mostly between one and three, a single case with four and another with five, over a total of 12 localities sampled; with STACEY data, also mostly between one and three, with two cases with four and a single case with six.

The phylogenetic tree for *Vermilacinia* (Fig. 7) is fully resolved at most nodes if one adopts a 90% BS value as reference and at all nodes if one adopts a > 80% BS value. The tree is divided into two main clades: one includes only saxicolous species with an almost perfect match between the ITS-barcode ABGD method and the other three more sophisticated methods for species delimitation. This clade includes four species recognized as new in this work. These are monophyletic and supported lineages that cannot be assigned to any of the species included in Spjut (1996).

The second clade has two branches: one with the saxicolous *V. laevigata*, not distinguished by the BPP and STACEY methods from the related *V. combeoides* and the other one with all accessions of epiphytic species, including the populations found in SW Africa. A single species, as circumscribed by Spjut (1996), is recovered by our statistical analyses: *V. cerebra*, representing the sister group to all other species. The other supported clades and statistical analyses demonstrate a complex situation: *V. cephalota*, one of two sorediate species in the Northern Hemisphere, is resolved into two different species, whereas the *V. corrugata* and the *V. howei-leopardina-nylanderii-zebrina* clades are unresolved: the BPP analysis recognized four species within *V. corrugata* and only three in the former assemblage; the STACEY analysis recognized two species in the *V. corrugata* lineage and only one in the *V. howei-leopardina-nylanderii-zebrina* one. Fifteen collections of *Vermilacinia* from Namibia all have the same ITS, including a single unique substitution in ITS2. The *Vermilacinia corrugata* clade is comprised of cryptic species, although Spjut (1996) described a morphological variation that might be segregated in further study; the type is in southern Baja California Sur where we did not collect.



**Figure 8.** Evolutionary tree for the genera *Niebla* and *Vermilacinia*, produced with the 6-locus matrix and using \*BEAST (Matrix 2). Values above branches represent posterior probabilities of support. Epithets in colour following insert: green = collected in USA/California; pink = collected in Mexico/Baja California; blue = collected in Mexico/Baja California Sur. Similarity matrix from the STACEY analysis on the right. Each rectangle represents posterior probability (white = 0, black = 1) of pairs of specimens to belong to the same species. Shades of grey represent intermediate values. Rectangles delimited by red lines represent the species delimitation with a 0.3 cut-off.

**Evolutionary tree for the genera *Namibialina* and *Ramalina* (Fig. 9)**

A paraphyletic assemblage of ten species forms the base of the phylogenetic tree of *Ramalina* (Fig. 9: “early diverging clades”). This includes all seven species that lack medullary compounds (*R. capitata*, *R. celastri*, *R. crinita*, *R. fraxinea*, *R. hoehneliana*, *R. polymorpha* and *R. sinensis*) and two that produce a  $\beta$ -depsidone or a depside, *R. rubrotincta* and *R. crispans*, respectively. Neither group forms a supported clade. A more

extensive sampling for the basal *R. sinensis*, which is geographically structured, revealed an impressive diversification, dated at 19 Myrs.

Following these early diverging clades, is a strongly supported clade resolved in four assemblages, all strongly supported. However, significant incongruence amongst the four loci has been detected at this level, affecting the topological position of two lineages, the *R. clementeana* one with a single species and the *R. fastigiata* lineage with *R. carpatica*, *R. sp. 1* and the eponym species. This matter remains to be resolved.

Apart from the paraphyletic early diverging assemblage, the tree here produced is divided into four main clades. The first (Fig. 9) includes the *fastigiata* gr.; the second includes the *brevisucula* gr., the *nodosa* gr., the *cribrosa* gr. and the *farinacea* gr.; the 3<sup>rd</sup> includes only *R. clementeana*, while the fourth is much more diverse, including, *inter alia*, the *bourgeana*-, the *decipiens*, the *huei*- and the *canariensis* groups.

## Discussion

### Phylogeny of fruticose genera in the Ramalinaceae

The phylogenetic tree, here produced for the fruticose taxa within the Ramalinaceae, is strongly supported and rejects their monophyly. Indeed, both lineages that support fruticose genera are nested within accessions referred to the crustose genus *Cliostomum* s.l.: *C. griffithii* is sister to all other lineages and *Cliostomum* s. str. (including the type species *C. corrugatum*) is sister to the lineage *Niebla* + *Vermilacinia* with poor support. Thus, both strongly supported lineages comprising fruticose taxa are sister groups to *Cliostomum* s. str., forming an unresolved strongly supported group of three lineages.

One lineage contains two genera (*Niebla* + *Vermilacinia*) with all species but one restricted to coastal deserts of the New World subjected to oceanic fog and the other is divided into two genera, one (*Namibialina*) only with species with the same ecological requirements, but with a disjunct distribution (SW Africa) and the other (*Ramalina*) widely distributed throughout the world, with a basal species (*R. sinensis*) that is widespread throughout the Northern Hemisphere. It further includes, *inter alia*, at least two clades (the *R. bourgeana* and the *R. decipiens* gr.; Krog and Østhaugen 1980; Sérusiaux et al. 2010; Pérez-Ortega et al. 2019) also associated with coastal arid habitats subjected to ocean fog, but again with a disjunct distribution as they thrive off the coasts of North Africa, mainly in the Canary Islands and Madeira archipelago.

Kistenich et al. (2018) further positioned a unique genus and species (*Cenozosia inanis*), endemic to the Atacama Desert in South America, as sister to *Cliostomum* and the other fruticose taxa now recognized in the Ramalinaceae. We could not support this hypothesis with our dataset; only a rather small LSU sequence is available for that species that could complement the loci used in this study and its inclusion in our analysis resolved it at the base of the *Niebla* + *Vermilacinia* clade in an unsupported position (tree not shown). *Cenozosia inanis* was described as an epiphyte (“in ramulis dejectis prope ...” Montagne 1842) and briefly presented by Bowler (1981) as follows: “The monotypic

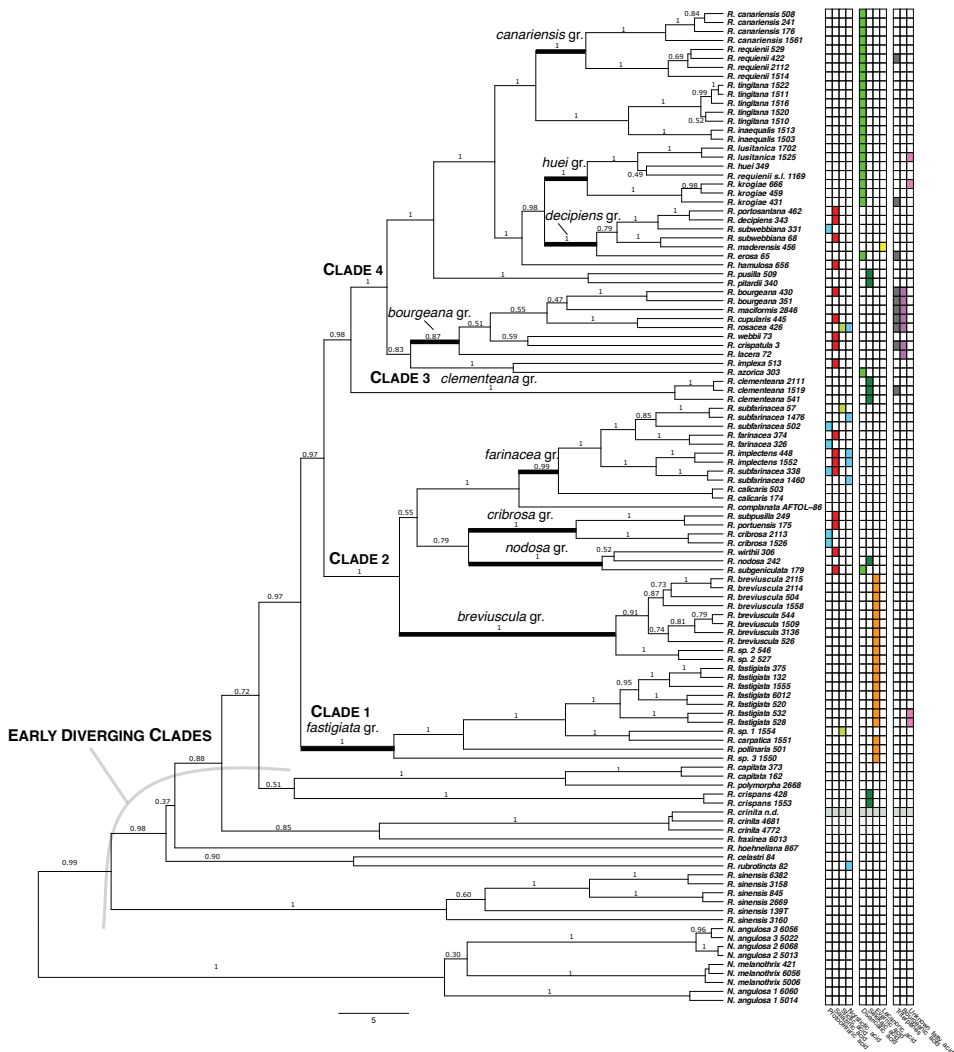


**Figure 9.** Evolutionary tree for the genera *Namibialina* and *Ramalina* (subset of Matrix 1). The tree is a close-up of Figure 6. Values above branches represent the posterior probabilities of support. Table on right side provides further information for all accessions: column 1-4:  $\beta$ -depsidones (protocetraric acid, salazinic acid, stictic acid, norstictic acid); column 5-8: depsides (divaricatic acid, sekikaic acid, evernic acid, lecanoric acid); column 9: triterpenes; column 10: bourgeanic acid; column 11: unknown fatty acid; greyish colour through columns 1-11 for two accessions (*R. complanata* and *R. crinita*) means that no data are available.

genus *Cenozosia* is a fistulose radiant of the South American *N. ceruchis* line. The thallus is either hollow or very loosely filled with medullary hyphae [...]. The anatomy of the cortex is the same as that of the *N. ceruchis* aggregate [...]. The “*N. ceruchis* line”, a corticolous species in the subgenus *Cylindricaria*, is more appropriately referred to as the *Vermilacinia tigrina* clade. In addition, Spjut (1996) noted under *V. flaccescens* that *Cenozosia inanis* is clearly distinct for its perforated cortex and chondroid strands that crisscross the

medulla. The phylogenetic position of this unique species requires further study and we expect it to be resolved at the base of the clade formed by *Vermilacinia* and *Niebla*.

### Time calibration and biogeographical patterns

The divergence between the *Ramalina* + *Namibialina* clade (RN) and the *Cliostomum* + *Vermilacinia* + *Niebla* clade (CVN) occurred before or at the beginning of the Eocene Climatic Optimum (55–50 Myrs) which was the warmest period during the Cenozoic (Zachos et al. 2001, 2008; Seton et al. 2012; Mudelsee et al. 2014). At the beginning of the subsequent climatic deterioration, the Long Term Eocene Cooling (LTEC, ca. 48 Myrs), fruticose taxa emerged:

- the RN clade evolved into two fruticose genera, *Ramalina* and *Namibialina*. Starting at c. 43 Myrs, *Ramalina* rapidly spread throughout the world, colonizing a wide range of habitats from saxicolous sea-shores to trunks and tiny branches in boreal, temperate and tropical forests. Its sister genus, *Namibialina*, radiated under more specialized ecological conditions in the coastal deserts of SW Africa, starting much later at c. 19–20 Myrs. Its diversification is thus much older than the full establishment of the cold-water upwelling system of the Benguela Current in the Late Miocene (10–7 Myrs; Heinrich et al. 2011; Rommerskirchen et al. 2011; Jung et al. 2014). The first-diverging species of *Ramalina* (*R. sinensis*) also started to diversify at that time.
- the poorly supported CVN clade divided in two taxa, one crustose (*Cliostomum* s. str.) and the other diverging at the mid Oligocene (ca. 30 Myrs) and splitting into two lineages of fruticose taxa. Therefore, the divergence of the duo *Vermilacinia* + *Niebla* is hardly younger than the establishment in northern Chile of the ecological conditions required (Oligocene to Middle Eocene; Rundel et al. 1991; Dunai et al. 2005; Le Roux 2012a, b; Gutiérrez et al. 2013; Koračín et al. 2014; Rundel et al. 2016). *Vermilacinia* diversified at 22 Myrs, that is before the Mid Miocene Climatic Optimum (MMOC) and *Niebla* started to diversify at 13 Myrs for *Niebla*, that is after the MMOC.

A similar geographical pattern is observed in three other lineages of lichenized fungi that have the same ecology, occurring on coastal rocks in fog deserts. These are: (a) the Redonographoideae which further includes two corticolous species (Lücking et al. 2013; Rivas Plata et al. 2013; Miranda-González et al. 2020), a small group of two genera and seven species (*Gymnographopsis* C.W. Dodge: three species, one in South Africa, one in Chile and one in Mexico; *Redonographa* Lücking et al.: four species, North and South America, Galapagos); (b) the genus *Santessonia* Hale and Vobis (Caliciaceae) in the Namib desert (three species: Sérusiaux and Wessels 1984) were assumed to form a monophyletic group with another set of three species from the Atacama Desert (Follmann 2006), but no molecular data are available; (c) the sister group formed in the Arthoniales by the monotypic *Combea* De Not. [*C. mollusca* (Ach.) Nyl.] endemic to the Namib and the monotypic *Dolichocarpus* R. Sant. (*D. chilensis* R. Sant.), endemic to the Atacama Desert (Ertz and Tehler 2011).

When the fruticose genera in the Ramalinaceae diverged c. 48 Myrs into the RN and CVN clades, the breakdown of Gondwana was almost complete. The Antarctic current had cooled the Antarctic continent to where all vegetation disappeared under immense glaciers (Anderson et al. 2011; Bohoyo et al. 2019). With the phylogenetic and biogeographical data available, a Southern Hemisphere origin for both clades can be argued, either in South Africa or in Patagonia and the closest Antarctica peninsula (N-W Antarctica). The only similar biogeographic pattern that we could detect in angiosperms is the Tecophilaeaceae, a small family of eight genera and 27 species in the Asparagales, mainly occurring in arid ecosystems and with a disjunct distribution in California, Chile and southern and tropical mainland Africa (Buerki et al. 2013). The biogeographical scenario, inferred from phylogenetic data, assigned the most recent common ancestor (MRCA) of the family as “widespread between South America and tropical Africa” and an origin in the late Cretaceous. Empirically, we can argue that this timing and biogeographical scenario fit the data for the fruticose genera in the Ramalinaceae.

### Phylogenies of the genera *Niebla* and *Vermilacinia* and species delimitation

The number of *Niebla* species recognized by the most sophisticated BPP and STACEY statistical methods at each locality is very low. A methodology bias can influence those data, as all ITS barcodes detected at each locality could not be included in the 6-locus dataset, because of poor amplification of several loci. Nevertheless, the hypothesis of a micro-endemism pattern of allopatric species cannot be ruled out and variation in space and time of fog conditions may provide support for this scenario. Indeed, their restricted geographical range and their radiation at c. 22 Myrs for *Vermilacinia* and at ca. 13 Myrs for *Niebla* clearly point to the paramount importance of climate change since the Miocene (Spjut 1996; Cerling et al. 1997; Herbert et al. 2016).

Pacific coastal fog relates to seasonal high/low pressure areas that impact the strength of an inversion layer and temperature of the California Current (for the Northern Hemisphere) or the Chile-Peru Current (for the Southern Hemisphere), location of upwelling water caused by wind and Coriolis force diverting water away from shore (“Ekman transport”) and topography, including offshore continental slope and shelf width (Zaytsev et al. 2003). As surface water moves away from the coast, colder water upwells, chilling the overlying humid marine air to saturation – creating fog. Land heated during day above sea temperatures lowers pressure causing fog to drift landward. Seasonal high pressure intensifies fog against the windward side of coastal ranges. The result is that fog is patchy, varying in its intensity and its flow inland (Rundel et al. 1991; Cartapanis et al. 2011). Further, several studies could highlight the instability (in surface affected and continuity) of fog over the last millions of years (Ortiz et al. 1997; Heusser 1998; Herbert et al. 2001; Snyder et al. 2003; Addison et al. 2018). We can therefore postulate that intermittence of fog, both in time and area affected, may provide a sufficient driving force for active speciation. Retreat of fog along a mountainous coastline with various bays and inlets would create localized habitats for *Niebla* and *Vermilacinia*, such as what

we see today along the Pacific Coast. During times when fog becomes more continuous along the coast, the previously isolated populations also expand and come into contact.

However, several alternative patterns can substantiate or dispute the hypothesis of micro-endemism such as incomplete lineage sorting or hybridization (Buschbom and Mueller 2005; Stewart et al. 2014) as recently suggested for the genus *Rhizoplaca* Zopf (Keuler et al. 2020). However, micro-endemism within a single radiation has been demonstrated for a lineage of *Sticta* in the MIOI (Madagascar and Indian Ocean Islands; Simon et al. 2018) and might represent a widespread pattern in lichenized fungi, as strongly suggested in several other studies (Sérusiaux et al. 2011; Lücking et al. 2014; Dal Forno et al. 2017; Lücking et al. 2017b).

### Insights into the species diversity of *Niebla* and *Vermilacinia*

Despite the incongruence of morphological species with phylogenetic reconstructions in *Niebla*, geographical lineages are apparent such as the *Niebla homalea* group (Fig. 7), characterized by a relatively thick cortex with a solid medulla, occurring largely in the California Floristic Province in contrast to lineages with a relatively thinner cortex and more fistulose medulla, occurring in the NVD. Additionally, distinct lineages for *Niebla homalea* in Northern California might relate to movement of the Pacific Plate relative to the North American Plate during the past 2 Myrs. A similar pattern is detected in *Ramalina menziesii*: the oldest of geographically defined lineages for this species ranging from the Pacific Northwest to the Vizcaíno deserts, was recognized as a unique lineage in the Vizcaíno deserts, having been isolated for perhaps 1–2 Myrs (Sork and Werth 2014).

None of the  $\beta$ -depsidones-producing species as Spjut (1996) delimited by morphological, chemical and ecological characters could be recognized. The main reason for this discrepancy is that Spjut (1996) applied the  $\beta$ -depsidone metabolite as a discriminant character: protocetraric acid for *N. pulchribarbara*, hypoprotocetraric acid for *N. brachyura* and *N. spatulata* and salazinic acid for the six other species (*N. arenaria*, *N. effusa*, *N. flabellata*, *N. josecuervoii*, *N. limicola* and *N. marinii*) and *N. homaleoides* for thalli lacking  $\beta$ -depsidones. All are related by the absence of triterpenes. Examples of the discrepancy between the work of Spjut (1996) and the species delimitation produced here with molecular data are (a) *N. brachyura* represented by four accessions that resolved into three different species by the BPP method and (b) the basal clade with only *N. flabellata* or *N. spatulata*, recognized as a single species by BPP, but as two by Spjut (1996) who used the two different metabolites to distinguish these two species (salazinic acid for *N. flabellata* and hypoprotocetraric acid for *N. spatulata*). This example is mainly applicable to collections from the SVD where thalli of the two depsidone chemotypes consistently occurred together at many sites, whereas the type specimen for *N. flabellata* (Spjut and Marin 9073H5, US) was collected in close association with the divaricatic acid-producing *N. caespitosa* (Spjut and Marin 9073C, US) in the southern NVD and the two species could only be distinguished by chemistry. *Niebla flabellata* is thus supported in the NVD by chemistry from similar morphs (*N. caespitosa* with divaricatic acid and

*N. lobulata* with sekikaic acid), but not by morphology from the related  $\beta$ -depsidone species. Thus, these species are still unresolved from a phylogenetic perspective.

The taxonomy proposed by Spjut (1996) relies on the combination of chemical and morphological characters. Although his *Niebla* taxonomy is not corroborated by molecular inferences and statistical speciation methods, that of saxicolous *Vermilacinia* is corroborated and this likely is to be found in South American species.

Spjut (1996) recognized two subgenera within *Vermilacinia*: subgenus *Vermilacinia* with the saxicolous *V. combeoides* as type species and subgenus *Cylindricaria* with the corticolous *V. corrugata* as type species. These two subgenera are recovered and can be confirmed if the saxicolous *V. combeoides* and *V. laevigata* are treated separately from the corticolous species all included in the subgenus *Vermilacinia*. This would require recognizing a third subgenus for the majority of saxicolous species – the alternative option would be not to recognize any subgenera.

Although future inclusion of data for species occurring in South America may bring in new structure for the *Vermilacinia* phylogenetic tree, it is nevertheless interesting to highlight that, for the Northern Hemisphere Pacific coasts, the corticolous habitat is a more recent autapomorphy. Contrarily to saxicolous species whose species delimitation is resolved, the terminal and, thus, most recent corticolous *Vermilacinia* are taxonomically problematic. Only the two oldest clades are fully resolved: *V. cerebrata* is resolved as a monophyletic group and the sorediate populations are resolved into two different species (*V. cephalota* for populations from USA/California and a yet undescribed species for those from Baja California). All others are resolved into two strongly supported clades: (1) one without any black bands can be attributed to *V. corrugata*, a species with a corrugated cortical surface that is deficient in terpenes except zeorin and occasionally T3 (Spjut 1996); it occurs in the Channel Islands and abundantly on shrubs in Baja California for nearly the entire length of the peninsula along the fringe of the coastal fog – to at least the vicinity of Isla Magdalena in Baja California Sur; (2) the second has black bands or irregular spots, around the lobes, the pycnidia or the apothecial discs; Spjut (1996) recognized six species in that morphologically (including production of punctiform soralia) and chemically variable group: *V. howei*, *V. leopardina*, *V. nylanderii*, *V. zebrina* plus *V. leonis* and *V. tigrina* (not represented in our dataset). Three species are delimited by the BPP analysis and a single one by STACEY. There is hardly any matching between the species delimited by Spjut (1996) in the “black bands” lineage. The accession from Namibia is not recognized as a different species, although an autapomorphic substitution in ITS2 is easily detected; we can therefore assume that this disjunct population is the result of a single, very recent colonization event. As for *Niebla*, more samples and data are needed to resolve the taxonomy of this genus.

As for the saxicolous and terricolous species of *Vermilacinia*, the taxonomical weight given to chemistry by Spjut (1996) for the recognition of species could find support in our dataset. The TLC data of the four accessions of *V. combeoides*, *V. laevigata* and *V. procerata* from USA/California included in Sérusiaux et al. (2010) are “triterpenes” without any other information; one can thus consider that this statement is coherent with the typical assemblage for those species: zeorin, T3 and [-]-16 $\alpha$ -hydroxykaurane. Indeed, this “T3 triterpene assemblage” is present throughout the clade and represents the plesiomorphic chemical assemblage, as is also the case for the related saxicolous species in South America. The T1

+ T2 assemblage, with zeorin and [-]-16 $\alpha$ -hydroxykaurane, is detected in two lineages, one with the newly described *V. lacunosa* and the second with *V. ligulata* and *V. reptilioderma*. Therefore, species with the T1 + T2 assemblage include *V. lacunosa* and *V. rosei* in the SVD and *V. johncassadyi* and *V. ligulata* in the NVD extending to just north of Punta Canoas on Mesa Camacho; only *V. reptilioderma*, the last T1 + T2 species, being present throughout that range. *Vermilacinia johncassadyi* and *V. rosei* also occur on the nearby island Cedros. All these species have a restricted range and we can confidently assume a micro-endemism pattern. Finally, the newly described *Vermilacinia lacunosa* is unique amongst the saxicolous *Vermilacinia* in the Northern Hemisphere for containing methyl 3,5-dichlorolecanorate (= tumidulin), otherwise known in the two South American species *V. flaccescens* and *V. granulans*. *Vermilacinia lacunosa* was recovered as a unique lineage within the phylogenetic tree, which reinforces the taxonomic significance of the secondary metabolites in the genus.

Spjut (1996) reported two saxicolous species to reach Tierra del Fuego in Argentina (*V. ceruchis* and *V. combeoides*). He now suspects that E. Tuckerman (1817–1886) mounted California specimens of *V. combeoides* on the same herbarium sheet close by specimens reportedly collected from Callao, Peru and Coquimbo, Chile for making comparisons. Spjut (1996) treated the Peru and Chile saxicolous specimens as variants of the terricolous *V. ceruchis*; however, based on our study of saxicolous *Vermilacinia* employing molecular data, they almost certainly are distinct from *V. ceruchis* and, therefore, we refer to them as *V. aff. ceruchis* and *V. aff. combeoides*; the former differs in having inflated branches with many lateral apothecia along a branch, the latter differs by the subterminal apothecia instead of strictly terminal apothecia. *Vermilacinia cf. flaccescens* has also been reported from Patagonia (Yang et al. 2018).

Delimiting species boundaries and establishing robust taxonomies for these two genera are challenging tasks that need more samples and data and more sophisticated techniques for species delimitation (Altermann et al. 2014; Magain et al. 2017; Grewe et al. 2018).

### Phylogeny of the genus *Namibialina* (Fig. 9)

Two typical species occurring in the coastal deserts of SW Africa are here assigned to the new genus *Namibialina*: “*Ramalina melanothrix*” recovered as a single taxon and “*Ramalina angulosa*” (Wirth 2010 a, b), recovered as a paraphyletic assemblage of three species. Although there are no clear-cut morphological, anatomical or chemical autapomorphies, we choose to recognize a new genus, sister to *Ramalina*, as its divergence time (from *Ramalina*) is dated at c. 48 Myrs, almost simultaneously to the emergence of the MRCA (Most Recent Common Ancestor) of the CVN clade comprising three genera, clearly different from one another on morphological and chemical characters.

The taxonomical status of *Ramalina melanothrix* is straightforward, while that of *R. angulosa* is not. First, the type material was not available for study and its nomenclature is confusing (see § Taxonomy and Nomenclature). Further, we suspect this morphotype is widespread from the coastal desert of Namibia (of which only a short portion ca. 120 km long was sampled; see above under Material and methods) down to the Cape area where the type was collected. A much higher diversity is expected

as three supported and sympatric species are easily detected in our material, differing from one another by the branching pattern including capillary cilia, the cortex surface, several characters associated with the cartilaginous strands under the cortex and production or not of apothecia.

### Phylogeny of the genus *Ramalina* (Fig. 9)

The subcosmopolitan genus *Ramalina* exhibits an impressive thallus variation as it ranges from luxuriant pendulous thalli up to several metres long, hanging down from branches of tall trees (such as in *R. hoehneliana* and *R. menziesii*) to unattached and almost pulverulent thalli hidden in rock crevices. Further, the thallus branches are very diverse as they can be terete or markedly compressed and applanate, hollow or solid, usually with a chondroid tissue and lax medulla; with or without fenestrations, reticulate ridges, pseudocyphellae, laminal striae, tiny lateral hooked fibrils, cilia, soralia; pycnidia with a black ostiole or not. The number of species is expected to be 230 (Lücking et al. 2017a) and 50 are represented in our study, including one here newly described and three that cannot be assigned to a validly published epithet (Figs 2, 6, 9–11).

All species lacking secondary metabolites, except for usnic acid in the cortex, are resolved at the base of the tree. However, these species do not form a single lineage and are intermingled in paraphyletic lineages with two species (*R. crispans* and *R. rubrotincta*) that do produce secondary metabolites.

Although the sampling of species included in this study may not be representative of the variation throughout the genus, chemistry-based branches supporting several species are numerous with, *inter alia*: (1) two clades characterized by the production of  $\beta$ -depsidones: the *farinacea* and the *cribrosa* clade, with one anomaly in *R. subgeniculata* whose thalli produce divaricatic acid, the  $\beta$ -depsidone salazinic acid being restricted to the apothecia; (2) two clades characterized by the production of evernic acid: the *breviuscula* and the *fastigiata* clade (the latter with one exception with sp. 1 which produces several  $\beta$ -depsidones); (3) the *bourgeana* clade characterized by the production of bourgeanic acid, with the exception of *R. webbii*, which does not produce that metabolite; and (4) two supported clades with all species producing divaricatic acid: the *canariensis*-clade and the *huei*-clade.

Strongly supported clades, however, can have a diverse chemistry, such as the *decipiens* clade, endemic to the Canary Islands and the Madeira archipelago (including Porto Santo), which have species producing either  $\beta$ -depsidones or depsides. Therefore, worldwide sampling is needed to further evaluate secondary chemistry to give support for deep node segregation, such as in other macrolichen genera (*Xanthoparmelia pulla*-group: De Paz et al. 2012; *Usnea cornuta*-group: Gerlach et al. 2019; *Cetrelia*: Mark et al. 2019). However, the model of chemical characters as support of evolutionary nodes is not universal as demonstrated by the *Bryoria fuscescens* group (Boluda et al. 2019) and *Thamnolia* (Onuț-Brännström et al. 2017).

Other interesting results include: (1) *R. requienii*, a rather common saxicolous species in the Mediterranean region and in the Canary Islands, from sea-level to montane regions, here resolved into two different species: one restricted to the Canary



**Figure 10.** *Ramalina breviuscula* aggr **A, B** *R. breviuscula*, type locality in France, eastern Pyrenees (photographs taken in the field) **C, D** *Ramalina* sp. 2 (France, Corsica). Scale: 1 mm (**C, D**). Photographs by E. Sérusiaux.

Islands and the Madeira archipelago and the other to the Mediterranean region; as the type was collected in France/Corsica (Krog and Østhaugen 1980) and as no available epithet could be assigned to this species, the new *Ramalina krogiae* is described below (Fig. 11). (2) Confirmation of sibling species (Culbertson 1986) with *R. inaequalis* and *R. tingitana*, here confirmed as two sympatric species (Fig. 2), sister to each other, thriving in the same habitat on rocky sea-shores in the western Mediterranean region. (3) The *R. farinacea* complex is here resolved into two clades: one includes the typically sorediate corticolous species *R. farinacea* and the saxicolous *R. subfarinacea*; the same ecomorphotype, however, is also resolved in the second clade, further comprising the non-sorediate and fertile *R. impletens*. Therefore, the classical taxonomy of this species complex (Aptroot and Shumm 2008: *R. impletens*, fertile; *R. farinacea*, sorediate and corticolous; *R. subfarinacea*, sorediate to isidiate and usually saxicolous) is not supported by molecular inferences. Further, both *subfarinacea* ecomorphotypes are sympatric along the northern coasts of Norway. These results are consistent with the library of DNA barcodes for Nordic countries (Marthinsen et al. 2019). (4) Two very variable groups, both producing evernic acid and not resolved as sister taxa: one includes the

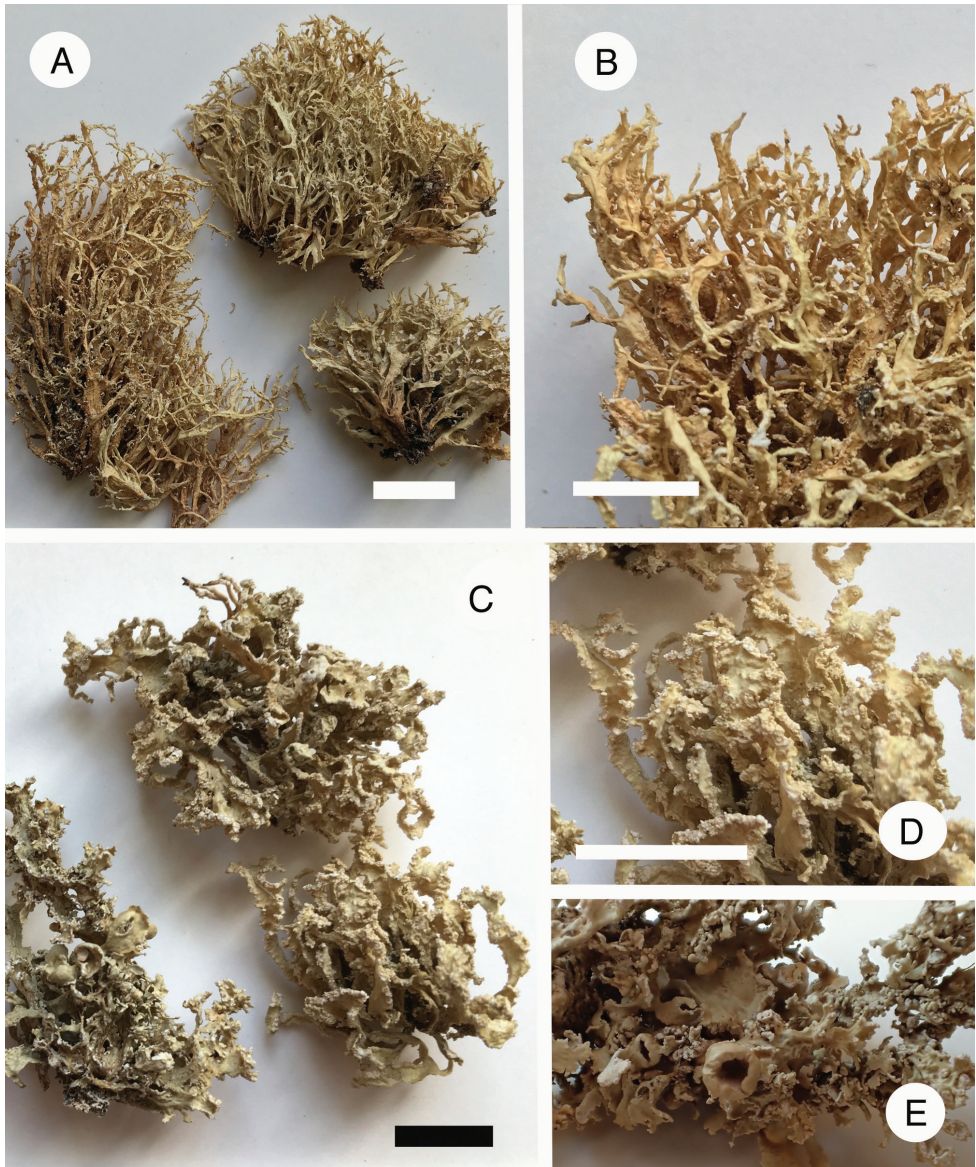


**Figure 11.** Species in *Ramalina* **A, B** *R. krogiæ* (holotype) **C–E** *R. requienii* (France, Corsica). Scale: 1 cm (**A–D**); scale in **E** identical to **D**. Photographs by E. Sérusiaux.

corticolous *R. fastigiata*, almost always fertile, usually forming densely tufted and richly branched, pulvinate thalli, but quite variable in size of thalli and lobes and especially in the spur-shaped lobe at the base of apothecia; and the saxicolous *R. breviuscula*, with fertile, densely tufted and branched, pulvinate thalli. Two morphotypes can be distinguished within the *breviuscula* lineage (Fig. 10): the first corresponds to material sampled at the type locality, widespread from sea-level outcrops to exposed ones at



**Figure 12.** Species in *Ramalina* **A** *R. crispans* (holotype: left-hand specimen; other specimen from Morocco: right-hand) **B** *R. lusitanica* (Morocco, leg. J. Gattefosse, BC) **C, D** *R. lusitanica* (Italy/Sardinia, accession LG DNA 1525). Scale: 1 mm (**C**). Photographs by E. Sérusiaux.

higher elevations (compact pulvinate thalli with young lobes typically dichotomously branched at their apices; lobes becoming tubular, remaining rather regular and not pitted); and the second one found only in Corsica at 930–940 m in a forest context (less compacted thalli with young lobes simple or not regularly branched and mature lobes irregular, remaining tubular, but many irregular holes) is here recognized as a separate species, so far unnamed. (5) Finally, accessions of fertile, epiphytic and divaricatic acid-producing populations from the western Mediterranean region are shown to be a well-delimited species, for which the epithet *lusitanica* is re-appropriated (Fig. 12).

As expected, detailed morphological and chemical studies supported by molecular inferences end up with taxonomical adjustments, descriptions of new taxa or resurrection of old epithets. An interesting case is the basal species *R. sinensis* which started its diversification c. 19 Myrs (Early Miocene) and produced four different lineages that might be worthy of recognition at species level: the earliest divergence isolated an accession from Western North America; the second (16–17 Myrs) isolated an accession from Taiwan (East Asia); the third one (9.5 Myrs) separated two accessions of the Caucasus region s.l. (Armenia and Iran) from two others from central Europe (Switzerland) and central Canada (Alberta).

## Conclusions

The Ramalinaceae include two strongly supported lineages of fruticose thalli: (1) *Ramalina* and *Namibialina* (gen. nov.) and (2) *Vermilacinia* and *Niebla*. Both form an unresolved clade with the crustose genus *Cliostomum*, excluding the well-known *C. griffithii* which is resolved in its own clade, sister to all others. The relationship of the monotypic *Cenozosia*, endemic to the Atacama Desert, remains to be determined.

Three of the fruticose genera are endemic to coastal fog deserts, *Namibialina* in SW Africa, *Vermilacinia* along the Pacific coasts in South America and North America, with a recent dispersal of a sorediate epiphytic species, *V. zebrina*, to Namibia and *Niebla* only in North America. All three genera are actively speciating and need further work to thoroughly address their taxonomy and diversification patterns.

The taxonomy of *Niebla* and *Vermilacinia* proposed by Spjut (1996) is largely confirmed, especially for the distinction between *Niebla* and *Vermilacinia* and the *a priori* assumption that all characters (secondary metabolites and morphology of thalli) can be employed for the delineation of species. An example is provided by *Niebla* as the deep nodes of its evolutionary structure are supported only by chemical characters. For *Niebla*, a larger sampling exercise, including all type localities, is needed to resolve its taxonomy at species level as the current species delimitation (Spjut 1996) is not supported by molecular data and inferences. Further, the model of micro-endemism of allopatric species cannot be ruled out at this stage. This model also finds strong support in the saxicolous species of *Vermilacinia*, whose phylogeny and species delimitation are fully resolved and includes four species here described as new for science. The corticolous species of *Vermilacinia* are partly resolved, the two most recent *V. corrugata*-clade and the “black-banded species”-clade need further work.

Our study confirms that the genus *Ramalina*, with a subcosmopolitan distribution and colonizing so many different habitats, is indeed a monophyletic group, based on 50 identified species (plus three without a specific epithet) represented for an estimated total of 230 species. The topology shown by the evolutionary tree confirms that all species that do not produce secondary metabolites (other than usnic acid produced in the cortex) are resolved at the base of the tree, but do not form a monophyletic group. Several clades supporting several species correspond to the production of peculiar secondary metabolites, but none of these constitutes an autapomorphy for a well-supported monophyletic clade, with the exception of bourgeanic acid which is unique to the *bourgeana*-clade. The data largely confirmed the present taxonomy with several corrections needed, the most interesting one being the diversity of the largely distributed basal species *R. sinensis* which started to diversify ca. 19 Myrs ago.

## Taxonomy and nomenclature

We here provide several notes on the taxonomy and nomenclature of a few taxa discussed in this paper, including re-assessment of three epithets and description of a new genus and five new species.

I *Namibialina*: a new genus for “*Trichoramalina melanothrix*”***Namibialina* Spjut & Sérus., gen. nov.**

Mycobank No: 833602

- = *Ramalina melanothrix* Laurer, Syn. Meth. Lich. 1(2): 290, tab. VIII, fig. 26, 1860  
= *Trichoramalina melanothrix* (Laurer) Rundel and Bowler, The Bryologist 77(2): 194, 1974  
= *Niebla melanothrix* (Laurer) Kistenich, Timdal, Bendiksby, S. Ekman, Taxon 67(5): 893, 2018

**Type species.** *Namibialina melanothrix* (Laurer) Spjut & Sérus., comb. nov.

**Description.** Thallus shrubby, usually arising from a single holdfast, stiff or flexuose, several cm in height when epiphytic or, saxicolous or developing terricolous shrubby cushions up to ca. 10–15 cm in diam. and 2–6 cm in height (fig. 2 in Wirth 2010b), typically pale green or yellowish-green. Branches usually dividing, regularly or not, dichotomous or not, apices usually with capillaceous or blackish terminal hairs; main branches terete-angular or flattened, distinctly canaliculate, because of well-developed longitudinal strands of cartilaginous tissue. Lateral branches and spinules sometimes present; typical isidia or soralia never observed. Medulla arachnoid, very thin. Cortex 2-layered, but not always typical. Apothecia present or absent, disciform, terminal or marginal and sometimes typically orientated perpendicular to the branch. Ascospores ellipsoid, straight or slightly bent, 1-septate, ca. 10–20 × 5–8 μm. Pycnidia sometimes abundant, with black ostioles. Secondary metabolites: usnic ac. in the cortex.

**Remarks.** The type species of *Trichoramalina* (Rundel and Bowler 1974), characterized by marginal black hairs, is *T. crinita* (Tuck.) Rundel and Bowler, a species endemic to the coastal areas of California and Baja California (Fig. 3). Kistenich et al. (2018) could demonstrate that it belongs to *Ramalina* and our own accessions support this phylogenetical position. The other species with black hairs (“*Trichoramalina*” *melanothrix*) is shown to have an isolated phylogenetic position and forms together with *Ramalina angulosa* (sensu Wirth 2010b) the sister group to all other accessions of *Ramalina* s. str. Although there are no clear-cut morphological, anatomical or chemical autapomorphies, a new genus is here introduced for this lineage endemic to SW Africa (Namibia and South Africa). Indeed, it diverged from *Ramalina* c. 48 Myrs ago early in the Eocene, almost simultaneously with the emergence of the MRCA (Most Recent Common Ancestor) of the CVN clade comprising three genera, clearly different from one another on morphological and chemical characters. Further, the basal species of *Ramalina* s. str. is *R. sinensis*, an epiphytic species widespread throughout the Northern Hemisphere, a complete contrast with *Namibialina* and that also started to diversify at c. 20 Myrs.

Two described species are here assigned to the new genus *Namibialina*: *Ramalina melanothrix* recovered as a single taxon and “*Ramalina angulosa*” (Lalley and Viles 2005; Wirth 2010a, b), recovered as a paraphyletic assemblage of three species, with *R. melanothrix* nested amongst them. All accessions available for DNA extraction and analysis were collected in Namibia, along ca. 120 km of coastline North of Swakopmund. There-

fore, we strongly suspect that a complex assemblage is hidden under these epithets, most probably much more diverse along the coastal deserts of SW Africa, from the southern part of Angola down to the Cape of Good Hope. It is currently under study.

Strands of cartilaginous tissue develop longitudinally under the cortex in all species of *Namibialina* and in several species of *Ramalina* resolved at the base of the tree, such as *R. sinensis* and *R. celastri*. In *Namibialina*, chondroid stands are “attached to the cortex”, not isolated in the medulla, the medulla is arachnoid, very thin and supported by a 2-layered cortex, sometimes the external layer indistinct (Rundel and Bowler 1974, Bowler 1981). Another shared plesiomorphy is the lack of secondary metabolites (except for usnic acid in the cortex) in *Namibialina* and in several basal species in *Ramalina* (*R. celastri*, *R. fraxinea*, *R. hoehneliana*, *R. sinensis* and others). However, Wirth (2010b) mentioned several secondary compounds in “*Ramalina angulosa*”:  $\pm$  bourgeanic,  $\pm$  sekikaic,  $\pm$  4'-O-demethylsekikaic and  $\pm$  salazinic acid.

The nomenclature of the above-mentioned epithets can be summarized as follows: Theodor Magnus Fries (Flora 44: 411, 1861) clearly recognized *Ramalina melanothrix* as different from what had been assigned to *R. angulosa*. He referred to an annotation of Johann Friederich Laurer using that epithet for a collection made by Johann Franz Drège “in Africa meridionali”. J.F. Drège is a very famous plant collector in the Cape area (Gunn and Codd 1981) and we can thus assume his specimen was collected in that area. However, in the same section, Th. Fries thoroughly described *Ramalina capensis*, with two varieties: “Formae duae, quas amplectitur, nominandae:  $\alpha$  *angulosa* Laur. [...] ramis apicalibus concoloribus et  $\beta$  *melanothrix* Laur. [...] apicibus thalli [...] nigricantibus”.

Further, a collection assumed to be a type from the Royal Botanic Garden Edinburgh E is available at: <https://plants.jstor.org/stable/viewer/10.5555/al.ap.specimen.e00465255>.

There is no doubt that this collection belongs to the “*angulosa*” assemblage. It has a label indicating it was collected in Tahiti, but annotations by B.J. Coppins (Feb. 1976) reads as “This is a Drège specimen from South Africa”.

## 2 *Niebla*

### Type species of *Niebla*

There has been a lot of debate regarding the type species of this genus (Krog and Østhaugen 1980; Sérusiaux et al. 2010). The genus name is a substitute name for *Desmazieria*, a homonym created by Camille Montagne in 1852 who recognized only one species in the genus (*D. homalea*). However, the name *Desmaziera*, although not spelled exactly the same, but nevertheless considered to be the same (homonym), had been given to a genus of grass (Poaceae) by Barthélemy Dumortier in 1822. The earliest name is the one that must be retained unless the later name is conserved, according to the ICN. Additionally, the type species name for *Niebla* is *Niebla homalea*, based on the name given to the one and only species that had been recognized by Montagne for the genus, not *Niebla ceruchis* as stated in Sérusiaux et al. (2010).

### Lectotypification for *Niebla procera*

The holotype of *Niebla procera* Rundel & Bowler at ASU is represented by two specimens shown in Bowler et al. (1994, fig. 4) in black and white and a mirror image is available in colour in the CNALH website (<https://lichenportal.org>). The CNALH image clearly shows that two specimens are involved. We identify *Vermilacinia procera* on the left and *Vermilacinia* cf. *paleoderma* on the right; therefore, we designate the left-hand specimen as the lectotype of “*Niebla procera*”.

The lichen metabolites reported for *N. procera* in Bowler et al. (1994) are “[–]-16 $\alpha$ -hydroxykaurane,  $\pm$  zeorin,  $\pm$  salazinic acid, terpenes, fatty acids,  $\pm$  usnic acid”. A fragment of the specimen on the right may have been removed for TLC (the upper part of a thallus branch appears scraped just below the tip). The morphological description given in Bowler et al. (1994) generally agrees with the specimen on the left. Both species have similar chemistry (Spjut 1996). Additionally, Bowler et al. (1994) cited specimens of “*Niebla procera*” mostly from islands, five of the Channel Islands, one from Isla Guadalupe (as *V. paleoderma* in Spjut 1996), one at the north end of Isla Cedros and from one location on the Vizcaíno Peninsula, 3.5 km W of Mexico Hwy 1 along the road to Punta Abreojos (generally *V. paleoderma* in Spjut 1996). They did not cite specimens from the NVD. They also recognized another species in the Channel Islands and adjacent coastal California (Ventura and Los Angeles counties), “*Niebla polymorpha*” [= *Vermilacinia polymorpha*, type from Santa Catalina Island, also shown present in the chaparral region of Baja California without reference to specimens (Bowler et al. 1994)]. We consider *V. procera* to occur mostly on the mainland, Baja California from near San Quintín to Marin County, California; Spjut (1996) also cited two specimens from the Channel Islands, one from Santa Catalina Island collected by Howe and one from Santa Cruz Island collected by C. Bratt. Saxicolous species of *Vermilacinia* south of Bahía de San Quintín, including Isla Guadalupe (Palmer s.n., US!), belong to the *V. paleoderma* group, which includes new species described in this paper; however, this group might also be present near Punta Escarpada in the NVD as suggested in Spjut (1996).

### 3 *Ramalina*

***Ramalina crispans* R.G. Werner, Scientific Annals of the School of Agriculture and Forestry, Aristotelian University, Thessaloniki IH<sup>3</sup>-B: 1 (1977).**

Mycobank No: 131128

Fig. 12A, right-hand specimen

**Type.** MOROCCO – Original publication reads “ad corticem *Quercus suberus* L. in Mamora silva prope Rabat” (Werner 1977: 1); label reads as “Forêt de Mamora près Rabat, sur *Quercus suber*”, 01.02.1936 s.n. (BC! – holotype).

**Description.** Thallus epiphytic, almost always on tiny branches, shrubby, usually rather small (less than 2–5 cm long), formed of densely intricate branches that

are solid, slightly flattened and irregularly thickened; soralia conspicuous albeit quite small, granular, often with small fibrils; pseudocyphellae common, ellipsoid or linear; apothecia and pycnidia unknown.

**Chemistry.** Acids in the sekikaic aggregate with sekikaic and homosekikaic acids as the main compounds detected; usnic acid.

**Distribution and ecology.** Mediterranean area and Cabo Verde archipelago; assumed to be present in the Canary Islands, the Madeira archipelago and the Azores archipelago; on branches, including twigs, never found on trunks, in open shrubland.

**Remarks.** This species was described as “spec. nova ad interim”, an unclear status that could be questioned under the ICN code art. 34.1 (b). Nevertheless, we adopt it pending further nomenclatural clarification. Following Aptroot and Schumm (2008), this species would key out as *R. peruviana* Ach. This epithet is used for any densely branched, sorediate *Ramalina* producing sekikaic acid throughout the world (Swinscow and Krog 1988 for tropical East Africa; Aptroot and Bungartz 2007 for the Galapagos Islands; Galloway 2007 for New Zealand; Aptroot and Schumm 2008 for North Atlantic Islands; Oh et al. 2014 for China). *Ramalina peruviana* Ach. is a validly published epithet and the original publication states “Habitat in Peruvia in confortito crefens ...”. No material from Peru or surrounding countries that could match the original description was available for DNA analysis. Therefore, we choose to use the epithet introduced by R. G. Werner for Mediterranean material of corticolous *Ramalina farinacea* look-alikes and producing sekikaic acid. Our dataset shows that accession from Cape Verde and Greece are identical; we assume that reports from the archipelagoes of the Azores, Canary Islands and Madeira belong to the same species.

**Additional specimens examined.** Cabo Verde archipelago – São Vicente, Monte Verde; assumed at 16°52.2'N, 024°56.0'W; alt. ca. 730 m; 04.2008; J. Lambinon 08/20 leg.; on shrubs (LG DNA 428); [DNA: GU726358 (LSU), GU827317 (ITS), MN757015 (RPB1), MN757230 (RPB2)]. Greece – Dodecanese, Karpathos Is., top of Mt Hagios Elias; 35°43.6'N, 027°10.5'E; alt. 710 m; 07.2007; H. Sipman & Th. Raus 56261 leg.; on *Erica* dwarf shrubs (B, LG DNA 1553); [DNA: MN811427 (ITS)]. Morocco – “Chellak ruinas prope Rabat”; 07.04.1934; R.G. Werner s.n.; “ad radices *Chamaropsis humilis*” (BC). TLC for both collections from Morocco (incl. type) by Amami N., Arroyo & Serriñá, annotation of May 2002.

***Ramalina krogiae* Guissard & Sérus., sp. nov.**

MycoBank No: 833605

Fig. 11A, B

**Diagnosis.** *Ramalina krogiae* is recognized by its saxicolous habitat, ascending, 1–2 dichotomous branched, rigid lobes, producing abundant granules, but no genuine soralia, nor apothecia, producing divaricatic acid and endemic to the Canary Islands and Madeira archipelagoes

**Type.** Spain – Canary Islands, La Gomera, W of Arure, N of Ermitago de Santo; 28°08.10'N, 017°19.23'W; alt. 825–830 m; 04.2009; E. Sérusiaux s.n. leg; subvertical

outcrops in open matorrales; (LG DNA 666! – holotype; TFMCI – isotype) [TLC: divaricatic and usnic acid; DNA: MN811446 (LSU), MN811250 (ITS), MN757049 (RPB1), MN757257 (RPB2)]

**Description.** Thallus saxicolous, ascending, usually rigid, when well-developed up to 3–4 cm high, usually with 1–2 dichotomous branching in the upper half of the branch, 3–4 mm large at most, usually less, branches contorted or irregularly twisted, small dissected and elongated lobes (small laciniae) usually present, together with tiny rounded or irregularly shaped granules, these granules sometimes abundant; cortex locally and usually irregularly broken off, but no typical production of soralia observed. Apothecia rare to abundant, lateral, disc usually strongly concave (“wide open” apothecia rarely seen) with a scrobiculate outer cortex, margins of the disc usually with cortex interruption and production of tiny granules. Ascospores straight or slightly concave, 1-septate, 9–13 × 4–5 µm. Pycnidia not found.

**Chemistry.** Divaricatic and usnic acid, triterpenoids.

**Distribution and ecology.** On exposed rocks at low elevation, in the Canary Islands and the Madeira archipelago.

**Etymology.** Epithet chosen after our most distinguished colleague Prof. Hildur Krog (1922–2014), author, inter alia, of a remarkable and detailed revision of the genus *Ramalina* in the Canary Islands (Krog and Østhagen 1980).

**Remarks.** Besides its distinct geographical range (Mediterranean region vs. Canary Islands and Madeira archipelago), the morphologically and chemically similar *R. requienii* can be distinguished by its usually larger lobes with sublinear pseudocyphellae and especially the lobes extremities rather typically labriform, with a lower surface with large patches of disrupted cortex and production of coarse soralia. In typical populations of *R. krogiae*, no such labriform and slightly, but distinctly, expanded lobes are formed and tiny granules produced on or around the rather large cortex interruptions at the lobe extremities are not observed. Therefore, the distinct phylogenetic relationships of *R. krogiae*, as well as its disjunct distribution, are complemented by morphological features, which albeit rather cryptic can be easily detected with some taxonomic expertise.

**Additional specimens examined.** Portugal – Madeira, Ponta de São Lourenço; 32°44'N, 16°40'W; alt. 150 m; 05.04.2007; D. Ertz 10520 leg.; rock outcrop near the sea; (BR, LG DNA 431); [DNA: GU726360 (LSU), GU827319 (ITS), MN757017 (RPB1), MN757232 (RPB2)]. Portugal – Porto Santo, between Pico de Castelo and la Capela de Nossa Senhora da Graça; 33°04.41'N, 016°19.37'W; alt. 200–220 m; 04.2007; M. Dewald, A. Hambuckers & E. Sérusiaux leg.; outcrops in pastures; (LG DNA 459); [DNA: MN811437 (LSU), MN811241 (ITS), MN757040 (RPB1)].

***Ramalina lusitanica* H. Magn., Bot. Notiser 109: 149 (1956)**

Mycobank No: 369922

Fig. 12B–D

**Type.** Portugal – Estramadura, Serra da Arrabida, between Setubal and Torre de Outao; 01.05.1931; G. Degelius leg.; on trees (UPS L-78721 ! – holotype).

**Description.** Thallus corticolous, usually on branchlets, erect or rarely partly pendulous, up to 4–5 cm in diam., with a fan-shaped appearance (with terminal apothecia) or a small-cushion one; lobes divided dichotomously or trichotomously, rather stiff, flat or slightly concave, up to 3–4 mm large just before the first division; upper surface slightly grooved or channelled, often longitudinally ridged; lower surface undulating, distinctly scrobiculate on well-developed lobes. Apothecia usually present and abundant, terminal or lateral on young lobes, up to 4–5 mm in diam., usually 2–3 mm, disc concave, with no spur or with the lobe margin that carry the apothecium developing into a ligulate to triangular spur. Ascospores straight or slightly concave,  $10\text{--}14 \times 3\text{--}5 \mu\text{m}$ . Pycnidia not found.

**Chemistry.** Divaricatic and usnic acid, unknown fatty acid.

**Distribution and ecology.** Corticolous on branchlets in forest or more open areas at low elevation in the western Mediterranean region, so far confirmed on DNA-basis from the islands of Corsica (France) and Sardinia (Italy); probably more widespread.

**Remarks.** The type collection of *Ramalina lusitanica* has many small and brittle fragments, with an upper surface with verruciform ridges, reticulate lower surface and several apothecia. Its author considered it was close to “*Ramalina evernioides*” that represents the taxon now named *R. lacera*; he added that it “cannot be considered a variety of that species on account of absolute absence of sorediate parts and of distinct reticulation”. We were able to produce DNA sequences out of material collected in Italy/Sardinia and France/Corsica and therefore to stabilize this epithet erratically used, because of confusion with *R. canariensis* and *R. lacera*. Typical specimens are easily recognized (when young) by their fan-shaped, rather rigid lobes, some being slightly concave, usually longitudinally striate, without fenestrations, usually with abundant and terminal apothecia and production of divaricatic acid.

*Ramalina lusitanica* is resolved as a distinct species in a clade together with *R. huei* and all accessions of *R. requienii* from Macaronesia, here assigned to the newly described *R. krogiae*. However, *R. huei* (Fig. 4D) develops pendulous thalli, usually exuberant (5–20 cm long) and with convoluted lobes, lateral apothecia and pseudocypbellae; when these are lateral, they induce separation of cortex layers, thus exposing the medulla; such features are not encountered in *R. lusitanica*. *Ramalina huei* thrives in the Canary Islands, the Cabo Verde archipelago and southern Portugal (Krog and Østhagen 1980; Aptroot and Schumm 2008). Interestingly, *R. lusitanica* is not closely related to the mainly epiphytic *R. canariensis* and the saxicolous *R. requienii*, both species producing divaricatic acid and occurring abundantly in the Mediterranean region.

Without identification of its secondary metabolite (divaricatic acid), the general appearance of this species brings it close to forms of *R. fastigiata* (producing evernic acid) or *R. panizzei* and *R. elegans* (both producing acids in the sekikaic group). Further information about these species can be found in Arroyo and Serriñá (1995) and Groner and LaGreca (1997).

We considered *Ramalina latzelii* Zahlbr., a species producing divaricatic acid and abundant apothecia, as a putative synonym. This epithet was reduced into synonymy with *R. canariensis* by Poelt (1969) and examination of the type material (W) confirms that it is, indeed, a fertile rather than sorediate form of that species; divaricatic acid is detected by TLC.

**Additional specimens examined.** France – Corsica, Terzanili; 41°25.21'N, 09°12.37'E; alt. 60 m; 10.2010; M. Guissard & E. Sérusiaux ; olive orchard (LG DNA 1702); [DNA : MN811471 (LSU), MN811275 (ITS), MN757073 (RPB1), MN757273 (RPB2)] Italy – Sardinia, E of Sanat Teresa, La Licciola; 41°13.33'N, 09°15.32'E; alt. 70 m; 10.2010; M. Guissard & E. Sérusiaux leg; on twigs in disused olive plantation; (LG DNA 1525); DNA : MN811462 (LSU), MN811266 (ITS), MN757064 (RPB1), MN757269 (RPB2)] Morocco – Oued “Rotbar, sur racines accidentellement découvertes de *Chamerops humilis*”, 01.06.1937, leg. J. Gattefosse leg. (BC). – Morocco, “forêt de Boulhaut à Aïn Sferdjla, sur *Rhus pentaphylla*”, 20.02.1939, J. Gattefosse leg. (BC). TLC for both collections from Morocco by Amami N., Arroyo & Serifiá, annotation of May 2002.

Type collection of *Ramalina latzelii* Zahlbr., Oesterr. Botan. Zeitschrift 60: 18 (1910): Croatia – “Dalmatien, Meleda, an *Pinus halep.* auf der Grabova”, ca. 200 m, 18.02.1908, leg. Dr. A. Latzel n° 22” (W! – holotype).

***Ramalina rosacea* (Massal.) Hepp, Flechten Europ. n° 356 (1857)**

MycoBank No: 403822

Bas.: *Ramalina polymorpha* var. *rosacea* Massal., Schedul. Critic., fasc. IX: 157 (1856). = *R. bourgeana* auct. europ., non Mont. ex Nyl.

**Type.** Corsica, Cavallo, Lich. Exs. Ital. 228 (BM! – isotype).

**Description.** Thallus saxicolous, firmly attached to the substrate (rock), formed of rigid, rather large lobes (2–8 cm large and 1–14 cm long) almost all attached with a single holdfast, lobes surface strongly reticulate-wrinkled. Apothecia usually present, marginal, usually at lobe extremities, with an outer exciple strongly scrobiculate. Ascospores straight or slightly curved, 1-septate, 10–12 × 3–5 µm. Pycnidia not found.

**Chemistry.** Bourgeanic, norstictic, stictic and cryptostictic acid, PCR-1 and triterpenes.

**Distribution and ecology.** Very rare, found on rocky sea-shores at two localities in the western parts of the Mediterranean Sea (France/Corsica and Spain; see below).

**Remarks.** The original material was collected on the island of Cavallo, a small islet south of Corsica (France) and distributed through the Lichenes Italici Exsiccati, n° 288. The original publication (Schedulae criticae in lichenes exsiccatos Italiae IX n° 286–323) can be accessed through the permanent link <http://mdz-nbn-resolving.de/urn:nbn:de:bvb:12-bsb10229836-1>. We could examine the material preserved in BM: an original handwritten annotation is “Cavallo”. It matches very well the recent collection made on the very same islet by Gonnet et al. (2017) which we could examine (including by TLC and ITS sequence). The secondary metabolites of that material were identified as usnic, bourgeanic and salazinic acids (Gonnet et al. 2017); we cannot confirm these results. Indeed, following the protocols designed by Culberson et al. (1981), we recognize the following as produced by the recent accession from Cavallo and two from Cabo de Gata (Spain): norstictic (+), stictic (++), cryptostictic (+++), and

bourgeanic acid and triterpenes. Besides bourgeanic acid and the triterpenes, the main compound is the poorly known cryptostictic acid, easily confused in solvent G with salazinic acid (Suppl. material 8). We thus confirm the results of Krog and Østhagen (1980), who stated that this material contains depsidones in the stictic acid group. This confusion was the source of a nomenclatural imbroglio as to the identity of the material recently collected at Cavallo with *R. bourgeana* (Roux et al. 2019).

Quite interestingly, this easily recognized species (at least in the local Mediterranean context) is absent elsewhere in southern Corsica and northern Sardinia where two of us (MG and ES) looked carefully for it in several localities, including on other islets of the Lavezzi archipelago, the archipelago to which the island of Cavallo belongs. See for more at: [http://www.afl-lichenologie.fr/Photos\\_AFL/Photos\\_AFL\\_R/Textes\\_R/Ramalina\\_bourgeana.htm](http://www.afl-lichenologie.fr/Photos_AFL/Photos_AFL_R/Textes_R/Ramalina_bourgeana.htm).

The ITS barcode sequence of this material is strictly identical with that of a second population of that species found at the Cabo de Gata in SE Spain, a coastal locality most famous for its lichen flora (Egea and Llimona 1994) and which also is the type locality of *Ramalina clementeana* (Llimona and Werner 1975). Our results clearly demonstrate that it is a unique taxon, different from accessions from Macaronesia and referred to as *R. bourgeana* Mont. ex Nyl. (1870), following Krog and Østhagen (1980). All other reports of both species (*R. bourgeana* and *R. rosacea*) from the Mediterranean region are not confirmed and refer to other species, mostly *R. tingitana*.

**Selected specimens examined.** FRANCE – Corsica, Cavallo Island; 41°22'N, 009°15'E; alt. 0–10 m; 2014; D. & O. Gonnet s.n. leg; rocky sea-shores (hb, LG DNA 4642); [DNA: MN788731 (ITS)]. SPAIN – Sierra del Cabo de Gata, path W of Torre de Vela Blanca to lighthouse; 36°43.82'N, 02°10.46'W; alt. 150 m; 2007; P. van den Boom 3835 leg; on exposed outcrops (hb van den Boom, LG DNA 426); [DNA: GU726357 (LSU), GU827316 (ITS), MN757014 (RPB1), MN757229 (RPB2)].

### *Ramalina sarabae* Knudsen et al.

**Remarks.** This species belongs to the *Ramalina lacera* group (Sérusiaux et al. 2010). It was recently described from the Channel Islands in California, USA (Knudsen et al. 2018). Its ITS sequence is available (Accession: NR\_160636.1) and appears identical with all our accessions of *R. lacera* (sensu Nash et al. 2002) from Mexico/Baja California and Baja California Sur, one accession of *R. lacera* s.l. from the archipelago Cabo Verde in the Atlantic Ocean off the coast of Mauritania and several accessions from the coastal areas of Namibia that would all be referred to as *R. lacera* following Wirth (2010b). The discovery of *R. sarabae*, throughout most of the peninsula of Baja California, in the Namib desert and the Cabo Verde archipelago creates an interesting relationship between these regions and it is worth mentioning that *R. sarabae* cannot be detected in any of the three other archipelagoes forming Macaronesia: Canary Islands, Madeira and Azores.

**Selected specimens examined.** CAPE VERDE ARCHIPELAGO – São Vicente, Monte Verde, just below the summit, NW slope; 16°52.2'N, 024°56.0'W; alt. 700 m;

2006; P. van den Boom 36603 & 36603b leg; on twigs (hb, LG DNA 1963 and 1964); [DNA 963: MN788729 (ITS); DNA 964: MN788730 (ITS)]; NAMIBIA – East of the road Swakopmund-Henties Bay; 22°20.38'S, 014°26.44'E; alt. 20 m; 04.2016; E. Sérusiaux s.n leg.; desert dunes, on twigs in “lichen field” (LG DNA 5012); [DNA: MN788735 (ITS)] – Omaruru distr., Laguneberg, N of Mile 72; ca. 21°49.8'S, 014°04.6'E; alt. 70 m; 09.2007; V. Wirth 40683 & 40686 leg; on twigs (KR, LG DNA 563 and 564); [DNA 563: MN788727 (ITS); DNA 564: MN788728 (ITS)]; – N-E of Cape Cross, southern part of the Laguneberg Range; 21°39.31'S, 013°59.55'E; alt. 100–130 m; 04.2016; E. Sérusiaux leg; rocky outcrops in “lichen field”, on twigs (LG DNA 5021); [DNA: MN788735 (ITS)] MEXICO – Baja California, laguna and peninsula of San Quintín; 30°29.74'N, 116°00.04'W; alt. 4 m; 02.2016; heavily disturbed chaparral over volcanic rocks; R. Spjut & E. Sérusiaux 17032 leg; on branches of *Aesculus parryi* (hb WBA, LG DNA 4676; [DNA: MN788731 (ITS)] – Baja California, El Rosario, Punta Baja; 29°58.26'N, 115°47.26'W; alt. 70 m, 02.2016; R. Spjut & E. Sérusiaux 17090 leg; on twigs and branches of small shrub (hb WBA, LG DNA 4728); [DNA: MN788732 (ITS)]; – Baja California Sur, SE of Bahía de Asunción, near the coast; 27°09.81'N, 114°14.75'W; alt. 20 m; 02.2016; R. Spjut & E. Sérusiaux 17136 leg; on twigs; (hb WBA, LG DNA 4756); [DNA: MN788733 (ITS)] – Baja California Sur; along the road from Bahía de Tortugas to Vizcaíno; 27°37.82'N, 113°25.19'W; alt. 70 m; 02.2016; R. Spjut 17233c & E. Sérusiaux leg; on twigs (hb WBA, LG DNA 4823); [DNA: MN788734 (ITS)].

#### 4 *Vermilacinia*

Saxicolous species of *Vermilacinia* are often described to have cylindrical prismatic branches, cylindrical for their lengthwise three-dimensional shape that in x-section are  $\pm$  round in outline but with short line segments to form a polygonal shape as opposed to teretiform being uniformly round in x-section. The lichen metabolites zeorin, T3 (terpene, UV+ orange), and [-]-16 $\alpha$ -hydroxykaurane are usually present. Exceptions are T3 lacking in species with T1 & T2 (Rf class 2–3, Solvent G) and zeorin sometimes absent in *V. combeoides* and *V. rigida*.

#### *Vermilacinia breviloba* Spjut & Sérus., sp. nov.

Mycobank No: 833607

Fig. 13A, B

**Diagnosis.** Similar to *V. robusta* by the inflated branches and to *V. polymorpha* by the relatively short length of branches; differs by the honeycomb-like cortex or by the contorted lobes.

**Type.** MEXICO – Baja California, Pacific Coast ca. 100 km N of Guerrero Negro, just N of Punta San Rosalillita west of road to Punta Negra along track to Puerto San Andrés in a narrow arroyo leading to a tidal inlet (estuary); 28°42.62'N, 114°16.19'W,

alt. 50 m, 26.01.2016, R. Spjut & E. Sérusiaux 17117 leg.; on steep north-facing rock ledges bordering south-side of tidal marsh, (LG ! – holotype; BCMEX !, US !, hb. Spjut at World Botanical Associates! – isotypes) [TLC : salazinic acid, triterpene 3, zeorin, [-]-16 $\alpha$ -hydroxykaurane ; DNA : MN811491 (LSU), MN811295 (ITS), MN757090 (RPB1), MN757285 (RPB2), MN757407 (GDP), MN757544 (EF-1 $\alpha$ )]

**Description.** Thallus 1–1.5 (-2.5) cm high and 0.5–1 cm broad; basal branches 1–5 or rarely more, short cylindrical, teretiform or prismatic, 1–3 mm diam., loosely united at brownish base,  $\pm$  erect, inflated, irregularly shriveled and contorted when dry, transversely segmented and ruptured when wet at  $\pm$  regular intervals, terminally divided into short lobes with or without apothecia; terminal lobes often many and close together or fewer and spreading, 4–6 mm long, 2–4 mm diam. Cortex two-layered, 35–50  $\mu$ m thick, outer thicker, melanized, externally pale olive green, with irregular reticulate cortical ridges, recessed-concave within ridges (honeycomb-like surface), occasionally plicate on inflated lobes. Medulla subfistulose, hyphae flexuous when wet, intertwining in a net arrangement,  $\pm$  periclinal, frequently uniting into minute knots; Photobiont in small yellow green to green round colonies  $\pm$  continuous around the perimeter of the medulla. Apothecia many, aggregate terminally on a primary branch, each subtended by a short stalk-like lobe partly deflated and constricted to junction with branch lobe, bowl-shaped when young, to 4 mm diam., lenticular with age; thalline margin thickened, incurved, entire or crenulate or incised, disc pale orange, concave; asci 8-spored; spores opaque, 1-septate, short ellipsoid, 6–7  $\times$  4–5  $\mu$ m. Pycnidia black, common on the upper half of branches in shallow concave depressions within cortical ridges, ostiole flush with cortical surface, immersed below; conidia not observed.

**Chemistry.** Salazinic acid, triterpene 3, zeorin, [-]-16 $\alpha$ -hydroxykaurane.

**Distribution and ecology.** Mexico, Baja California, North Vizcaíno Desert, between Punta Santa Rosalillita and Punta Negra. Only known from that locality. On rock ledges of north-facing cliffs bordering estuary inland from the sea, occurring with species of *Niebla*, *Vermilacinia cedrosensis* and *V. paleoderma*, within a semicircular arc of volcanic coastal hills with steep ravines and narrow ridges trending in various directions, 200–400 m in altitude, extending approx. 20 km along the coast and to 7 km inland at midpoint near the Punta Negra Road (Google Earth 2019). Fog often lingers amongst the higher ridges and peaks during the day (Spjut 1996). A diversity of saxicolous *Vermilacinia* occurs here: *V. breviloba*, *V. cedrosensis*, *V. ligulata*, *V. paleoderma*, *V. pustulata*, *V. reptilioderma* and *V. rigida*. Vegetation on hills near type locality consists of spiny shrubs and succulents of *Pachycormus discolor*, *Stenocereus thurberi*, *Cylindropuntia* spp., *Fouquieria diguetii* and *Agave shawii*. The subshrub *Xylonnagra arborea* was observed on rocks amongst the lichens and salt-scrub of *Atriplex julacea* and *Frankenia palmeri* bordered a salt marsh of aquatic species not studied.

**Etymology.** Epithet *breviloba* refers to the short lobes.

**Remarks.** *Vermilacinia breviloba* appears related morphologically to *V. polymorpha* and *V. robusta*, neither of which could be included in our phylogeny. *Vermilacinia polymorpha* was described by Bowler et al. (1994) from a specimen collected by Janet Marsh on Santa Catalina Island. *V. robusta*, a widespread species, differs by its much larger, terminally round inflated branches with a relatively smooth cortical surface. *Vermilacinia polymorpha* differs by its deflated-canaliculate branches near base. Both

*V. polymorpha* and *V. robusta* occur in the USA/California and Mexico/BC Chaparral, mostly in the Channel Islands; the latter species is also on Isla Guadalupe.

**Additional specimens examined.** Same locality as the type: R. Spjut & E. Sérusiaux 17121, 17126, 17128b, 17129b.

**Conservation Status.** Prior to year 2000, Puerto San Andrés was accessible directly from San Andrés Ranch, which appeared occupied at the time and not far from where *V. breviloba* occurs (Spjut pers. obs.). In January 2016, the ranch was not seen while we observed a new earth road that circumvented the estuary by passing north over a saddle and down across a wide arroyo to the north end of Puerto San Andrés, ca. 7 km southeast of Punta Rocosa via a precipitous rocky coastline (Google Earth 2019). A mixed community of local fishermen and nomads appear to reside at Puerto San Andrés. The most disturbance to lichens – evident to Spjut – was on the volcanic hill along the earth road that passes between the estuary and the arroyo north of the pass and also at the north end of Puerto San Andrés. An example is a strongly inflated form of *N. podetiaforma* observed in May 1985 to be common on pebbles on the rain shadow side of the hill (Spjut 1996, coll. Spjut and Marin 9077, distributed to many herbaria). This species was not seen there during our Jan 2016 visit. Two other earth tracks from Punta Negra road towards the coast could not be found in January 2016, one that seemed to have been created sometime between May 1986 and March 1988 that led to Punta Rocosa through Krutsio Ranch and a much older track originating about midway between Punta Negra and Santa Rosalillita that led into the hills along a narrow arroyo where Spjut, Marin and McCloud in May 1986 found closer foot access to the higher elevation ridges. This latter track, which was not evident from ground level in Jan 2016, is evident from Google Earth (2019), whereas the track to Krutsio Ranch appears to have weathered beyond recognition along with the ranch. Thus, much of this rocky coastal region between San Andrés and Punta Negra is protected by its isolation from being inaccessible by road. Additionally, the type locality is accessible only by foot in a direction opposite to where visitors travel to Puerto San Andrés.

***Vermilacinia lacunosa* Spjut & Sérus., sp. nov.**

Mycobank No: 833608

Fig. 13C, D

**Diagnosis.** Similar to *V. reptilioderma* morphologically by the cylindrical-prismatic branches and chemically by the triterpenes T1 and T2, but differing in chemistry by the additional lichen substance, methyl 3,5-dichlorolecanorate (tumidulin).

**Type.** MEXICO – Baja California Sur, Vizcaíno Peninsula, 2.5 km SE of Punta Eugenia, rock outcrops along coastal hills trending west-east separated by wide arroyo, just east of the coastal community of La Lobera; 27°49.701'N, 115°03.454'W; alt. 35–40 m; 29.01.2016, R. Spjut & E. Sérusiaux 17174 leg.; on calcareous rocks of north facing slope; (LG! – holotype; BCMEX!; US!; hb. Spjut at World Botanical Associates! – isotypes) [TLC: Triterpenes 1 & 2, zeorin, [-]-16 $\alpha$ -hydroxykaurane, usnic acid, methyl 3,5-dichlorolecanorate (= tumidulin), two unknown triterpenes; DNA: MN811420 (ITS), MN757203 (RPB1), MN757370 (RPB2), MN757488 (GDP)]



**Figure 13.** New species of saxicolous *Vermilacinia* **A,B** *V. breviloba* (holotype) **C,D** *V. lacunosa* (holotype) **E,F** *V. pustulata* (holotype) **G,H** *V. reticulata* (holotype). Scale: 1 mm (**A,C**). Photographs by R. Spjut.

**Description.** Thallus divided into many subcylindrical branches from a basal reddish-brown to blackish holdfast, to 2.5 cm high and broad. Primary branches ascending to erect,  $\pm$  ellipsoid-arcuate in x-section, simple or once dichotomously divided near mid region, terminating in aggregate of up to 8, commonly 5, apothecia or with single apothecium, or apothecia not fully developed on most branches, occasional branches without apothecia tapering to obtusely rounded apex; surface of branches commonly lacunose, deeply recessed within reticulate or circular cortical ridges when dry. Cortex pale yellow green, 50–125  $\mu\text{m}$  thick, each of two layers equal in thickness, outer melanized, inner pale. Medulla hyphae flexuous when wet, intertwining in a net arrangement,  $\pm$  periclinal, frequently uniting into short knots; photobiont in small yellow green clusters irregularly discontinuous around perimeter. Apothecia sessile, differentiated from branch by constriction or very short stalk-like lobe, bowl-shaped, to 2 mm diam. Alternatively, wider with shallower disc in age, thalline margin not differentiated by thicker cortex, incurved, entire or crenulate with age, disc pale yellow green or yellowish with age, concave; asci 8-spored; spores not observed outside asci. Pycnidia black, common on upper branches and on apothecia, mostly along cortical ridges, immersed except for ostiole flush with surface, conidia straight, short, needle-like.

**Chemistry.** Triterpenes 1 & 2, zeorin, [-]-16 $\alpha$ -hydroxykaurane, usnic acid, methyl 3,5-dichlorolecanorate (tumidulin), unknown triterpenes just below and above T1 and T2, respectively (TLC solvent G).

**Distribution and ecology.** Mexico, Baja California Sur, Vizcaíno Peninsula. Known only from a single collection on calcareous rocks on the north slope facing towards a wide arroyo just inland from the sea on the far western Vizcaíno Peninsula, occurring with *Vermilacinia paleoderma* and vascular plants *Fouquieria diguetii*, *Pachycormus discolor*, *Eriogonum pondii* and *Gossypium* sp. This region lies within the El Vizcaíno Biosphere Reserve, the largest reserve in Mexico. Additional details on the vegetation of the Vizcaíno Peninsula can be found in Peinado et al. (2005).

**Etymology.** Epithet *lacunosa* refers to the cortical depressions or 'holes' in the branch.

**Remarks.** *Vermilacinia lacunosa* is a distinct saxicolous species for containing the rare lichen metabolite methyl 3,5-dichlorolecanorate (tumidulin), identified by its high Rf on TLC plates in two specimens, previously known only from South American epiphytic species of *Vermilacinia* (Spjut 1996), such as *V. flaccescens* (Nyl.) Spjut and Hale. Sipman (2011) subsequently reported finding what he interpreted to be tumidulin in a new sorediate species he named *Niebla granulans*, here regarded as *Vermilacinia* [*V. granulans* (Sipman) Spjut and Sérusiaux (comb. nov.); bas. *Niebla granulans* Sipman, Bibliotheca Lichenologica 106: 300, 2011] found on twigs at Zapallar in the Valparaíso region of Chile. He distinguished it by apical punctiform soralia in contrast to lateral disciform soralia of *V. cephalota*; he further differentiated it from *V. cephalota* by the intricately branched habit; however, Spjut has collected much branched *V. cephalota* near Bahía de Asunción and distinguished *V. leonis* in the Magadlena Region of Baja California Sur for its larger much branched thalli (Spjut 1996). Additionally, Sipman (2011) reported four undetermined terpenoid compounds, one of which was

likely a diagnostic *Vermilacinia* compound, [-]-16 $\alpha$ -hydroxykaurane, based on his observation of “blooming of terpenoid crystals in herbarium specimens.” The species was noted to lack chondroid strands, pycnidia and apothecia.

In contrast, Sipman (2011) described *Niebla nashii*, another Chilean sorediate species from Coquimbo that he compared to *Ramalina lacera* (With.) J.R. Laundon. He distinguished it by possessing isolated medullary chondroid strands, as well as tumidulin and bourgeanic acid, while he also noted that key [*Vermilacinia*] terpenoids, pycnidia and apothecia were absent. Judging from Sipman’s image of the type specimen, it lacks the characteristic cortical ridging of *Niebla*. Further, Sérusiaux et al. (2010) found bourgeanic acid associated with depsides in Mediterranean species of *Ramalina* – that had been treated in *Niebla* by Rundel and Bowler (1978) and Bowler and Marsh (2004) – to be nested within the genus *Ramalina*. Other collections identified *Niebla* spp. from Patagonia in Chile (National Park of Torres Del Paine) – that were reported to contain tumidulin – “exhibited significant inhibitory activity on spheroid formation in CRC cells and decreased the expression of CSC markers in CRC cells” (Yang et al. 2018). DNA extracts are needed to assess the phylogenetic relationships of the Chile specimens reported to contain tumidulin.

**Conservation Status.** The type locality of *Vermilacinia lacunosa*, 2.5 km southeast of the fishing community of Punta Eugenia, is vulnerable to off-road travel. Spjut observed the Punta Eugenia community to have expanded considerably since his first visit there in 1986. Although the type locality lies within the El Vizcaíno Biosphere Reserve, this reserve is referred to as a wildlife refuge. However, to the northeast is the protected area of flora and fauna at Valle de los Cirios in the southern portion of Baja California. “The El Vizcaíno overlaps with smaller protected areas on land and in the waters, including the protected grey whale (*Eschrichtius robustus*) sanctuaries at Ojo de Liebre (Scammon’s Lagoon), Guerrero Negro, and San Ignacio. Protection is provided by international organizations including UNESCO, Ramsar and Western Hemisphere Shorebird Reserve Network (WHSRN). The area is not only important to plant and animal life, but more than 300 ancient rock painting sites have been discovered throughout the reserve” (CONANP-20: <http://www.parkswatch.org/parkprofile.php?l=eng&country=mex&park=vibr&page=inf&p=mex>; accessed 09.06.2019).

***Vermilacinia pustulata* Spjut & Sérus., sp. nov.**

MycoBank No: 833609

Fig. 13E, F

**Diagnosis.** Similar to *V. cedrosensis* in the flexuous long cylindrical branches with a pale yellow-green cortex, but differs by the pustular cortical protrusions, in contrast to pitted and transversely reticulated cortex of *V. cedrosensis*.

**Type.** MEXICO – Baja California Sur, Vizcaíno Peninsula, ca. 11 km NW of Bahía Tortugas, 2.6 km NE of Rompiente along the west side of peninsular Coast, west to

southwest along track off the Bahía Tortugas-Punta Eugenia Road; 27°44.969'N, 114°56.690'W; alt. 140–160 m; 30.01.2016, R. Spjut & E. Sérusiaux 17191 leg.; on white calcareous rock outcrops along coastal hills trending northwest, (LG! – holotype; BCMEX!; US!; hb. Spjut at World Botanical Associates! – isotypes); [TLC : Salazinic acid, triterpene 3, zeorin, [-]-16 $\alpha$ -hydroxykaurane, unknown triterpene UV+ bright blue Rf just below T3, traces of several other unknown triterpenes; DNA : MN811556 (LSU), MN811360 (ITS), MN757151 (RPB1), MN757492 (GDP), MN757618 (EF-1 $\alpha$ )]

**Description.** Thallus divided into many long, uniformly narrow cylindrical-tereti-form, flexuous branches from a pale brown to blackened base, to 7.0 cm long and 1 cm diam. at base. Primary branches fastigiate, ascending near base, flexuous above, simple or dichotomously divided, 1–2 mm diam., terminating in aggregate of few to several apothecia, occasional branches obtuse to a blunt apex; surface of branches densely pustular and blistered, conspicuously in a line along one side. Cortex pale yellow green or whitish-green, 40–60  $\mu$ m thick. Medulla with strong orange pigmentation in central region within the lower half of branches, becoming pale yellow and then clear in upper half or medulla pale yellow or without noticeable pigmentation; photobiont in small yellowish-green colonies irregularly dispersed around the perimeter of medulla. Apothecia mostly terminal, occasionally subterminal well below apex, developing from a short terminal expansion and flattened lobe, bowl-shaped when young, to 5 mm diam.; thalline margin lip-like, incurved to disc, becoming deeply lobulate; disc pale yellow green to pale grey or white or yellowish with age, plane to slightly concave; asci 8-spored; mature spores not seen outside asci. Pycnidia black, conspicuous on conical protrusions, immersed except for ostiole flush with surface.

**Chemistry.** Salazinic acid, triterpene 3, zeorin, [-]-16 $\alpha$ -hydroxykaurane, unknown triterpene UV+ bright blue Rf just below T3, traces of several other unknown triterpenes, one above salazinic acid and another above T3 (TLC in Solvent G).

**Etymology.** Epithet *pustulata* refers to the pustular outgrowths on the cortex.

**Distribution and ecology.** Mexico, Baja California Sur, Vizcaíno Peninsula and Baja California, Punta Morro Santo Domingo and Puerto San Andrés.

**Remarks.** *Vermilacinia pustulata* is closely related to *V. cedrosensis* from which it can be distinguished by its surface of branches densely pustular and blistered, conspicuously in a line along one side. This species is resolved as sister to *V. reptilioderma*, a species easily distinguished by its cylindrical-prismatic branches and production of the triterpenes T1 and T2. All species delimitation methods recognized the two as different, except for STACEY which merged them. This incongruence may require further investigation.

**Conservation Status.** The species appears threatened at type locality by trash discarded in the open desert, observed to be increasing in density as one approaches within several km from the west side of Bahía Tortugas. Fortunately, the species occurs elsewhere.

**Additional specimens examined.** MEXICO – Baja California, west of Villa Jesus María along shoreline at Punta Morro Santo Domingo; elev. 10 m; 12.2016; S. Leavitt et al. 16–938 leg. (BRY!); *ibid.*; vicinity of Puerto San Andrés; 19.05.1986; R. Spjut 9893A1 leg. (hb. Spjut at World Botanical Associates).

***Vermilacinia reticulata* Spjut & Sérus., sp. nov.**

MycoBank No: 833610

Fig. 13G, H

**Diagnosis.** Recognized by its thallus divided into subcylindrical-prismatic branches, appearing quadrangular in x-section, with sharply raised  $\pm$  wavy ridges in a reticulate pattern, the primary branches shortly 5-lobed near apex.

**Type.** MEXICO – Baja California Sur, Vizcaíno Peninsula, 2.5 km SE of Punta Eugenia, rock outcrops along coastal hills trending west-east separated by wide arroyo, just east of the coastal community of La Lobera; 27°49.701'N, 115°03.454'W; alt. 35–40 m; 29.01.2016, R. Spjut & E. Sérusiaux 17153 leg.; on calcareous rocks of north facing slope; (LG! – holotype; BCMEX!; US!; hb Spjut at World Botanical Associates! – isotypes)[TLC : Salazinic acid, triterpene T3, zeorin, [-]-16 $\alpha$ -hydroxykaurane, unknown triterpenes ; DNA : MN811551 (LSU), MN811355 (ITS), MN757146 (RPB1), MN757332 (RPB2), MN757486 (GDP), MN757613 (EF-1 $\alpha$ )]

**Description.** Thallus divided into several or many subcylindrical-prismatic branches from a common basal attachment, up to 6 cm high and 5.5 cm broad. Primary branches ascending, once dichotomously divided near mid region, terminally shortly 5-lobed, with apothecia or, if without apothecia, obtusely rounded to bluntly pointed apex, compressed, 4-lobed or angled in x-section, occasional branches dilated and flattened to apex, sharply recessed along cortical ridges mostly in a reticulate pattern. Cortex pale yellow green or bluish green, smooth and deeply recessed within the  $\pm$  reticulate or circular ridges along the face of the branch, 2-layered or a dense algal layer in outer medulla closely adhering as a third supportive layer, 75–150  $\mu$ m thick. Medulla with a central dense grey area and outer white area. Apothecia on a short compressed lobe slightly constricted at junction with primary branch, bowl-shaped, to 2 mm diam. or up to 5 mm diam. with less concave disc or appearing to abort development, the branch terminally inflated and lobulate; thalline margin incurved, entire or crenulate with age, disc pale yellow green or yellowish with age or cream, concave; spores opaque, 1-septate, fusiform-curved, 8–10  $\mu$ m. Pycnidia black, common to abundant on upper half of branches, immersed except ostiole flush with surface; conidia needle-like.

**Chemistry.** Salazinic acid, triterpene T3, zeorin, [-]-16 $\alpha$ -hydroxykaurane, unknown triterpenes UV + light blue without border, UV+ dark blue with border at Rf just above salazinic acid (TLC in solvent G).

**Distribution and ecology.** Mexico, Baja California Sur, Vizcaíno Peninsula, known from a single location on conglomerate outcrops along north to northeast facing slopes near Punta Eugenia, occurring with *Vermilacinia paleoderma*.

**Remarks.** *Vermilacinia reticulata* is distinguished from *V. paleoderma* by the sharply delineated cortical ridges and deeply recessed surface within, often appearing in a reticulate pattern. TLC revealed an unknown UV+ dark blue with a well-defined border under UV+ just above salazinic acid. Thalli with concentrated development of pycnidia on rugose cortical ridges resemble *Niebla rugosa*, which differs by the steplad-

der arrangement of the cortical ridges, in addition to the chemical and medulla character features that define the genus and species. *Vermilacinia reticulata* is sister to a clade comprising *V. paleoderma* and the newly described *V. breviloba*.

**Etymology.** Epithet *reticulata* refers to the cortical ridges exhibiting a nice and obvious reticulate pattern.

**Conservation Status.** The species may be threatened by off-road travel as discussed under *V. lacunosa*.

**Additional specimens.** Same at the all type locality: R. Spjut & E. Sérusiaux 17175a [DNA: MN811502 (LSU), MN811306 (ITS), MN757420 (GDP), MN757557 (EF-1 $\alpha$ )], 17179c [DNA: MN811504 (LSU), MN811308 (ITS), MN757101 (RPB1), MN757423 (GDP), MN757559 (EF-1 $\alpha$ )], 17173D [DNA: MN811552 (LSU), MN811356 (ITS), MN757147 (RPB1), MN757487 (GDP, MN757614 (EF-1 $\alpha$ ))] (all: LG, hb Spjut at World Botanical Institutes).

### Key to saxicolous and terricolous species of *Vermilacinia*

Key based on Spjut (1996), specimens collected by Spjut and Sérusiaux (2016), specimens from BRY loaned to WBA: 400 specimens collected by Steve Leavitt et al. in Baja California, Dec 2016 and another ca. 20 specimens from Chile, March 2017. New species are marked with \*.

- 1       Thallus branches densely compacted into hemispherical moss-like cushions (Cladonia-Cladina habit), 0.5–2.5(–5.0) cm high, often broader or in irregularly shaped clumps with basal prostrate branches from which ascending to erect secondary branches arise; terminal branches long to short bifurcate or abruptly pointed to obtuse apex; apothecia absent or undeveloped on most branches or, if developed, strictly subterminal with extended spur-like branch ..... **2**
- Thallus branches not tightly compacted into moss-like cushions, generally > 3.0 cm high, taller than wide; branches ribbon-like (flattened and contorted), blade-like (compressed-straight) or long tubular or cylindrical-prismatic, generally erect-fastigiate or spreading outward from one another, often branching in mid region, as well as near apex, not regularly bifurcate near apex; apothecia terminal or nearly so, often aggregate, rarely absent..... **6**
- 2       Thallus terricolous; basal branches prostrate to ascending near tip, with occasional upright secondary branches or thallus of numerous capillary matted branches (< 1.0 mm diam.; *Ramalina ceruchis* var. *tumidula* (Tayl.) Howe, probably a distinct species); terminal branches long bifurcate and attenuate to apex; apothecia absent; Peru, Chile..... ***V. ceruchis***
- Thallus terricolous or saxicolous, branches ascending to erect; mainly N America ..... **3**

- 3 Branches (0.5-) 1–2.0 (-5.0) mm diam., terminally swollen, then abruptly tapered to a pointed obtuse apex, simple to occasionally bifurcate or rarely trifurcate near apex, never isidiate; thallus similar to *V. combeoides* that differs by the development of terminal apothecia or by truncated apices on branches without apothecia. .... ***V. pumila***
- Branches mostly  $\leq$  1.0. mm diam.; with short acicular terminal branchlets or isidiate ..... **4**
- 4 Branches not united by holdfast; terminal branches equally short bifurcate to apex; isidioid branchlets and/or isidia lacking ..... ***V. ceruchooides***
- Branches arising from a common base or holdfast, unequally very short bifurcate or trifurcate near apex, occasional to frequent isidioid branchlets below apex; isidia often present; rarely sorediate..... **5**
- 5 Pycnidia absent or only at apex of terminal or isidioid branchlets; isidia often present; apothecia absent; California and Baja California Chaparral, Chile Atacama Desert..... ***V. acicularis***
- Pycnidia common to near base of branches; apothecia present, with short spur branchlets; rare, California Chaparral – San Luis Obispo County, Morro Bay ..... ***V. tuberculata***
- 6 Apothecia subterminal well below apex or lateral – facing perpendicular away from primary branch; Peru, Chile (*V. ceruchis* variants, Spjut 1996)..... ***V. cf. ceruchis***
- Apothecia terminal or subterminal; N America..... **7**
- 7 Pair of triterpenes present in  $R_f$  class 2–3 (TLC, Solvent G)..... **8**
- Triterpenes absent in  $R_f$  class 2–3 ..... **12**
- 8 Methyl 3,5-dichlorolecanorate (tumidulin) present..... ***V. lacunosa*\***
- Tumidulin absent..... **9**
- 9 Branches irregularly shaped, neither blade-like nor cylindrical, expanded near apex; Islas San Roque and Cedros, western Vizcaíno Peninsula ..... ***V. rosei***
- Branches  $\pm$  regular in shape, compressed or teretiform, sublinear to  $\pm$  oblong ..... **10**
- 10 Branches cylindrical-prismatic ..... ***V. reptilioderma***
- Branches compressed, ribbon-like (flattened, contorted) or bladelike..... **11**
- 11 Branches twisted (ribbon-like) ..... ***V. ligulata***
- Branches straight to recurved (blade-like) ..... ***V. johncassadyi***
- 12 Branches more blade-like (compressed) than cylindrical..... **13**
- Branches generally cylindrical-round or cylindrical-prismatic or tubular-inflated..... **14**
- 13 Basal branches 0.5–2 cm long, closely fastigate; rare, N Vizcaíno Desert – coastal ridge south of Punta Negra N of Punta Santa Rosalillita..... ***V. rigida***
- Basal branches mostly 3–6 cm long; spreading apart from base towards apex; California and Baja California Chaparral ..... ***V. laevigata***
- 14 Primary branches tubular inflated, loosely united at base ..... **15**

- Primary branches not tubular inflated, generally cylindrical, recessed within reticulate or round cortical ridges, closely united at base ..... **18**
- 15 Primary branches irregularly shaped, expanded near apex; S Vizcaíno Desert – Isla San Roque, Chile – Atacama Desert [BRY specimen].....  
..... *V. varicosa*
- Primary branches  $\pm$  regular in shape, cylindrical, teretiform or prismatic .....  
**16**
- 16 Basal branches cylindrical prismatic, as least in part, near apex distinctly lobed or with aggregate apothecia; N Vizcaíno Desert – San Andrés Cañon .....  
..... *V. breviloba*\*
- Basal branches tubular inflated, simple or irregularly shortly lobed near apex ..... **17**
- 17 Branches broadly rounded to apex; California and Baja California Chaparral, mostly islands ..... *V. robusta*
- Branches abruptly tapered to pointed apex; Chile – Atacama Desert.....  
..... *V. aff. robusta*
- 18 Basal branches mostly simple, closely fastigiate; apothecia terminal and solitary; zeorin often absent; California and Baja California Chaparral, mainland and islands ..... *V. combeoides*
- Basal branches spreading outwards above base; apothecia often terminally aggregate, sessile or on short branches or solitary and subterminal; zeorin present ... **19**
- 19 Branches with bladderlike swellings; pycnidia prominent on elevated rugose cortical ridges; rare, N Vizcaíno Desert – between Punta Canoas and Puerto Catarina..... *V. vesiculosa*
- Bladder-like swellings absent; pycnidia on various cortical angular ridges or at base of cortical depressions or at apex of pustular protrusions ..... **20**
- 20 Branches cylindrical-teretiform, often flexuous; cortex with shallow depressions or pits and often with transverse fissural cracks..... **21**
- Branches cylindrical-prismatic; cortex not cracked transversely ..... **23**
- 21 Cortex dark green, persistent, blackened irregularly from base to apex, notably where in contact with substrate; California and Baja California Chaparral..... *V. procera*
- Cortex relatively thin, yellowish-green, often eroding towards apex, the branches appearing white due to exposed medulla; Vizcaíno Deserts ..... **22**
- 22 Pycnidia mostly in shallow cortical depressions or pits; cortex mostly pitted; apothecia rim entire to slightly lobed ..... *V. cedrosensis*
- Pycnidia mostly on conical tubercles; cortex also pustular; apothecia lobulate..... *V. pustulata*\*
- 23 Branch surface honeycomb-like, with deep,  $\pm$  angular depressions.....  
..... *V. reticulata*\*
- Branch surface with various shallow depressions, crater-like or with pastry-like creases or relatively smooth and uneven..... **24**

- 24 Thallus much branched; pycnidia only at apex of branches; apothecia absent; terminal branches shortly bifurcate to sharp pointed apex; branch surface regularly recessed at ‘branch nodes’, sharply angled along ridges; rare, N Vizcaíno Desert – Punta Morro Santo Domingo, Atacama Desert ..... *V. aff. paleoderma*
- Primary branches sparingly divided; pycnidia below apex; apothecia on some branches; surface of branches variable ..... **25**
- 25 Branches  $\pm$  oblong ( $< 10\times$  longer than wide), deflated in part, canaliculate, especially near base, rounded along margins, usually with smooth concave depressions; California and Baja California Chaparral..... *V. polymorpha*
- Branches  $\pm$  linear to broad linear ( $> 10\times$  longer than wide), cylindrical prismatic; cortex irregularly creased, reticulately ridged, angularly recessed, plicate or the surface smooth and uneven; Vizcaíno Deserts..... *V. paleoderma*

### Data accessibility

Alignments and trees have been deposited in TreeBASE (Accession No: S25433).

### Acknowledgements

Field studies in many parts of the world where we could sample fruticose Ramalinaceae were made possible with the help and advice of many friends and colleagues; we would like to mention: Dr. F. Chase (National Herbarium of Namibia in Windhoek), Prof. J.M. Delgadillo (University of Ensenada BC, Mexico), Dr. D. Ertz (Jardin Botanique Meise, Belgium), Prof. E. Fischer (Universität Koblenz-Landau, Germany), Dr. A. Hambuckers (University of Liège, Belgium), Prof. X. Llimona (Herbarium of the University of Barcelona, España), Dr. Cl. Roux and Ms and Mr. O. Gonnet (Association Française de Lichénologie), Dr. H.J.M. Sipman (Botanischer Garten und Botanisches Museum Berlin), Mr. P. van den Boom (Son, The Netherlands) and Prof. Volkmar Wirth (Staatl. Museums für Naturkunde Karlsruhe). We thank the staff members of the Belgian Embassy in Mexico and the Mexican Embassy in Brussels for their help in getting the relevant permits to collect in Mexico. We also thank very much Dr. F. Chase for help and advice for the collection permit in the Skeleton Coast Park in Namibia. We warmly thank the Directors and staff members of the following herbaria for their help and loan of relevant material: B, BCN, BM, P, W and WIND. We would like to acknowledge Mr. L. Gohy for technical assistance with DNA extractions and amplifications at the University of Liège. Mr. Antoine Simon is a PhD student at the University of Liège and acknowledges the financial support by FRIA, a grant of the Belgian Research Foundation (F.R.S.-FNRS). Finally, we thank the referees for their critical and helpful notes and suggestions.

Sampling the targeted lichens in Mexico/Baja California was conducted under permit PPFE/DGOPA-006/15 issued by the Secretaría de Agricultura, Ganadería, Desarrollo rural, Pesca y Alimentación, Permiso de Pesca de Fomento a extranejeros on

08.12.2015. Sampling the targeted lichens in the coastal Namib desert, especially in the Skeleton Coast Park was conducted under research/collecting permit 2109/2015 issued by The Ministry of Environment and Tourism of Namibia on 06.01.2016. We thank both official bodies for their interest in our research.

## References

- Addison JA, Barron J, Finney B, Kusler J, Bukry D, Heusser LE, Alexander CR (2018) A Holocene record of ocean productivity and upwelling from the northern California continental slope. *Quaternary International* 469: 96–108. <https://doi.org/10.1016/j.quaint.2017.02.021>
- Agnan Y, Probst A, Séjalon-Delmas N (2016) Evaluation of lichen species resistance to atmospheric metal pollution by coupling diversity and bioaccumulation approaches: A new bioindication scale for French forested areas. *Ecological Indicators* 72: 99–110. <https://doi.org/10.1016/j.ecolind.2016.08.006>
- Altermann S, Leavitt SD, Goward T, Nelsen MP, Lumbsch HT (2014) How do you solve a problem like *Letharia*? A new look at cryptic species in lichen-forming fungi using Bayesian clustering and SNPs from multilocus sequence data. *PLoS One*, 9(5): e97556. <https://doi.org/10.1371/journal.pone.0097556>
- Altschul SF, Gish W, Miller W, Myers EW, Lipman DJ (1990) Basic local alignment search tool. *Journal of Molecular Biology* 215(3): 403–410. [https://doi.org/10.1016/S0022-2836\(05\)80360-2](https://doi.org/10.1016/S0022-2836(05)80360-2)
- Anar M, Asian A, Ceker S, Kizil HE, Alpsyoy L, Agar G (2015) Determination of antigenotoxic effects of four lichen species by using human lymphocytes. *Fresenius Environmental Bulletin* 24(12): 4251–4256.
- Anderson JB, Warny S, Askin RA, Wellner JS, Bohaty SM, Kirshner AE, Livsey DN, Simms AR, Smith TR, Ehrmann W, Lawver LA, Barbeau D, Wise SW, Kulhanek DK, Weaver FM, Majewski W (2011) Progressive Cenozoic cooling and the demise of Antarctica's last refugium. *Proceedings of the National Academy of Sciences*, 108(28): 11356–11360. <https://doi.org/10.1073/pnas.1014885108>
- Aptroot A, Bungartz F (2007) The lichen genus *Ramalina* on the Galapagos. *The Lichenologist* 39(6): 519–542. <https://doi.org/10.1017/S0024282907006901>
- Aptroot A, Schumm F (2008) Key to *Ramalina* species known from Atlantic islands, with two new species from the Azores. *Sauteria* 15: 21–57.
- Arroyo R, Serriá E (1995) *Ramalina elegans* (Lichenes, Ramalinaceae) a taxon which has been mistaken for *Ramalina calicaris* and *R. fastigiata* in the Iberian Peninsula. *Cryptogamic Botany* 5(1): 22–27.
- Beimforde C, Feldberg K, Nylinder S, Rikkinen J, Tuovila H, Dörfelt H, Gube M, Jackson DJ, Reitner J, Seyfullah LJ, Schmidt AR (2014) Estimating the Phanerozoic history of the Ascomycota lineages: combining fossil and molecular data. *Molecular Phylogenetics and Evolution* 78: 386–398. <https://doi.org/10.1016/j.ympev.2014.04.024>
- Biosca EG, Flores R, Santander RD, Díez-Gil JL, Barreno E (2016) Innovative approaches using lichen enriched media to improve isolation and culturability of lichen associated bacteria. *PLoS ONE* 11(8): e0160328. <https://doi.org/10.1371/journal.pone.0160328>

- Bohoyo F, Larter RD, Galindo-Zaldívar J, Leat PT, Maldonado A, Tate AJ, Flexas MM, Gowlanland EJM, Arndt JE, Dorschel B, Kim YD, Hong JK, López-Martínez J, Maestro A, Bermúdez O, Nitsche FO, Livermore RA, Riley TR (2019) Morphological and geological features of Drake Passage, Antarctica, from a new digital bathymetric model. *Journal of Maps* 15(2): 49–59. <https://doi.org/10.1080/17445647.2018.1543618>
- Boluda CG, Rico VJ, Divakar PK, Nadyeina O, Myllys L, McMullin RT, Zamora JC, Scheidegger C, Hawksworth DL (2019) Evaluating methodologies for species delimitation: the mismatch between phenotypes and genotypes in lichenized fungi (*Bryoria* sect. *Implexae*, Parmeliaceae). *Persoonia*: 42: 75–100. <https://doi.org/10.3767/persoonia.2019.42.04>
- Born J, Linder HP, Desmet P (2007) The Greater Cape Floristic Region. *Journal of Biogeography* 34: 147–162. <https://doi.org/10.1111/j.1365-2699.2006.01595.x>
- Bouckaert R, Heled J, Kühnert D, Vaughan T, Wu CH, Xie D, Suchard MA, Rambaut A, Drummond AJ (2014) BEAST 2: a software platform for Bayesian evolutionary analysis. *PLoS Computational Biology*, 10(4). <https://doi.org/10.1371/journal.pcbi.1003537>
- Bowler PA (1981) Cortical diversity in the Ramalinaceae. *Canadian Journal of Botany* 59(4): 437–452. <https://doi.org/10.1139/b81-062>
- Bowler PA, Marsh JE (2004) *Niebla*. In: Nash III TH, Ryan B, Diederich P, Gries C, Bungartz F (Eds), *Lichen Flora of the Greater Sonoran Desert Region*. Lichens Unlimited, vol. 2. Arizona State University, Tempe, Arizona, 368–380.
- Bowler PA, Rundel PW (1977) Synopsis of a new lichen genus, *Fistulariella* Bowler & Rundel (Ramalinaceae). *Mycotaxon* 6: 195–202.
- Buerki S, Manning JC, Forest F (2013) Spatio-temporal history of the disjunct family Tephthilaaceae: a tale involving the colonization of three Mediterranean-type ecosystems. *Annals of Botany* 111(3): 361–373. <https://doi.org/10.1093/aob/mcs286>
- Buschbom J, Mueller GM (2005) Testing “species pair” hypotheses: evolutionary processes in the lichen-forming species complex *Porpidia flavocoerulescens* and *Porpidia melinodes*. *Molecular Biology and Evolution* 23(3): 574–586. <https://doi.org/10.1093/molbev/msj063>
- Bustamante DE, Oliva M, Leiva S, Mendoza JE, Bobadilla L, Angulo G, Calderon MS (2019) Phylogeny and species delimitations in the entomopathogenic genus *Beauveria* (Hypocreales, Ascomycota), including the description of *B. peruviansis* sp. nov. *MycoKeys*, 58: 47–68. <https://doi.org/10.3897/mycokeys.58.35764>
- Candan M, Tay F, Avan I, Tay T (2017) Removal of copper (II) and nickel (II) ions from aqueous solution using non-living lichen *Ramalina fraxinea* biomass: Investigation of kinetics and sorption isotherms. *Desalination and Water Treatment* 75: 148–157. <https://doi.org/10.5004/dwt.2017.20749>
- Cartapanis O, Tachikawa K, Bard E (2011) Northeastern Pacific oxygen minimum zone variability over the past 70 kyr: Impact of biological production and oceanic ventilation. *Paleoceanography* 26(4) PA4208. <https://doi.org/10.1029/2011PA002126>
- Casano LM, Braga MR, Álvarez R, del Campo EM, Barreno E (2015) Differences in the cell walls and extracellular polymers of the two *Trebouxia* microalgae coexisting in the lichen *Ramalina farinacea* are consistent with their distinct capacity to immobilize extracellular Pb. *Plant Science* 236: 195–204. <https://doi.org/10.1016/j.plantsci.2015.04.003>
- Catalá S, del Campo EM, Barreno E, García-Breijo FJ, Reig-Armiñana J, Casano LM (2016) Coordinated ultrastructural and phylogenomic analyses shed light on the hidden phycobi-

- ont diversity of *Trebouxia* microalgae in *Ramalina fraxinea*. *Molecular Phylogenetics and Evolution* 94: 765–777. <https://doi.org/10.1016/j.ympev.2015.10.021>
- Cerling TE, Harris JM, MacFadden BJ, Leakey MG, Quade J, Eisenmann V, Ehleringer JR (1997) Global vegetation change through the Miocene/Pliocene boundary. *Nature* 389(6647): 153–158. <https://doi.org/10.1038/38229>
- Clauzade G, Roux C (1985) Likenoj de Okcidenta Europo. *Ilustrita Determinlibro*. Bulletin de la Société Botanique du Centre-Ouest, Nouvelle Série, Numero Special 7. Royan, 893 pp.
- Cubero OF, Crespo A, Fatehi J, Bridge PD (1999) DNA Extraction and PCR amplification method suitable for fresh, herbarium-stored, lichenized, and other Fungi. *Plant Systematics and Evolution* 216: 243–249. <https://doi.org/10.1007/BF01084401>
- Culberson WL (1986) Chemistry and sibling speciation in the lichen-forming fungi: ecological and biological considerations. *The Bryologist* 89(2): 123–131. <https://doi.org/10.2307/3242752>
- Culberson CF, Culberson WL, Johnson A (1981) A standardized TLC analysis of  $\beta$ -orcinol depsidones. *The Bryologist* 84(1): 16–29. <https://doi.org/10.2307/3242974>
- Dal Forno M, Bungartz F, Yáñez-Ayabaca A, Lücking R, Lawrey JD (2017) High levels of endemism among Galapagos basidiolichens. *Fungal Diversity* 85(1): 45–73. <https://doi.org/10.1007/s13225-017-0380-6>
- Darriba D, Taboada GL, Doallo R, Posada D (2012) jModelTest 2: more models, new heuristics and parallel computing. *Nature Methods* 9(8): 772. <https://doi.org/10.1038/nmeth.2109>
- De Paz GA, Cubas P, Crespo A, Elix JA, Lumbsch HT (2012) Transoceanic dispersal and subsequent diversification on separate continents shaped diversity of the *Xanthoparmelia pulla* group (Ascomycota). *PLoS One* 7(6): e39683. <https://doi.org/10.1371/journal.pone.0039683>
- Devkota S, Chaudhary RP, Werth S, Scheidegger C (2017) Indigenous knowledge and use of lichens by the lichenophilic communities of the Nepal Himalaya. *Journal of Ethnobiology and Ethnomedicine* 13: 15. <https://doi.org/10.1186/s13002-017-0142-2>
- Diederich P, Lücking R, Aptroot A, Sipman HJM, Braun U, Ahti T, Ertz D (2017) New species and new records of lichens and lichenicolous fungi from the Seychelles. *Herzogia* 30(1): 182–236. <https://doi.org/10.13158/heia.30.1.2017.182>
- Domínguez-Moruco N, Augusto S, Trabalón L, Pocurull E, Borrull F, Schuhmacher M, Domingo JL, Nadal M (2015) Monitoring PAHs in the petrochemical area of Tarragona County, Spain: comparing passive air samplers with lichen transplants. *Environmental Science and Pollution Research* 24(13): 11890–11900. <https://doi.org/10.1007/s11356-015-5612-2>
- Drummond AJ, Ho SY, Phillips MJ, Rambaut A (2006) Relaxed phylogenetics and dating with confidence. *PLoS Biology* 4(5): e88. <https://doi.org/10.1371/journal.pbio.0040088>
- Drummond AJ, Rambaut A (2007) BEAST: Bayesian evolutionary analysis by sampling trees. *BMC Evolutionary Biology* 7(1): 214. <https://doi.org/10.1186/1471-2148-7-214>
- Drummond AJ, Suchard MA, Xie D, Rambaut A (2012) Bayesian phylogenetics with BEAUti and the BEAST 1.7. *Molecular Biology and Evolution* 29(8): 1969–1973. <https://doi.org/10.1093/molbev/mss075>
- Dunai TJ, González López GA, Juez-Larré J (2005) Oligocene/Miocene age of aridity in the Atacama Desert revealed by exposure dating of erosion sensitive landforms. *Geology* 33: 321–324. <https://doi.org/10.1130/G21184.1>
- Edwards SV, Xi Z, Janke A, Faircloth BC, McCormack JE, Glenn TC, Zhong B, Wu S, Lemmon EM, Lemmon AR, Leaché AD, Liu L, Davis CC (2016) Implementing and test-

- ing the multispecies coalescent model: a valuable paradigm for phylogenomics. *Molecular Phylogenetics and Evolution* 94: 447–462. <https://doi.org/10.1016/j.ympev.2015.10.027>
- Egea JM, Llimona X (1994) La flore et la végétation lichéniques des laves acides du parc naturel de la Sierra del Cabo de Gata (SE de l'Espagne) et des régions voisines. *Bulletin de la Société Linnéenne de Provence* 45: 263–281.
- Ekman S (1997) The genus *Cliostomum* revisited. *Symbolae Botanicae Upsalienses* 32(1): 17–28.
- Ekman S (2001) Molecular phylogeny of the Bacidiaceae (Lecanorales, lichenized Ascomycota). *Mycological Research* 105: 783–797. <https://doi.org/10.1017/S0953756201004269>
- Elix JA, McCarthy PM (1998) Checklist of Pacific Island lichens. *Bibliotheca Lichenologica* 70: 1–361.
- Ertz D, Tehler A (2011) The phylogeny of Arthoniales (Pezizomycotina) inferred from nuLSU and RPB2 sequences. *Fungal Diversity* 49(1): 47–71. <https://doi.org/10.1007/s13225-010-0080-y>
- Ezcurra MD, Agnolín FL (2011) A new global palaeobiogeographical model for the late Mesozoic and early Tertiary. *Systematic Biology* 61(4): 553–566. <https://doi.org/10.1093/sysbio/syr115>
- Felsenstein J (1985) Confidence limits on phylogenies: an approach using the bootstrap. *Evolution* 39(4): 783–791. <https://doi.org/10.1111/j.1558-5646.1985.tb00420.x>
- Follmann G (2006) Two new roccelloid Physciaceae from Pacific South America and a synopsis of the genus *Santessonia*. *The Journal of the Hattori Botanical Laboratory* 100: 651–670.
- Furmanek Ł, Czarnota P, Seaward MRD (2019) Antifungal activity of lichen compounds against dermatophytes: A review. *Journal of Applied Microbiology* 127(2): 308–325. <https://doi.org/10.1111/jam.14209>
- Galloway DJ (2007) *Flora of New Zealand: Lichens, including lichen-forming and lichenicolous fungi*, Vol 1 and 2 (No. Ed. 2). Manaaki Whenua Press, Landcare Research, 2261 pp.
- Gardes M, Bruns TD (1993) ITS primers with enhanced specificity for basidiomycetes, application to the identification of mycorrhizae and rusts. *Molecular Ecology* 2: 113–118. <https://doi.org/10.1111/j.1365-294X.1993.tb00005.x>
- Gasparyan A, Sipman HJM (2016) The epiphytic lichenized fungi in Armenia: Diversity and conservation. *Phytotaxa* 281(1): 1–68. <https://doi.org/10.11646/phytotaxa.281.1.1>
- Gasparyan A, Sipman HJM, Lücking R (2017) *Ramalina europaea* and *R. labiosorediata*, two new species of the *R. pollinaria* group (Ascomycota: Ramalinaceae), and new typifications for *Lichen pollinarius* and *L. squarrosus*. *The Lichenologist* 49(4): 301–319. <https://doi.org/10.1017/S0024282917000226>
- Gerlach ADCL, Toprak Z, Naciri Y, Caviro EA, da Silveira RMB, Clerc P (2019) New insights into the *Usnea cornuta* aggregate (Parmeliaceae, lichenized Ascomycota): Molecular analysis reveals high genetic diversity correlated with chemistry. *Molecular Phylogenetics and Evolution* 131: 125–137. <https://doi.org/10.1016/j.ympev.2018.10.035>
- Gernhard T (2008) The conditioned reconstructed process. *Journal of Theoretical Biology* 253(4): 769–778. <https://doi.org/10.1016/j.jtbi.2008.04.005>
- Gonnet D, Gonnet O, Gardiennet A, Roux C (2017) Les lichens et champignons lichénicoles de l'île de Cavallo (archipel des Lavezzi, Corse). *Ecologia Mediterranea* 43: 171–175. <https://doi.org/10.3406/ecmed.2017.2022>
- Grewe F, Lagostina E, Wu H, Printzen C, Lumbsch HT (2018) Population genomic analyses of RAD sequences resolves the phylogenetic relationship of the lichen-forming fun-

- gal species *Usnea antarctica* and *Usnea aurantiacoatra*. MycoKeys 43: 91–113. <https://doi.org/10.3897/mycokeys.43.29093>
- Groner U, LaGreca S (1997) The ‘Mediterranean’ *Ramalina panizzei* north of the Alps: morphological, chemical and rDNA sequence data. The Lichenologist 29(5): 441–454. <https://doi.org/10.1006/lich.1997.0098>
- Guéra A, Gasulla F, Barreno E (2016) Formation of photosystem II reaction centers that work as energy sinks in lichen symbiotic Trebouxiophyceae microalgae. Photosynthesis Research 128(1): 15–33. <https://doi.org/10.1007/s11120-015-0196-8>
- Gumboski E, Eliasaro S, Scur M, Lorenz-Lemke A, Borges da Silveira R (2018) A new riparian species of *Ramalina* (Ramalinaceae) from Brazil, with a key to neotropical saxicolous species. The Lichenologist 50(5): 541–553. <https://doi.org/10.1017/S0024282918000361>
- Gunn M, Codd LEW (1981) Botanical Exploration Southern Africa. CRC Press, 400 pp.
- Gutiérrez NM, Hinojosa LF, Le Roux JP, Pedroza V (2013) Evidence for an Early-Middle Miocene age of the Navidad Formation (central Chile): Paleontological, paleoclimatic and tectonic implications. Andean Geology 40(1): 66–78. <https://doi.org/10.5027/andgeoV40n1-a03>
- Heinrich S, Zonneveld KAF, Bickert T, Willems H (2011) The Benguela upwelling related to the Miocene cooling events and the development of the Antarctic circumpolar current: evidence from calcareous dinoflagellate cysts. Paleoceanography and Paleoclimatology 26(3): PA3209. <https://doi.org/10.1029/2010PA002065>
- Herbert TD, Lawrence KT, Tzanova A, Peterson LC, Caballero-Gill R, Kelly CS (2016) Late Miocene global cooling and the rise of modern ecosystems. Nature Geoscience 9(11): 843–847. <https://doi.org/10.1038/ngeo2813>
- Herbert TD, Schuffert JD, Andreasen D, Heusser L, Lyle M, Mix A, Ravelo AC, Stott LD, Herguera JC (2001) Collapse of the California Current during glacial maxima linked to climate change on land. Science 293(5527): 71–76. <https://doi.org/10.1126/science.1059209>
- Heusser L (1998) Direct correlation of millennial-scale changes in western North American vegetation and climate with changes in the California Current system over the past ~60 kyr. Paleoceanography and Paleoclimatology 13(3): 252–262. <https://doi.org/10.1029/98PA00670>
- Hofstetter V, Miadlikowska J, Kauff F, Lutzoni F (2007) Phylogenetic comparison of protein-coding versus ribosomal RNA-coding sequence data: a case study of the Lecanoromycetes (Ascomycota). Molecular Phylogenetics and Evolution 44(1): 412–426. <https://doi.org/10.1016/j.ympev.2006.10.016>
- Huang JP, Kraichak E, Leavitt SD, Nelsen MP, Lumbsch HT (2019) Accelerated diversifications in three diverse families of morphologically complex lichen-forming fungi link to major historical events. Scientific Reports 9(1): 8518. <https://doi.org/10.1038/s41598-019-44881-1>
- Johannesson HS, Johannesson KHP, Stenlid J (2000) Development of primer sets to amplify fragments of conserved genes for use in population studies of the fungus *Daldinia loculata*. Molecular Ecology 9(3): 375–377. <https://doi.org/10.1046/j.1365-294x.2000.00874-6.x>
- Jones GR (2015) Species delimitation and phylogeny estimation under the multispecies coalescent. BioRxiv, 010199. <https://doi.org/10.1101/010199>
- Jung G, Prange M, Schulz M (2014) Uplift of Africa as a potential cause for Neogene intensification of the Benguela upwelling system. Nature Geoscience 7: 741–747. <https://doi.org/10.1038/ngeo2249>

- Katoh K, Asimenos G, Toh H (2009) Multiple alignment of DNA sequences with MAFFT. *Methods in Molecular Biology* 537: 39–64. [https://doi.org/10.1007/978-1-59745-251-9\\_3](https://doi.org/10.1007/978-1-59745-251-9_3)
- Katoh K, Misawa K, Kuma K, Miyata T (2002) MAFFT: a novel method for rapid multiple sequence alignment based on fast Fourier transform. *Nucleic Acids Research* 30: 3059–3066. <https://doi.org/10.1093/nar/gkf436>
- Kauff F, Lutzoni F (2002) Phylogeny of the Gyalectales and Ostropales (Ascomycota, Fungi): among and within order relationships based on nuclear ribosomal RNA small and large subunits. *Molecular Phylogenetics and Evolution* 25: 138–156. [https://doi.org/10.1016/S1055-7903\(02\)00214-2](https://doi.org/10.1016/S1055-7903(02)00214-2)
- Keuler RA, Garretson A, Saunders T, Erickson R, Andre NS, Grewe F, Smith H, Lumbsch H, Clair LLS, Leavitt S (2020) Genome-scale data reveal the potential role of hybrid speciation in lichen-forming fungi. *Scientific Reports* 10(1): 1–14. <https://doi.org/10.1038/s41598-020-58279-x>
- Kim M-K, Kim MA, Yim JH, Lee D-H, Cho SK, Yang SG (2018) Ramalin, an antioxidant compound derived from Antarctic lichen, prevents progression of liver fibrosis induced by dimethylnitrosamine (DNM) in rats. *Biochemical and Biophysical Research Communications* 504(1): 25–33. <https://doi.org/10.1016/j.bbrc.2018.08.103>
- Kistenich S, Timdal E, Bendiksby M, Ekman S, 2018. Molecular systematics and character evolution in the lichen family Ramalinaceae (Ascomycota: Lecanorales). *Taxon* 67: 891–904. <https://doi.org/10.12705/675.1>
- Knudsen K, Lendemer JC, Kocourková J (2018) *Ramalina sarabae* (Ramalinaceae), a new species from the Channel Islands of California, USA. *The Bryologist* 121(4): 513–520. <https://doi.org/10.1639/0007-2745-121.4.513>
- Koračin D, Dorman CE, Lewis JM, Hudson JG, Wilcox EM, Torregrosa A (2014) Marine fog: A review. *Atmospheric Research* 143: 142–175. <https://doi.org/10.1016/j.atmosres.2013.12.012>
- Krog H (1994) Typification and interpretation of *Ramalina arabum*. *Acta Botanica Fennica* 150: 99–104.
- Krog H, James PW (1977) The genus *Ramalina* in Fennoscandia and the British Isles. *Norwegian Journal of Botany* 24: 15–43.
- Krog H, Østhagen H (1980) The genus *Ramalina* in the Canary Islands. *Norwegian Journal of Botany* 27: 255–296.
- Lalley JS, Viles HA (2005) Terricolous lichens in the northern Namib Desert of Namibia: distribution and community composition. *The Lichenologist* 37(1): 77–91. <https://doi.org/10.1017/S0024282904014203>
- Leavitt SD, Esslinger TL, Divakar PK, Lumbsch HT (2012) Miocene divergence, phenotypically cryptic lineages, and contrasting distribution patterns in common lichen-forming fungi (Ascomycota: Parmeliaceae). *Biological Journal of the Linnean Society* 107(4): 920–937. <https://doi.org/10.1111/j.1095-8312.2012.01978.x>
- Lee E, Lee CG, Yim JH, Lee HK, Pyo S (2016) [2015] Ramalin-Mediated Apoptosis Is Enhanced by Autophagy Inhibition in Human Breast Cancer Cells. *Phytotherapy Research* 30(2): 426–438. <https://doi.org/10.1002/ptr.5544>
- Lemoine F, Entfellner JBD, Wilkinson E, Correia D, Felipe MD, Oliveira T, Gascuel O (2018) Renewing Felsenstein's phylogenetic bootstrap in the era of big data. *Nature* 556(7702): 452–456. <https://doi.org/10.1038/s41586-018-0043-0>

- Le Roux JP (2012a) A review of Tertiary climate changes in southern South America and the Antarctic Peninsula. Part 1: Oceanic conditions. *Sedimentary Geology* 247: 1–20. <https://doi.org/10.1016/j.sedgeo.2011.12.014>
- Le Roux JP (2012b) A review of Tertiary climate changes in southern South America and the Antarctic Peninsula. Part 2: continental conditions. *Sedimentary Geology* 247: 21–38. <https://doi.org/10.1016/j.sedgeo.2011.12.001>
- Liu YJ, Whelen S, Hall BD (1999) Phylogenetic relationships among ascomycetes: evidence from an RNA polymerase II subunit. *Molecular Biology and Evolution* 16(12): 1799–1808. <https://doi.org/10.1093/oxfordjournals.molbev.a026092>
- Llimona X, Werner RG (1975) Quelques lichens nouveaux ou intéressants de la Sierra de Gata (Almería, SE de l'Espagne). *Acta Phytotaxonomica Barcinonensia* 16: 1–32.
- López Berdonces MA, Higuera PL, Fernández-Pascual M, Borreguero AM, Carmona M (2016) The role of native lichens in the biomonitoring of gaseous mercury at contaminated sites. *Journal of Environmental Management* 186: 207–213. <https://doi.org/10.1016/j.jenvman.2016.04.047>
- Lücking R, Dal-Forno M, Sikaroodi M, Gillevet PM, Bungartz F, Moncada B, Yáñez-Ayabaca A, Chaves JL, Coca LF, Lawrey JD (2014) A single macrolichen constitutes hundreds of unrecognized species. *Proceedings of the National Academy of Sciences* 111: 11091–11096. <https://doi.org/10.1073/pnas.1403517111>
- Lücking R, Hodkinson BP, Leavitt SD (2017a) The 2016 classification of lichenized fungi in the Ascomycota and Basidiomycota – Approaching one thousand genera. *The Bryologist* 119(4): 361–417. <https://doi.org/10.1639/0007-2745-119.4.361>
- Lücking R, Moncada B, Smith CW (2017b) The genus *Lobariella* (Ascomycota: Lobariaceae) in Hawaii: late colonization, high inferred endemism and three new species resulting from “micro-radiation”. *The Lichenologist* 49(6): 673–691. <https://doi.org/10.1017/S0024282917000470>
- Lücking R, Tehler A, Bungartz F, Rivas Plata E, Lumbsch HT (2013) Journey from the West: Did tropical Graphidaceae (lichenized Ascomycota: Ostropales) evolve from a saxicolous ancestor along the American Pacific coast? *American Journal of Botany* 100(5): 844–856. <https://doi.org/10.3732/ajb.1200548>
- Luo A, Ling C, Ho SY, Zhu CD (2018) Comparison of methods for molecular species delimitation across a range of speciation scenarios. *Systematic Biology* 67(5): 830–846. <https://doi.org/10.1093/sysbio/syy011>
- Lutsak T, Fernández-Mendoza F, Kirika P, Wondrafrash M, Printzen C (2020) Coalescence-based species delimitation using genome-wide data reveals hidden diversity in a cosmopolitan group of lichens. *Organisms Diversity & Evolution* 20: 189–218. <https://doi.org/10.1007/s13127-019-00424-0>
- Magain N, Miadlikowska J, Mueller O, Gajdeczka M, Truong C, Salamov A, Dubchak I, Grigoriev IV, Goffinet B, Sérusiaux E, Lutzoni F (2017) Conserved genomic collinearity as a source of broadly applicable, fast evolving, markers to resolve species complexes: A case study using the lichen-forming genus *Peltigera* section *Polydactylon*. 25<sup>th</sup> anniversary issue of *Molecular Phylogenetics and Evolution* 117: 10–29. <https://doi.org/10.1016/j.ympev.2017.08.013>
- Mark K, Randlane T, Thor G, Hur JS, Obermayer W, Saag A (2019) Lichen chemistry is concordant with multilocus gene genealogy in the genus *Cetrelia* (Parmeliaceae, Ascomycota). *Fungal Biology* 123(2): 125–139. <https://doi.org/10.1016/j.funbio.2018.11.013>

- Marthinsen G, Rui S, Timdal E (2019) OLICh: A reference library of DNA barcodes for Nordic lichens. *Biodiversity Data Journal*, 7: e36252. <https://doi.org/10.3897/BDJ.7.e36252>
- McMullin RT (2015) The Lichens of Prince Edward Island, Canada: A Second Checklist, with Species Ranked for Conservation Status. *Rhodora* 117: 454–484. <https://doi.org/10.3119/15-12>
- Miadlikowska J, Kauff F, Högnabba F, Oliver JC, Molnár K, Fraker E, Gaya E, Hafellner J, Hofstetter V, Gueidan C, Otálora MAG, Hodkinson B, Kukwa M, Lücking R, Björk C, Sipman HJM, Burgaz AR, Thell A, Passo A, Myllys L, Goward T, Fernández-Brime S, Hestmark G, Lendemer J, Lumbsch HT, Schmull M, Schoch CL, Sérusiaux E, Maddison DR, Arnold AE, Lutzoni F, Stenroos S (2014) A multigene phylogenetic synthesis for the class Lecanoromycetes (Ascomycota): 1307 fungi representing 1139 infrageneric taxa, 317 genera and 66 families. *Molecular Phylogenetics and Evolution* 79: 132–168. <https://doi.org/10.1016/j.ympev.2014.04.003>
- Miller MA, Pfeiffer W, Schwartz T (2010) Creating the CIPRES Science Gateway for inference of large phylogenetic trees. In: *Proceedings of the Gateway Computing Environments Workshop (GCE)*, 14 Nov 2010, New Orleans, LA, 1–8. <https://doi.org/10.1109/GCE.2010.5676129>
- Miranda-González R, Lücking R, Barcenás-Peña A, Herrera-Campos M (2020) The new genus *Jocatoa* (Lecanoromycetes: Graphidaceae) and new insights into subfamily Redonographoideae. *The Bryologist* 123(2): 127–143. <https://doi.org/10.1639/0007-2745-123.2.127>
- Montagne C (1842) Troisième centurie de plantes cellulaires exotiques nouvelles, Décades V–VIII. *Annales des Sciences Naturelles* 18: 241–282.
- Moya P, Molins A, Martínez-Alberola F, Muggia L, Barreno E (2017) Unexpected associated microalgal diversity in the lichen *Ramalina farinacea* is uncovered by pyrosequencing analyses. *PLoS ONE* 12(4): e0175091. <https://doi.org/10.1371/journal.pone.0175091>
- Mudelsee M, Bickert T, Lear CH, Lohmann G (2014) Cenozoic climate changes: A review based on time series analysis of marine benthic  $\delta^{18}\text{O}$  records. *Reviews of Geophysics* 52(3): 333–374. <https://doi.org/10.1002/2013RG000440>
- Myllys L, Stenroos S, Thell A (2002) New genes for phylogenetic studies of lichenized fungi: glyceraldehyde-3-phosphate dehydrogenase and beta-tubulin genes. *The Lichenologist* 34(3): 237–246. <https://doi.org/10.1006/lich.2002.0390>
- Nash III TH, Ryan D, Diederich P, Gries C, Bungartz F (2004) Lichen flora of the greater Sonoran desert region. Vol. 2 Lichens Unlimited, Arizona State University, 742 pp.
- Nash III TH, Ryan D, Gries C, Bungartz F (2002) Lichen flora of the greater Sonoran desert region. Vol. 1 Lichens Unlimited, Arizona State University, 1–532.
- Oh SO, Wang XY, Wang LS, Liu PG, Hur JS (2014) A note on the lichen genus *Ramalina* (Ramalinaceae, Ascomycota) in the Hengduan Mountains in China. *Mycobiology* 42(3): 229–240. <https://doi.org/10.5941/MYCO.2014.42.3.229>
- Onuț-Brännström I, Tibell L, Johannesson H (2017) A worldwide phylogeography of the whiteworm lichens *Thamnomlia* reveals three lineages with distinct habitats and evolutionary histories. *Ecology and Evolution* 7(10): 3602–3615. <https://doi.org/10.1002/ece3.2917>
- Orange A, James PW, White FJ (2010) *Microchemical Methods for the Identification of Lichens*. British Lichen Society, 101 pp.
- Ortiz J, Mix A, Hostetler S, Kashgarian M (1997) The California current of the last glacial maximum: Reconstruction at 42 degrees N based on multiple proxies. *Paleoceanography* 12: 191–205. <https://doi.org/10.1029/96PA03165>

- Paukov A, Sipman HJM, Kukwa M, Repin R, Teptina A (2017) New lichen records from the mountains Kinabalu and Tambuyukon (Kinabalu Park, Malaysian Borneo). *Herzogia* 30(1): 237–252. <https://doi.org/10.13158/heia.30.1.2017.237>
- Peinado M, Delgadillo J, Aguirre JL (2005) Plant associations of El Vizcaíno biosphere reserve, Baja California Sur, Mexico. *The Southwestern Naturalist* 50(2): 129–150. [https://doi.org/10.1894/0038-4909\(2005\)050\[0129:PAOEVB\]2.0.CO;2](https://doi.org/10.1894/0038-4909(2005)050[0129:PAOEVB]2.0.CO;2)
- Pérez-Ortega S, Pérez-Vargas I, Blázquez M, Garrido-Benavent I, Aptroot A, Bungartz F, Blanchon D, Cáceres MES, Divakar PK, Ertz D, Fernández-Mendoza F, Flakus A, Gasparyan A, Gockman O, Kirika P, Knight A, Lagreca S, Leavitt S, de los Ríos A (2019) First genus-wide phylogeny of the genus *Ramalina* (lichenized Ascomycota) sheds light on the endemic diversity in Macaronesia. Island Biology III International Conference, La Réunion 8–13 July 2019, Abstract, 25–26.
- Prieto M, Wedin M (2013) Dating the diversification of the major lineages of Ascomycota (Fungi). *PloS One* 8(6): e65576. <https://doi.org/10.1371/journal.pone.0065576>
- Puillandre N, Lambert A, Brouillet S, Achaz G (2012) ABGD, Automatic Barcode Gap Discovery for primary species delimitation. *Molecular Ecology* 21(8): 1864–1877. <https://doi.org/10.1111/j.1365-294X.2011.05239.x>
- R Core Team (2015) A language and environment for statistical computing. R Foundation for Statistical Computing, Vienna, Austria.
- Rannala B, Yang Z (2003) Bayes estimation of species divergence times and ancestral population sizes using DNA sequences from multiple loci. *Genetics* 164(4): 1645–1656.
- Rambaut A, Drummond AJ, Xie D, Baele G, Suchard MA (2018) Posterior summarisation in Bayesian phylogenetics using Tracer 1.7. *Systematic Biology* 67(5): 901–904. <https://doi.org/10.1093/sysbio/syy032>
- Rehner SA, Samuels GJ (1994) Taxonomy and phylogeny of *Gliocladium* analysed from nuclear large subunit ribosomal DNA sequences. *Mycological Research* 98(6): 625–634. [https://doi.org/10.1016/S0953-7562\(09\)80409-7](https://doi.org/10.1016/S0953-7562(09)80409-7)
- Rikkinen J, Poinar Jr GO (2008) A new species of *Phyllopsora* (Lecanorales, lichen-forming Ascomycota) from Dominican amber, with remarks on the fossil history of lichens. *Journal of Experimental Botany* 59(5): 1007–1011. <https://doi.org/10.1093/jxb/ern004>
- Rivas Plata E (2011) Historical biogeography, ecology and systematics of the family Graphidaceae (Lichenized Ascomycota: Ostropales). PhD Thesis submitted at the Graduate College of the University of Illinois, Chicago, Illinois, 238 pp.
- Rivas Plata E, Parnmen S, Staiger B, Mangold A, Frisch A, Weerakoon G, Hernández JEM, Cáceres MES, Kalb K, Sipman HJM, Common RS, Nelsen MP, Lücking R, Lumbsch HT (2013) A molecular phylogeny of Graphidaceae (Ascomycota, Lecanoromycetes, Ostropales) including 428 species. *Mycology* 6: 55–94. <https://doi.org/10.3897/mycokeys.6.3482>
- Rommerskirchen F, Condon T, Mollenhauer G, Dupont L, Schefuß E (2011) Miocene to Pliocene development of surface and subsurface temperatures in the Benguela Current system. *Paleoceanography* 26: 1–15. <https://doi.org/10.1029/2010PA002074>
- Roux C et al. [89 co-authors] (2019) Catalogue des lichens et champignons lichénicoles de France métropolitaine. Association française de lichénologie (AFL)(Fontainebleau); Catalogue 3 (v. 15 du 2019/03/01). [accessed on-line]

- Rundel PW, Arroyo MT, Cowling RM, Keeley JE, Lamont BB, Vargas P (2016) Mediterranean biomes: Evolution of their vegetation, floras, and climate. *Annual Review of Ecology, Evolution, and Systematics* 47: 383–407. <https://doi.org/10.1146/annurev-ecolsys-121415-032330>
- Rundel PW, Bowler PA (1974) The lichen genus *Trichoramalina*. *The Bryologist* 77: 188–194. <https://doi.org/10.2307/3241555>
- Rundel PW, Bowler PA (1978) *Niebla*, a new generic name for the lichen genus *Desmazieria* (Ramalinaceae). *Mycotaxon* 6: 497–499.
- Rundel PW, Dillon MO, Palma B, Mooney HA, Gulmon SL, Ehleringer JR (1991) The phytogeography and ecology of the coastal Atacama and Peruvian deserts. *Aliso* 13(1): 1–49. <https://doi.org/10.5642/aliso.19911301.02>
- Samarakoon MC, Hyde KD, Promputtha I, Ariyawansa HA, Hongsanant S (2016) Divergence and ranking of taxa across the kingdoms Animalia, Fungi and Plantae. *Mycosphere* 7(11): 1678–1689. <https://doi.org/10.5943/mycosphere/7/11/5>
- Sanders WB, de los Ríos A (2019) Cell wall dynamics under conditions of diffuse growth in the thick-walled cortical tissue (prosoplectenchyma) of *Ramalina usnea*. *The Lichenologist* 51(3): 269–280. <https://doi.org/10.1017/S0024282919000082>
- Sanders WB, Tokamov SA (2015) Diffuse growth in the fruticose beard lichen *Ramalina usnea* (L.) R. Howe. *Lichenologist* 47(1): 51–58. <https://doi.org/10.1017/S0024282914000504>
- Schoch CL, Seifert KA, Huhndorf S, Robert V, Spouge JL, Levesque CA, Fungal Barcoding Consortium (2012) Nuclear ribosomal internal transcribed spacer (ITS) region as a universal DNA barcode marker for Fungi. *Proceedings of the National Academy of Sciences of the United States of America* 109: 6241–6246. <https://doi.org/10.1073/pnas.1117018109>
- Schwarz G (1978) Estimating the dimension of a model. *The Annals of Statistics* 6(2): 461–464. <https://doi.org/10.1214/aos/1176344136>
- Sérusiaux E, van den Boom PPG, Brand MA, Coppins BJ, Magain N (2012) *Lecania falcata*, a new species from Spain, the Canary Islands and the Azores, close to *Lecania chlorotiza*. *The Lichenologist* 44(5): 577–590. <https://doi.org/10.1017/S0024282912000308>
- Sérusiaux E, van den Boom PPG, Ertz D (2010) A two-gene phylogeny shows the lichen genus *Niebla* (Lecanorales) is endemic to the New World and does not occur in Macaronesia nor in the Mediterranean basin. *Fungal Biology* 114: 528–537. <https://doi.org/10.1016/j.funbio.2010.04.002>
- Sérusiaux E, Villarreal AJC, Wheeler T, Goffinet B (2011) Recent origin, active speciation and dispersal for the lichen genus *Nephroma* (Peltigerales) in Macaronesia. *Journal of Biogeography* 38(6): 1138–1151. <https://doi.org/10.1111/j.1365-2699.2010.02469.x>
- Sérusiaux E, Wessels D (1984) *Santessonia* (Lecanorales, Buelliaceae) in the Namib Desert (South West Africa). *Mycotaxon* 19: 479–502.
- Seton M, Müller RD, Zahirovic S, Gaina C, Torsvik T, Shephard G, Talsma A, Gurnis M, Turner M, Maus S, Chandler M (2012) Global continental and ocean basin reconstructions since 200 Ma. *Earth-Science Reviews* 113(3–4): 212–270. <https://doi.org/10.1016/j.earscirev.2012.03.002>
- Simon A, Goffinet B, Magain N, Sérusiaux E (2018) High diversity, high insular endemism and recent origin in the lichen genus *Sticta* (lichenized Ascomycota, Peltigerales) in Madagascar and the Mascarenes. *Molecular Phylogenetics and Evolution* 122: 15–28. <https://doi.org/10.1016/j.ympev.2018.01.012>

- Sipman HJM (2011) New and notable species of *Enterographa*, *Niebla* and *Sclerophyton* s. lat. from coastal Chile. *Bibliotheca Lichenologica* 106: 297–308.
- Snyder MA, Sloan LC, Diffenbaugh NS, Bell JL (2003) Future climate change and upwelling in the California Current. *Geophysical Research Letters* 30(15): 1823. <https://doi.org/10.1029/2003GL017647>
- Sork VL, Werth S (2014) Phylogeography of *Ramalina menziesii*, a widely distributed lichen-forming fungus in western North America. *Molecular Ecology* 23(9): 2326–2339. <https://doi.org/10.1111/mec.12735>
- Sparrius LB, Aptroot A, Sipman HJM, Pérez-Vargas I, Matos P, Gerlach A, Vervoort M (2017) Estimating the population size of the endemic lichens *Anzia centrifuga* (Parmeliaceae) and *Ramalina* species (Ramalinaceae) on Porto Santo (Madeira archipelago). *The Bryologist* 120(3): 293–301. <https://doi.org/10.1639/0007-2745-120.3.293>
- Spjut RW (1995a) *Vermilacinia* (Ramalinaceae, Lecanorales), a new genus of lichens. In: Daniëls, FJA, Schulz M, Peine J, (Eds): *Flechten Follmann. Contributions to lichenology in Honour of Gerhard Follmann*. Geobotanical and Phytotaxonomical Study Group, Botanical Institute, University of Cologne, Cologne, 337–351.
- Spjut RW (1995b) Occurrence of *Mobergia calculiformis* (Physciaceae, Lecanorales) in peninsular Baja California. In: Daniëls, FJA, Schulz M, Peine J, (Eds): *Flechten Follmann. Contributions to lichenology in Honour of Gerhard Follmann*. Geobotanical and Phytotaxonomical Study Group, Botanical Institute, University of Cologne, Cologne, 475–482.
- Spjut RW (1996) *Niebla* and *Vermilacinia* (Ramalinaceae) from California and Baja California. *Sida, Botanical Miscellany* 14: 1–208.
- Stamatakis A (2006) RAxML-VI-HPC: maximum likelihood-based phylogenetic analyses with thousands of taxa and mixed models. *Bioinformatics* 22: 2688–2690. <https://doi.org/10.1093/bioinformatics/btl446>
- Stamatakis A, Hoover P, Rougemont J (2008) A rapid bootstrap algorithm for the RAxML Web servers. *Systematic Biology* 57: 758–771. <https://doi.org/10.1080/10635150802429642>
- Stewart JE, Timmer LW, Lawrence CB, Pryor BM, Peever TL (2014) Discord between morphological and phylogenetic species boundaries: incomplete lineage sorting and recombination results in fuzzy species boundaries in an asexual fungal pathogen. *BMC Evolutionary Biology* 14(1): 38. <https://doi.org/10.1186/1471-2148-14-38>
- Suh SS, Kim TK, Kim JE, Hong JM, Nguyen TTT, Han SJ, Youn UJ, Yim JH, Kim IC (2017) Anticancer activity of ramalin, a secondary metabolite from the antarctic lichen *Ramalina terebrata*, against colorectal cancer cells. *Molecules* 22(8): 1361. <https://doi.org/10.3390/molecules22081361>
- Swinscow TDV, Krog H (1988) *Macrolichens of East Africa*. British Museum (Natural History), London, 390 pp.
- Vilgalys R, Hester M (1990) Rapid genetic identification and mapping of enzymatically amplified ribosomal DNA from several *Cryptococcus* species. *Journal of Bacteriology* 172: 4238–4246. <https://doi.org/10.1128/JB.172.8.4238-4246.1990>
- Ward JD, Corbett I (1990) Towards an age for the Namib. In: Seely MK (Ed.) *Namib ecology: 25 years of Namib research*. Transvaal Museum Monograph 7. Transvaal Museum, Pretoria, 17–26.

- Werner RG (1977) Lichens nouveaux pour le Maroc ou la science avec regard sur la Grèce. *Scientific Annals of the School of Agriculture and Forestry, Aristotelian University Thessaloniki, IH'-B*: 1–15.
- White TJ, Bruns T, Lee S, Taylor J (1990) Amplification and direct sequencing of fungal ribosomal RNA genes for phylogenetics. *PCR protocols: a guide to methods and applications* 18: 315–322. <https://doi.org/10.1016/B978-0-12-372180-8.50042-1>
- Wirth V (2010a) Flechtengesellschaften der Namibwüste. *Carolinea* 68: 49–60.
- Wirth V (2010b) Lichens of the Namib Desert: A guide to their identification. Klaus Hess Verlag: Göttingen, 96 pp.
- Yang Y, Bhosle S, Yu Y, Park SY, Zhou, R, Taş İ, CDB Gamage, Kim KK, Pereira I, Hur J-S, Ha H-H, Kim H (2018) Tumidulin, a Lichen Secondary Metabolite, Decreases the Stemness Potential of Colorectal Cancer Cells. *Molecules* 23(11): 2968. <https://doi.org/10.3390/molecules23112968>
- Yang Z, Rannala B (2010) Bayesian species delimitation using multilocus sequence data. *Proceedings of the National Academy of Sciences* 107(20): 9264–9269. <https://doi.org/10.1073/pnas.0913022107>
- Yang Z, Rannala B (2014) Unguided species delimitation using DNA sequence data from multiple loci. *Molecular Biology and Evolution* 31(12): 3125–3135. <https://doi.org/10.1093/molbev/msu279>
- Yang Z, Rannala B (2017) Bayesian species identification under the multispecies coalescent provides significant improvements to DNA barcoding analyses. *Molecular Ecology* 26(11): 3028–3036. <https://doi.org/10.1111/mec.14093>
- Yu G, Smith DK, Zhu H, Guan Y, Lam TTY (2017) ggtree: an R package for visualization and annotation of phylogenetic trees with their covariates and other associated data. *Methods in Ecology and Evolution* 8(1): 28–36. <https://doi.org/10.1111/2041-210X.12628>
- Zachos JC, Dickens GR, Zeebe RE (2008) An early Cenozoic perspective on greenhouse warming and carbon-cycle dynamics. *Nature* 451(7176): 279–283. <https://doi.org/10.1038/nature06588>
- Zachos J, Pagani M, Sloan L, Thomas E, Billups K (2001) Trends, rhythms, and aberrations in global climate 65 Ma to present. *Science* 292(5517): 686–693. <https://doi.org/10.1126/science.1059412>
- Zaytsev O, Cervantes-Duarte R, Montante O, Gallegos-Garcia A (2003) Coastal upwelling activity on the Pacific Shelf of the Baja California Peninsula. *Journal of Oceanography* 59: 489–502. <https://doi.org/10.1023/A:1025544700632>
- Zhang J, Kapli P, Pavlidis P, Stamatakis A (2013) A general species delimitation method with applications to phylogenetic placements. *Bioinformatics* 29(22): 2869–2876. <https://doi.org/10.1093/bioinformatics/btt499>

## Supplementary material 1

### Three Major Ecogeographic Areas of Evolution in Fruticose Ramalinaceae

Authors: Richard Spjut, Antoine Simon, Martin Guissard, Nicolas Magain, Emmanuël Sérusiaux

Data type: occurrence

Explanation note: Three geographical areas play a special role in the evolutionary history and present range of the fruticose genera of the Ramalinaceae: (1) the coasts of California/USA and Baja California/Mexico; (2) the Atacama and Sechura deserts along the western coasts of South America and (3) the coasts of Namibia and South-West of South Africa. These areas are briefly presented in this section, focusing on their biodiversity, especially for lichenized fungi, and their recent climatic history. Chapter (1) further includes updates on the ecogeographical data and evolutionary interpretation for the genera *Niebla* and *Vermilacinia* in Baja California.

Copyright notice: This dataset is made available under the Open Database License (<http://opendatacommons.org/licenses/odbl/1.0/>). The Open Database License (ODbL) is a license agreement intended to allow users to freely share, modify, and use this Dataset while maintaining this same freedom for others, provided that the original source and author(s) are credited.

Link: <https://doi.org/10.3897/mycokeys.73.47287.suppl1>

## Supplementary material 2

### Table S2. PCR conditions and primers for each locus

Authors: Richard Spjut, Antoine Simon, Martin Guissard, Nicolas Magain, Emmanuël Sérusiaux

Data type: molecular

Explanation note: PCR conditions and primers for each locus: ITS, LSU, RPB1, RPB2, GDP and EF-1 $\alpha$ .

Copyright notice: This dataset is made available under the Open Database License (<http://opendatacommons.org/licenses/odbl/1.0/>). The Open Database License (ODbL) is a license agreement intended to allow users to freely share, modify, and use this Dataset while maintaining this same freedom for others, provided that the original source and author(s) are credited.

Link: <https://doi.org/10.3897/mycokeys.73.47287.suppl2>

### Supplementary material 3

#### Table S3. Table of accessions of the lichen collections studied

Authors: Richard Spjut, Antoine Simon, Martin Guissard, Nicolas Magain, Emmanuël Sérusiaux

Data type: species data

Explanation note: Table of accessions of the lichen collections studied, with the following data: name; locality and year of collection; collector(s) and herbarium references; reference accession number in DNA data bank at Uliège (LG herbarium); secondary chemical compounds (as detected by TLC) and GenBank accessions numbers of each locus examined (ITS, LSU, *RPB1*, *RPB2*, *GDP* and *EF-1 $\alpha$* ). The first column points to the accessions that were included in the time-calibrated phylogeny for the four genera of fruticose Ramalinaceae studied (*Namibialina*, *Niebla*, *Ramalina* and *Vermilacinia*) and several accessions of their crustose sister genus *Cliostomum*, including the type species *C. corrugatum*. The last five columns (M to Q) refer to the results of species delimitations methods run on *Niebla* and *Vermilacinia* (ABGD; PTP; BPP and STACEY analyses).

Copyright notice: This dataset is made available under the Open Database License (<http://opendatacommons.org/licenses/odbl/1.0/>). The Open Database License (ODbL) is a license agreement intended to allow users to freely share, modify, and use this Dataset while maintaining this same freedom for others, provided that the original source and author(s) are credited.

Link: <https://doi.org/10.3897/mycokeys.73.47287.suppl3>

### Supplementary material 4

#### Table S4. Time calibration

Authors: Richard Spjut, Antoine Simon, Martin Guissard, Nicolas Magain, Emmanuël Sérusiaux

Data type: species data

Explanation note: Time calibration based on a fossil of *Phyllopsora* and constraint on the Ramalinaceae node conducted on the evolutionary tree.

Copyright notice: This dataset is made available under the Open Database License (<http://opendatacommons.org/licenses/odbl/1.0/>). The Open Database License (ODbL) is a license agreement intended to allow users to freely share, modify, and use this Dataset while maintaining this same freedom for others, provided that the original source and author(s) are credited.

Link: <https://doi.org/10.3897/mycokeys.73.47287.suppl4>

## Supplementary material 5

### Table S5. Comparison of the identification of the *Niebla* collections

Authors: Richard Spjut, Antoine Simon, Martin Guissard, Nicolas Magain, Emmanuël Sérusiaux

Data type: species data

Explanation note: Comparison of the identification of the *Niebla* collections following Spjut (1996) and the number of accessions in the 6-loci analysis and the species as delimited by the BPP and STACEY analysis.

Copyright notice: This dataset is made available under the Open Database License (<http://opendatacommons.org/licenses/odbl/1.0/>). The Open Database License (ODbL) is a license agreement intended to allow users to freely share, modify, and use this Dataset while maintaining this same freedom for others, provided that the original source and author(s) are credited.

Link: <https://doi.org/10.3897/mycokeys.73.47287.suppl5>

## Supplementary material 6

### Table S6. Data for the *Niebla* collections studied

Authors: Richard Spjut, Antoine Simon, Martin Guissard, Nicolas Magain, Emmanuël Sérusiaux

Data type: species data

Explanation note: Data for the *Niebla* collections studied: number of localities for each species recognized by BPP and number of species for each locality sampled.

Copyright notice: This dataset is made available under the Open Database License (<http://opendatacommons.org/licenses/odbl/1.0/>). The Open Database License (ODbL) is a license agreement intended to allow users to freely share, modify, and use this Dataset while maintaining this same freedom for others, provided that the original source and author(s) are credited.

Link: <https://doi.org/10.3897/mycokeys.73.47287.suppl6>

## Supplementary material 7

### Table S7. Data for the *Niebla* collections studied

Authors: Richard Spjut, Antoine Simon, Martin Guissard, Nicolas Magain, Emmanuël Sérusiaux

Data type: species data

Explanation note: Data for the *Niebla* collections studied: number of localities for each species recognized by STACEY and number of species for each locality sampled.

Copyright notice: This dataset is made available under the Open Database License (<http://opendatacommons.org/licenses/odbl/1.0/>). The Open Database License (ODbL) is a license agreement intended to allow users to freely share, modify, and use this Dataset while maintaining this same freedom for others, provided that the original source and author(s) are credited.

Link: <https://doi.org/10.3897/mycokeys.73.47287.suppl7>

## Supplementary material 8

### Identification of the chemistry of *Ramalina rosacea*

Authors: Richard Spjut, Antoine Simon, Martin Guissard, Nicolas Magain, Emmanuël Sérusiaux

Data type: species data

Explanation note: Identification of the chemistry of *Ramalina rosacea*, a coastal saxicolous species of the *R. bourgeana*-group, endemic to the Western Mediterranean sea-shores (2 localities known).

Copyright notice: This dataset is made available under the Open Database License (<http://opendatacommons.org/licenses/odbl/1.0/>). The Open Database License (ODbL) is a license agreement intended to allow users to freely share, modify, and use this Dataset while maintaining this same freedom for others, provided that the original source and author(s) are credited.

Link: <https://doi.org/10.3897/mycokeys.73.47287.suppl8>

# Neodactylariales, Neodactylariaceae (Dothideomycetes, Ascomycota): new order and family, with a new species from China

Min Qiao<sup>1\*</sup>, Hua Zheng<sup>1\*</sup>, Ruili Lv<sup>1</sup>, Zefen Yu<sup>1</sup>

<sup>1</sup> *Laboratory for Conservation and Utilization of Bio-resources, Key Laboratory for Microbial Resources of the Ministry of Education, Yunnan University, Kunming, Yunnan, 650091, China*

Corresponding author: Zefen Yu ([zfyuqm@hotmail.com](mailto:zfyuqm@hotmail.com))

---

Academic editor: T. Lumbsch | Received 8 May 2020 | Accepted 21 August 2020 | Published 11 September 2020

---

**Citation:** Qiao M, Zheng H, Lv R, Yu Z (2020) Neodactylariales, Neodactylariaceae (Dothideomycetes, Ascomycota): new order and family, with a new species from China. *MycKeys* 73: 69–85. <https://doi.org/10.3897/mycokeys.73.54054>

---

## Abstract

During a mycological survey of aquatic hyphomycetes on submerged decaying leaves in southwest China, a distinct new fungus was collected. The collection was cultured and sequenced and a BLAST search of its ITS and LSU sequence against data in GenBank revealed a dothideomycetous affiliation, with the closest related taxa in the genus *Neodactylaria*. Phylogenetic analyses of a multigene matrix containing sequences from four genes (LSU, SSU, *rpb2*, and *tef1*), representing broad groups of Dothideomycetes, revealed its placement within Dothideomycetes, but without a supported familial or ordinal affiliation. Based on further phylogenetic analyses and morphological investigations, the new fungus is described here as a new species of *Neodactylaria*, *N. simaoensis* **sp. nov.**, and placed in a new family Neodactylariaceae **fam. nov.** and a new order Neodactylariales **ord. nov.**

## Keywords

Dothideomycetes, new family, new order, new species, phylogenetic analysis, taxonomy

## Introduction

The kingdom Fungi contains an estimated 700,000 to over 5 million species, amongst which only about 120,000 have been described (Lynne 2016). Dothideomycetes is one

---

\* Authors contributed equally to this work.

of the largest and most significant classes of fungi within Ascomycota (Kirk et al. 2008; Schoch et al. 2009a; Hyde et al. 2013). Thousands of species have been included in the class Dothideomycetes, and many of them are important plant pathogens (Cortinas et al. 2006; Crous et al. 2007; Wikee et al. 2011, 2013a, b; Manamgoda et al. 2012), human and animal pathogens (Siu and Lzumi 2004; da Cunha et al. 2012, 2013), or used in biotechnological applications (Verkley et al. 2004; Damm et al. 2008; de Wit et al. 2012; Ohm et al. 2012; Stergiopoulos et al. 2012; Hyde et al. 2014). The members of Dothideomycetes are still increasing with the discovery of many novel species and inclusion of DNA sequence data. In the past few years, molecular phylogenetic studies have advanced our understanding of the systematics of Dothideomycetes (Inderbitzin et al. 2001; Schoch et al. 2009b; Hirayama et al. 2010; Suetrong et al. 2011; Hyde et al. 2013; Wijayawardene et al. 2014; Liu et al. 2017; Jiang et al. 2020). Wijayawardene et al. (2014) recommended 23 orders and 110 families in Dothideomycetes based on culture characteristics and molecular phylogenetic analyses. More recently, Liu et al. (2017) provided an updated phylogenetic assessment of Dothideomycetes at the order level by using molecular clock methods and accepted 29 orders. However, the latest research by Wijayawardene et al. (2018) expanded this to 33. Despite the progress in our understanding of the systematics of Dothideomycetes, a number of newly described and/or previously reported taxa are currently *incertae sedis* and their family and order level positions within the Dothideomycetes remain obscure; many taxa lack sequencing data or appropriate classification rank to accommodate them (Hyde et al. 2013; Wijayawardene et al. 2018).

The genus *Neodactylaria* Guevara-Suarez et al., typified by *N. obpyriformis* Guevara-Suarez et al., was originally described from human bronchoalveolar lavage in the USA (Crous et al. 2017). The genus is characterized by having integrated, polyblastic and sympodial extended conidiogenous cells producing solitary, septate, obpyriform or rostrate conidia (Crous et al. 2017). Morphologically, *Neodactylaria* is similar to two *Dactylaria* species, *D. kumamotoensis* Matsush. and *D. madrasensis* Matsush., and several *Pyricularia* species, such as *P. grisea* Cooke ex Sacc. and *P. pennisetigena* Klaubauf, M.-H. Lebrun & Crous. However, in the phylogeny inferred from sequences of the large subunits of nuclear ribosomal DNA (LSU), *Neodactylaria* was placed within Dothideomycetes, but the ordinal and familial position was unresolved.

Southwestern China is one of the world's 34 biodiversity hotspots (Myers et al. 2000; Zhang et al. 2020). During a survey of aquatic hyphomycetes on submerged decaying leaves from this area, several new species have been reported (Guo et al. 2019; Qiao et al. 2019a, b; Yu et al. 2019). In a further study, an unidentified fungus was collected, which had a similar morphology to *Heliocephala proliferans* V. Rao et al. (Pezizomycotina *incertae sedis*; Rao et al. 1984; Mel'nik et al. 2013), but detailed morphological examination showed that the conidiogenous cells were terminal or intercalary, with short-cylindrical denticles, and the conidia were 1- or 2-septate and constricted at the septum. Sequence data obtained from cultures of conidia confirmed that this species does not belong in *Heliocephala*. A BLAST search of its LSU gene sequences against the public sequence records in GenBank (Sayers et al. 2019) confirmed its dothideo-

mycetous affinity and that it was closely related to members of the genus *Neodactylaria*. Subsequently, we obtained the type species of *Neodactylaria*, *N. obpyriformis* Guevara-Suarez et al., from the CBS-KNAW Fungal Biodiversity Centre (Netherlands) and processed it with full morphological and phylogenetic analyses. Our new collection prompted the study of the molecular phylogenetic relationships of taxa within *Neodactylaria*, as well as the higher order phylogenetic relationship of *Neodactylaria* within the Dothideomycetes.

Our comparative analyses identified that the newly collected fungus is a species of *Neodactylaria*, *N. simaoensis*. However, due to their significant divergence, there was no apparent family or order for placement of *Neodactylaria*. We propose that the genus be placed in a new family and new order within Dothideomycetes.

## Materials and methods

### Isolation and morphological study

Submerged dicotyledonous leaves were collected from a stream in Simao, Yunnan Province, southern China. Samples were preserved in zip-lock plastic bags, labelled and transported to the laboratory. Each rotted leaf was cut into several 3–4 × 4–5 cm sized fragments, and these were incubated on CMA (20 g cornmeal, 18 g agar, 1000 ml distilled water), supplemented by two antibiotics (penicillin G, 0.04 g/l; and streptomycin, 0.03 g/l; Gams et al. 1998), for 5 days at room temperature. Individual conidia were isolated using a sterilised toothpick under a BX51 microscope and cultivated on CMA plates. Morphological observations were conducted on cultures growing on CMA after incubation at 25 °C for 1 week. Colony colour was based on the colour charts of Rayner (1970).

Pure cultures have been deposited in the Herbarium of the Laboratory for Conservation and Utilization of Bio-resources, Yunnan University, Kunming, Yunnan, P.R. China (YMF, formerly Key Laboratory of Industrial Microbiology and Fermentation Technology of Yunnan).

### DNA extraction, polymerase chain reaction (PCR) amplification and sequencing

Pure cultures were grown on PDA for 5 days at 25 °C. Actively-growing mycelia were scraped off the surface of a culture and transferred to 2 ml Eppendorf micro-centrifuge tubes. Total genomic DNA was extracted according to the procedures in Turner et al. (1997). To determine the phylogenetic position of *Neodactylaria*, we amplified five nuclear genomic loci, including the internal transcribed spacer (ITS), the 28S large subunit ribosomal RNA (LSU), the 18S small subunit ribosomal RNA (SSU), the translation elongation factor1-alpha partial gene (*tef1*) and the RNA polymerase II subunit 2 (*rpb2*). The following primers were used: the ITS region was amplified us-

ing the primers ITS1 and ITS4 (White et al. 1990); the LSU nuc rDNA region was amplified with primers LROR and LR7 (Vilgalys and Hester 1990); the SSU nuc rDNA region was amplified with primers NS1 and NS4 (White et al. 1990); an approx. 1.1 kb fragment of the *rpb2* gene was amplified using the primer pair fRPB2-5f and fRPB2-7cr (Liu et al. 1999); an approximately 1.0 kb fragment of the *tefl* gene was amplified with the primers TEF983F and TEF2218R (initially obtained from S. Rehner: <http://ocid.nacse.org/research/deeephyphae/EF1primer.pdf>).

PCR reactions were prepared in a 25 µl final volume as described by Zheng et al. (2019, 2020a). PCR amplifications were performed in an Eppendorf Mastercycler thermal cycler. PCR conditions were as follows: an initial 4 min denaturing step at 94 °C, followed by 35 cycles of 75 s at 94 °C, 90 s at 52 °C (for *rpb2*, LSU, and SSU) and 100 s at 72 °C. After a final extension step of 7 min at 72 °C, the samples were stored at 4 °C. Conditions for amplification of the ITS and *tefl* regions were an initial step of three cycles at an annealing temperature of 54 °C, followed by 30 cycles with the annealing temperature set at 48 °C. When needed, a ‘touchdown’ (Don et al. 1991) protocol preceded the PCR cycle. PCR products were then purified using a commercial kit (Bioteke Biotechnology Co. Ltd, China). Each fragment was sequenced from both directions using the forward and reverse primers in separate reactions using a LI-COR 4000L automatic sequencer as described by Kindermann et al. (1998). The sequences obtained have been submitted to GenBank at the National Center for Biotechnology Information (NCBI) and the accession numbers are listed in Table 1.

### Sequence alignment and phylogenetic analysis

Preliminary BLAST searches with ITS, SSU, LSU, *rpb2*, and *tefl* gene sequences of the new isolate against GenBank and UNITE databases (Nilsson et al. 2019) identified sequences closely related to our isolates. However, we were only able to robustly determine their placements within the class Dothideomycetes. To infer a phylogenetic relationship for our strain, an initial alignment of the newly generated sequences (SSU, LSU, *rpb2*, and *tefl*) and 74 representatives belonging to 33 orders of the Dothideomycetes, extracted from recent studies (Mapook et al. 2016; Nieuwenhuijzen et al. 2016; Voglmayr et al. 2016; Hernandez-Restrepo et al. 2017; Liu et al. 2017; Wijayawardene et al. 2018) with a species from the sibling class, Arthoniomycetes, as the outgroup, was performed using the online MAFFT interface (Katoh and Standley 2013; <http://mafft.cbrc.jp/alignment/server/>). This alignment was used to infer a preliminary phylogenetic relationship for the new sequences based on Bayesian inference (BI) analyses (data not shown).

Based on the initial analysis, a second alignment combined SSU, LSU, and *tefl* sequence data were constructed from the closest relatives to our strain in Botryosphaerales, Dothideales, Hysteriales, Minutisphaerales, Myriangiales, Patellariales, Phaeotrichales, Pleosporales, Tubeufiales, and Venturiales. In the second alignment, *Schismatomma decolorans* (DUKE 47570) was used as an outgroup taxon. All sequence data were aligned using MAFFT (v. 7.110) online program (<http://mafft.cbrc.jp/alignment/server/>) (Katoh and Standley 2013). The alignments were checked and uninformative gaps minimized

**Table 1.** Species, strains, and their corresponding GenBank accession numbers of sequences used for phylogenetic analyses.

Species	Strain <sup>ab</sup>	GenBank accession numbers <sup>c</sup>		
		LSU	SSU	<i>tefl</i>
<i>Acanthostigma chiangnaiense</i> Boonmee & K.D. Hyde	MFLUCC 10-0125 <sup>T</sup>	JN865197	JN865185	KF301560
<i>Allophaeosphaeria muriformis</i> Ariyaw., Camporesi & K.D. Hyde	MFLUCC 13-0349 <sup>T</sup>	KP765681	KP765682	–
<i>Bambusaria bambusae</i> (J.N. Kapoor & H.S. Gill) Jaklitsch, D.Q. Dai, K.D. Hyde and Voglmayr	CBS 139763	KP687813	KP687962	KP687983
<i>Botryobambusa fusicocum</i> Phook., Jian K. Liu & K.D. Hyde	MFLUCC 11-0143 <sup>T</sup>	JX646809	JX646826	–
<i>Botryosphaeria agaves</i> (Henn.) E.J. Butler	MFLUCC 11-0125 <sup>T</sup>	JX646808	JX646825	–
<i>Botryosphaeria dothidea</i> (Moug.) Ces. & De Not.	CBS 115476	DQ678051	DQ677998	DQ767637
<i>Caphiniforma atrovirens</i> (Mehl & Slippers) A. Alves & A.J.L. Phillips	MFLUCC 11-0425 <sup>T</sup>	JX646817	JX646833	–
<i>Dematiopleospora mariae</i> Wanås., Camporesi, E.B.G. Jones & K.D. Hyde	MFLUCC 13-0612 <sup>T</sup>	KJ749653	KJ749652	KJ749655
<i>Dothidea hippophaes</i> Fuckel	CBS 188.58	DQ678048	U42475	DQ677887
<i>Dothidea insculpta</i> Wallr.	CBS 189.58	DQ247802	DQ247810	DQ471081
<i>Glioniopsis praelonga</i> (Schwein.) Underw. & Earle	CBS 112415	FJ161173	FJ161134	FJ161090
<i>Helicangiospora lignicola</i> Boonmee, Bhat & K.D. Hyde	MFLUCC 11-0378 <sup>T</sup>	KF301531	KF301539	KF301552
<i>Helicoma chiangnaiense</i> Boonmee & K.D. Hyde	MFLUCC 10-0115	JN865188	JN865176	KF301551
<i>Helicoma fagacearum</i> Boonmee & K.D. Hyde	MFLUCC 11-0379	KF301532	KF301540	KF301553
<i>Hysterium angustatum</i> Alb. & Schwein.	CBS 236.34	FJ161180	GU397359	FJ161096
<i>Hysterobrevium smilacis</i> (Schwein.) E. Boehm & C.L. Schoch	CBS 114601	FJ161174	FJ161135	FJ161091
<i>Hysteropatella clavisporea</i> (Peck) Höhn.	CBS 247.34	AY541493	DQ678006	DQ677901
<i>Kellermania macrospora</i> (Durieu & Mont.) Minnis & A.H. Kenn.	CBS 131716 <sup>T</sup>	JX444874	JX444902	–
<i>Kellermania yuccigena</i> Ellis & Everh.	CBS 131727	JX444883	JX444908	–
<i>Minutisphaera aspera</i> Raja, Oberlies, Shearer & A.N. Mill.	DSM 29478 <sup>T</sup>	KP309993	KP309999	–
<i>Minutisphaera fimbriatosporea</i> Shearer, A.N. Mill. & A. Ferrer	A242-8a	HM196367	HM196374	–
<i>Minutisphaera japonica</i> Kaz. Tanaka, Raja & Shearer	JCM 18560 <sup>T</sup>	AB733440	AB733434	–
<i>Murispora rubicunda</i> (Niessl) Y. Zhang ter, J. Fourn. & K.D. Hyde	IFRD 2017	FJ795507	GU456308	GU456289
<i>Myriangium duriae</i> Mont. & Berk.	CBS 260.36	DQ678059	AY016347	DQ677900
<i>Myrmaecium rubrum</i> (Aptroot, Aa & Petrini) Jaklitsch & Voglmayr	CBS 109505	GU456324	GU456303	GU456260
<i>Myrmaecium fulvopruinatum</i> (Berk.) Jaklitsch & Voglmayr	CBS 139058	KP687861	KP687968	KP688030
<i>Myrmaecium rubricosum</i> (Fr.) Fuckel	CBS 139068	KP687885	KP687979	KP688053
<i>Neodactylaria obpyriformis</i> Guevara-Suarez, Deanna A. Sutton, Wiederh. & Gené	CBS 142668	<b>MK562751</b>	<b>MK562750</b>	–
<i>Neodactylaria simaoensis</i> H. Zheng & Z.F. Yu	YMF 1.3984	<b>MH379210</b>	<b>MK562747</b>	<b>MK562748</b>
<i>Oedohysterium insidens</i> (Schwein.) E. Boehm & C.L. Schoch	CBS 238.34	FJ161182	FJ161142	FJ161097
<i>Panawiesneriomyces syzygii</i> Crous & M.J. Wingf.	CBS 141333 <sup>T</sup>	KX228339	–	–
<i>Patellaria atrata</i> (Hedw.) Fr.	CBS 958.97	GU301855	GU296181	GU349038
<i>Phaeotrichum benjaminii</i> Malloch & Cain	CBS 541.72	AY004340	AY016348	DQ677892
<i>Phyllosticta ampellicida</i> (Engelm.) Aa	CBS 237.48	DQ678085	DQ678034	–
<i>Phyllosticta citricarpa</i> (McAlpine) Aa	CBS 102374	GU301815	GU296151	GU349053
<i>Populocrescentia forlicsenensis</i> Wanås., Camporesi, E.B.G. Jones & K.D. Hyde	MFLUCC 14-0651 <sup>T</sup>	KT306952	KT306955	–
<i>Pseudogliophragma indica</i> Phadke & V.G. Rao	MTCC 11985 <sup>T</sup>	KM052851	KM052852	–
<i>Psilogleonium araucanum</i> (Speg.) E. Boehm, Marinc. & C.L. Schoch	CBS 112412	FJ161172	FJ161133	FJ161089
<i>Saccharata proteae</i> (Wakef.) Denman & Crous	CBS 115206	GU301869	GU296194	GU349030
<i>Schismatomma decolorans</i> (Erichsen) Clauzade & Vězda	DUKE 47570	AY548815	AY548809	DQ883725
<i>Speiropsis pedatospora</i> Tubaki	CBS 397.59	KR869797	–	–
<i>Trematosphaeria pertusa</i> Fuckel	CBS 122368	FJ201990	FJ201991	GU456276
<i>Trematosphaeria pertusa</i> Fuckel	CBS 122371	FJ201992	FJ201993	GU349085
<i>Trichodelitischia bisporala</i> (P. Crouan & H. Crouan) Munk	CBS 262.69	GU348996	GU349000	GU349020
<i>Trichodelitischia munkii</i> N. Lundq.	Kruys 201	DQ384096	DQ384070	–
<i>Tubeufia chiangnaiensis</i> Boonmee & K.D. Hyde	MFLUCC 11-0514 <sup>T</sup>	KF301538	KF301543	KF301557
<i>Tubeufia javanica</i> Penz. & Sacc.	MFLUCC 12-0545 <sup>T</sup>	KJ880036	KJ880035	KJ880037
<i>Valsaria insitiva</i> (Tode) Ces. & De Not.	CBS 127882 <sup>T</sup>	KP687886	KP687980	KP688054
<i>Valsaria lopastomoides</i> Jaklitsch & Voglmayr	CBS 139062 <sup>T</sup>	KP687868	KP687972	KP688037
<i>Valsaria neotropica</i> Jaklitsch, J. Fourn. & Voglmayr	CBS 139064 <sup>T</sup>	KP687874	KP687974	KP688042
<i>Valsaria robiniae</i> (Schwein.) Cooke	CBS 139063	KP687870	KP687973	KP688039
<i>Valsaria rudis</i> (P. Karst. & Har.) Theiss. & Syd. ex Petr. & Syd.	CBS 139066 <sup>T</sup>	KP687879	KP687976	KP688047
<i>Valsaria spartii</i> Maubl.	CBS 139070 <sup>T</sup>	KP687843	KP687964	KP688013

<sup>a</sup> ex-type strains are indicated with <sup>T</sup> after the strain number. <sup>b</sup> Abbreviations of culture collections (where known): CBS, Westerdijk Fungal Biodiversity Institute, Utrecht, The Netherlands; DSMZ, German Collection of Microorganisms and Cell Cultures, Braunschweig, Germany; G, University of North Carolina, Greensboro, Department of Chemistry and Biochemistry Fungal Culture Collection; DUKE, Duke University Herbarium, Durham, North Carolina; IFRDCC, International Fungal Research and Development Culture Collection; JCM, Japan Collection of Microorganism, RIKEN BioResource Center, Japan; MFLUCC, Mae Fah Luang University Culture Collection, Chiang Rai, Thailand; YMF, the Herbarium of the Laboratory for Conservation and Utilization of Bio-resources, Yunnan University, China. <sup>c</sup> Sequences obtained in this study are shown in bold.

manually where necessary in BioEdit 7.0.1 (Hall 1999). Maximum likelihood (ML) and BI were used in the analyses following the methodology as described in Mapook et al. (2016). The nucleotide substitution models use for analyses was determined using jModelTest 2.0 (Posada 2008). The GTR+I+G model with inverse gamma rate were selected for individual data from each partition with the combined aligned dataset. The phylogenetic tree was visualized in FigTree v. 1.4 (Rambaut 2012) and the layout of the tree was done in Adobe Illustrator v. CS5.1. The alignment of phylogenetic analyses was deposited in TreeBASE (<https://www.treebase.org>, submission number 24051).

## Results

### Molecular phylogeny

Following the results of preliminary phylogenetic analysis of the initial alignment (data not shown), the phylogenetic reconstruction of the second alignment was performed including SSU, LSU, and *tefl* sequences from 53 strains representing 10 different orders in the Dothideomycetes and one order in the Arthoniomycetes (Table 1). The three-gene dataset comprised of LSU sequences for all 52 ingroup sequences, 50 SSU sequences, and 36 *tefl* sequences. After exclusion of ambiguous regions and introns, the combined dataset included 2555 characters (826 for LSU, 1012 for SSU, and 717 for *tefl*). In the BI analysis, the alignment has 952 distinct patterns, 600 parsimony-informative, 205 singleton sites, and 1750 constant sites.

The best tree (RAxML) obtained using the ML analysis is shown as Fig. 1, with the support values from the ML and BI analyses plotted at the nodes. In this tree, our newly proposed species and *N. obpyriformis* formed a distinct clade within Dothideomycetes with significant ML bootstrap support (100%) and Bayesian sposterior probability (1.0). Moverover, the *Neodactylaria* clade is sister to the Pleosporales clade, but only with low bootstrap support values (51%) and Bayesian posterior probabilities (0.72). The results suggested that our strain belongs to the genus *Neodactylaria*. The order Pleosporales has characters that are very different from those of species of *Neodactylaria* and, therefore, we introduce a new order and new family, Neodactylariales and Neodactylariaceae, respectively, for this group of fungi. In addition, combined with morphological differences, our strain was described and illustrated herein as a new species of *Neodactylaria*.

### Taxonomy

#### **Neodactylariales H. Zheng & Z.F. Yu, ord. nov.**

Mycobank No: 830161

**Type family.** Neodactylariaceae H. Zheng & Z.F. Yu.

**Description.** Asexual morph from human-associated organs or saprobic on plant debris. Conidiophores acroauxic, macronematous, mononematous, branched

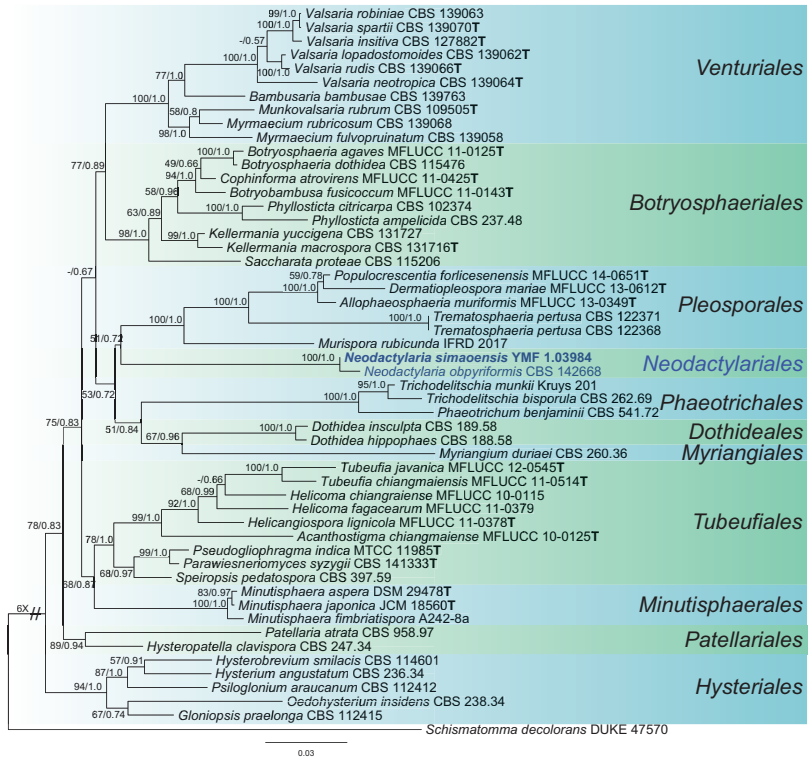


**Figure 1.** Maximum likelihood (RAxML) tree obtained by phylogenetic analyses of the combined LSU, SSU, and *tef1* sequence alignment of 53 taxa belonging to the 11 orders shown to the right of the tree. The numbers of nodes in clades represent Maximum likelihood bootstrap support values (ML-BS, 0–100) and Bayesian posterior probabilities (BPP, 0–1.0). ML-BS greater than 50% and BPP above 0.5 are indicated at the nodes (ML-BS/BPP). The scalebar represents the number of changes. *Schizmatomma decolorans* DUKE 47570 was used as outgroup. The strain numbers are noted after the species names with ex-type strains indicated with <sup>T</sup>. The proposed new order is in boldface.

or unbranched. Conidiogenous cells mono- and polyblastic, sympodially extended. Conidia solitary, hyaline or pale pigmented, smooth, verrucous or echinulate. Sexual morph not observed.

### **Neodactylariaceae H. Zheng & Z.F. Yu, fam. nov.**

Mycobank No: 830162

**Type genus.** *Neodactylaria* Guevara-Suarez, Deanna A. Sutton, Wiederh. & Gené.

**Description.** Mycelium superficial or immersed, composed of branched, septate, hyaline to subhyaline hyphae. Conidiophores macronematous, mononematous, straight or flexuous, septate, unbranched. Conidiogenous cells terminal or intercalary, polyblastic, sympodial, with short-cylindrical denticles. Conidial secession schizolytic. Conidia solitary, smooth or finely echinulate. Sexual morph not observed.

***Neodactylaria* Guevara-Suarez, Deanna A. Sutton, Wiederh. & Gené, in Crous et al. *Persoonia* 38: 345 (2017)**

**Type species.** *Neodactylaria obpyriformis* Guevara-Suarez, Deanna A. Sutton, Wiederh. & Gené.

**Description.** Mycelium superficial or immersed, composed of branched, septate, smooth-walled, hyaline to subhyaline hyphae. Conidiophores macronematous, mononematous, straight or flexuous, septate, unbranched, smooth-walled, pale to mid-brown. Conidiogenous cells polyblastic, sympodial extended, integrated, terminal or intercalary, denticulate, with short cylindrical denticles, pale to medium-brown. Conidial secession schizolytic. Conidia obpyriform to obclavate, unicellular or septate, attenuate, subulate or rostrate toward the obtuse apex, with a tiny, protuberant basal hilum, smooth or finely echinulate, subhyaline or pale brown. Sexual morph not observed.

***Neodactylaria simaoensis*, H. Zheng & Z.F. Yu, sp. nov.**

Mycobank No: 830160

Fig. 2

**Diagnosis.** It is characterised by straight or flexuous, 2–4-septate, unbranched conidiophores, with denticulate conidiogenous cells and obclavate to long obpyriform, subulate or slightly rostrate towards the obtuse or rounded apex and 1–2 (–3)-septate conidia. Differs from *N. obpyriformis* by longer and slightly wider conidia and more septa.

**Type.** China, Yunnan Province, Simao country, 100°59'19"N, 22°46'38"E, ca 1330 m alt., from submerged unidentified dicotyledonous leaves, 28 Oct 2013, Z.F. Yu, live culture YMF 1.03984 – *holotype*, dried slide YMFT 1.03984.

**Description.** Mycelium partly superficial or partly immersed, composed of branched, septate, hyaline to subhyaline, creeping, 1.0–2.0 µm wide hyphae. Conidiophores macronematous, mononematous, straight or flexuous, slightly geniculate towards the apex, 2–4-septate, unbranched, hyaline or pale brown, 38–86 (–129) × 3–4 µm, arising from the creeping hyphae pale brown. Conidiogenous cells polyblastic, indeterminate, sympodial extended, integrated, terminal or intercalary, denticulate with protuberant cylindrical denticles. Conidia solitary, obclavate to long obpyriform, subulate or slightly rostrate towards the obtuse or rounded apex, lumina micro-guttulate, 1–2 (–3)-septate, constricted at the septa, pale to mid brown, 15–40 × 3.6–6.5 µm, with a subhyaline, protuberant basal hilum up to 1 µm long.

**Culture characteristics.** Colonies attaining 1 cm in diameter on CMA after 7 days at 25 °C. On CMA, colonies flat, floccose at the centre, lacking aerial mycelium towards periphery, white to cream-coloured, reverse same colour, sporulation abundant. On PDA, colonies flat, white to cream-coloured, margin entire; sporulation sparse.

**Habitat and distribution.** In submerged dicotyledonous leaves from southwestern China.



**Figure 2.** Culture and anamorph of *Neodactylaria simaoensis* (YMF 1.03984) **A** culture on CMA **B–D** conidia **E** conidia and conidiophores **F** immature conidium and conidiogenous cells **G** conidiophores and conidia under low power microscope. Scale bars: 1 cm (**A**); 10  $\mu$ m (**B–F**); 50  $\mu$ m (**G**).

**Teleomorph.** Not known.

**Etymology.** The species epithet indicates its occurrence in the county of Simao, China.

**Notes.** Based on a Blast search of NCBI's GenBank nucleotide database, the closest hits using the ITS sequences of *N. simaoensis* (GenBank MH379209) is *N. obpyriformis* (GenBank NR\_154267, Identities = 545/569(96%), Gaps = 4/569(0%)). Morphologically, the new species, *N. simaoensis*, shares several characters with *N. obpyriformis* (type species): both have white to cream-coloured colonies, with short-cylindrical denticles as conidiogenous cells and obpyriform to slightly rostrate conidia (Crous et al. 2017). However, *N. simaoensis* differs from *N. obpyriformis* by having obviously longer and slightly wider conidia ( $15\text{--}40 \times 3.6\text{--}6.5 \mu\text{m}$  vs  $10\text{--}14 \times 3\text{--}5 \mu\text{m}$ ) and more septa.

## Discussion

Aquatic hyphomycetes, which have always been important members of the Dothideomycetes, play critical roles in the decomposition of organic compounds and nutrient cycling in aquatic habitats. Since Ingold (1942, 1943) first reported aquatic hyphomycetes in the 1940s, research on this group have been steadily increasing throughout the world. It was estimated that over 300 species of over 80 genera of aquatic hyphomycetes are reported worldwide (Kirk et al. 2008; Guo et al. 2015). Studies of aquatic hyphomycetes have revealed a huge fungal diversity. Our study again underlined the importance of these microorganisms for fungal taxonomic discovery.

In this study, a preliminary phylogenetic analysis combined SSU, LSU, *rpb2*, and *tef1* sequences from 74 representative taxa of Dothideomycetes and Arthoniomycetes revealed the *Neodactylaria* as a unique clade within Dothideomycetes (data not shown). The second phylogenetic analyses using three loci (SSU, LSU, *tef1*) also showed our new collected strain and *N. obpyriformis* form a strongly supported monophyletic and distinct clade (ML-BS = 100%, BPP = 1.0) within the Dothideomycetes (Fig. 1). In this tree, the *Neodactylaria* clade is close to the *Pleosporales* but with low support (ML-BS = 51%, BPP = 0.72). The original study on *N. obpyriformis*, which conducted a phylogenetic analysis of the LSU sequence, also showed that *Neodactylaria* is related to Dothideomycetes, but with an uncertain taxonomic position at the ordinal level and family level (Crous et al. 2017). Thus, we establish a new order (Neodactylariales) and family (Neodactylariaceae) within the Dothideomycetes for this unique clade.

The genus *Neodactylaria* is morphologically similar to two species of the genus *Dactylaria*, *D. kumamotoensis* and *D. madresensis*, which were described by Matsushima from soil and plant debris in Japan and India, respectively (Matsushima 1981, 1984). Although these two fungi in *Dactylaria* could be congeneric with *N. simaoensis*, they are only known from the type collection and no living cultures are available for molecular comparison. Morphologically, the conidia of *N. simaoensis* are smaller than *D. kumamotoensis* and are distinguished from *D. madresensis* by their size and the number of septa. In addition, the genus *Dactylaria* is heterogeneous. Related information showed that the classification position of *D. kumamotoensis* was in the order Helotiales, the class Leotiomycetes (<http://www.indexfungorum.org/Names/NamesRecord>).

asp?RecordID=111390), but most *Dactylaria* species were placed in the Sordariomycetes (Crous et al. 2017). Thus, although the genus *Neodactylaria* shares some morphological characters with the genus *Dactylaria*, *Neodactylaria* was placed in the Dothideomycetes by phylogenetical analysis and was phylogenetically distant from *Dactylaria*.

In the Dothideomycetes, many orders show various morphological characteristics and lifestyles, such as the order Pleosporales. In our new order, the two species within genus *Neodactylaria* also have different habitats: *N. obpyriformis* was found from human bronchoalveolar lavage in the USA, but *N. simaoensis* was found from submerged decaying leaves in China. Therefore, it seems fungi in this genus may be broadly distributed in different habitats.

The class Dothideomycetes is one of the most important and diverse classes in the phylum Ascomycota. It comprises pathogenic fungi, aquatic hyphomycetes, fungi with different life cycles and habitats, and also fungi with biotechnological potential (Wijayawardene et al. 2014; Santos et al. 2015; Woudenberg et al. 2015; Zheng et al. 2020b). In recent years, this class has received significant attention, and several papers have highlighted its importance to fungal taxonomy, based on its fungal diversity and on new studies performed to improve the classification of dothideomycetous fungi (Schoch et al. 2009a; Hyde et al. 2013; Wijayawardene et al. 2014). In Dothideomycetes, most families comprise both sexual genera and asexual genera and only a few families are totally comprised of asexual genera, such as Cladosporiaceae Nann., which contains seven asexual hyphomycetous genera and Neodevriesiaceae Quaedvlieg & Crous, which contains one asexual hyphomycetous genus (Wijayawardene et al. 2014). However, the order Lichenocniales, only comprising one family, was also established with an asexual genus (Hyde et al. 2013). Here, we added a new order containing only an asexual genus to Dothideomycetes. These results show asexual genera have equal status to sexual genera at various taxon ranks. In addition, the description of Neodactylariales, as a new order in this study, highlights the need to collect fungal biodiversity from a range of diverse environments and substrates, as these diverse niches frequently harbour fungal lineages that are still missing in current phylogenetic studies.

## Acknowledgements

This work was financed by the National Natural Science Foundation Program of PR China (31760012, 31770026). We are grateful to two reviewers for critically reviewing the manuscript and for providing helpful suggestions to improve this paper.

## References

- Cortinas MN, Burgess T, Dell B, Xu D, Crous PW, Wingfield BD, Wingfield MJ (2006) First record of *Colletogloeopsis zuluense* comb. nov., causing stem canker of *Eucalyptus* in China. *Mycological Research* 110: 229–236. <https://doi.org/10.1016/j.mycres.2005.08.012>
- Crous PW, Braun U, Groenewald JZ (2007) *Mycosphaerella* is polyphyletic. *Studies in Mycology* 58: 1–32. <https://doi.org/10.3114/sim.2007.58.01>

- Crous PW, Wingfield MJ, Burgess TI, Hardy GESTJ, Barber PA, Alvarado P, Barnes CW, Buchanan PK, Heykoop M, Moreno G, Thangavel R, van der Spuy S, Barili A, Barrett S, Cacciola SO, Cano-Lira JF, Crane C, Decock C, Gibertoni TB, Guarro J, Guevara-Suarez M, Hubka V, Kolařík M, Lira CRS, Ordoñez ME, Padamsee M, Ryvarden L, Soares AM, Stchigel AM, Sutton DA, Vizzini A, Weir BS, Acharya K, Aloí F, Baseia IG, Blanchette RA, Bordallo JJ, Bratek Z, Butler T, Cano-Canals J, Carlavilla JR, Chander J, Cheewangkoon R, Cruz RHSE, da Silva M, Dutta AK, Ercole E, Escobio V, Esteve-Raventós F, Flores JA, Gené J, Góis JS, Haines L, Held BW, Jung MH, Hosaka K, Jung T, Jurjević Ž, Kautman V, Kautmanova I, Kiyashko AA, Kozanek M, Kubátová A, Lafourcade M, La Spada F, Latha KPD, Madrid H, Malysheva EF, Manimohan P, Manjón JL, Martín MP, Mata M, Merényi Z, Morte A, Nagy I, Normand AC, Paloi S, Pattison N, Pawłowska J, Pereira OL, Petterson ME, Picillo B, Raj KNA, Roberts A, Rodríguez A, Rodríguez-Campo FJ, Romański M, Ruszkiewicz-Michalska M, Scanu B, Schena L, Semelbauer M, Sharma R, Shouche YS, Silva V, Staniaszek-Kik M, Stielow JB, Tapia C, Taylor PWJ, Toome-Heller M, Vabeikhokhei JMC, van Diepeningen AD, Van Hoa N, Van Tri M, Wiederhold NP, Wrzosek M, Zothanzama J, Groenewald JZ (2017) Fungal Planet description sheets: 558–624. *Persoonia* 38: 240–384. <https://doi.org/10.3767/003158517X698941>
- Da Cunha KC, Sutton DA, Fothergill AW, Cano J, Gené J, Madrid H, De Hoog S, Crous PW, Guarro J (2012) Diversity of *Bipolaris* species in clinical samples in the United States and their antifungal susceptibility profiles. *Journal of Clinical Microbiology* 50: 4061–4066. <https://doi.org/10.1128/JCM.01965-12>
- Da Cunha KC, Sutton DA, Fothergill AW, Gené J, Cano J, Madrid H, De Hoog S, Crous PW, Guarro J (2013) In vitro antifungal susceptibility and molecular identity of 99 clinical isolates of the opportunistic fungal genus *Curvularia*. *Diagnostic Microbiology and Infectious Disease* 76: 168–174. <https://doi.org/10.1016/j.diagmicrobio.2013.02.034>
- Damm U, Verkley GJM, Crous PW, Fourie PH, Haegi A, Riccioni L (2008) Novel *Paraconiothyrium* species on stone fruit trees and other woody hosts. *Persoonia* 20: 9–17. <https://doi.org/10.3767/003158508X286842>
- De Wit PJGM, Van der Burgt A, Ökmen B, Stergiopoulos I, Abd-Elsalam KA, Aerts AL, Bahkali AH, Beenen HG, Chettri P, Cox MP, Datema E, De Vries RP, Dhillon B, Ganley AR, Griffiths SA, Guo Y, Hamelin RC, Henrissat B, Kabir MS, Jashni MK, Kema G, Klaubauf S, Lapidus A, Lévassieur A, Lindquist E, Mehrabi R, Ohm RA, Owen TJ, Salamov A, Schwelm A, Schijlen E, Sun H, Van den Burg HA, Van Ham RCHJ, Zhang S, Goodwin SB, Grigoriev IV, Collemare J, Bradshaw RE (2012) The genomes of the fungal plant pathogens *Cladosporium fulvum* and *Dothistroma septosporum* reveal adaptation to different hosts and lifestyles but also signatures of common ancestry. *PLOS Genetics* 8(11): 1–22. <https://doi.org/10.1371/journal.pgen.1003088>
- Don R, Cox P, Wainwright B, Baker K, Mattick J (1991) ‘Touchdown’ PCR to circumvent spurious priming during gene amplification. *Nucleic Acids Research* 19: 4008. <https://doi.org/10.1093/nar/19.14.4008>
- Gams W, Hoekstra ES, Aptroot A (1998) CBS Course of Mycology, Fourth Edition. Centraal-bureau voor Schimmelcultures, Baarn.
- Guo MT, Qian WY, Li JY, Yu ZF (2015) One genus and three species of aquatic hyphomycetes new to china. *Mycosystema* 2015(6): 1205–1208.

- Guo JS, Zhang Z, Qiao M, Yu ZF (2019) *Phalangispora sinensis* sp. nov. from Yunnan, China and two new members of *Wiesneriomycetaceae*. *International Journal of Systematic and Evolutionary Microbiology* 69(10): 3207–3213. <https://doi.org/10.1099/ijsem.0.003612>
- Hall TA (1999) BioEdit: a user-friendly biological sequence alignment editor and analysis program for Windows 95/98/NT. *Nucleic Acids Symposium Series* 41: 95–98.
- Hernandez-Restrepo M, Gené J, Castaneda-Ruiz RF, Mena-Portales J, Crous PW, Guarro J (2017) Phylogeny of saprobic microfungi from Southern Europe. *Studies in Mycology* 86: 53–97. <https://doi.org/10.1016/j.simyco.2017.05.002>
- Hirayama K, Tanaka K, Raja HA, Miller AN, Shearer CA (2010) A molecular phylogenetic assessment of *Massarina ingoldiana* sensu lato. *Mycologia* 102: 729–746. <https://doi.org/10.3852/09-230>
- Hyde KD, Jones EBG, Liu JK, Ariyawansa HA, Zhang M (2013) Families of Dothideomycetes. *Fungal Diversity* 63: 1–313. <https://doi.org/10.1007/s13225-013-0263-4>
- Hyde KD, Nilsson RH, Alias SA, Ariyawansa HA, Blair JE, Cai L, De Cock AWAM, Dissanayake AJ, Glockling SL, Goonasekara ID, Gorczak M, Hahn M, Jayawardena RS, Van Kan JAL, Laurence MH, Lévesque CA, Li XH, Liu JK, Maharachchikumbura SSN, Manamgoda DS, Martin FN, McKenzie EHC, McTaggart AR, Mortimer PE, Nair PVR, Pawłowska J, Rintoul TL, Shivas RG, Spies CFJ, Summerell BA, Taylor PWJ, Terhem RB, Udayanga D, Vaghefi N, Walther G, Wilk M, Wrzosek M, Xu JX, Yan JY, Zhou N (2014) One stop shop: backbones trees for important phytopathogenic genera: I. *Fungal Diversity* 67: 21–125. <https://doi.org/10.1007/s13225-014-0298-1>
- Inderbitzin P, Landvik S, Abdel-Wahab MA, Berbee ML (2001) *Aliquandostipitaceae*, a new family for two new tropical ascomycetes with unusually wide hyphae and dimorphic ascospores. *American Journal of Botany* 88: 52–61. <https://doi.org/10.2307/2657126>
- Ingold CT (1942) Aquatic Hyphomycetes of decaying alder leaves. *Transactions of the British Mycological Society* 25: 339–417. [https://doi.org/10.1016/S0007-1536\(42\)80001-7](https://doi.org/10.1016/S0007-1536(42)80001-7)
- Ingold CT (1943) Further observations on aquatic Hyphomycetes. *Transactions of the British Mycological Society* 26: 104–115. [https://doi.org/10.1016/S0007-1536\(43\)80015-2](https://doi.org/10.1016/S0007-1536(43)80015-2)
- Jiang SH, Hawksworth DL, Lücking R, Wei JC (2020) A new genus and species of foliicolous lichen in a new family of Strigulales (Ascomycota: Dothideomycetes) reveals remarkable class-level homoplasy. *IMA Fungus* 11: 1–1. <https://doi.org/10.1186/s43008-019-0026-2>
- Katoh K, Standley DM (2013) MAFFT multiple sequence alignment software version 7: improvements in performance and usability. *Molecular Biology and Evolution* 30: 772–780. <https://doi.org/10.1093/molbev/mst010>
- Kindermann J, El-Ayouti Y, Samuels GJ, Kubicek CP (1998) Phylogeny of the genus *Trichoderma* based on sequence analysis of the internal transcribed spacer region 1 of the rDNA clade. *Fungal Genetics and Biology* 24: 298–309. <https://doi.org/10.1006/fgbi.1998.1049>
- Kirk PM, Cannon PF, Minter DW, Stalpers JA (2008) *Ainsworth & Bisby's Dictionary of the Fungi*, Tenth Edition. CABI, Wallingford. <https://doi.org/10.1079/9780851998268.0000>
- Liu JK, Hyde KD, Jeewon R, Phillips AJL, Maharachchikumbura SSN, Ryberg M, Liu ZY, Zhao Q (2017) Ranking higher taxa using divergence times: a case study in Dothideomycetes. *Fungal Diversity* 84: 75–99. <https://doi.org/10.1007/s13225-017-0385-1>

- Liu YJ, Whelen S, Hall BD (1999) Phylogenetic relationships among ascomycetes: evidence from an RNA polymerase II subunit. *Molecular Biology and Evolution* 16: 1799–1808. <https://doi.org/10.1093/oxfordjournals.molbev.a026092>
- Lynne B (2016) Genetics – variation, sexuality, and evolution. In: Watkinson SC, Boddy L, Money NP (Eds) *The Fungi*, Third Edition. Academic Press, London, 99–139. <https://doi.org/10.1016/B978-0-12-382034-1.00004-9>
- Manamgoda DS, Cai L, McKenzie EHC, Crous PW, Madrid H, Chuksatirote E, Shivas RG, Tan YP, Hyde KD (2012) A phylogenetic and taxonomic re-evaluation of the *Bipolaris-Cochliobolus-Curvularia* complex. *Fungal Diversity* 56: 131–144. <https://doi.org/10.1007/s13225-012-0189-2>
- Mapook A, Hyde KD, Dai D, Li J, Jones EBG, Bahkali AH, Boonmee S (2016) *Muyocopronales*, ord. nov., (Dothideomycetes, Ascomycota) and a reappraisal of *Muyocopron* species from northern Thailand. *Phytotaxa* 265(3): 225–237. <https://doi.org/10.11646/phytotaxa.265.3.3>
- Matsushima T (1981) *Matsushima Mycological Memoirs 2*. Matsushima Fungus Collection, Kobe, 68 pp.
- Matsushima T (1984) *Matsushima Mycological Memoirs No.3*: *Mycologia* 76(2): 1–90. <https://doi.org/10.2307/3793127>
- Mel'nik VA, Castaneda-Ruiz RF, Granados M (2013) A new species of *Heliocephala* from Vietnam. *Mycotaxon* 123: 281–284. <https://doi.org/10.5248/123.281>
- Myers N, Mittermeier RA, Mittermeier CG, da Fonseca GA, Kent J (2000) Biodiversity hotspots for conservation priorities. *Nature* 403: 853–858. <https://doi.org/10.1038/35002501>
- Nieuwenhuijzen VE, Miadlikowska J, Houbraken J, Adan OO, Lutzoni F, Samson RA (2016) Wood staining fungi revealed taxonomic novelties in Pezizomycotina: New order Superstratomycetales and new species *Cyanodermella oleoligni*. *Studies in Mycology* 85: 107–124. <https://doi.org/10.1016/j.simyco.2016.11.008>
- Nilsson RH, Larsson K-H, Taylor AFS, Bengtsson-Palme J, Jeppesen TS, Schigel D, Kennedy P, Picard K, Glöckner FO, Tedersoo L, Saar I, Kõljalg U, Abarenkov K (2019) The UNITE database for molecular identification of fungi: handling dark taxa and parallel taxonomic classifications. *Nucleic Acids Research* 47: 259–264. <https://doi.org/10.1093/nar/gky1022>
- Ohm RA, Feau N, Henrissat B, Schoch CL, Horwitz BA, Barry KW, Condon BJ, Copeland AC, Dhillon B, Glaser F, Hesse CN, Kostı I, LaButti K, Lindquist EA, Lucas S, Salamov AA, Bradshaw RE, Ciuffetti L, Hamelin RC, Kema GHJ, Lawrence C, Scott JA, Spatafora JW, Turgeon BG, De Wit PJGM, Zhong S, Goodwin SB, Grigoriev IV (2012) Diverse life styles and strategies of plant pathogenesis encoded in the genomes of eighteen Dothideomycetes Fungi. *PLoS Pathogens* 8(12): e1003037. <https://doi.org/10.1371/journal.ppat.1003037>
- Qiao M, Tian WG, Castañeda-Ruiz RF, Xu JP, Yu ZF (2019a) Two new species of *Verruconis* from Hainan, China. *MycoKeys* 48: 41–53. <https://doi.org/10.3897/mycokeys.48.32147>
- Qiao M, Zheng H, Zhang Z, Yu ZF (2019b) *Seychellomyces sinensis* sp. nov. from China. *Mycotaxon* 134(2): 391–398. <https://doi.org/10.5248/134.391>
- Posada D (2008) jModelTest: phylogenetic model averaging. *Molecular Biology and Evolution* 25: 1253–1256. <https://doi.org/10.1093/molbev/msn083>
- Rambaut A (2012) FigTree v1.4.2. <http://tree.bio.ed.ac.uk/software/figtree/>
- Rao V, Reddy KA, Hoog GSD (1984) *Heliocephala*, a new genus of dematiaceous Hyphomycetes. *Persoonia* 12: 239–242.

- Rayner RW (1970) A Mycological Colour Chart. Commonwealth Mycological Institute and British Mycological Society, Kew.
- Santos MGS, Bezerra JDP, Svedese VM, Sousa MA, Silva DCV, Maciel MHC, Paiva LM, Porto ALF, Souza-Motta CM (2015) Screening of endophytic fungi from cactus of the Brazilian tropical dry forest according to their L-asparaginase activity. *Sydowia* 67: 147–156.
- Sayers EW, Cavanaugh M, Clark K, Ostell J, Pruitt KD, Karsch-Mizrachi I (2019) GenBank. *Nucleic Acids Research* 47: 94–99. <https://doi.org/10.1093/nar/gky989>
- Schoch CL, Crous PW, Groenewald JZ, Boehm EW, Burgess TI, De Gruyter J, De Hoog GS, Dixon LJ, Grube M, Gueidan C, Harada Y, Hatakeyama Hirayama SK, Hosoya T, Huhndorf SM, Hyde KD, Jones EBG, Kohlmeyer J, Krays A, Li YM, Lücking R, Lumbsch HT, Marvanová L, Mbatchou JS, McVay AH, Miller AN, Mugambi GK, Muggia L, Nelsen MP, Nelson P, Owensby CA, Phillips AJL, Phongpaichit S, Pointing SB, Pujade-Renaud V, Raja HA, Plata ER, Robbertse B, Ruibal C, Sakayaroj J, Sano T, Selbmann L, Shearer CA, Shirouzu T, Slipers B, Suetrong S, Tanaka K, Volkmann-Kohlmeyer B, Wingfield MJ, Wood AR, Woudenberg JHC, Yonezawa H, Zhang Y, Spatafora JW (2009b) A class-wide phylogenetic assessment of Dothideomycetes. *Studies in Mycology* 64: 1–15. <https://doi.org/10.3114/sim.2009.64.01>
- Schoch CL, Sung GH, Lopez-Giraldez F, Townsend JP, Miadlikowska J, Hofstetter V, Robbertse B, Matheny PB, Kauff F, Wang Z, Gueidan C, Andrie RM, Trippe K, Ciuffetti LM, Wynns A, Fraker E, Hodkinson BP, Bonito G, Groenewald JZ, Arzanlou M, De Hoog GS, Crous PW, Hewitt D, Pfister DH, Peterson K, Gryzenhout M, Wingfield MJ, Aptroot A, Suh SO, Blackwell M, Hillis DM, Griffith GW, Castlebury LA, Rossman AY, Lumbsch HT, Lücking R, Büdel B, Rauhut A, Diederich P, Ertz D, Geiser DM, Hosaka K, Inderbitzin P, Kohlmeyer J, Volkmann-Kohlmeyer B, Mostert L, O'Donnell K, Sipman H, Rogers JD, Shoemaker RA, Sugiyama J, Summerbell RC, Untereiner W, Johnston PR, Stenroos S, Zuccaro A, Dyer PS, Crittenden PD, Cole MS, Hansen K, Trappe JM, Yahr R, Lutzoni F, Spatafora JW (2009a) The Ascomycota tree of life: a phylum-wide phylogeny clarifies the origin and evolution of fundamental reproductive and ecological traits. *Systematic Biology* 58: 224–239. <https://doi.org/10.1093/sysbio/syp020>
- Siu K, Lzumi AK (2004) Phaeohiphomyces caused by *Coniothyrium*. *Cutis* 73: 127–130.
- Stergiopoulos I, Kourmpetis YAI, Slot JC, Bakker FT, De Wit JPGM, Rokas A (2012) In silico characterization and molecular evolutionary analysis of a novel superfamily of fungal effector proteins. *Molecular Biology and Evolution* 29: 3371–3384. <https://doi.org/10.1093/molbev/mss143>
- Suetrong S, Boonyuen N, Pang K, Ueapattanakit J, Klaysuban A, Sri-indrasutdhi V, Sivichai S, Jones EBG (2011) A taxonomic revision and phylogenetic reconstruction of the Jahnuales (Dothideomycetes), and the new family Manglicolaceae. *Fungal Diversity* 51: 163–188. <https://doi.org/10.1007/s13225-011-0138-5>
- Turner D, Kovacs W, Kuhls K, Lieckfeldt E, Peter B, Arisan-Atac I, Strauss J, Samuels GJ, Börner T, Kubicek CP (1997) Biogeography and phenotypic variation in *Trichoderma* sect. *Longibrachiatum* and associated *Hypocrea* species. *Mycological Research* 101: 449–459. <https://doi.org/10.1017/S0953756296002845>
- Verkley GJM, da Silva M, Wicklow DT, Crous PW (2004) *Paraconiothyrium*, a new genus to accommodate the mycoparasite *Coniothyrium minitans*, anamorphs of *Paraphaeosphaeria*, and four new species. *Studies in Mycology* 50: 323–335.

- Vilgalys R, Hester M (1990) Rapid genetic identification and mapping of enzymatically amplified ribosomal DNA from several *Cryptococcus* species. *Journal of Bacteriology* 172: 4238–4246. <https://doi.org/10.1128/JB.172.8.4238-4246.1990>
- Voglmayr H, Gardiennet A, Jaklitsch WM (2016) *Asterodiscus* and *Stigmatodiscus*, two new apothecial Dothideomycete genera and the new order Stigmatodiscales. *Fungal Diversity* 80(1): 271–284. <https://doi.org/10.1007/s13225-016-0356-y>
- White TJ, Bruns T, Lee S, Taylor J (1990) Amplification and direct sequencing of fungal ribosomal RNA genes for phylogenetics. *PCR Protocols: a guide to methods and applications* 18: 315–322. <https://doi.org/10.1016/B978-0-12-372180-8.50042-1>
- Wijayawardene NN, Crous PW, Kirk PM, Hawksworth DL, Boonmee S, Braun U, Dai DQ, D'souza MJ, Diederich P, Dissanayake A, Doilom M, Hongsanan S, Jones EBG, Groenewald JZ, Ruvishika Jayawardena R, Lawrey JD, Liu JK, Lücking R, Madrid H, Manamgoda DS, Muggia L, Nelsen MP, Phookamsak R, Suetrong S, Tanaka K, Thambugala KM, Wanasinghe DN, Wikee S, Zhang Y, Aptroot A, Ariyawansa HA, Bahkali AH, Bhat DJ, Gueidan C, Chomnunti P, De Hoog GS, Knudsen K, Li WJ, McKenzie EHC, Miller AN, Phillips AJL, Piątek M, Raja HA, Shivas RS, Slippers B, Taylor JE, Tian Q, Wang Y, Woudenberg JHC, Cai L, Jaklitsch WM, Hyde KD (2014) Naming and outline of Dothideomycetes – 2014 including proposals for the protection or suppression of generic names. *Fungal Diversity* 69: 1–55. <https://doi.org/10.1007/s13225-014-0309-2>
- Wijayawardene NN, Hyde KD, Lumbsch HT, Liu JK, Maharachchikumbura SSN, Ekanayaka AH, Tian Q, Phookamsak R (2018) Outline of Ascomycota: 2017. *Fungal Diversity* 88: 167–263. <https://doi.org/10.1007/s13225-018-0394-8>
- Wikee S, Lombard L, Crous PW, Nakashima C, Motohshi K, Chukeatirote E, Alias SA, McKenzie EHC, Hyde KD (2013a) *Phyllosticta capitalensis*, a widespread endophyte of plants. *Fungal Diversity* 60: 91–105. <https://doi.org/10.1007/s13225-013-0235-8>
- Wikee S, Lombard L, Nakashima C, Motohashi K, Chukeatirote E, Alias SA, McKenzie EHC, Hyde KD (2013b) A phylogenetic re-evaluation of *Phyllosticta* (Botryosphaerales). *Studies in Mycology* 76: 1–29. <https://doi.org/10.3114/sim0019>
- Wikee S, Udayanga D, Crous PW, Chukeatirote E, McKenzie EHC, Bahkali AH, Dai DQ, Hyde KD (2011) *Phyllosticta* – an overview of current status of species recognition. *Fungal Diversity* 51: 43–61. <https://doi.org/10.1007/s13225-011-0146-5>
- Woudenberg JHC, Seidl MF, Groenewald JZ, de Vries M, Stielow JB, Thomma BPHJ, Crous PW (2015) *Alternaria* section *Alternaria*: Species, formae speciales or pathotypes? *Studies in Mycology* 82: 1–21. <https://doi.org/10.1016/j.simyco.2015.07.001>
- Yu ZF, Lv YF, Feng B, Qiao M (2019) *Lemonniera yulongensis* sp. nov. from Yunnan, China. *Mycotaxon* 134(1): 177–181. <https://doi.org/10.5248/134.177>
- Zhang Y, Qiao M, Xu JP, Baral HO, Zhang KQ, Yu ZF (2020) Morphological and molecular characterization of two new species of *Orbilbia* (Orbiliomycetes) from China. *International Journal of Systematic and Evolutionary Microbiology* 70: 2664–2676. <https://doi.org/10.1099/ijsem.0.004088>
- Zheng H, Yang XQ, Xu JP, Yu ZF (2020a) *Beltrania sinensis* sp. nov., a new endophytic fungus from China and a key to species of the genus. *International Journal of Systematic and Evolutionary Microbiology* 70(2): 1178–1185. <https://doi.org/10.1099/ijsem.0.003897>

- Zheng H, Yu ZF, Xu JP, Castañeda-Ruiz RF, Qiao M (2020b) *Ramichloridium endophyticum* sp. nov., a new species of endophytic fungi from *Potamogeton pectinatus* in Tibet, China. *International Journal of Systematic and Evolutionary Microbiology* 70: 3433–439. <https://doi.org/10.1099/ijsem.0.004190>
- Zheng H, Zhang Z, Liu DZ, Yu ZF (2019) *Memnoniella sinensis* sp. nov., a new species from China and a key to species of the genus. *International Journal of Systematic and Evolutionary Microbiology* 69(10): 3161–3169. <https://doi.org/10.1099/ijsem.0.003605>



# *Caliciopsis moriondi*, a new species for a fungus long confused with the pine pathogen *C. pinea*

Duccio Migliorini<sup>1</sup>, Nicola Luchi<sup>1</sup>, Alessia Lucia Pepori<sup>1</sup>, Francesco Pecori<sup>1</sup>, Chiara Aglietti<sup>1,2</sup>, Fabio Maccioni<sup>1</sup>, Isabel Munck<sup>3</sup>, Stephen Wyka<sup>4</sup>, Kirk Broders<sup>4,5</sup>, Michael J. Wingfield<sup>6</sup>, Alberto Santini<sup>1</sup>

**1** Institute for Sustainable Plant Protection – National Research Council (IPSP-CNR), Via Madonna del Piano 10, I-50019, Sesto Fiorentino, Firenze, Italy **2** Department of Agrifood Production and Environmental Sciences, University of Florence, Piazzale delle Cascine 28, I-50144, Firenze, Italy **3** Forest Health Protection, USDA Forest Service, 271 Mast Road, Durham, NH 03824, Durham, USA **4** Department of Bioagricultural Sciences and Pest Management, Colorado State University, Fort Collins, Colorado, USA **5** Smithsonian Tropical Research Institute, Apartado 0843-03092, Balboa, Ancon, Panama **6** Forestry and Agricultural Biotechnology Institute (FABI), University of Pretoria, Private Bag X20, Pretoria 0028, South Africa

Corresponding author: Nicola Luchi (nicola.luchi@ipsp.cnr.it); Alberto Santini (alberto.santini@cnr.it)

---

Academic editor: D. Haelewaters | Received 8 April 2020 | Accepted 5 August 2020 | Published 25 September 2020

**Citation:** Migliorini D, Luchi N, Pepori AL, Pecori F, Aglietti C, Maccioni F, Munck I, Wyka S, Broders K, Wingfield MJ, Santini A (2020) *Caliciopsis moriondi*, a new species for a fungus long confused with the pine pathogen *C. pinea*. MycoKeys 73: 87–108. <https://doi.org/10.3897/mycokeys.73.53028>

---

## Abstract

The genus *Caliciopsis* (Eurotiomycetes, Coryneliales) includes saprobic and plant pathogenic species. *Caliciopsis* canker is caused by *Caliciopsis pinea* Peck, a species first reported in the 19<sup>th</sup> century in North America. In recent years, increasing numbers of outbreaks of *Caliciopsis* canker have been reported on different *Pinus* spp. in the eastern USA. In Europe, the disease has only occasionally been reported causing cankers, mostly on *Pinus radiata* in stressed plantations. The aim of this study was to clarify the taxonomy of *Caliciopsis* specimens collected from infected *Pinus* spp. in Europe and North America using an integrative approach, combining morphology and phylogenetic analyses of three loci. The pathogenicity of the fungus was also considered. Two distinct groups were evident, based on morphology and multilocus phylogenetic analyses. These represent the known pathogen *Caliciopsis pinea* that occurs in North America and a morphologically similar, but phylogenetically distinct, species described here as *Caliciopsis moriondi* **sp. nov.**, found in Europe and at least one location in eastern North America. *Caliciopsis moriondi* differs from *C. pinea* in various morphological features including the length of the ascomata, as well as their distribution on the stromata.

## Keywords

*Caliciopsis* canker, *Caliciopsis* spp., forest pathogen, one new species, pine trees, taxonomy

## Introduction

Species in the Coryneliaceae (Eurotiomycetes) have a worldwide distribution; they occur in both hemispheres and in both temperate and tropical climates (Fitzpatrick 1942). The family accommodates seven genera including *Caliciopsis* Peck, *Corynelia* Ach. ex Fr., *Coryneliopsis* Butin, *Coryneliospora* Fitzp., *Fitzpatrickella* Benny, Samuelson & Kimbr., *Hypsotheca* Ellis & Everh., *Lagenulopsis* Fitzp. and *Tripospora* Sacc. (Crous et al. 2019; Wood et al. 2016; Wijayawardene et al. 2020). The genus *Caliciopsis* includes both saprobic and plant pathogenic species. Recently, a taxonomic key for the genus *Caliciopsis* has been presented (Garrido-Benavent and Perez-Ortega 2015). *Caliciopsis nigra* [now recombined to *Hypsotheca nigra* (Crous et al. 2019)] is the causal agent of cankers on stems of the Mediterranean cypress, *Cupressus sempervirens* and common juniper, *Juniperus communis* (Intini 1980) and *C. indica* is a pathogen on *Garcinia indica* leaves (Pratibha et al. 2010). *Caliciopsis arceuthobii* infects the flowers of several species of dwarf mistletoe in the genus *Arceuthobium* (Ramsfield et al. 2009), *Caliciopsis rhoina* is associated with bark and trunk cankers on *Toona sinensis* (Rikkinen 2000), while *Caliciopsis brevipes* was reported on needles and bark of *Araucaria araucana* and *C. cochlearia* on needles and twigs of *A. araucana*, *Fitzroya cupressoides*, *Austrocedrus chilensis*, *Pilgerodendron uviferum* and *Podocarpus nubigenus* (Butin 1970). More recently, *Caliciopsis pleomorpha* [now recombined in *Hypsotheca* as *H. pleomorpha* (Crous et al. 2019)] has been reported as the causal agent of a canker disease on various *Eucalyptus* species in Australia (Pascoe et al. 2018).

*Caliciopsis* canker has been reported as an emerging disease of *Pinus* in the eastern USA (Munck et al. 2015, 2016; Costanza et al. 2018; Haines et al. 2018; Schulz et al. 2018a, b; Whitney et al. 2018) and is caused by the fungus *Caliciopsis pinea*. The pathogen gives rise to cankers and abundant resin bleeding on branches and stems of young and mature *Pinus strobus* trees, which can lead to crown wilting and defoliation and, in some cases, killing significant portions of the tree crowns. In the USA, *C. pinea* has been known since at least 1920 (Fitzpatrick 1920). It was considered “not uncommon” in eastern North America on *P. strobus* and on various conifer species in western North America (Ray 1936). After the accidental introduction of white pine blister rust (*Cronartium ribicola* J.C. Fisch.) into the USA in the early 1900s, *Caliciopsis* canker was ignored.

*Caliciopsis pinea* is considered native to North America (Harrison 2009). In Europe, Lanier (1965) reported this species for the first time from France on *P. halepensis*, *P. insignis*, *P. nigra* and *P. pinaster*, although the pathogen had been known in the region since the late 1800s (Rehm 1896). The disease was also reported in Italy (Capretti 1978, 1980) on several different *Pinus* species, both native and non-native. While all of these reports of *Caliciopsis* canker have been attributed to *C. pinea*, a recent study by Munck et al. (2015) suggested that a closely related, but distinct lineage of the fungus was present on *P. nigra* and *P. radiata* in Italy. Recently, an extensive survey of pine plantations in central-south Italy revealed several *P. radiata* stands showing crown yellowing, die-back and profuse resin production on the stems and shoots associated with depressed cankers. Fungal fruiting bodies resembling those of *Caliciopsis* in all stages of development were found on the cankered tissues (N. Luchi unpublished data).

No comprehensive phylogenetic study has been undertaken on *Caliciopsis* spp. associated with cankers on *Pinus* spp. including both Europe and North America. Given the findings of Munck et al. (2015), it is possible that a distinct species of *Caliciopsis* is present in Europe. Furthermore, this fungus could have a host range, ecology and epidemiology different to those of its North American congener. The aim of this study was to compare pine-infecting *Caliciopsis* isolates from Europe and North America, based on morphological features and phylogenetic inference and to determine whether these represent a single or more than one species.

## Materials and methods

### Sampling and isolation of fungal strains

Isolates used in this study were obtained from a number of surveys of *Caliciopsis* canker on native and non-native *Pinus* spp. in plantations and naturally regenerated eastern white pine stands growing in different areas of Europe (EU) and North America (NA). Isolates from NA were obtained from Georgia, North Carolina, Tennessee and Virginia (this study) and Maine, Massachusetts, New Hampshire in the USA (Munck et al. 2015). Isolates from EU were obtained from France, Italy and Spain (Table 1).

Samples from Italy were obtained from pine trees with *Caliciopsis* canker symptoms from three different locations in Tuscany (Central Italy). Five shoots with *Caliciopsis* canker from five different trees were collected at each of the three Italian sites. Other isolates from *Pinus* and other host species used in this study included *Caliciopsis pinea* LSVN1233 (from France, supplied by Dr. R. Ioos), *C. pinea* SP 1 (from Spain, supplied by Dr. P. Capretti), *C. pinea* CBS 139.64 (from Canada), *C. orientalis* CBS 138.64 (from Canada) and *C. pseudotsugae* CBS 140.64 (from Canada). All isolates are maintained in the culture collections of the Institute for Sustainable Plant Protection – National Research Council (IPSP-CNR, Italy) and the Department of Bioagricultural Sciences, Colorado State University.

Samples were placed in paper bags and transferred to the laboratory for isolation. Pine twigs (5 cm long; 0.5 to 1 cm diameter) were surface disinfested with 75% ethanol (1 min) and 3% sodium hypochlorite (NaOCl) (3 min), after which they were rinsed three times in sterile water. A sterile scalpel was used to remove the outer portions. Necrotic tissues were cut in small pieces and placed in 90-mm Petri dishes containing 1.5% Potato Dextrose Agar (PDA, DIFCO, Detroit, Michigan, USA), amended with streptomycin (0.050 g/l). All plates were incubated in the dark at 20 °C for 10–15 days. Fungal colonies with a morphology resembling *C. pinea* were transferred to fresh plates to obtain pure cultures.

### Morphology and culture characteristics

*Caliciopsis* fruiting bodies on cankered bark of the Italian specimens were mounted on glass slides in 80% lactic acid, amended with bromothymol blue and examined using a

**Table 1.** List of *Caliciopsis* spp. and *Corynelia* spp. used in comparisons of the morphology and culture characteristics and phylogenetic analyses and inoculation tests in this study.

Species	Isolate ID	Substrate	Location <sup>1</sup>	GenBank accession numbers		
				ITS	EF1- $\alpha$	Bt1
<i>Caliciopsis pinea</i>	US 27	<i>Pinus strobus</i>	Blackwater, NH, USA	KY099598	MK913567	MN150097
	US 42	<i>P. strobus</i>	Farmington, NH, USA	MK785367	MK913566	MN150096
	US 52	<i>P. strobus</i>	Bethel, ME, USA	MK785366	MK913565	MN150095
	US 67	<i>P. strobus</i>	Greenfield, NH, USA	MK785365	MK913564	MN150098
	US 71	<i>P. strobus</i>	Parsonsfield, ME, USA	MK785364	MK913563	MN150101
	US 76	<i>P. strobus</i>	Bear Brook, NH, USA	MK785363	MK913562	MN150102
	US 81	<i>P. strobus</i>	West Groton, MA, USA	KY099601	MK913561	MN150094
	US 100	<i>P. strobus</i>	Merrimack, NH, USA	MK785361	MK913560	MN150092
	US 110	<i>P. strobus</i>	Burns Farm, Milford, NH, USA	MK785360	MK913559	MN150091
	US 124	<i>P. strobus</i>	Albany, ME, USA	MK785359	MK913558	MN150090
	US 137	<i>P. strobus</i>	Alternatate Brownfield, ME, USA	MK785358	MK913557	MN150089
	US 139	<i>P. strobus</i>	Sebago Lake, ME, USA	MK785357	MK913556	MN150100
	US 149	<i>P. strobus</i>	Brownfield, ME, USA	MK785356	MK913555	MN150088
	US 151	<i>P. strobus</i>	Little Ossipee Farm, Livingston, USA	MK785355	MK913554	MN150087
	US 161	<i>P. strobus</i>	Androscoggin River Park, ME, USA	MK785354	MK913553	MN150086
	US 163	<i>P. strobus</i>	Androscoggin River Park, ME, USA	MK785353	MK913552	MN150085
	US 167	<i>P. strobus</i>	Bowdoinham, ME, USA	MK785352	MK913551	MN150084
	US 172	<i>P. strobus</i>	Naples, ME, USA	MK785351	MK913550	MN150083
	US 199	<i>P. strobus</i>	Sauford, ME, USA	MK785350	MK913549	MN150082
	US 206	<i>P. strobus</i>	Androscoggin River Park, ME, USA	MK785349	MK913548	MN150081
	US 220	<i>P. strobus</i>	New Castle, ME, USA	MK785348	MK913547	MN150080
	US 222b	<i>P. strobus</i>	Palmer, MA, USA	MK785347	MK913546	MN150099
	US 225a	<i>P. strobus</i>	Douglas, MA, USA	MK785346	MK913545	MN150078
	US 230d	<i>P. strobus</i>	Peru, ME, USA	KY099602	MK913544	MN150077
	US 232b	<i>P. strobus</i>	Barre, MA, USA	MK785344	MK913543	MN150076
	US 234a	<i>P. strobus</i>	Hollis, NH, USA	MK785343	MK913542	MN150075
	US 237	<i>P. strobus</i>	Macon, NC, USA	MK785342	MK913541	MN150074
	US 238	<i>P. strobus</i>	Neola, VA, USA	MK785341	MK913540	MN150073
	US 240	<i>P. strobus</i>	Lyme, NH, USA	MK785340	MK913539	MN150072
	US 252	<i>P. strobus</i>	USA	MK785339	MK913538	MN150071
US 255	<i>P. strobus</i>	Unicio State Park, GA, USA	MK785338	MK913537	MN150070	
US 256	<i>P. strobus</i>	Wartburg, TN, USA	MK785336	MK913536	MN150069	
US 257	<i>P. strobus</i>	Unicio State Park, GA, USA	MK785336	MK913535	MN150079	
<i>C. moriondi</i>	IT 1, CBS 146717	<i>P. radiata</i>	Carcheri, Tuscany, Italy	MN156540	MK913586	MN150120
	IT 2	<i>P. radiata</i>	Carcheri, Tuscany, Italy	MK785385	MK913585	MN150119
	IT 4	<i>P. radiata</i>	Carcheri, Tuscany, Italy	MK785384	MK913584	MN150118
	IT 5	<i>P. radiata</i>	Carcheri, Tuscany, Italy	MK785383	MK913583	MN150117
	IT 6	<i>P. radiata</i>	Carcheri, Tuscany, Italy	MK785382	MK913582	MN150116
	IT 7	<i>P. radiata</i>	Carcheri, Tuscany, Italy	MK785381	MK913581	MN150115
	IT 9	<i>P. radiata</i>	Carcheri, Tuscany, Italy	MK785380	MK913580	MN150114
	IT 11	<i>P. radiata</i>	Carcheri, Tuscany, Italy	MK785379	MK913579	MN150113
	IT 13	<i>P. radiata</i>	Carcheri, Tuscany, Italy	MK785378	MK913578	MN150112
	IT 14	<i>P. radiata</i>	Carcheri, Tuscany, Italy	MK785377	MK913577	MN150111
	IT 15	<i>P. radiata</i>	Carcheri, Tuscany, Italy	MK785376	MK913576	MN150110
	SP 1	<i>P. radiata</i>	San Sebastian de Garabandal, Spain	MK785372	MK913571	MN150106
	IT 17	<i>P. nigra</i>	Antella, Tuscany, Italy	MK785375	MK913575	MN150109
	IT 20	<i>P. radiata</i>	Carcheri, Tuscany, Italy	MK785374	MK913574	MN150108
	IT 22	<i>P. radiata</i>	Fucecchio, Tuscany, Italy	MK785373	MK913573	MN150107
<i>C. orientalis</i>	LSVN1233	<i>P. radiata</i>	Pyrénées Atlantiques, France	MK785386	MK913572	MN150121
	US 64	<i>P. resinosa</i>	Bear Brook State Park, NH, USA	MK913571	MK913570	MN150105
	US 65	<i>P. resinosa</i>	Bear Brook State Park, NH, USA	MK785370	MK913569	MN150104
	US 66	<i>P. resinosa</i>	Bear Brook State Park, NH, USA	MK785369	MK913568	MN150103
	CBS 138.64	<i>Tsuga canadensis</i>	Nashville, Canada	KP881690	MK91358	MN150122
<i>C. pinea</i>	CBS 139.64	<i>P. strobus</i>	Chalk River, Canada	KP881691	DQ677937	MN150093

<i>C. pseudotsugae</i>	CBS 140.64	<i>P. menziesii</i>	Cowichan Lake, Canada	MK785387	MK913587	MN150123
<i>C. beckhausii</i>	MA 18186	<i>Quercus ilex</i> subsp. <i>rotundifolia</i>	Spain	NR132090		
<i>C. calicioides</i>	211	<i>Populus trichocarpa</i>	Wentachee National Forest, WA, USA	JX968549		
<i>C. eucalypti</i>		<i>Eucalyptus marginata</i>	Western Australia, Australia	KY173391		
<i>C. indica</i>	GFCC 4947	<i>Garcinia indica</i>	India	NR119752		
<i>C. valentina</i>		<i>Quercus ilex</i> subsp. <i>rotundifolia</i>	Spain	NR132091		
<i>Corynelia uberata</i>	ARW 686	<i>Afrocarpus falcatus</i>	Western Cape, South Africa	KP881707		
<i>Co. fructigena</i>	ARW 250	<i>Podocarpus latifolius</i>	Western Cape, South Africa	KP881704		
<i>Co. africana</i>	ARW 247	<i>Podocarpus latifolius</i>	Western Cape, South Africa	KP881693		
<i>Hypsobeca pleomorpha</i>	VPRI 15646	<i>Eucalyptus</i>	Australia	MG641785		
<i>Lagemulopsis bispora</i>	ARW 249	<i>Podocarpus latifolius</i>	Western Cape, South Africa	KP881709		

\* ITS sequences obtain from GenBank.

<sup>1</sup> Canada (CA), France (FR), Italy (IT), Spain (SP) and United States of America (USA). States abbreviations are Georgia (GA), Maine (ME), Massachusetts (MA), New Hampshire (NH), North Carolina (NC), Tennessee (TE), Virginia (VA), and Washington (WA).

dissection microscope (SMZ800, Nikon, Japan). The length and width of 50 released ascospores and 30 fruiting bodies were measured under a light microscope (Axioskop 50 Zeiss, Germany) and images captured with a Nikon Digital Sight DS-5M camera (Nikon Instruments Software-Elements Basic Research). The means and range dimensions of fruiting bodies and ascospores were compared with those reported in literature (Table 2). The morphology of fungal colonies was determined for cultures grown for four weeks on 1.5% Malt Extract Agar (MEA, DIFCO, Detroit, Michigan, USA) and 1.5% PDA.

### Daily growth rate in culture

Six-mm diameter mycelial plugs were taken from the margins of actively growing seven-day-old colonies on PDA, using a flame-sterilised cork borer and were placed at the centres of 90-mm Petri dishes containing 1.5% PDA or 1.5% MEA. Five replicates were used for each of five selected strains (IT6, IT9, IT16, IT17, IT22) at each temperature. Dishes were incubated at 4 °C, 15 °C and 20 °C. Two measurements of colony diameter perpendicular to each other were made at 3, 7, 14, 21 and 28 days and daily growth rate was calculated as an average for each strain on each substrate. Data were analysed using a factorial ANOVA, considering temperature and substrate as the independent factor and daily growth rate as the dependent factor.

### DNA extraction and PCR amplification

Fungal isolates, including those from the Westerdijk Fungal Biodiversity Institute (CBS 138.64, CBS 139.64 and CBS 140.64) listed in Table 1, were grown in 90-mm Petri dishes containing MEA covered with 300PT cellophane membrane (Celsa, Varese,

**Table 2.** Morphological characteristics of *C. pinea* isolates described in literature and in this study and compared with *C. moriondi*. Measurements are presented as height × width, both measured reported as (min value) mean±/ -SD (max value).

	<i>C. moriondi</i>	<i>C. pinea</i>	<i>C. pinea</i>	<i>C. pinea</i>	<i>C. pinea</i>	<i>C. pinea</i>	<i>C. pinea</i>
Host	<i>P. radiata</i>	<i>P. pinaster</i>	<i>P. nigra</i> var. <i>astrata</i>	<i>C. pinea</i>	<i>P. mugo</i>	<i>C. pinea</i>	<i>C. pinea</i>
Reference	This study	Capretti 1978	Capretti 1980	Rehm 1896	Fitzpatrick 1920	Lanier 1965	
Sampling location	France, Italy, Spain, USA (New Hampshire)	Italy	Italy	Germany	Eastern North America	France	
Ascospore height	(450) 845±24 (1240) µm	2–5mm	–	100–140 µm	1–3 mm	2–3 mm	
Stalk width	(51) 79±2 (135) µm	–	–	Apical	100–125 µm	–	
Ascigerous swelling	terminal	Apical	Apical	400 × 175–275 µm	Apical	Apical or sub-apical	
Swelling size	(106)281±8(406) × (81)142±5(268) µm	–	–	Ellipsoidal to ovoidal or globose	175 µm in diameter	–	
Ascospore shape	Small, oval	Small, oval	Small, oval	Ellipsoidal to ovoidal or globose	Ellipsoidal	Ellipsoidal, brown-hyaline	
Ascospore size	(3)4.4±0.07(6.2) × (1.8)2.5±0.04(3.5) µm	(3.5)4.6(6.3) × (3.1)3.7(4.2) µm	(3.7)5.3(7.9) × (2.8)4.2(4.4) µm	3.5–6 × 2–4 µm	5–6 × 3 µm	5–6 × 3–3.5 µm	
Asci size	(26)37±6(53) × (5.3)6.3±0.4(7.4) µm	–	–	12–17 × 5–8 µm	20 × 8 µm	–	
Colonies on malt agar	White-hyaline appressed to the agar. Turning to brown in time.	White-brown with frequent anastomoses	White-brown with frequent anastomoses	–	* 1	–	

Italy) and incubated at 20 °C in the dark for 10 days. Fresh mycelium (ca. 80 mg) was scraped from the surface of the cellophane and ground in 2 ml microfuge tubes with two tungsten beads (3 mm) (Qiagen, Hilden, Germany) and 400 µl Buffer P1 (EZNA Plant DNA Kit, Omega Bio-tek, Norcross, GA, USA) using a Mixer Mill 300 (Qiagen, Hilden, Germany) [2 min; 20 Hz]. DNA was extracted from all samples using the EZNA Plant DNA Kit (Omega Bio-tek, Norcross, Georgia, USA), following the manufacturer's instructions. The DNA concentration was measured using a Nanodrop ND-1000 spectrophotometer (NanoDrop Technologies, Wilmington, Delaware, USA).

For the phylogenetic analyses, partial regions of three loci were amplified. Amplification of the internal transcribed spacer ITS region (including spacers ITS1 and ITS2 and the 5.8S gene of the rDNA) was done using primers ITS1 and ITS4 (White et al. 1990), of  $\beta$ -tubulin 1 (Bt1) gene using primers Bt2a and Bt2b (Glass and Donaldson 1995) and of translation elongation factor 1- $\alpha$  (EF1- $\alpha$ ) gene using primers EF1-983F and EF-gr (Rehner and Buckley 2005). PCR reaction mixtures (25 µl) contained 1 µl of genomic DNA, 2.5 µl of each 10 µM primer, 0.5 µl of 10 mM dNTPs (GeneSpin, Milan, Italy), 2.5 µl of 10X PCR Buffer (GeneSpin), 3 µl of 25 nM MgCl and 0.5 µl (5 U/µl) of Taq polymerase (TaqPol, GeneSpin). Amplifications were carried out in a Mastercycler (Eppendorf, Hamburg, Germany) using the following PCR conditions: for ITS and Bt1: initial denaturation at 95 °C for 5 min; followed by 35 cycles of denaturation at 94 °C for 90 sec, annealing at 56 °C for 1 min and extension at 72 °C for 2 min; and a final elongation step at 72 °C for 10 min. For EF1- $\alpha$ : initial denaturation at 95 °C for 8 min; followed by 35 cycles of denaturation at 95 °C for 30 sec, annealing at 55 °C for 30 sec and extension at 72 °C for 1 min; and a final elongation step at 72 °C for 5 min (modified from Pepori et al. 2015). Amplification products were separated by electrophoresis on gels containing 1% (w/v) of agarose LE (GeneSpin). The approximate length (bp) of the amplification products was determined using the 100-bp DNA ladder Ready to Load (Genespin). PCR amplicons were purified with a miPCR Purification Kit (Metabion International, Planegg, Germany) and sequenced in both directions at Macrogen (Seoul, South Korea). The quality of amplified nucleotide sequences was checked with the software package Geneious version 10.0.9 (Biomatters, Auckland, New Zealand). Generated sequences were submitted to NCBI GenBank (Table 1).

### Multi-locus phylogenetic analyses

BLAST searches of the generated sequences were done against the NCBI GenBank database (<https://blast.ncbi.nlm.nih.gov/Blast.cgi>) to identify the most closely-related sequences. Sequences were compared to those of known *Caliciopsis* species and other Coryneliaceae obtained from GenBank: ITS sequences of *Caliciopsis beckhausii* (NR\_132090), *C. calicioides* (JX968549), *C. eucalypti* (KY173391), *C. indica* (NR\_119752), *C. orientalis* (KP881690), *C. pinea* (KP881691, KY099598, KY099601, KY099602), *Hypsoteca pleomorpha* (MG641785), *C. valentina* (NR\_132091), *Corynelia uberata* (KP881707), *Co. fructigena* (KP881704), *Co. africana* (KP881693),

*Lagenulopsis bispora* (KP881709); EF1- $\alpha$  sequence of *Caliciopsis pinea* (DQ677937). *Lagenulopsis bispora* (KP881709) was selected as outgroup in the ITS dataset, whereas *C. orientalis* (CBS 138.64) and *C. pseudotsugae* (CBS 140.64) were selected as outgroup taxa in the EF1- $\alpha$  and Bt1 datasets. The software package Geneious (Auckland, New Zealand) was used for manual optimisation and alignment (ClustalW) of the sequences. Gaps were treated as missing data.

Phylogenetic analyses of all obtained sequences were performed using MEGA 7 (Kumar et al. 2016), Maximum Parsimony (MP) was performed using the heuristic search option with random stepwise addition with 1000 replicates, tree bisection and reconnection (TBR) as branch swapping algorithm and random taxon addition of sequences for the construction of MP trees. All characters were weighted equally and character state transitions were treated as unordered. Parameters measured for parsimony included tree length (TL), consistency index (CI), rescaled consistency index (RC), retention index (RI) and homoplasy index (HI). Bootstrap support values were evaluated using 5000 bootstrap replicates (Hills and Bull 1993).

Datasets were also analysed by Bayesian Inference (BI) using MrBayes 3.1.2 (Ronquist and Huelsenbeck 2003), with a General Time Reversible (GTR) model and gamma distributed rate variation across sites. Six Markov Chain Monte Carlo (MCMC) chains (Larget and Simon 1999) were run for 3 million generations, starting from a random tree and using the default temperature. Every 100<sup>th</sup> tree was sampled and the first 100,000 generations were discarded as burn-in. The burn-in period was determined after testing for stationarity of likelihood values, that is, by plotting numbers of generation versus the log probability and checking for the convergent diagnostic PSRF, which approached 1 (Ronquist et al. 2005). The consensus tree was calculated in MrBayes with the command sumt (Ronquist et al. 2005). The resulting phylogenetic tree was visualised using TreeView (Page 1996) and edited in TreeGraph2 (Stöver and Müller 2010).

## Inoculation tests

An inoculation experiment was carried out at the IPSP-CNR nursery facilities, located at Antella, Province of Florence, Italy (43°43'N, 11°22'E; 170 m a.s.l.). Three-year-old seedlings of *Pinus halepensis*, *P. pinaster* and *P. pinea*, with 36 plants per species, were planted in a randomised block design. The plants were maintained in rows 1 m apart and grown in a substrate comprised of commercially-produced loam and drip irrigated. The site had been completely cleared and ploughed prior to planting and was weeded each month.

Inoculations were performed in June 2014. A 6-mm diameter cork borer was used to remove the bark and expose the cambium on each plant. A plug of mycelium of the test fungus that had been grown in Petri dishes on 1.5% PDA for 20 days at 25 °C in the dark was inserted, with the mycelium side placed downwards into each wound. For inoculations, four different Italian *Caliciopsis* isolates (IT5, IT7, IT20 and IT22), recovered from infected *Pinus* sp. in the field, were used (Table 1). The inoculation trial

was performed using eight trees per isolate on each of the *Pinus* spp. Four plants for each *Pinus* sp. were mock-inoculated using sterile PDA as controls.

Pathogenicity was assessed, based on the length of lesions (mm) after six months. Statistical analyses were performed by using Statistica 10.0 (StatSoft Inc. 1984–2011). To fulfil Kock's postulates, re-isolations were carried out from the lesions on all the inoculated and control plants.

## Results

### Morphology and culture characteristics

Fruiting bodies on bark taken from infected trees were black ascomata assembled in tufts with ascigerous swellings at the apices containing ascospores. The Italian specimens had different morphological characteristics from those reported in literature for *Caliciopsis pinea* (Table 2, Figures 1, 2). Colonies of the Italian strains grown on MEA were white, appressed to the agar surface, turning to brown with time.

### Growth in culture

No growth was detected for any isolate at 4 °C. Isolates showed significantly greater growth at 20 °C. Mean daily growth rate (mm/day) at 4 °C =  $0 \pm 0$ ; at 15 °C =  $0.037 \pm 0.017$ ; at 20 °C =  $0.076 \pm 0.028$ ;  $F = 412.371$ ;  $p < 0.000$ ). No significant differences in growth were recorded on the different growth media ( $F = 0.801$ ;  $p = 0.373$ ).

### DNA sequence analysis

The final combined ITS–EF1- $\alpha$ –Bt1 data matrix of *Caliciopsis* included 53 ingroup and 2 outgroup sequences (length = 137, CI = 0.9444, RI = 0.99633, RC = 0.98178, HI = 0.940979) (Figure 3), comprising 1611 alignment characters, including gaps. Of these, 1434 characters were constant and 112 characters were parsimony informative (Figure 3). Single ITS, EF1- $\alpha$  and Bt1 datasets included, respectively, 458, 762 and 373 characters (Figure 4, Suppl. material 1: Figure S1 and Suppl. material 2: Figure S2)

Phylogenetic analysis, resulting in the most parsimonious tree from the concatenated dataset, showed that isolates, previously identified as *Caliciopsis pinea*, based on morphology, grouped in two different clades. One of these clades (Clade I) included most of the US strains and the *C. pinea* isolate CBS 139.64. The other clade (Clade II) included all EU isolates and three US strains from *P. resinosa* from a single location in New Hampshire (US64, US65, US66). Maximum Parsimony and Bayesian Inference produced nearly identical topologies for all single locus datasets: ITS, which included different species of *Caliciopsis* and other Coryneliaceae (*Corynelia africana*, *C. fructigena*, *C. uberata*

and *Lagenulopsis bispora*) (length = 168, CI = 0.721154, RI = 0.922043, RC = 0.762881, HI = 0.664935); Bt1 (length = 62, CI = 0.926829, RI = 0.98404, RC = 0.936428, HI = 0.912039); EF1- $\alpha$  gene (length = 66, CI = 0.9999, RI = 0.9998, RC = 0.9988, HI = 0.9888) (Figure 4, Suppl. material 1: Figure S1 and Suppl. material 2: Figure S2).

Across the three loci sequenced, there were 31 fixed polymorphisms separating Clade I from Clade II. Of these, 12 were in the ITS region, 11 in EF1- $\alpha$  and 7 in Bt1 (Figure 5). The USA isolates US64, US65 and US66 shared the same fixed polymorphisms present in Clade II samples. However, samples US64 together with isolates SP1, LSVN1233 and IT17 did not have the insertion in position 459 of ITS, which was one of the fixed polymorphisms in Clade II samples. Ten fixed polymorphisms were specific to Clade I. Of these, two were in the ITS, two in the EF1- $\alpha$  and six in the Bt1, where three in position 105, 122 and 128 were in common with isolates in Clade II. Fixed, unique polymorphisms were identified in all three loci, which produced congruent trees from the individual loci that separated Clade I (*C. pinea*) from Clade II isolates, suggesting that the latter isolates represent a novel species different from *C. pinea*.

## Taxonomy

***Caliciopsis moriondi* N. Luchi, D. Migliorini & A. Santini, sp. nov.**

MycoBank No: 833212

Figures 1, 2

**Types.** ITALY, Florence, Lastra a Signa, Carcheri, 43°71.58'N, 11°07.36'E, 110 m a.s.l., isolated from branches of *Pinus radiata*, 10 Oct. 2014, *leg.* N. Luchi, D. Migliorini & A. Santini, CBS 146717 (**holotype**); (IT1). ex-holotype sequences MN156540 (ITS), MK913586 (EF1- $\alpha$ ), MN150120 (Bt1); duplicate deposited at Fungal Collection of the Institute for Sustainable Plant Protection-National Research Council (IT1; **isotype**). ITALY, Florence, Fucecchio, 43°47'17"N, 10°46'37"E, isolated from diseased *Pinus radiata*, 5 Dec. 2014, *leg.* N. Luchi, deposited at Fungal Collection of the Institute for Sustainable Plant Protection-National Research Council (IT22, **paratype**). ITALY, Florence, Lastra a Signa, Carcheri, 43°71.58'N, 11°07.36'E, isolated from diseased *Pinus radiata*, 10 Oct. 2014, *leg.* N. Luchi, deposited at Fungal Collection of the Institute for Sustainable Plant Protection-National Research Council (IT4, **paratype**). ITALY, Florence, Antella 43°44.00'N, 11°19.52'E, isolated from diseased *Pinus nigra*, 24 Nov. 2014, *leg.* D. Migliorini, deposited at Fungal Collection of the Institute for Sustainable Plant Protection-National Research Council (IT17, **paratype**). SPAIN, San Sebastián de Garabandal, 43°12.04'N, 4°25.25'W, isolated from diseased *Pinus radiata*, 25 May 2011, *leg.* P. Capretti, deposited at Fungal Collection of the Institute for Sustainable Plant Protection-National Research Council (SP1, **paratype**).

**Description.** Stromata developing beneath the surface of host periderm as small, more or less circular structures, giving little external evidence of their presence at early stages. Continued growth causing the bark to break and the minute cushion-shaped

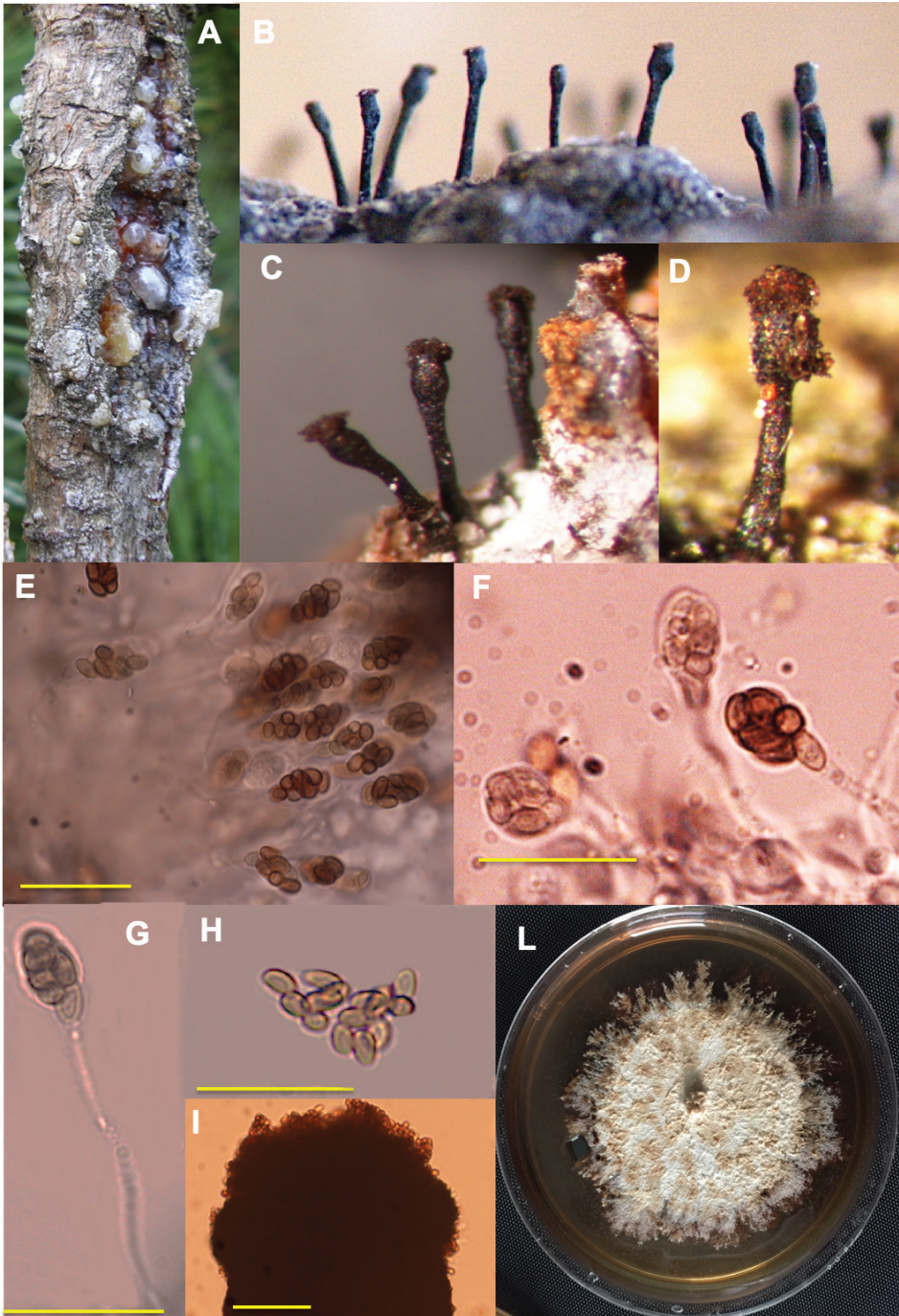


**Figure 1.** *Caliciopsis moriondi* structures **A** cankers on a *Pinus radiata* trunk **B–D** ascomata growing from a canker **B** image of *C. pinea* ascigerous columns from an archive of 1970 (provided by Prof. Paolo Capretti) **E–G** asci **H** ascospores **I** ascigerous, terminal portion **L** four weeks colony grown at 20 °C on MEA. Scale bars: 2.5  $\mu\text{m}$  (**F–H**), 5  $\mu\text{m}$  (**I**).

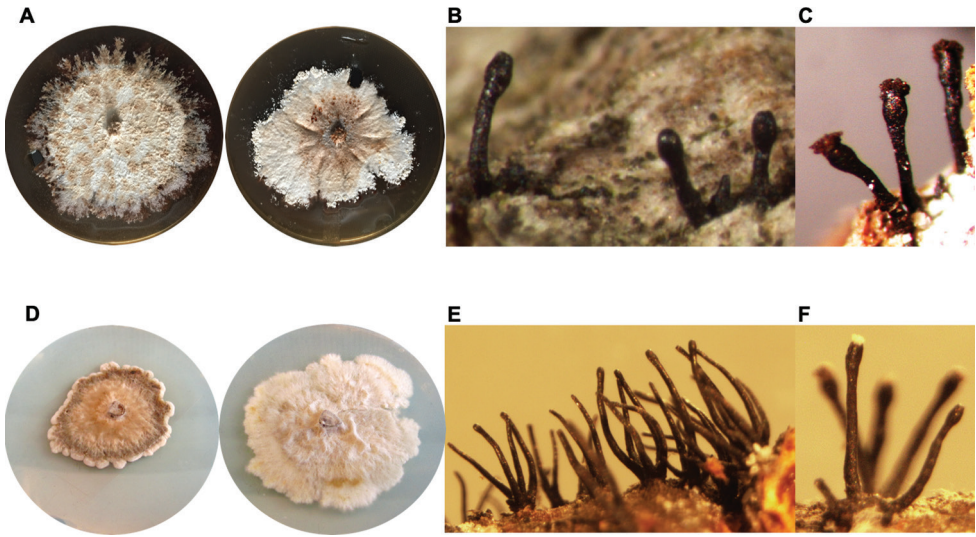


**Figure 2.** Morphological differences between *Caliciopsis moriondi* and *C. pinea* **A–C** *Caliciopsis moriondi*: **A** four-week-old colonies grown at 20 °C on MEA **B, C** ascomata growing from a canker of *Pinus radiata* **D–F** *Caliciopsis pinea*: **D** four-week-old colonies grown at 20 °C on MEA **E, F** ascomata growing from a canker of *P. radiata*.

stromata, developing a lobed appearance and increasing in diameter and thickness, in black short-stalked columnar ascomata. Ascomata mostly frequent protruding at the margin of cankers, single or double, rarely triple, stalks not branched, (0.45)  $0.84 \pm 0.02$  (1.2) mm high and (51)  $79 \pm 2$  (135)  $\mu\text{m}$  width. Ascigerous swelling, terminal, (106)  $281 \pm 8$  (406)  $\mu\text{m}$  high and (81)  $142 \pm 5$  (268)  $\mu\text{m}$  diameter, forming a brownish pulverulent mass of extruded ascospores. Asci bitunicate, clavate, 8-spored, slightly curved, pedicellate, (26)  $37 \pm 6$  (53)  $\mu\text{m}$  long; pedicel 1–3  $\mu\text{m}$  diameter; sporiferous part (12)  $13 \pm 0.4$  (14.2)  $\mu\text{m}$  long and (5.3)  $6.3 \pm 0.4$  (7.4)  $\mu\text{m}$  wide. Ascospores yellow-green colour, sub-globose to ellipsoidal and often aggregated in small masses, (3)  $4.4 \pm 0.07$  (6.2)  $\mu\text{m}$  long and (1.8)  $2.5 \pm 0.04$  (3.5)  $\mu\text{m}$  wide, brown when mature. Spermogonia sub-globose, papillate, sessile, aggregated below ascomatal tubes. Conidia unicellular, hyaline, smooth, slightly fusiform.

**Culture characteristics.** Cultures incubated on 2% PDA, showed optimal temperature for growth at 20 °C, with slow-growth rate (1.4 mm/day). Colonies white appressed to the agar, circular to irregular, becoming fawn-colored with age, areas towards margin floccose; mycelium velutinous with funicolose areas or strongly funicolose in the inner and older parts of the mycelium. Reverse colony brownish, with brown diffusion zone in old cultures; branching septate hyphae, with frequent anastomoses and tips with dendroid branching.

**Inoculation tests.** All isolates from Italy and residing in Clade II inoculated on seedlings gave rise to symptoms and lesions of variable length after six months. These were all significantly different to those of the controls ( $F = 119.21$ ,  $p < 0.000$ ;  $F = 60.84$ ,  $p < 0.000$ , respectively). Inoculated plants did not show a crown dieback,

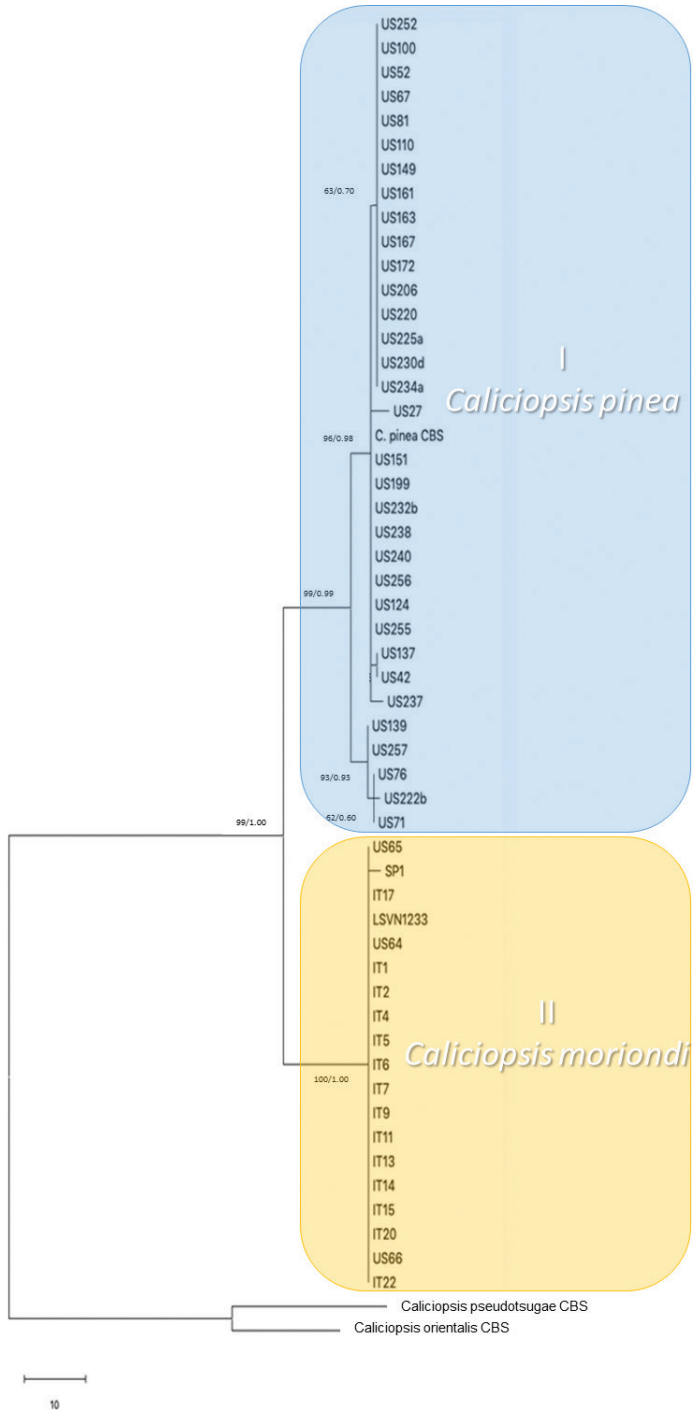


**Figure 3.** One of the most parsimonious trees (length = 137) from the combined sequence datasets of the ITS rDNA, Bt1 and EF1- $\alpha$  loci is shown (CI = 0.9444, RI = 0.99633, RC = 0.98178, HI = 0.94098). MP bootstraps and Bayesian posterior probabilities are indicated alongside the branches. *C. pseudotsugae* and *C. orientalis* EF1- $\alpha$  were selected as outgroup taxa.

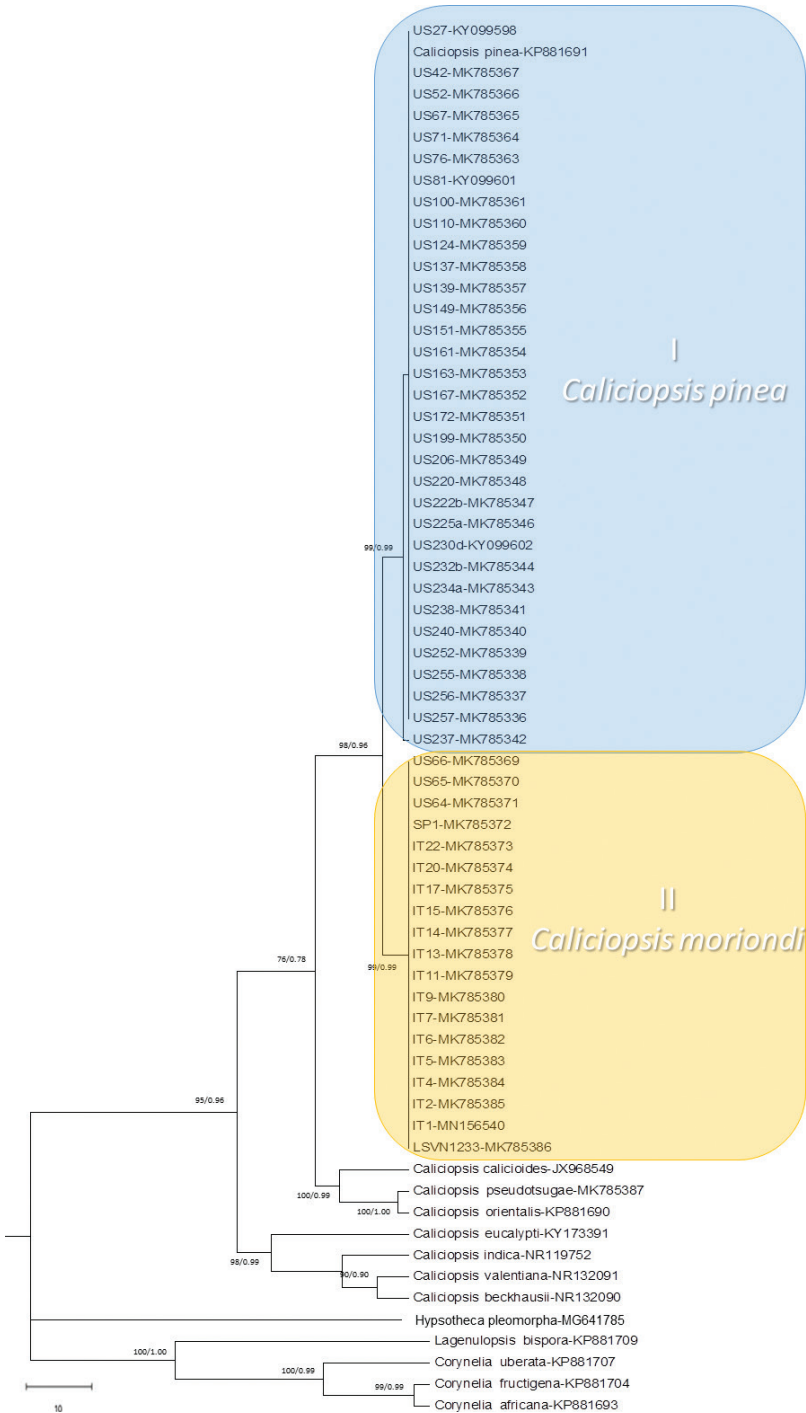


**Figure 4.** One of the most parsimonious trees of aligned ITS dataset (length = 168, CI = 0.721154, RI = 0.922043, RC = 0.762881, HI = 0.664935). The MP and Bayesian posterior probability are indicated next to the branches.



but all had profuse resin production at the inoculation points. *Caliciopsis moriondi* fruiting bodies were clearly visible on *P. halepensis*, while no fructifications were seen in any of the other inoculated *Pinus* species.

The lengths of lesions caused by the inoculated isolates were significantly longer on *P. halepensis* ( $28.6 \pm 9.04$  mm) and *P. pinaster* ( $30.1 \pm 7.13$  mm) than on *P. pinea* ( $16.4 \pm 3.16$  mm) ( $F = 297.43$ ,  $p < 0.000$ ). *Caliciopsis moriondi* was successfully re-isolated from all the seedlings inoculated with the pathogen, while no *Caliciopsis* species were re-isolated from mock-inoculated seedlings.

**Hosts and distribution.** Pathogen of pine trees *P. nigra*, *P. radiata* and *P. resinosa*, causing cankers and resin production in Europe (France, Italy, Spain) and North America (New Hampshire, USA).

**Etymology.** The name *moriondi* honours Prof. Francesco Moriondo (1926–2014). Francesco Moriondo was the founder of forest pathology as a discipline distinct from plant pathology in Italy. In this respect, he preferred a more ecological view of the topic as opposed to the typical mechanistic approach. During his career, he encouraged many young students to consider the reasons for the appearance of symptoms on trees, rather than considering only the causative agents. He also emphasised the importance of minor pathogens in the ecosystem, of which *Caliciopsis moriondi* (then *C. pinea*) was one.

**Notes.** *Caliciopsis moriondi* is commonly associated with a canker disease on *Pinus* spp. It differs subtly from *C. pinea*, based on morphological traits, including shorter ascomata, protruding and isolated from the stroma, rarely in groups of two-three, but never in more numerous groups, such as is common for *C. pinea* (Table 2).

## Discussion

This study included a large number of isolates previously believed to be *Caliciopsis pinea*. Analysis of DNA sequences of the ITS, Bt1 and EF1- $\alpha$  regions clearly showed that these isolates represented two distinct taxa. One of these represented *C. pinea* and the other an undescribed species, which we have formally described here as *C. moriondi*.

*Caliciopsis moriondi* can be distinguished from *C. pinea* based on various morphological features including the length of the ascomata, as well as by their distribution on the stromata. In the absence of sequence data, previous authors confused isolates obtained in Europe with *C. pinea*, which was originally described from North America by Fitzpatrick (1920). *Caliciopsis moriondi* as the fungus is now known, has been found in Italy, France and Spain, mainly on *P. radiata* trees and, on one occasion, on *P. nigra*. Based on the wide sampling in this study, it appears likely that *C. pinea* does not occur in Europe.

Delatour (1969) described *Caliciopsis pinea* as a weak pathogen by basing his assessment on inoculations of *P. pinaster* in France. The results of the present study suggest that it is more likely that this author was working with *C. moriondi*. This view is supported by the illustrations of *C. pinea* by Lanier (1965) showing ascomata very similar to those of *C. moriondi*.

*Caliciopsis moriondi* was able to cause only mild symptoms when inoculated on Mediterranean *Pinus* spp. in pathogenicity trials. The symptoms were most noticeable on *P. halepensis* and less severe on *P. pinaster* and *P. pinea*, confirming the results of Delatour (1969). *Caliciopsis moriondi* was able to produce ascocarps when inoculated on *P. halepensis*, but not on *P. pinaster* and *P. pinea*.

Interestingly, the European isolates of *Caliciopsis moriondi* were mainly found on *Pinus radiata*. Our inoculation tests, as well as those of Delatour (1969), suggest that the non-native *P. radiata* is more susceptible than Mediterranean *Pinus* spp. Unfortunately, *P. radiata* and *P. nigra* plants were not available when this pathogenicity test was undertaken. A further inoculation experiment on these two *Pinus* spp., which are widely planted in Europe, will be necessary in order to assess their susceptibility to *C. moriondi*.

The results of this study suggest that *Caliciopsis moriondi* is native to Europe. This is supported by the fact that it caused only mild symptoms on artificially inoculated European *Pinus* spp. Yet on naturally infected non-native *P. radiata*, it gave rise to symptoms similar to those caused by the pitch canker pathogen *Fusarium circinatum*, which is an important quarantine pathogen in Europe and also commonly found on *P. radiata* (Capretti et al. 2013). Future studies will be necessary to determine whether infections on these trees are caused by *F. circinatum* or *C. moriondi* and the duplex real-time PCR assay developed and validated by Luchi et al. (2018) should be useful in this regard.

*Caliciopsis moriondi* and *C. pinea* are two vicariant species and it appears that the European *C. moriondi* has been accidentally introduced in North America. We hypothesise that this might have occurred at the end of the 1800s when European nurseries produced large volumes of *Pinus* spp. for the establishment of North American plantations (Maloy 1997). *Caliciopsis moriondi* could easily have moved on infected, but asymptomatic, seedlings at that stage.

The results of this study suggest that *Caliciopsis pinea* is not present in Europe. Its pathogenicity on European pines has never been assessed. Since the beginning of the present century, there has been a renewed interest in this species due to the damage it causes to the plantations of *P. strobus* in the north-eastern United States (Munck et al. 2015, 2016). An accidental introduction of this species into Europe could pose a threat to European pine plantations and natural forests. Consequently, it will be important to assess the susceptibility of European *Pinus* spp. to this pathogen and to prepare an *ad hoc* pest risk assessment for it.

## Acknowledgements

We thank Dr. Renaud Ioos (Agency for Food, Environmental and Occupational Health & Safety, France) and Dr. Kaitlin Mooneyham for kindly providing isolates from France and Virginia, respectively. The Nucleo Carabinieri per la Biodiversità (Cecina, Italy) is thanked for providing plants used in the pathogenicity tests. We also wish to thank Prof. Paolo Capretti (University of Florence, Italy) who supported us in studying *Caliciopsis* and who followed in the footsteps of Prof. Francesco Moriondo.

This study has received funding from the project “Holistic management of emerging forest pests and diseases” (HOMED) a European Union’s Horizon 2020 Programme for Research & Innovation under grant agreement No 771271.

## References

- Butin H (1970) Zwci neue *Caliciopsis*-Arctn auf chilenischen Koniferen. Journal of Phytopathology 69(1): 71–77. <https://doi.org/10.1111/j.1439-0434.1970.tb03903.x>
- Capretti P (1978) *Caliciopsis pinea* Peck parassita di *Pinus pinaster* e *Pinus insignis*. Phytopathologia Mediterranea 17(2): 101–104.
- Capretti P (1980) *Pinus nigra* var. *austriaca*, nuovo ospite di *Caliciopsis pinea* Peck. Informatore Fitopatologico 30(5): 19–21.
- Capretti P, Luchi N, Migliorini D (2013) Occurrence of *Caliciopsis pinea* Peck on pine: interactions with other fungal pathogens. In: Mendel University in Brno (Ed.) Proceedings of the IUFRO working party 7.02.02 Foliage, shoot and stem diseases of forest trees, ‘Biosecurity in natural forests and plantations, genomics and biotechnology for biosecurity in forestry’, Brno, Czech Republic (33).
- Costanza KKL, Whitney TD, McIntire CD, Livingston WH, Gandhi KJK (2018) A synthesis of emerging health issues of eastern white pine (*Pinus strobus*) in eastern North America. Forest Ecology and Management 423: 3–17. <https://doi.org/10.1016/j.foreco.2018.02.049>
- Crous PW, Schumacher PK, Akulov A, Thangavel R, Hernández-Restrepo M, Carnegie AJ, Cheewangkoon R, Wingfield MJ, Summerell BA, Quaedvlieg W, Coutinho TA. (2019) New and interesting fungi. 2. Fungal Systematics and Evolution 3(1): 57–134. <https://doi.org/10.3114/fuse.2019.03.06>
- Delatour C (1969) Contribution à l’étude du *Caliciopsis pinea* Peck: résultats complémentaires d’inoculations artificielles. Annales Des Sciences Forestières 26(2): 285–295. <https://doi.org/10.1051/forest/19690205>
- Fitzpatrick HM (1920) Monograph of the Coryneliaceae. Mycologia 12(4): 206–237. <https://doi.org/10.1080/00275514.1920.12016837>
- Fitzpatrick HM (1942) Revisionary studies in the Coryneliaceae. II. The genus *Caliciopsis*. Mycologia 34(5): 489–514. <https://doi.org/10.1080/00275514.1942.12020918>
- Garrido-Benavent I, Pérez-Ortega S (2015) Unravelling the diversity of European *Caliciopsis* (Coryneliaceae, Ascomycota): *Caliciopsis valentina* sp. nov. and *C. beckhausii* comb. nov., with a worldwide key to *Caliciopsis*. Mycological Progress 14(3): 1–10. <https://doi.org/10.1007/s11557-015-1034-2>
- Glass NL, Donaldson GC (1995) Development of primer sets designed for use with the PCR to amplify conserved genes from filamentous ascomycetes. Applied and Environmental Microbiology 61(4): 1323–1330. <https://doi.org/10.1128/AEM.61.4.1323-1330.1995>
- Haines SL, Costanza KKL, Livingston WH (2018) Compartmentalization process in eastern white pine (*Pinus strobus* L.) documented using a native fungal pathogen. Forest Ecology and Management 423: 94–105. <https://doi.org/10.1016/j.foreco.2018.03.003>

- Harrison KJ (2009) Forest disease records on eastern white pine in Atlantic Canada: 1950 to 1996. *Forestry Chronicle* 85(4): 604–608. <https://doi.org/10.5558/tfc85604-4>
- Hillis DM, Bull JJ (1993) An empirical test of Bootstrapping as a method for assessing confidence in phylogenetic analysis. *Systematic Biology* 42(2): 182–192. <https://doi.org/10.1093/sysbio/42.2.182>
- Intini M (1980) *Caliciopsis nigra* Schrader ex Fries, a parasite of *Cupressus sempervirens*. *Informatore Fitopatologico* 30(10): 7–9.
- Kumar S, Stecher G, Tamura K (2016) MEGA7: molecular evolutionary genetics analysis version 7.0 for bigger datasets. *Molecular Biology and Evolution* 33(7): 1870–1874. <https://doi.org/10.1093/molbev/msw054>
- Lanier L (1965) Note sur une espèce cryptogamique nouvelle pour la France sur différents Pins dont le Pin maritime des Landes. *Revue Forestière Française* 1: 1–34. <https://doi.org/10.4267/2042/24685>
- Larget B, Simon DL (1999) Markov chain Monte Carlo algorithms for the Bayesian analysis of phylogenetic trees. *Molecular Biology and Evolution* 16(6): 750–759. <https://doi.org/10.1093/oxfordjournals.molbev.a026160>
- Luchi N, Pepori AL, Bartolini P, Ioos R, Santini A (2018) Duplex real-time PCR assay for the simultaneous detection of *Caliciopsis pinea* and *Fusarium circinatum* in pine samples. *Applied Microbiology and Biotechnology* 102: 7135–7146. <https://doi.org/10.1007/s00253-018-9184-1>
- Maloy OC (1997) White pine blister rust control in North America: A case history. *Annual Review of Phytopathology* 35: 87–109. <https://doi.org/10.1146/annurev.phyto.35.1.87>
- Munck IA, Livingston W, Lombard K, Luther T, Ostrofsky WD, Weimer J, Wyka S, Broders K (2015) Extent and severity of *Caliciopsis* canker in New England, USA: An emerging disease of Eastern White Pine (*Pinus strobus* L.). *Forests* 6: 4360–4373. <https://doi.org/10.3390/f6114360>
- Munck IA, Luther T, Wyka S, Keirstead D, McCracken K, Ostrofsky W, Searles W, Lombard K, Weimer J, Allen B (2016) Soil and stocking effects on caliciopsis canker of *Pinus strobus* L. *Forests* 7(269): 1–10. <https://doi.org/10.3390/f7110269>
- Page RD (1996) Tree View: An application to display phylogenetic trees on personal computers. *Bioinformatics* 12(4): 357–358. <https://doi.org/10.1093/bioinformatics/12.4.357>
- Pascoe IG, McGee PA, Smith IW, Dinh SQ, Edwards J (2018) *Caliciopsis pleomorpha* sp. nov. (Ascomycota: Coryneliales) causing a severe canker disease of *Eucalyptus cladocalyx* and other eucalypt species in Australia. *Fungal Systematics and Evolution* 2: 45–56. <https://doi.org/10.3114/fuse.2020.05.13>
- Peck CH (1880) Report of the Botanist (1879) Annual Report on the New York State Museum of Natural History 33. <https://www.biodiversitylibrary.org/item/110212#page/291/mode/1up>
- Pepori AL, Kolařík M, Bettini PP, Vettrai AM, Santini A (2015) Morphological and molecular characterisation of *Geosmithia* species on European elms. *Fungal Biology* 119(11): 1063–1074. <https://doi.org/10.1016/j.funbio.2015.08.003>
- Pratibha J, Amandeep K, Shenoy B, Bhat D (2010) *Caliciopsis indica* sp. nov. from India. *MYCOSPHERE ONLINE-Journal of Fungal Biology* 1: 65–72. <http://irgu.unigoa.ac.in/drs/handle/unigoa/2394>

- Ramsfield TD, Shamoun SF, Van Der Kamp BJ (2009) The phenology and impact of *Caliciopsis arceuthobii* on lodgepole pine dwarf mistletoe, *Arceuthobium americanum*. *Botany* 87(1): 43–48. <https://doi.org/10.1139/B08-089>
- Ray WW (1936) Pathogenicity and cultural experiments with *Caliciopsis pinea*. *Mycologia* 28(3): 201–208. <https://doi.org/10.1080/00275514.1936.12017130>
- Rehm H (1896) Rabenhorst Kryptogamen Flora. Pilze – Ascomyceten 1(3): 1–382.
- Rehner SA, Buckley E (2005) A *Beauveria* phylogeny inferred from nuclear ITS and EF1- $\alpha$  sequences: evidence for cryptic diversification and links to *Cordyceps* teleomorphs. *Mycologia* 97(1): 84–98. <https://doi.org/10.1080/15572536.2006.11832842>
- Rikkinen J (2000) Two new species of *Caliciopsis* (Coryneliaceae) from Hunan Province, China. *Karstenia* 40(1–2): 147–151. <https://doi.org/10.29203/ka.2000.365>
- Ronquist F, Huelsenbeck JP (2003) MrBayes 3: Bayesian phylogenetic inference under mixed models. *Bioinformatics* 19(12): 1572–1574. <https://doi.org/10.1093/bioinformatics/btg180>
- Ronquist F, Huelsenbeck JP, van der Mark P (2005) MrBayes 3.1 Manual.
- Schulz AN, Mech AM, Asaro C, Coyle DR, Cram MM, Lucardi RD, Gandhi KJK (2018a) Assessment of abiotic and biotic factors associated with eastern white pine (*Pinus strobus* L.) dieback in the Southern Appalachian Mountains. *Forest Ecology and Management* 423: 59–69. <https://doi.org/10.1016/j.foreco.2018.02.021>
- Schulz AN, Mech AM, Cram MM, Asaro C, Coyle DR, Lucardi RD, Lucas S, Gandhi KJK (2018b) Association of *Caliciopsis pinea* Peck and *Matsucoccus macrocitrices* Richards with eastern white pine (*Pinus strobus* L.) seedling dieback. *Forest Ecology and Management* 423: 70–83. <https://doi.org/10.1016/j.foreco.2018.03.013>
- Stöver BC, Müller KF (2010) TreeGraph 2: combining and visualizing evidence from different phylogenetic analyses. *BMC Bioinformatics* 11(1): 1–7. <https://doi.org/10.1016/j.foreco.2018.03.013>
- TreeView (2006, 2008) TreeView. <http://taxonomy.zoology.gla.ac.uk/rod/treeview.html>
- White TJ, Bruns TD, Lee SB, Taylor JW (1990) Analysis of phylogenetic relationships by amplification and direct sequencing of ribosomal RNA genes. In: Innis MA, Gelfand DH, Sninsky JJ, White TJ (Eds) *PCR Protocols: a guide to methods and applications*. Academic Press, San Diego, 315–322. <https://doi.org/10.1016/B978-0-12-372180-8.50042-1>
- Whitney TD, Cram MM, Barnes BF, Yao J, Lucardi RD, Gandhi KJK (2018) Tree-level distribution of a novel insect-pathogen complex and its potential contribution to eastern white pine dieback. *Forest Ecology and Management* 423: 49–58. <https://doi.org/10.1016/j.foreco.2018.02.002>
- Wijayawardene NN, Hyde KD, Al-Ani LKT, Tedersoo L, Haelewaters D, Rajeshkumar KC, Zhao RL, Aptroot A, Leontyev DV, Saxena RK, Tokarev YS, Dai DQ, Letcher PM, Stephenson SL, Ertz D, Lumbsch HT, Kukwa M, Issi IV, Madrid H, Phillips AJL, Selbmann L, Pfliegler WP, Horváth E, Bensch K, Kirk PM, Kolaříková K, Raja HA, Radek R, Papp V, Dima B, Ma J, Malosso E, Takamatsu S, Rambold G, Gannibal PB, Triebel D, Gautam AK, Avasthi S, Suetrong S, Timdal E, Fryar SC, Delgado G, Réblová M, Doilom M, Dola-

- tabadi S, Pawłowska JZ, Humber RA, Kodsueb R, Sánchez-Castro I, Goto BT, Silva DKA, de Souza FA, Oehl F, da Silva GA, Silva IR, Błaszowski J, Jobim K, Maia LC, Barbosa FR, Fiuza PO, Divakar PK, Shenoy BD, Castañeda-Ruiz RF, Somrithipol S, Lateef AA, Karunarathna SC, Tibpromma S, Mortimer PE, Wanasinghe DN, Phookamsak R, Xu J, Wang Y, Tian F, Alvarado P, Li DW, Kušan I, Matočec N, Mešić A, Tkalčec Z, Maharachchikumbura SSN, Papizadeh M, Heredia G, Wartchow F, Bakhshi M, Boehm E, Youssef N, Hustad VP, Lawrey JD, Santiago ALCMA, Bezerra JDP, Souza-Motta CM, Firmino AL, Tian Q, Houbraken J, Hongsanan S, Tanaka K, Dissanayake AJ, Monteiro JS, Grossart HP, Suija A, Weerakoon G, Etayo J, Tsurukau A, Vázquez V, Mungai P, Damm U, Li QR, Zhang H, Boonmee S, Lu YZ, Becerra AG, Kendrick B, Brearley FQ, Motiejūnaitė J, Sharma B, Khare R, Gaikwad S, Wijesundara DSA, Tang LZ, He MQ, Flakus A, Rodriguez-Flakus P, Zhurbenko MP, McKenzie EHC, Stadler M, Bhat DJ, Liu JK, Raza M, Jeewon R, Nassonova ES, Prieto M, Jayalal RGU, Erdoğan M, Yurkov A, Schnittler M, Shchepin ON, Novozhilov YK, Silva-Filho AGS, Gentekaki E, Liu P, Cavender JC, Kang Y, Mohammad S, Zhang LF, Xu RF, Li YM, Dayarathne MC, Ekanayaka AH, Wen TC, Deng CY, Pereira OL, Navathe S, Hawksworth DL, Fan XL, Dissanayake LS, Kuhnert E, Grossart HP, Thines M (2020) Outline of Fungi and fungus-like taxa. *Mycosphere* 11(1): 1060–1456. <https://doi.org/10.5943/mycosphere/11/1/8>
- Wood AR, Damm U, Van der Linde EJ, Groenewald JZ, Cheewangkoon R, Crous PW (2016) Finding the missing link: Resolving the Coryneliomycetidae within Eurotiomycetes. *Persoonia – Molecular Phylogeny and Evolution of Fungi* 37: 37–56. <https://doi.org/10.3767/003158516X689800>

## Supplementary material I

### Figure S1. One of the most parsimonious trees from EF1- $\alpha$ sequence datasets

Authors: Duccio Migliorini, Nicola Luchi, Alessia Lucia Pepori, Francesco Pecori, Chiara Aglietti, Fabio Maccioni, Isabel Munck, Stephen Wyka, Kirk Broders, Michael J. Wingfield, Alberto Santini

Data type: Alignment of genomic sequences

Explanation note: One of the most parsimonious trees from EF1- $\alpha$  gene sequence datasets is shown (length = 66, CI = 0.9999, RI = 0.9998, RC = 0.9988, HI = 0.9888).

The MP and Bayesian posterior probability are indicated next to the branches. *C. pseudotsugae* and *C. orientalis* are used as outgroup.

Copyright notice: This dataset is made available under the Open Database License (<http://opendatacommons.org/licenses/odbl/1.0/>). The Open Database License (ODbL) is a license agreement intended to allow users to freely share, modify, and use this Dataset while maintaining this same freedom for others, provided that the original source and author(s) are credited.

Link: <https://doi.org/10.3897/mycokeys.73.53028.suppl1>

## Supplementary material 2

### Figure S2. One of the most parsimonious trees from Bt1 sequence datasets

Authors: Duccio Migliorini, Nicola Luchi, Alessia Lucia Pepori, Francesco Pecori, Chiara Aglietti, Fabio Maccioni, Isabel Munck, Stephen Wyka, Kirk Broders, Michael J. Wingfield, Alberto Santini

Data type: Alignment of genomic sequences

Explanation note: One of the most parsimonious trees from Bt1 sequence datasets is shown (CI = 0.9268, RI = 0.9840, RC = 0.936428, HI = 0.912039). The MP and Bayesian posterior probability are indicated next to the branches. *C. pseudotsugae* and *C. orientalis* are used as outgroup.

Copyright notice: This dataset is made available under the Open Database License (<http://opendatacommons.org/licenses/odbl/1.0/>). The Open Database License (ODbL) is a license agreement intended to allow users to freely share, modify, and use this Dataset while maintaining this same freedom for others, provided that the original source and author(s) are credited.

Link: <https://doi.org/10.3897/mycokeys.73.53028.suppl2>

# Four new species of *Trichoderma* in the *Harzianum* clade from northern China

Xin Gu<sup>1\*</sup>, Rui Wang<sup>1\*</sup>, Quan Sun<sup>1</sup>, Bing Wu<sup>2</sup>, Jing-Zu Sun<sup>2</sup>

**1** School of Agriculture, Ningxia University, Yinchuan, Ningxia 750021, China **2** State Key Laboratory of Mycology, Institute of Microbiology, Chinese Academy of Sciences, No. 3 Park 1, Beichen West Road, Chaoyang District, Beijing 100101, China

Corresponding author: Jing-Zu Sun ([sunjz@im.ac.cn](mailto:sunjz@im.ac.cn))

---

Academic editor: T. Lumbsch | Received 24 February 2020 | Accepted 8 September 2020 | Published 8 October 2020

---

**Citation:** Gu X, Wang R, Sun Q, Wu B, Sun J-Z (2020) Four new species of *Trichoderma* in the *Harzianum* clade from northern China. MycoKeys 73: 109–132. <https://doi.org/10.3897/mycokeys.73.51424>

---

## Abstract

The *Harzianum* clade of *Trichoderma* comprises many species, which are associated with a wide variety of substrates. In this study, four new species of *Trichoderma*, namely *T. lentinulae*, *T. vermifimicola*, *T. xixiacum*, and *T. zelobreve*, were encountered from a fruiting body and compost of *Lentinula*, soil, and vermicompost. Their colony and mycelial morphology, including features of asexual states, were described. For each species, their DNA sequences were obtained from three loci, the internal transcribed spacer (ITS) regions of the ribosomal DNA, the gene encoding the second largest nuclear RNA polymerase subunit (RPB2), the translation elongation factor 1- $\alpha$  encoding gene (TEF1- $\alpha$ ). The analysis combining sequences of the three gene regions distinguished four new species in the *Harzianum* clade of *Trichoderma*. Among them, *T. lentinulae* and *T. xixiacum* clustered with *T. lixii*, from which these new species differ in having shorter phialides and smaller conidia. Additionally, *T. lentinulae* differs from *T. xixiacum* in forming phialides with inequilateral to a strongly-curved apex, cultural characteristics, and slow growth on PDA. *Trichoderma vermifimicola* is closely related to *T. simmonsii*, but it differs from the latter by producing phialides in verticillate whorls and smaller conidia. *Trichoderma zelobreve* is the sister species of *T. breve* but is distinguished from *T. breve* by producing shorter and narrower phialides, smaller conidia, and by forming concentric zones on agar plates. This study updates our knowledge of species diversity of *Trichoderma*.

## Keywords

compost, fungicolous, Hypocreaceae, mycoparasite

---

\* Authors contributed equally to this work

## Introduction

The genus *Trichoderma* Pers., introduced by Persoon (1794), is cosmopolitan, including saprotrophs and mycoparasites in a diversity of ecosystems, such as agricultural fields, prairies, forests, salt marshes, and fungal fruiting body (Gazis and Chaverri 2010; Chaverri et al. 2015; Qiao et al. 2018). Species of this genus have been widely used in the biocontrol of plant pathogens (Chaverri et al. 2015; Degenkolb et al. 2015; Bunbury-Blanchette and Walke 2019) and production of enzymes and bioactive compounds (Sun et al. 2016). Nevertheless, some of them are associated with green mold diseases in the commercial production of mushrooms (Innocenti et al. 2019; Sun et al. 2019a). Morphologically, the asexual-morphs are similar in producing branched tree-like conidiophores with cylindrical to nearly subglobose phialides and ellipsoidal to globose conidia, but their variation is insufficient to differentiate the *Trichoderma* species (Chaverri et al. 2015; Qin and Zhuang 2017; Qiao et al. 2018). Multilocus molecular phylogeny, based on combined sequence data of the internal transcribed spacer (ITS) regions, RNA polymerase II subunit (RPB2), and the translation elongation factor 1- $\alpha$  gene (TEF1- $\alpha$ ), enables rapid and accurate identification of the *Trichoderma* species (Druzhinina et al. 2005; Atanasova et al. 2013; Chaverri et al. 2015). Currently, the combination of multi-gene phylogenetic analysis and phenotypic characteristics is extensively applied in species delimitation of *Trichoderma* (du Plessis et al. 2018; Qiao et al. 2018; Innocenti et al. 2019).

*Trichoderma harzianum* Rifai is one of the most well-known *Trichoderma* species, due to its antifungal properties and effective bio-control ability, used to suppress soil-borne plant pathogens (Chaverri et al. 2015; Degenkolb et al. 2015; Bunbury-Blanchette and Walker 2019). As a cosmopolitan and ubiquitous fungus, it has been isolated from diverse substrates, such as soil, plant tissue, and mushrooms (Chaverri et al. 2015; Jaklitsch and Voglmayr 2015; Innocenti et al. 2019; Sun et al. 2019b). Since Chaverri et al. (2015) provided a systematic revision of species in the *Harzianum* clade, numerous new species have been described (Jaklitsch and Voglmayr 2015; Qin and Zhuang 2016a; Sun et al. 2016; Chen and Zhuang 2017b; Qiao et al. 2018). Currently, more than 60 species are placed in the *Harzianum* clade (Jaklitsch and Voglmayr 2015; Qin and Zhuang 2016a, b, 2017; Chen and Zhuang 2017b; Qiao et al. 2018; Phookamsak et al. 2019; ).

It is estimated that 136 new species of *Trichoderma* have been recognised since 2015 ([www.indexfungorum.org](http://www.indexfungorum.org) 2020), with 84 among these reported from China (Sun et al. 2012; Qin and Zhuang 2016a, b, 2017; Chen and Zhuang 2017a, b; Qiao et al. 2018), which evidenced that China has a high species diversity of *Trichoderma* (Zhu and Zhuang 2015; Jiang et al. 2016). In our survey of *Trichoderma*, eighteen isolates were obtained from soil, mushroom substrates, and vermicompost from northern China. Four new species belonging to the *Harzianum* clade were identified based on morphological features and DNA sequence data at three loci: the genes encoding RNA polymerase II subunit (RBP2) and translation elongation factor 1- $\alpha$  gene (TEF1- $\alpha$ ), and the internal transcribed spacer (ITS) regions of the nuclear ribosomal RNA gene.

## Materials and methods

### Sampling sites and strains isolation

Since *Trichoderma* is easily isolated from soil, mushroom substrates, and earthworm substrates, the soil, mushroom substrates, and earthworm were therefore collected from Yinchuan, Ningxia Hui Autonomous Region, and Chaoyang district, Beijing, China. All the samples were stored at 4 °C before fungal isolation. *Trichoderma* strains were isolated by gradient dilution and the spread plate method or directly from the mushroom substrates. Three dilutions ( $10^{-1}$ ,  $10^{-2}$ , and  $10^{-3}$ ) were prepared with 1 g soil and sterile water, and 100 µl of each dilution was spread on a 9 cm diameter Petri dish of PDA agar with 100 mg/L chloramphenicol added. The plates were then incubated at 25 °C. Each of the individual colonies was transferred to a new PDA dish after 1–3 days and incubated at 25 °C. Dried cultures from the single spore or specimens of new species were deposited in the Herbarium Mycologicum Academiae Sinicae (HMAS) and the ex-type strains were preserved in the China General Microbiological Culture Collection Center (CGMCC).

### Morphological analysis

For morphological studies, we used three different media: cornmeal dextrose agar (CMD, Difco, BD Science, USA), PDA (Difco, BD Science, USA), and synthetic low nutrient agar (SNA, Difco, BD Science, USA) (Chaverri et al. 2015). Each strain was first cultured on an SNA plate for 3 days and a small agar piece of 0.5 cm diameter with mycelium was then transferred, respectively, to new CMD, PDA, and SNA plates. Strains were incubated in 9 cm diam with three replicates. Petri dishes at 25 °C with a 12 h natural light and 12 h darkness interval. Colony diameter at 25 °C was measured three days after inoculation, and the time when mycelium entirely covered the surface of the agar plate was also recorded. Micromorphological characters were examined from the cultures of one-week-old colonies on SNA (Chaverri et al. 2015). A Nikon Ellipse 80i light microscope, equipped with differential interference contrast (DIC) optics, was used to capture digital images.

### DNA extraction, PCR and sequencing

Genomic DNA of each strain was extracted from fresh mycelium growing on PDA after 5 days of growth following the rapid “thermolysis” method described in Zhang et al. (2010). For the amplification of ITS, RPB2, and TEF1- $\alpha$  gene fragments, ITS4 and ITS5 for ITS (White et al. 1990), EF1-728F (Carbone and Kohn 1999) and TEF1LLerev (Jaklitsch et al. 2005) for TEF1, and RPB2-5F and RPB2-7R for rpb2 (Liu et al. 1999) were used. Each PCR reaction consisted of 12.5 µl T5

Super PCR Mix (containing Taq polymerase, dNTP, and  $Mg^{2+}$ , Beijing TsingKe Biotech Co. Ltd., Beijing), 1.0  $\mu$ l of forward primer (10  $\mu$ M), 1.0  $\mu$ l of reverse primer (10  $\mu$ M), 0.5  $\mu$ l DMSO, 3  $\mu$ l DNA template and 7  $\mu$ l double sterilized water. PCR reactions were in Eppendorf Mastercycler, following the protocols described by Sun et al. (2016). PCR products were purified with the PCR product purification kit (TIANGEN Biotech, Beijing, China), and sequencing was carried out in both directions on an ABI 3730 XL DNA sequencer (Applied Biosystems, Foster City, California) with primers used during PCR amplification.

### Phylogenetic analyses

Preliminary BLAST searches with ITS, RPB2, and TEF1- $\alpha$  gene sequences of the new isolates against NCBI, TrichOKey (Druzhinina and Kopchinski 2006), and TrichoBlast (Kopchinskiy et al. 2005) databases identified species closely related to our isolates. Based on this information, sequences of ITS, RPB2, and TEF1- $\alpha$  of 133 strains, representing 59 species were downloaded from GenBank, following recent publications (Qin and Zhuang 2017; Qiao et al. 2018; Innocenti et al. 2019). Among them, 139 strains are belonging to the *Harzianum* clade, and *Trichoderma ceramicum*, *T. parestonicum*, and *T. estonicum* were chosen to represent the outgroup.

Tree alignment files were generated by using MAFFT version 7.03 with the Q-INS-I strategy (Kato and Standley 2013). Conserved blocks were selected from the initial alignments with Gblocks 0.91 b (Castresana 2000). The appropriate nucleotide substitution model for each gene was determined by using MrModeltest v2.4 (Nylander 2004). HKY + I + G was estimated as the best-fit model for RPB2, and GTR + I + G was estimated as the best-fit model for TEF1- $\alpha$  and ITS under the output strategy of AIC. The partition homogeneity test ( $p = 0.01$ ) indicated that the individual partitions were not significantly incongruent (Cunningham 1997), thus the aligned sequences of ITS, RPB2, and TEF1- $\alpha$  were combined for analyses. The multi-locus phylogenetic analyses included 1065 characters for RPB2, 587 characters for TEF1- $\alpha$ , and 555 characters for ITS. All characters were weighted equally and gaps were treated as missing characters.

Maximum Likelihood (ML) analyses were performed by RAxML (Stamatakis 2006), using the GTR-GAMMA-I model. The maximum likelihood bootstrap proportions (MLBP) were using 1000 replicates. Bayesian Inference (BI) analyses were conducted with MrBayes v3.2.6 (Ronquist et al. 2012). Metropolis-coupled Markov Chain Monte Carlo (MCMC) searches were calculated for 10,000,000 generations, sampling every 100<sup>th</sup> generation with the best best-fit model for each gene. Two independent analyses with six chains each (one cold and five heated) were carried out until the average standard deviation of the split frequencies dropped below 0.01. The initial 25% of the generations of MCMC sampling were discarded as burn-in. The refinement of the phylogenetic tree was used for estimating Bayesian

inference posterior probability (PP) values. The Tree was viewed in FigTree v1.4 (Rambaut 2012), values of Maximum likelihood bootstrap proportions (MLBP) greater than 50% and Bayesian inference posterior probabilities (BIPP), greater than 95% at the nodes, are shown along branches. The final alignments and the trees obtained have been deposited in TreeBASE (TreeBASE accession number: 25400).

## Results

### Phylogeny

The preliminary BLAST searches with ITS, RPB2, and TEF1- $\alpha$  gene sequences of the new isolates suggest our isolates were highly similar to species from *Trichoderma* in the *Harzianum*-complex. Therefore, as the next step phylogenetic analyses were conducted by using a single gene of ITS, RPB2, TEF1- $\alpha$ , and multi-gene dataset of cascaded ITS, RPB2, and TEF1- $\alpha$ , respectively. The phylogenetic trees showed that our isolates were placed in the *Harzianum* clade (Fig. 1, Suppl. material 1: Fig. S1, Suppl. material 2: Fig. S2, Suppl. material 3: Fig. S3). In the phylogenetic tree conducted by a combined matrix of ITS, RPB2, and TEF1- $\alpha$  sequences, isolates of *T. lentinulae*, *T. xixiacum*, and *T. lixii* formed a well-supported clade (MLBP/BIBP = 73%/1.00). Within this clade, isolates of *T. lentinulae* and *T. xixiacum* formed a subclade with maximum support. Isolates of *T. vermifimicola* clustered together with *T. simmonsii* (BIBP = 1.00), both forming a subclade with maximum support (MLBP/BIBP = 100%/1.00, Fig. 1). *Trichoderma zelobreve* and *T. breve*, were distinguished by maximum support to respective clades while forming a highly supported clade (MLBP/BIBP = 100%/1.00, Fig. 1).

The ITS gene could not distinguish our isolates from other species within the *Harzianum* clade (Suppl. material 1: Fig. S1). In the phylogenetic tree resulted from the RPB2 gene, *Trichoderma lentinulae*, *T. xixiacum*, and *T. lixii* formed a highly supported clade (MLBP/BIBP = 100%/1.00), but within this clade, *T. lentinulae*, *T. xixiacum* were not distinguished (Suppl. material 2: Fig. S2). Isolates of *T. vermifimicola* formed a distinct clade (MLBP/BIBP = 100%/1.00) and grouped with *T. simmonsii*, *T. guizhouense*, and *T. rugulosum* but weakly supported (Suppl. material 3: Fig. S3). *Trichoderma zelobreve* and *T. breve* also formed a highly supported clade (MLBP/BIBP = 98%/1.00), but *T. zelobreve* and *T. breve*, were distinguished by maximum support to respective clades while forming a highly supported clade (MLBP/BIBP = 100%/1.00, Suppl. material 2: Fig. S2). In the phylogenetic tree resulted from the TEF1- $\alpha$  gene, *T. zelobreve* and *T. breve* also formed a highly supported clade (MLBP/BIBP = 98%/1.00), but were not distinct from each other (Suppl. material 3: Fig. S3). Isolates of *T. lentinulae*, *T. xixiacum*, *T. vermifimicola*, and *T. simmonsii* clustered together but this clade was not well-supported. Within this clade, isolates of *T. lentinulae* formed a well-supported subclade (MLBP/

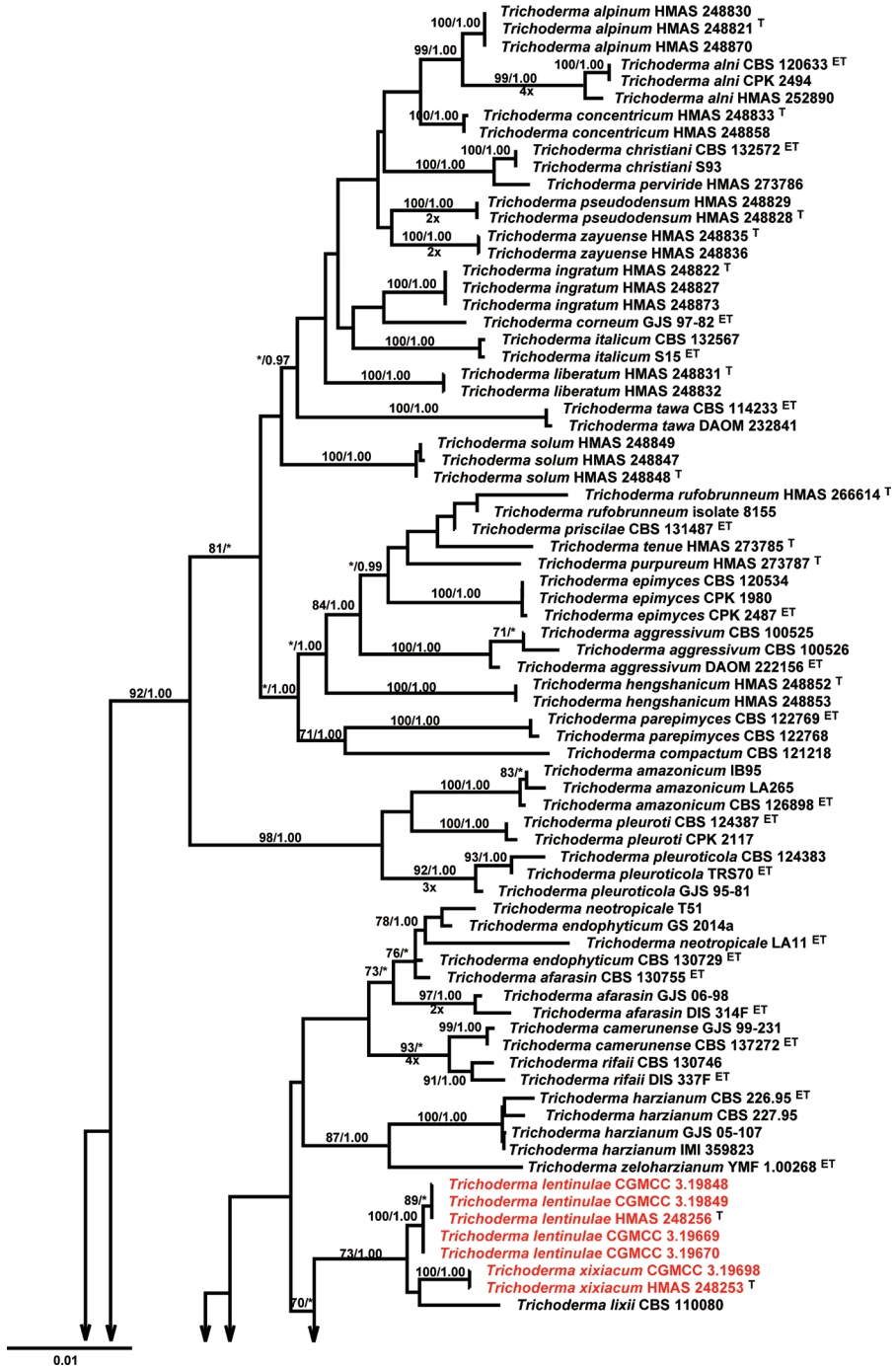


**Figure 1.** Phylogenetic tree based on Maximum Likelihood analysis of a combined ITS, RPB2, and TEF1 $\alpha$  sequence dataset. *Trichoderma estonicum*, *Trichoderma parastinicum*, *Trichoderma ceramicum* were chosen as the outgroup. Bootstrap Values higher than 70% from RAXML (BSML) (left) and Bayesian posterior probabilities greater than 0.95 (BYPP) (right) are given above the nodes. <sup>T</sup> indicates the type; <sup>ET</sup> indicates the ex-living type. Isolates obtained in this study are in red.

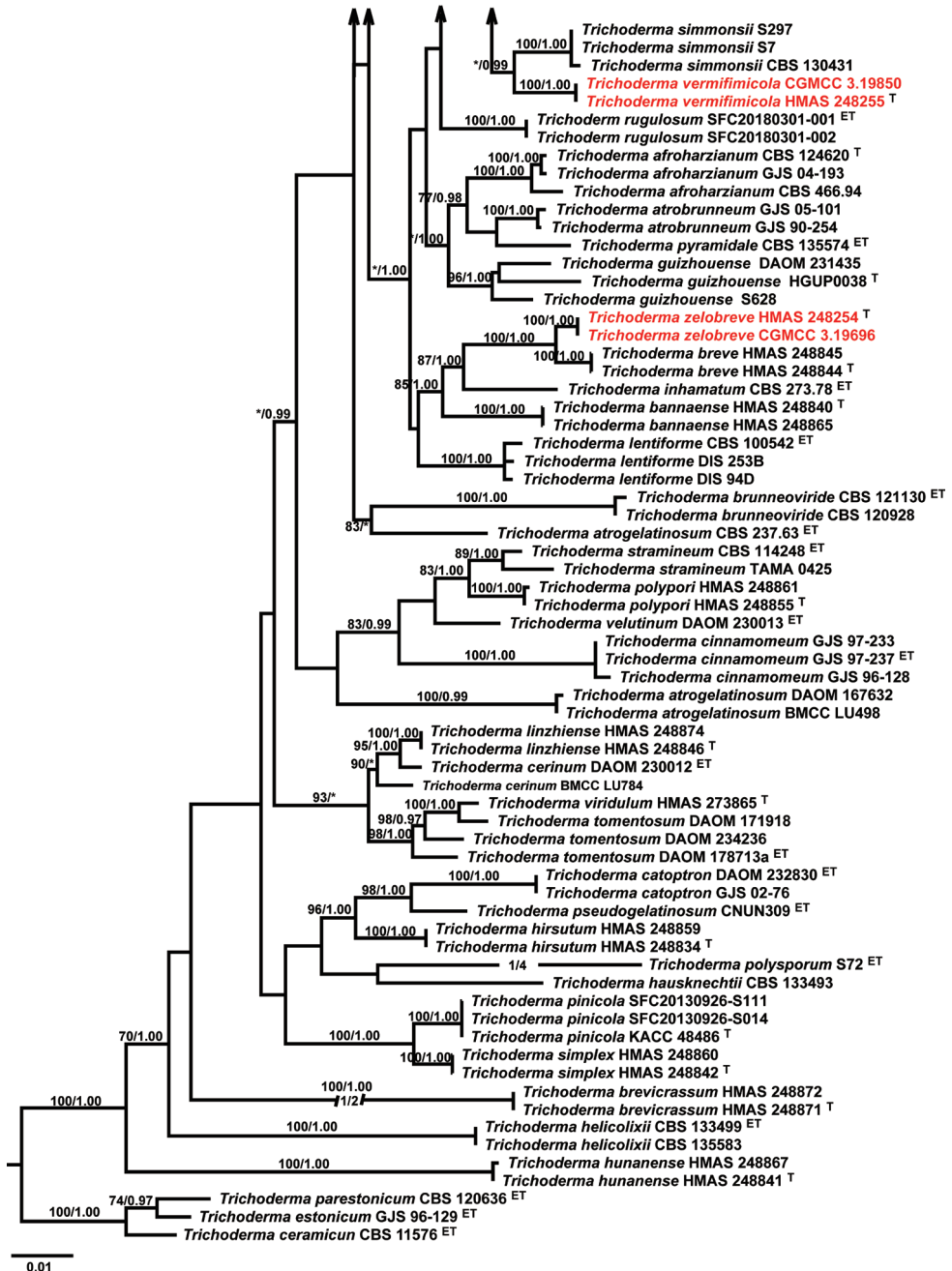


Figure 1. Continued.

BIBP = 91%/1.00). *Trichoderma xixiacum* and *T. vermifimicola* formed a highly supported subclade (MLBP/BIBP = 100%/1.00). Within this group, isolates of *T. vermifimicola* clustered together with well-supported (MLBP/BIBP = 93%/1.00, Suppl. material 3: Fig. S3).

## Taxonomy

### *Trichoderma lentinulae* Jing Z. Sun & X.Z. Liu, sp. nov.

Mycobank No: 833233

Fig. 2

**Etymology.** Latin, *lentinulae*, refers to the host from which the fungus was isolated.

**Type.** CHINA. Haidian District, Beijing, 39°57'40"N, 116°19'40"E, ca. 27 m elev., from a fruiting body and mushroom spawn of *Lentinula edodes*, 19 Oct 2018, Jing Z. Sun (HMAS 248256, holotype), ex-type culture CGMCC 3.19847.

**Description.** On CMD after 72 h, colony radius 57–58 mm at 25 °C, covering the plate at 30 °C, 4–5 mm at 35 °C. Colony hyaline, weak, indistinctly radial. Aerial hyphae short, inconspicuous. No diffusing pigment noted, odor indistinct (Fig. 2B). Conidial production noted after 3 days, scant, effuse in aerial hyphae, becoming blue-green after 7 days. Chlamydospores not observed.

On PDA after 72 h, colony radius 45–46 mm at 25 °C, mycelium covering the plate at 30 °C, 11–12 mm at 35 °C. Colony white to yellowish-white, regularly circular, indistinctly zonate; mycelium dense and radial. No diffusing pigment, not distinct odor (Fig. 2A). Conidial production noted after 3 days, starting around the original inoculum, effuse in the aerial hyphae, first white, turning green after 3 d. Chlamydospores unobserved.

On SNA after 72 h, colony radius 51–52 mm at 25 °C, 52–53 mm at 30 °C, 4–5 mm at 35 °C. Colony hyaline, indistinctly zonate; mycelium loose, especially at the margin. Aerial hyphae loose. No diffusing pigment, not distinct odor (Fig. 2C). Conidial production noted after 2 days, starting around the inoculum, effuse in the aerial hyphae. Small pustules formed around the inoculum, first white, turning green after 3 d, with hairs protruding beyond the surface. Conidiophores pyramidal with opposing branches, less frequently solitary, closely-spaced branches, each branch, and the main axis terminating in 2–5 cruciately to nearly verticillately disposed phialides (Fig. 2F, H, I). Phialides ampulliform, typically strongly constricted below the tip, less frequently lageniform and then usually apex and inequilateral to strongly curved, hyaline, (3.5–)4.0–6.0(–6.5) × (2.0–)2.5–3.0(–3.5) μm ( $\bar{x}$  = 4.5 × 3.0 μm, n = 30), length/width ratio (1.5–)2.0–3.0(–5.0) ( $\bar{x}$  = 2.0, n = 30), base 1.0–2.5 μm ( $\bar{x}$  = 1.5 μm)(Fig. 2G, H, I). Conidia ovoid to globose, smooth, hyaline when young, becoming green to dark green with age, (2.0–)2.5–3.0(–3.5) × (1.5–)2.0–2.5(–3.0) μm ( $\bar{x}$  = 2.5 × 2.2 μm, n = 50), length/width ratio (1.0–)1.1–1.4 (–1.5) ( $\bar{x}$  = 1.2, n = 50) (Fig. 2J). Chlamydospores common, apex or intercalary, ellipsoid or subglobose, (3.5–)5.0–6.5(–7.0) × (3.0–)4.0–5.0(–6.0) μm ( $\bar{x}$  = 5.5 × 4.5 μm, n = 30), length/width ratio (1.0–)1.2–1.5 (–1.7) ( $\bar{x}$  = 1.2, n = 30) (Fig. 2K–M).

**Additional specimen examined.** CHINA. Haidian District, Beijing, 39°57'40"N, 116°19'40"E, ca. 27 m elev., From a fruiting body and mushroom spawn of *Lentinula edodes*, 19 Oct 2018, Jing Z. Sun, living culture CGMCC 3.19848; Xixia District, Yinchuan, Ningxia Hui Autonomous Region, 38°38'52"N, 106°9'33"E, ca. 1127 m elev., from rhizosphere soil of *Lycium chinensis*, 17 Oct 2018, Jing Z. Sun, living culture CGMCC 3.19699; *ibid.*, living culture CGMCC 3.19670.

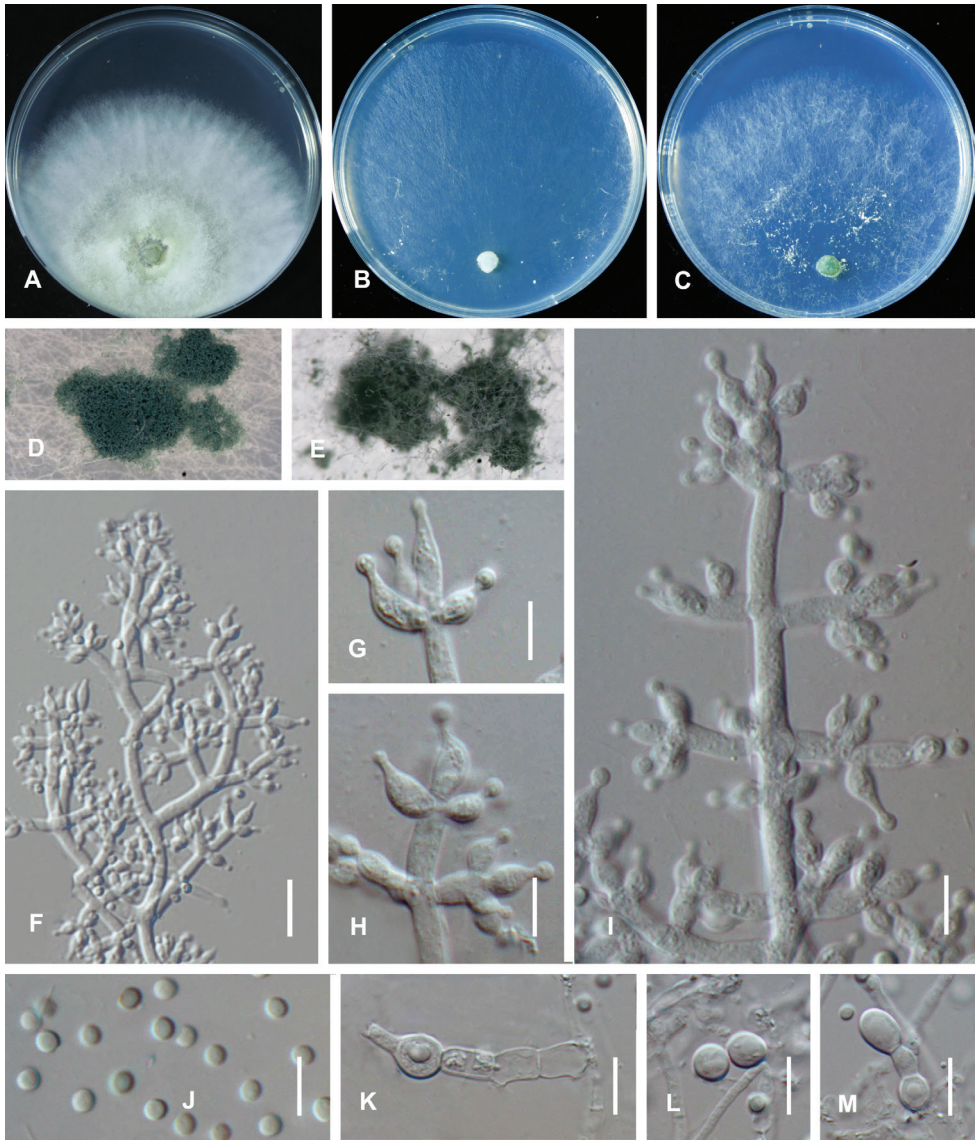


**Figure 2.** *Trichoderma lentinulae* (CGMCC 3.19847). Cultures at 25 °C after 3 days (**A** on PDA **B** on CMD **C** on SNA) **D** condiation pustules on CMD after 10 days **E** condiation pustules on CMD after 10 d **F** conidiophores **G–I** Conidiophores and phialides **J** conidia **K–M** chlamydsopores. Scale bars: 25 µm (**F**); 10 µm (**G–M**).

**Teleomorph.** Undetermined.

**Note.** The species is characterized by tree-like conidiophores, phialides verticillate or in whorls of 3–4, spindle-like to fusiform phialides ( $4.0\text{--}6.0 \times 2.5\text{--}3.0 \mu\text{m}$ ) and ovoid to subglobose conidia. Differs from *T. lixii* by shorter and wider phialides and smaller conidia. Differs from *Trichoderma xixiacum* by compact, relatively smaller phialides, and the pustules not forming distinctly zonate of pustules on SNA.

***Trichoderma vermifimicola* Jing Z. Sun & X.Z. Liu, sp. nov.**

MycoBank No: 833234

Fig. 3

**Etymology.** Latin, *vermifimicola*, refers to the habitat of the type species.

**Type.** CHINA. Yongning, Yinchuan, the Ningxia Hui Autonomous Region, 40°0'41"N, 116°23'37"E, ca. 1678 m elev., from the substrates for earthworm cultivation, 18 Oct 2018, Jing Z. Sun (HMAS 248255, holotype), ex-type culture CGMCC 3.19694.

**Description.** On CMD after 72 h, colony radius 49–51 mm at 25 °C, 51–52 mm at 30 °C, 4–5 mm at 35 °C. Colony hyaline, irregularly circular, indistinctly zonate; mycelium loose. Aerial hyphae short, inconspicuous. No diffusing pigment, not distinct odor. Conidial production noted after 3 days, starting around the inoculum (Fig. 3B). Small pustules formed at the colony margin, first white, turning blue-green after 7 d, with hairs protruding beyond the surface. Chlamydo spores unobserved.

On PDA after 72 h, colony radius 55–58 mm at 25 °C, 55–56 mm at 30 °C, 5–6 mm at 35 °C. Colony white-green to bright green, regularly circular, distinctly zonate; mycelium dense and radial. Aerial hyphae short, inconspicuous. No diffusing pigment, not distinct odor. Conidial production noted after 2 days, starting around the inoculum, effuse in the aerial hyphae, first white, turning green after 2 d (Fig. 3A). Chlamydo spores unobserved.

On SNA after 72 h, colony radius 48–50 mm at 25 °C, 51–52 mm at 30 °C, 3–4 mm at 35 °C. Colony hyaline, regularly circular, distinctly zonate; mycelium loose, especially at the margin. Aerial hyphae short, inconspicuous. No diffusing pigment, not distinct odor. Conidial production noted after 2 days, starting around the inoculum, effuse in the aerial hyphae. Small pustules formed along with two concentric rings, first white, turning yellow-green after 3 d, with hairs protruding beyond the surface (Fig. 3C). Conidiophores pyramidal with opposing branches, the distance between branches relatively large, each branch terminating in a whorl of 2–3 phialides, phialides sometimes solitary on the main axis (Fig. 3E, H, K); whorls typically cruciate, but often nearly verticillate (Fig. 3K); rarely conidiophores nodose and phialides disposed in more or less botryose clusters (Fig. 3H). Phialides ampulliform to lageniform, often constricted below the tip to form a narrow neck, hyaline, (4.4–)5.0–10.5(–11.2) × (2.0–)2.5–3.0(–3.5) μm ( $\bar{x}$  = 6.6 × 2.7 μm, n = 30), length/width ratio (1.5–)1.8–2.8(–5.3) ( $\bar{x}$  = 2.4, n = 30), base 1.6–2.5 μm ( $\bar{x}$  = 1.9 μm) (Fig. 3G, I, K). Conidia ovoid to subglobose, smooth, hyaline when young, becoming green to dark green with age, (2.0–)2.3–2.6(–3.0) × (1.5–)2.0–2.4(–2.8) μm ( $\bar{x}$  = 2.4 × 2.2 μm, n = 50), length/width ratio (1.0–)1.1–1.4(–1.7) ( $\bar{x}$  = 1.2, n = 50) (Fig. 3J). Chlamydo spores unobserved. No odor; no diffusing pigment observed.

**Additional specimen examined.** CHINA. Xixia District, Yinchuan, Ningxia Hui Autonomous Region, 38°38'52"N, 106°9'33"E, ca. 1127 m elev., from rhizosphere soil of *Lycium chinensis*, 17 Oct 2018, Jing Z. Sun, living CGMCC 3.19697.

**Teleomorph.** Undetermined.

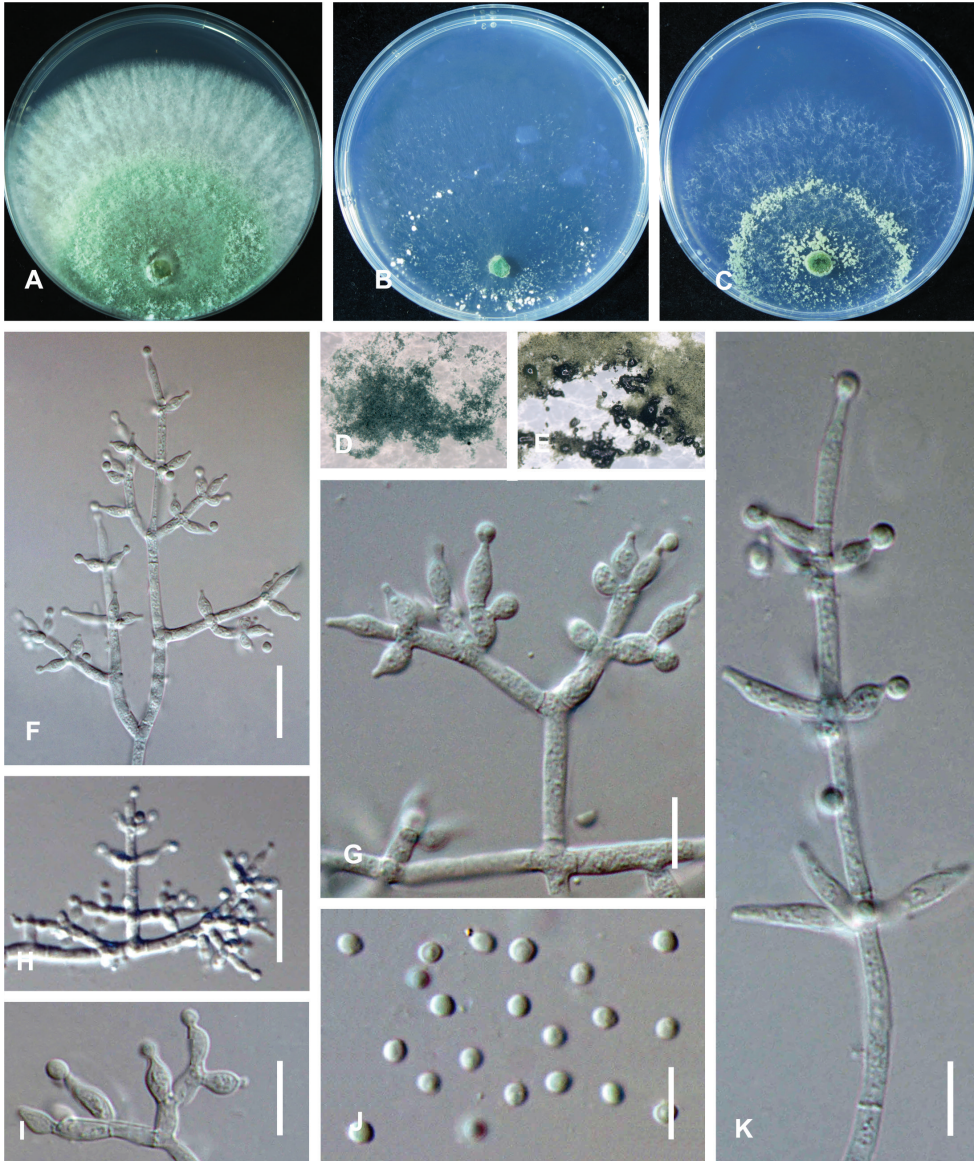


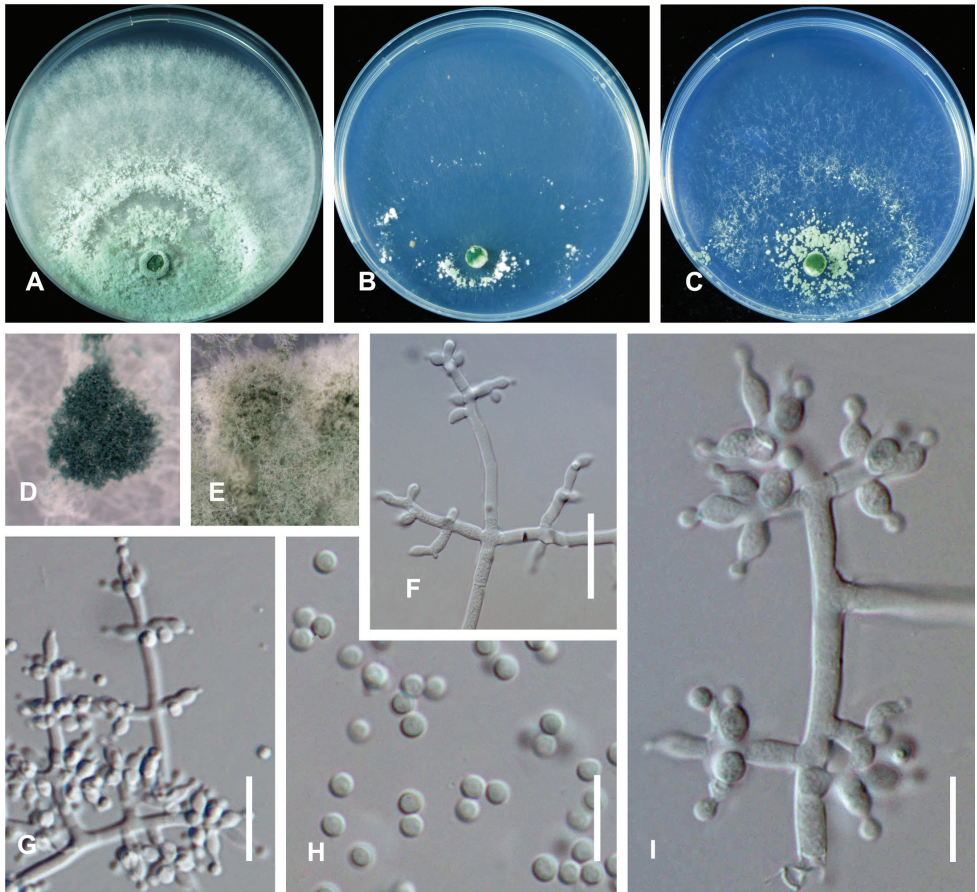
**Figure 3.** *Trichoderma vermifimicola* (CGMCC 3.19694). Cultures at 25 °C after 3 days (**A** on PDA **B** on CMD **C** on SNA) **D** conidiation pustules on CMD after 10 days **E** conidiation pustules on SNA after 10 d **F, H** conidiophores **G, J, K** conidiophores and phialides **I** conidia. Scale bars: 25  $\mu\text{m}$  (**F, H**); 10  $\mu\text{m}$  (**G, J–K**).

**Note.** Characterized by tree-like conidiophores, verticillate or in whorls of 3–4, ampulliform to lageniform phialides (5.0–10.5  $\times$  2.5–3.0  $\mu\text{m}$ ), ovoid to subglobose conidia (2.4–2.6  $\times$  2.0–2.5  $\mu\text{m}$ ). Differs from *Trichoderma simmonsii* by forming loose branches in whorls, relatively longer and thinner phialides, smaller conidia, and the fewer pustules on SNA.

***Trichoderma xixiacum* Jing Z. Sun & X.Z. Liu, sp. nov.**

MycoBank No: 833235

Fig. 4

**Etymology.** Latin, *xixiacum*, refers to the type locality.**Type.** CHINA. Xixia District, Yinchuan, Ningxia Hui Autonomous Region, 38°38'52"N, 106°9'33"E, ca. 1127 m elev., from rhizosphere soil of *Lycium chinensis*, 17 Oct 2018, Jing Z. Sun (HMAS 248253, holotype), ex-type culture CGMCC 3.19697.**Description.** On CMD after 72 h, colony radius 55–56 mm at 25 °C, covering the plate at 30 °C, 9–11 mm at 35 °C. Colony hyaline, indistinctly zonate, mycelia loose. Aerial hyphae short, inconspicuous. No diffusing pigment, not distinct odor (Fig. 4B). Conidial production noted after 3 days, effuse in aerial hyphae, becoming blue-green after 4 days. Chlamydozoospores unobserved.**Figure 4.** *Trichoderma xixiacum* (CGMCC 3.19697). Cultures at 25 °C after 3 d (A on PDA B on CMD C on SNA) D conidiation pustules on CMD after 10 d E conidiation pustules on SNA after 10 d F, G, I conidiophores and phialides H conidia. Scale bars: 10 µm (F, G); 10 µm (H, I).

On PDA after 72 h, colony radius 59–60 mm at 25 °C, covering the plate at 30 °C, 7–8 mm at 35 °C. Colony white to yellow-white, regularly circular, indistinctly zonate; mycelium dense and radial. Aerial hyphae conspicuous. No diffusing pigment, not distinct odor (Fig. 4A). Conidial production noted after 3 days, starting around the original inoculum, effuse in the aerial hyphae, first white, turning blue-green after 7 d. Chlamydospores unobserved.

On SNA after 72 h, colony radius 51–52 mm at 25 °C, 52–53 mm at 30 °C, 4–5 mm at 35 °C. Colony hyaline, indistinctly zonate; mycelium loose, especially at the margin. Aerial hyphae short. No diffusing pigment, not distinct odor (Fig. 4C). Conidial production noted after 2 days, starting around the inoculum, effuse in the aerial hyphae. Small pustules formed around the inoculum, first white, turning green after 3 d, with hairs protruding beyond the surface. Conidiophores pyramidal with opposing branches, less frequently solitary, closely-spaced branches, each branch, and the main axis terminating in 2–5 cruciately to nearly verticillately disposed phialides (Fig. 4F, G, I). Phialides ampulliform to lageniform, often constricted below the tip to form a narrow neck, hyaline, (3.2–)3.5–7.0(–9.3) × (2.3–)2.6–3.3(–3.6) μm ( $\bar{x}$  = 5.0 × 3.0 μm, n = 50), length/width ratio (1.2–)1.5–2.5(–4) ( $\bar{x}$  = 1.8, n = 50), base 1.6–2.2 μm ( $\bar{x}$  = 1.8 μm, n = 50) (Fig. 4I). Conidia subglobose to globose, smooth, hyaline when young, becoming green to dark green with age, (2.0–)2.3–2.7(–3.0) × (1.6–)2.0–2.6(–3.0) μm ( $\bar{x}$  = 2.5 × 2.2 μm, n = 50), length/width ratio 1.0–1.3(–1.7) ( $\bar{x}$  = 1.1, n = 50) (Fig. 4H). Chlamydospores unobserved. No odor; no diffusing pigment observed.

**Additional specimen examined.** CHINA. Xixia District, Yinchuan, Ningxia Hui Autonomous Region, 38°38'52"N, 106°9'33"E, ca. 1127 m elev., from rhizosphere soil of *Lycium chinensis*, 17 Oct 2018, Jing Z. Sun, living CGMCC 3.19697.

**Teleomorph.** Undetermined.

**Note.** Characterized by tree-like conidiophores, verticillate or in whorls of 3–4, ampulliform to lageniform phialides (3.5–7.0 × 2.6–3.4 μm), subglobose to globose conidia (2.2–2.6 × 2.0–2.4 μm). Differs from *Trichoderma lentinulae* by compact, relatively smaller phialides, and the character of pustules on SNA. Differs from *Trichoderma lixii* by shorter and wider phialides and smaller conidia.

***Trichoderma zelobreve* Jing Z. Sun & X.Z. Liu, sp. nov.**

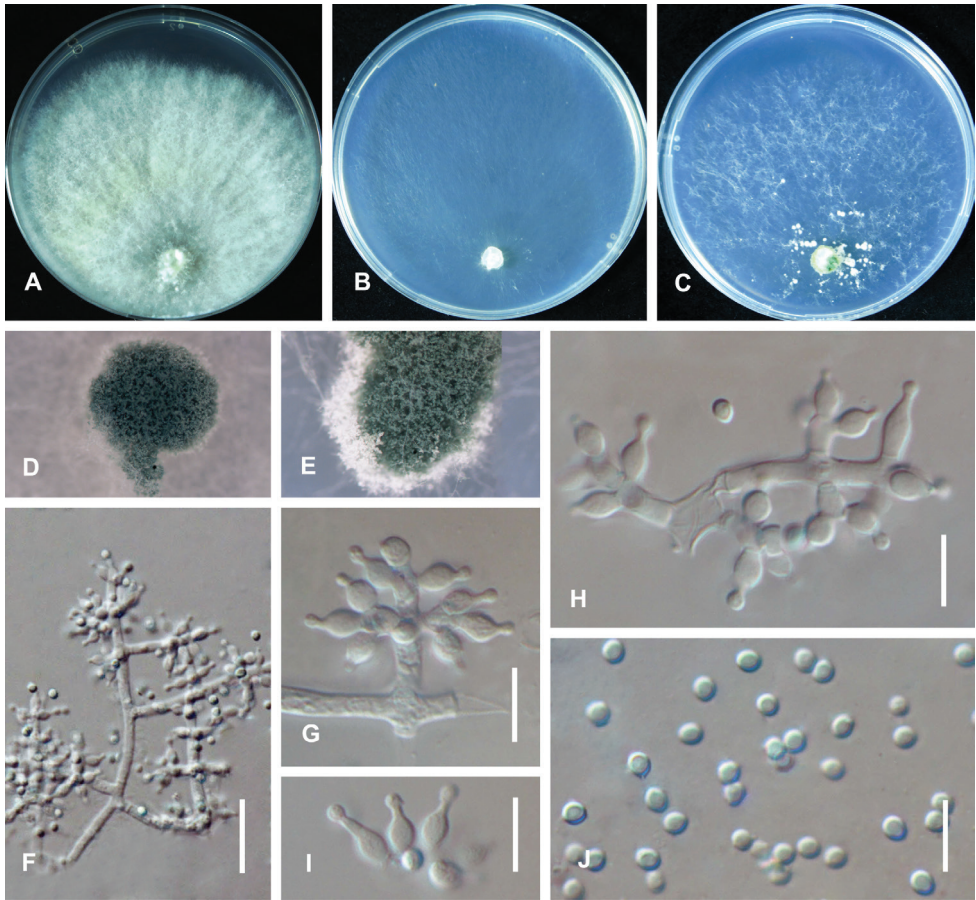
Mycobank No: 833236

Fig. 5

**Etymology.** Greek *zelo*, meaning emulation + *breve*, referred to *Trichoderma breve*.

**Type.** CHINA. Chaoyang District, Beijing, 40°0'41"N, 116°23'37"E, ca. 35 m elev., 19 Oct 2018, isolated from soil, Jing Z. Sun (HMAS 248254, holotype), ex-type culture CGMCC 3.19695.

**Description.** On CMD after 72 h, colony radius covering the plate at 25 °C and 30 °C, 11–12 mm at 35 °C. Colony hyaline, indistinctly radial; Aerial inconspicuous. No diffusing pigment, not distinct odor (Fig. 5B). Conidial production noted after



**Figure 5.** *Trichoderma zelobreve* (CGMCC 3.19695). Cultures at 25 °C after 3 days (**A** on PDA **B** on CMD **C** on SNA) **D** conidiation pustules on CMD after 10 days **E** conidiation pustules on SNA after 10 d **F** conidiophores **G, I** conidiophores and phialides **H** phialides with conidia **J** conidia. Scale bars: 25 µm (**F**); 10 µm (**G–J**).

5 days, starting around the original inoculum. Small pustules formed at the colony margin, first white, olivaceous after 6 d, with hairs protruding beyond the surface. Chlamydospores unobserved.

On PDA after 72 h, colony radius 55–58 mm at 25 °C, covering the plate at 30 °C, 8–9 mm at 35 °C. Colony white to yellow-white; mycelium dense and radial. Aerial conspicuous. No diffusing pigment, not distinct odor (Fig. 5A). Conidial production noted after 3 days, starting around the inoculum, effuse in the aerial hyphae, first white, turning green after 4 d. Chlamydospores unobserved.

On SNA after 72 h, colony radius 62–63 mm at 25 °C, covering the plate at 30 °C, 7–8 mm at 35 °C. Colony hyaline, regularly circular; mycelium loose. Aerial conspicuous. No diffusing pigment, not distinct odor (Fig. 5A). Conidial production noted after 2 days, starting around the inoculum, effuse in the aerial hyphae. Small pustules

formed along with two concentric rings, first white, turning yellow-green after 3 d, with hairs protruding beyond the surface. Conidiophores pyramidal with opposing branches, the distance between branches relatively large (Fig. 5F). Phialides, sometimes solitary, often paired or in whorls of 2–3 (Fig. 5F); whorls typically cruciate but often nearly verticillate; rarely conidiophores nodose and phialides disposed in more or less botryose clusters (Fig. 5G, H). Phialides ampulliform to lageniform, often constricted below the tip to form a narrow neck, hyaline (Fig. 5G, H, I),  $(3.5\text{--}4.0\text{--}6.0(-7.0) \times (2.2\text{--}2.6\text{--}3.2(-3.5)) \mu\text{m}$  ( $\bar{x} = 4.8 \times 2.9 \mu\text{m}$ ,  $n = 30$ ), length/width ratio  $(1.1\text{--}1.4\text{--}2.1(-2.5))$  ( $\bar{x} = 1.5$ ,  $n = 30$ ), base  $1.4\text{--}2.1 \mu\text{m}$  ( $\bar{x} = 1.7 \mu\text{m}$ ). Conidia ovoid to subglobose, smooth, hyaline when young, becoming green to dark green with age,  $(2.0\text{--}2.3\text{--}2.6(-2.9)) \times (1.5\text{--}1.8\text{--}2.2(-2.5)) \mu\text{m}$  ( $\bar{x} = 2.4 \times 2.0 \mu\text{m}$ ,  $n = 30$ ), length/width ratio  $(0.8\text{--}1.1\text{--}1.4(-1.7))$  ( $\bar{x} = 1.2$ ,  $n = 30$ ) (Fig. 5J). Chlamydo spores unobserved.

**Additional specimen examined.** CHINA. Chaoyang District, Beijing,  $40^{\circ}0'41''\text{N}$ ,  $116^{\circ}23'37''\text{E}$ , ca. 35 m elev., isolated from soil, 19 Oct 2018, Jing Z. Sun, living culture CGMCC 3.19696.

**Teleomorph.** Undetermined.

**Note.** Characterized by tree-like conidiophores, branches paired or in whorls of 3–4, ampulliform to lageniform ( $4.0\text{--}6.0 \times 2.6\text{--}3.2 \mu\text{m}$ ), ovoid to subglobose conidia ( $2.2\text{--}2.6 \times 1.8\text{--}2.2 \mu\text{m}$ ). Differs from *Trichoderma breve* by shorter phialides and smaller conidia, as well as the cultural characteristics and growth rates.

## Discussion

A combination of phylogenetic, morphological, ecological, and biogeographical data has robustly resolved the taxonomy of *Trichoderma* (Jaklitsch and Voglmayr 2015; Qin and Zhuang 2016a; Sun et al. 2016; Chen and Zhuang 2017b; Qiao et al. 2018). In this study, phylogenetic analysis based on a single gene of ITS could not distinguish species of *Trichoderma* in the *Harzianum* clade from each other (Suppl. material 1: Fig. S1), which confirmed that the ITS region is not suitable for species delimitation of *Trichoderma* (Jaklitsch et al. 2012; Qin et al. 2018). Sequences of RPB2 and TEF1- $\alpha$  were powerful due to their suitable interspecific variations (Jaklitsch and Voglmayr 2015), and these have extensively been used in solving the taxonomy of *Trichoderma* (Jaklitsch and Voglmayr 2015; Qin and Zhuang 2016a; Chen and Zhuang 2017a, b; Qiao et al. 2018). Despite the phylogenetic analyses based on the single gene of RPB2 and TEF1- $\alpha$  generally revealed the phylogenetic relationship within the *Harzianum* clade (Suppl. material 1: Fig. S2, Suppl. material 3: Fig. S3), but the relationships among *T. lentinulae*, *T. xixiacum*, *T. vermifimicola*, *T. zelibreve*, and their closed taxa were not well distinct. Consideration of the universality and reliability of barcodes for species in the *Trichoderma* genus (Qiao et al. 2018), combined ITS, RPB2, and TEF1- $\alpha$  dataset was used for phylogenetic analysis in this study, revealing phylogenetic relationship among species in *Harzianum* clades, and suggesting that *T. lentinulae*, *T. xixiacum*, *T. vermifimicola*, and *T. zelibreve* are distinguishable from each other and species within and outside of *Harzianum* clade as well.

**Table 1.** Species, strains and their corresponding GenBank accession numbers of sequences used for phylogenetic analyses.

Species	Voucher/ culture Nos.	Origin	Substrate	GenBank accession No.		
				ITS	RPB2	TEF1-a
<i>Trichoderma asfarasin</i>	CBS 130755 <sup>ET</sup>	Cameroon	Soil	AY027784		AF348093
	DIS 314F	Cameroon	Wood	FJ442259	FJ442778	FJ463400
	GJS 06 98	Cameroon	Soil	FJ442630		FJ463327
<i>Trichoderma afroharzianum</i>	CBS 124620 <sup>ET</sup>	Peru	<i>Moniliophthora roreri</i>	FJ442265	FJ442691	FJ463301
	CBS 466.94	Netherlands		KP009262	KP009150	KP008851
	GJS 04-193	Cameroon	Soil	FJ442233	FJ442709	FJ463298
<i>Trichoderma aggressivum</i>	CBS 100525	UK	Mushroom compost	AF057600	AF545541	AF348095
	DAOM 2221 56 <sup>ET</sup>		Mushroom compost	AF456924	FJ442752	AF348098
	CBS 100526	Ireland	Mushroom compost	FJ442607	KP009166	KP008993
<i>Trichoderma alni</i>	CBS 120633 <sup>ET</sup>	UK, England	<i>Alnus glutinosa</i>	EU518651	EU498349	EU498312
	CPK 2494			EU518652	EU498350	EU498313
	HMAS 252890				KT343763	KT343758
<i>Trichoderma alpinum</i>	HMAS 248821 <sup>T</sup>	China, Sichuan	Soil	KY687906	KY687958	KY688012
	HMAS 248830			KY687912	KY687961	KY688015
	HMAS 248870			KY687953	KY687963	KY688017
<i>Trichoderma amazonicum</i>	CBS 126898 <sup>ET</sup>	Peru	<i>Hevea brasiliensis</i>	HM142358	HM142367	HM142376
	IB95			HM142359	HM142368	HM142377
	LA265			HM142360	HM142369	HM142379
<i>Trichoderma atrobrunneum</i>	GJS 05-101			FJ442677	FJ442745	FJ463392
	GJS 90-254			AF443926	FJ442735	AF443943
<i>Trichoderma atrogelatinosum</i>	BMCC LU498	New Zealand				KJ871087
	CBS 237.63 <sup>ET</sup>	New Zealand		MH858272	KJ842201	
	DAOM 167632					KJ871083
<i>Trichoderma bannaense</i>	HMAS 248840 <sup>T</sup>	China, Yunan	Soil	KY687923	KY687979	KY688037
	HMAS 248865			KY687948	KY688003	KY688038
<i>Trichoderma breve</i>	HMAS 248844 <sup>T</sup>	China, Beijing	Soil	KY687927	KY687983	KY688045
	HMAS 248845			KY687928	KY687984	KY688046
<i>Trichoderma brevicrassum</i>	HMAS 248871 <sup>T</sup>		Soil	KY687954	KY688008	KY688064
	HMAS 248872		Soil	KY687955	KY688009	KY688065
<i>Trichoderma brunneoviride</i>	CBS 120928			EU518661	EU498358	EU498318
	CBS 121130 <sup>ET</sup>			EU518659	EU498357	EU498316
<i>Trichoderma camerunense</i>	CBS 137272 <sup>ET</sup>	Cameroon	Soil	AY027780	–	AF348107
	GJS 99 231			AY027783		AF348108
<i>Trichoderma catoptron</i>	DAOM 232830				KJ842166	KJ871245
	GJS 02 76 <sup>ET</sup>	Sri Lanka	Wood	AY737766		AY737726
<i>Trichoderma ceramicum</i>	CBS 114576			FJ860743	FJ860531	FJ860628
<i>Trichoderma cerinum</i>	BMCC LU784					KJ871244
	DAOM 230012 <sup>ET</sup>	Nepal		KC171336	KJ842184	KJ871242
<i>Trichoderma christiani</i>	CBS 132572 <sup>ET</sup>	Spain			KJ665244	KJ665439
	S93				KJ665245	KJ665442
<i>Trichoderma cinnamomeum</i>	GJS 96-128				AY391916	AY391977
	GJS 97-233				AY391919	AY391978
<i>Trichoderma cinnamomeum</i>	GJS 97-237 <sup>ET</sup>	USA, Missouri	Decaying wood	AY737759	AY391920	AY737732
<i>Trichoderma compactum</i>	CBS 121218			AY941822	KF134789	KF134798
<i>Trichoderma concentricum</i>	HMAS 248833 <sup>T</sup>	China, Hubei	Soil	KY687915	KY687971	KY688027
	HMAS 248858			KY687941	KY687997	KY688028
<i>Trichoderma corneum</i>	GJS 97-82 <sup>ET</sup>	Thailand			KJ665252	KJ665455
<i>Trichoderma endophyticum</i>	CBS 130729 <sup>ET</sup>	Ecuador	<i>Theobroma gileri</i>	FJ442243		FJ463319
	GS 2014a			FJ884177		FJ967822
<i>Trichoderma epimyces</i>	CBS 120534 <sup>ET</sup>	Austria		EU518663	EU498360	EU498320
	CPK 1980			EU518662	EU498359	EU498319
	CPK 2487 <sup>ET</sup>			EU518665	EU498361	EU498322

Species	Voucher/ culture Nos.	Origin	Substrate	GenBank accession No.		
				ITS	RPB2	TEF1-a
<i>Trichoderma estonicum</i>	GJS 96-129			AY737767	AF545514	AF534604
<i>Trichoderma guizhouense</i>	DAOM 231435			EF191296		EF191321
	HGUP0038 <sup>T</sup> S628			JN191311	JQ901400	JN215484
<i>Trichoderma harzianum</i>	CBS 226.95 <sup>ET</sup>	U.K.	Soil	AJ222720	AF545549	AF348101
	CBS 227.95			AF057605		AF348100
	GJS 05 107			FJ442679	FJ442708	FJ463329
	IMI 359823			EF113587		AF348092
<i>Trichoderma hausknechtii</i>	CBS 133493	France			KJ665276	KJ665515
<i>Trichoderma helicolixii</i>	CBS 133499 <sup>ET</sup>	Spain			KJ665278	KJ665517
<i>Trichoderma helicolixii</i>	CBS 135583				KJ665277	KJ665516
<i>Trichoderma hengshanicum</i>	HMAS 248852 <sup>T</sup>	China, Hubei	Soil	KY687935	KY687991	KY688054
	HMAS 248853			KY687936	KY687992	KY688055
<i>Trichoderma hirsutum</i>	HMAS 248834 <sup>T</sup>	China, Hubei	Soil	KY687916	KY687972	KY688029
	HMAS 248859			KY687942	KY687998	KY688030
<i>Trichoderma hunanense</i>	HMAS 248841 <sup>T</sup>	China, Hunan	Soil	NR_154571	KY687980	KY688039
	HMAS 248867			KY687950	KY688005	KY688040
<i>Trichoderma ingratum</i>	HMAS 248822 <sup>T</sup>	China, Sichuan	Soil	KY687917	KY687973	KY688018
	HMAS 248827			KY687909	KY687966	KY688021
	HMAS 248873			KY687956	KY688010	KY688022
<i>Trichoderma inhamatum</i>	CBS 273.78 <sup>ET</sup>	Colombia	Soil	FJ442680	FJ442725	AF348099
<i>Trichoderma italicum</i>	CBS 132567				KJ665282	KJ665525
	S15 <sup>ET</sup>	Italy			KJ665283	KJ665526
<i>Trichoderma lentiforme</i>	CBS 100542 <sup>ET</sup>	French Guiana	Decorticated wood	AF469189	–	AF469195
	DIS 253B			FJ442619	FJ442756	FJ851875
	DIS 94D			FJ442615	FJ442749	FJ463379
<i>Trichoderma lentinulae</i>	HMAS 248256 <sup>T</sup>	China	<i>Lentinula</i>	MN594469	MN605867	MN605878
	CGMCC 3.19848	China	<i>Lentinula</i>	MN594470	MN605868	MN605879
	CGMCC 3.19849	China	<i>Lentinula</i>	MN594471	MN605869	MN605880
	CGMCC 3.19699	China	Soil	MN594478	MN605876	MN605887
	CGMCC 3.19670	China	Soil	MN594479	MN605877	MN605888
<i>Trichoderma liberatum</i>	HMAS 248831 <sup>T</sup>	China, Hubei	Soil	KY687913	KY687969	KY688025
<i>Trichoderma liberatum</i>	HMAS 248832			KY687914	KY687970	KY688026
<i>Trichoderma linzhiense</i>	HMAS 248846 <sup>T</sup>	China, Tibet	Soil	KY687929	KY687985	KY688047
	HMAS 248874			KY687957	KY688011	KY688048
<i>Trichoderma lixii</i>	CBS 110080 <sup>ET</sup>	Thailand	Decayed <i>Ganoderma</i>	AF443920	KJ665290	AF443938
<i>Trichoderma neotropicale</i>	LA11 <sup>ET</sup>			HQ022407		HQ022771
	T51			FJ884180		FJ967825
<i>Trichoderma parestonicum</i>	CBS 120636 <sup>ET</sup>			FJ860803	FJ860565	
<i>Trichoderma parepimyces</i>	CBS 122768			FJ860801	FJ860563	FJ860665
	CBS 122769 <sup>ET</sup>	Austria	Wood	MH863234	FJ860562	FJ860664
<i>Trichoderma perviride</i>	HMAS 273786	China, Hubei	Wood	KX026962	KX026954	
<i>Trichoderma pinicola</i>	KACC 48486 <sup>ET</sup>	Korea	root of <i>Pinus densiflora</i>	MH050354	MH025993	MH025981
	SFC20130926-S014				MH025991	MH025978
	SFC20130926-S111				MH025992	MH025980
<i>Trichoderma pleuroti</i>	CBS 124387 <sup>ET</sup>	Korea	<i>Pleurotus</i> substrate	HM142363	HM142372	HM142382
	CPK 2117					EU279975
<i>Trichoderma pleuroticola</i>	CBS 124383 <sup>ET</sup>	Korea	<i>Pleurotus</i> substrate	HM142362	HM142371	HM142381
	GJS 95 81			AF345948		AF348102
	TRS70 <sup>ET</sup>			KP009264	KP009172	KP008951
<i>Trichoderma polypori</i>	HMAS 248855 <sup>T</sup>	Hunan	Soil	KY687938	KY687994	KY688058
	HMAS 248861			KY687944	KY688000	KY688059
<i>Trichoderma polysporum</i>	S72					KJ665685

Species	Voucher/ culture Nos.	Origin	Substrate	GenBank accession No.		
				ITS	RPB2	TEF1-a
<i>Trichoderma priscilae</i>	CBS 131487 <sup>ET</sup>	Spain			KJ665333	KJ665691
<i>Trichoderma pseudodensum</i>	HMAS 248828 <sup>T</sup>	Hubei	Soil	KY687910	KY687967	KY688023
	HMAS 248829			KY687911	KY687968	KY688024
<i>Trichoderma pseudogelatinosum</i>	CNUN309 <sup>ET</sup>	Japan	Shiitake mushroom	HM769754	HM920173	HM920202
<i>Trichoderma purpureum</i>	HMAS 273787 <sup>T</sup>	China, Hubei			KX026961	KX026953
<i>Trichoderma pyramidale</i>	CBS 135574 <sup>ET</sup>	Italy	<i>Olea europaea</i>		KJ665334	KJ665699
<i>Trichoderma rifaii</i>	CBS 130746	Ecuador	<i>Theobroma gileri</i>	FJ442663		FJ463324
	DIS 337F <sup>ET</sup>			FJ442621	FJ442720	FJ463321
<i>Trichoderma rufobrunneum</i>	HMAS 266614 <sup>T</sup>	China, Jilin	Rotten wood	KF729998	KF730010	KF729989
	isolate 8155				KF730007	KF729992
<i>Trichoderma rugulosum</i>	SFC20180301-001 <sup>T</sup>			MH050353	MH025986	MH025984
	SFC20180301-002				MH025987	MH025985
<i>Trichoderma simmonsii</i>	CBS 130431	USA, Maryland	Decaying wood bark	AF443917	FJ442757	AF443935
	S297					KJ665711
	S7				KJ665337	KJ665719
<i>Trichoderma simplex</i>	HMAS 248842 <sup>T</sup>	China, Guangxi	Soil	KY687925	KY687981	KY688041
	HMAS 248860			KY687943	KY687999	KY688042
<i>Trichoderma solum</i>	HMAS 248847			KY687930	KY687986	KY688049
	HMAS 248848 <sup>T</sup>	China, Hubei	Soil	KY687931	KY687987	KY688050
	HMAS 248849			KY687932	KY687988	KY688051
<i>Trichoderma stramineum</i>	CBS 114248 <sup>ET</sup>	Sri Lanka	Decaying wood	AY737765	AY391945	AY737746
	TAMA 0425			AB856609	AB856748	AB856675
<i>Trichoderma tawa</i>	CBS 114233 <sup>ET</sup>	Thailand	Decaying bark	AY737756	AY391956	FJ463313
	DAOM 232841				KJ842187	EU279972
<i>Trichoderma tenue</i>	HMAS 273785 <sup>ET</sup>	China, Hubei	Wood		KX026960	KX026952
<i>Trichoderma tomentosum</i>	DAOM 171918			AY605715		AY605759
	DAOM 178713a <sup>ET</sup>	Canada, Ontario	<i>Ulmus</i> wood	EU330958	AF545557	AY750882
	DAOM 234236			EU280083		EU279971
<i>Trichoderma velutinum</i>	DAOM 230013 <sup>ET</sup>	Nepal	Soil	AF149873	JN133569	AY937415
	HMAS 273865 <sup>T</sup>	China, Heilongjiang	Soil		KX026965	KX026957
<i>Trichoderma vermifimicola</i>	CGMCC 3.19850	China	Compost	MN594472	MN605870	MN605881
	HMAS 248255 <sup>T</sup>	China	Compost	MN594473	MN605871	MN605882
<i>Trichoderma xixiacum</i>	HMAS 248253 <sup>T</sup>	China	Soil	MN594476	MN605874	MN605885
	CGMCC 3.19698	China	Soil	MN594477	MN605875	MN605886
<i>Trichoderma zayuense</i>	HMAS 248835 <sup>T</sup>	China, Tibet	Soil	KY687918	KY687974	KY688031
	HMAS 248836			KY687919	KY687975	KY688032
<i>Trichoderma zelobreve</i>	HMAS 248254 <sup>T</sup>	China	Mushroom	MN594474	MN605872	MN605883
	CGMCC 3.19696	China	Soil	MN594475	MN605873	MN605884
<i>Trichoderma zeloharzianum</i>	YMF 1.00268 <sup>ET</sup>	China, Yunan	Soil	MH113932	MH158996	MH183181

*Trichoderma lentinulae* was phylogenetically close to *T. xixiacum* and *T. lixii* but represents a taxon (Fig. 1). Morphologically, it differed from *T. xixiacum* in producing less frequently lageniform phialides with inequilateral to a strongly-curved apex. The conidia of *T. lentinulae* are usually more slender ( $\bar{x} = 2.0$ ), than those of *T. xixiacum* ( $\bar{x} = 1.8$ ). In addition, the conidia of *T. lentinulae* (length/width ratio,  $\bar{x} = 1.2$ ) are slightly more slender than *T. xixiacum* (length/width ratio,  $\bar{x} = 1.1$ ). The two species also differ from each other in their cultural characteristics and growth rates (Figs 2A–C, 4 A–C). *Trichoderma lentinulae* differed from *T. lixii* in producing less fre-

quently lageniform phialide with inequilateral to a strongly-curved apex. Additionally, *T. lentinulae* forms 2–5 apex phialides on the main axis (Fig. 2F, I) in contrast to 2–4 apex phialides of *T. lixii* (Chaverri et al. 2015). *Trichoderma lentinulae* is also clearly distinguished from *T. lixii* (phialides, 6.5–3.5  $\mu\text{m}$ ; conidia, 3.0–2.7  $\mu\text{m}$ ) (Chaverri et al. 2015) in producing shorter phialides ( $\bar{x} = 4.5 \times 3.0 \mu\text{m}$ ) and smaller conidia ( $\bar{x} = 2.5 \times 2.2 \mu\text{m}$ ). *Trichoderma vermifimicola* was phylogenetically associated with *T. simmonsii* (Fig. 1). Morphologically, it is hard to distinguish *T. vermifimicola* from *T. simmonsii*, because both form similar tree-like conidiophores, ampulliform to lageniform phialides and ovoid to subglobose conidia, but phialide whorls of *T. vermifimicola* were often nearly verticillate rather than cruciate in *T. simmonsii* (Chaverri et al. 2015). Furthermore, *T. simmonsii* grew fast (PDA 25–55 mm, SNA 10–35 mm) at 35 °C than *T. vermifimicola*. Additionally, the length/width ratio phialide of *T. vermifimicola* is larger ( $\bar{x} = 2.4$ ) than that of *T. simmonsii* ( $\bar{x} = 1.9$ ) (Chaverri et al. 2015), and *T. vermifimicola* also produces smaller conidia ( $\bar{x} = 2.4 \times 2.2 \mu\text{m}$ ) (Fig. 3) than *T. simmonsii* (3.0–2.7  $\mu\text{m}$ ) (Chaverri et al. 2015). *Trichoderma zelibreve* was closely related to *Trichoderma breve* in the multi-gene phylogenetic analysis (Fig. 1). Morphologically, both fungi have short phialides, however, *T. zelibreve* differs from *T. breve* by producing shorter and narrower phialides (4.0–6.0  $\times$  2.6–3.2  $\mu\text{m}$ ) than that of *T. breve* (6.7–10.0  $\times$  2.8–3.9  $\mu\text{m}$ ) (Chen and Zhuang 2017a). The conidia of *T. zelibreve* are smaller ( $\bar{x} = 2.4 \times 2.0 \mu\text{m}$ ) than those of *T. breve* ( $\bar{x} = 3.0 \times 2.8 \mu\text{m}$ ). Additionally, *T. zelibreve* does not form a zonate colony on CMD, PDA, and SNA, whereas the colony of *T. breve* presents concentric zones on CMD and PDA and finely concentric zones on SNA (Chen and Zhuang 2017a). In a previous study, the phylogenetic analysis indicated that *T. breve* was a sister taxon of *T. bannaense*, but morphologically more similar to *T. harzianum* (Chen and Zhuang (2017a). Herein, our phylogenetic analyses presented *T. breve* was associated with *T. zelibreve* (Fig. 1), resulted from the little genetic variation of sequences of ITS and TEF1- $\alpha$  between them. The phylogenetic analysis in Chaverri et al. (2015) presented that *T. simmonsii* was associated with *T. camerunense*. In this study, our phylogenetic analysis presented that *T. simmonsii* was phylogenetically closed to *T. vermifimicola*, and *T. camerunense* phylogenetic to *T. rifaii* (Fig 1, Suppl. material 3: Fig S3). In a previous study, these species were recognized as the cryptic species in under *T. harzianum* (Chaverri et al. (2015).

Currently, the *Harzianum* clade contains more than 60 species which were isolated from soil, plant tissues, and other fungi (Jaklitsch and Voglmayr 2015; Qin and Zhuang 2016a; Chen and Zhuang 2017b; Qiao et al. 2018; Sun et al. 2019a, b). Several studies have confirmed that species in this clade are important because of their mycoparasitism (Chaverri et al. 2015; Chen and Zhuang 2017a; Sun et al. 2019). When numerous biological control agents were explored deriving from species in the *Harzianum* clade (Chaverri et al. 2015, several taxa, such as *T. atrobrunneum* *T. pleuroti*, and *T. pleuroticola* were recognized as causing agents of “Green mold” disease of cultivated mushroom (Innocenti et al. 2019; Sun et al. 2019a, b). In this study, *T. lentinulae* was isolated from a fruiting body and the cultivated substrates of *L. edodes*, causing the decay of the host as well. How *T. lentinulae* affect the cultivation of *Lentinula edodes* is worthy of further studies. Since *T. lentinulae* was isolated from mushroom, *T. lentinulae* and *T. vermifimicola*

were isolated from the mushroom spawn and substrates for earthworm cultivation, *T. xixiacum* and *T. zelobreve* were isolated from soil, confirming that species in the *Harzianum* clade have flexible nutrition modes (Chaverri and Samuels 2013; Zhang et al. 2018). The new species introduced here are not only potential candidates for biological agent exploration, but also improve our understanding of the diversity of *Trichoderma*, especially of the *Harzianum* clade in China.

## Acknowledgements

This research was jointly supported by Key Research and Development Programs in Ningxia Hui Autonomous Region (2018BBF02004) and the Natural Science Foundation of China (no. 31600024).

## References

- Atanasova L, Druzhinina IS, Jaklitsch WM, Mukherjee P, Horwitz B, Singh U (2013) Two hundred *Trichoderma* species recognized on the basis of molecular phylogeny. *Trichoderma: Biology and Applications* CABI, Wallingford: 10–42. <https://doi.org/10.1079/9781780642475.0010>
- Bunbury-Blanchette AL, Walker AK (2019) *Trichoderma* species show biocontrol potential in dual culture and greenhouse bioassays against *Fusarium* basal rot of onion. *Biological Control* 130: 127–135. <https://doi.org/10.1016/j.biocontrol.2018.11.007>
- Carbone I, Kohn LM (1999) A method for designing primer sets for speciation studies in filamentous ascomycetes. *Mycologia* 91: 553–556. <https://doi.org/10.1080/00275514.1999.12061051>
- Castresana J (2000) Selection of conserved blocks from multiple alignments for their use in phylogenetic analysis. *Molecular Biology and Evolution* 17: 540–552. <https://doi.org/10.1093/oxfordjournals.molbev.a026334>
- Chaverri P, Branco-Rocha F, Jaklitsch W, Gazis R, Degenkolb T, Samuels GJ (2015) Systematics of the *Trichoderma harzianum* species complex and the re-identification of commercial biocontrol strains. *Mycologia* 107: 558–590. <https://doi.org/10.3852/14-147>
- Chaverri P, Samuels GJ (2013) Evolution of habitat preference and nutrition mode in a cosmopolitan fungal genus with evidence of interkingdom host jumps and major shifts in ecology. *Evolution* 67: 2823–2837. <https://doi.org/10.1111/evo.12169>
- Chen K, Zhuang WY (2016) *Trichoderma shennongjianum* and *Trichoderma tibetense*, two new soil-inhabiting species in the Strictipile clade. *Mycoscience* 57: 311–319. <https://doi.org/10.1016/j.myc.2016.04.005>
- Chen K, Zhuang WY (2017a) Discovery from a large-scaled survey of *Trichoderma* in soil of China. *Scientific Reports* 7, 9090. <https://doi.org/10.1038/s41598-017-07807-3>
- Chen K, Zhuang WY (2017b) Three new soil-inhabiting species of *Trichoderma* in the Stromaticum clade with test of their antagonism to pathogens. *Current Microbiology* 74: 1049–1060. <https://doi.org/10.1007/s00284-017-1282-2>

- Cunningham CW (1997) Can three incongruence tests predict when data should be combined? *Molecular Biology and Evolution* 14: 733–740. <https://doi.org/10.1093/oxfordjournals.molbev.a025813>
- Degenkolb T, Nielsen KF, Dieckmann R, Branco-Rocha F, Chaverri P, Samuels GJ, Thrane U, von Dohren H, Vilcinskis A, Bruckner H (2015) Peptaibol, secondary-metabolite, and hydrophobin pattern of commercial biocontrol agents formulated with species of the *Trichoderma harzianum* Complex. *Chemistry & Biodiversity* 12: 662–684. <https://doi.org/10.1002/cbdv.201400300>
- Druzhinina IS, Kopchinskiy AG (2006) TrichOKEY v. 2 – A DNA Oligonucleotide BarCode Program for the Identification of Multiple Sequences of *Hypocrea* and *Trichoderma*. In: Meyer W, Pearce C (Eds) *International Proceedings of the 8<sup>th</sup> International Mycological Congress*. Cairns, Australia, Medimond, Bologna, Italy.
- Druzhinina IS, Kopchinskiy AG, Komoń M, Bissett J, Szakacs G, Kubicek CP (2005) An oligonucleotide barcode for species identification in *Trichoderma* and *Hypocrea*. *Fungal Genetics and Biology* 42: 813–828. <https://doi.org/10.1016/j.fgb.2005.06.007>
- du Plessis IL, Druzhinina IS, Atanasova L, Yarden O, Jacobs K (2018) The diversity of *Trichoderma* species from soil in South Africa, with five new additions. *Mycologia* 110: 559–583. <https://doi.org/10.1080/00275514.2018.1463059>
- Gazis R, Chaverri P (2010) Diversity of fungal endophytes in leaves and stems of wild rubber trees (*Hevea brasiliensis*) in Peru. *Fungal Ecology* 3: 240–254. <https://doi.org/10.1016/j.funeco.2009.12.001>
- Innocenti G, Montanari M, Righini H, Roberti R (2019) *Trichoderma* species associated with green mould disease of *Pleurotus ostreatus* and their sensitivity to prochloraz. *Plant Pathology* 68: 392–398. <https://doi.org/10.1111/ppa.12953>
- Jaklitsch WM, Komoń M, Kubicek CP, Druzhinina IS (2005) *Hypocrea voglmayrii* sp. nov. from the Austrian Alps represents a new phylogenetic clade in *Hypocreales* *Trichoderma*. *Mycologia* 97: 1365–1378. <https://doi.org/10.1080/15572536.2006.11832743>
- Jaklitsch WM, Voglmayr H (2015) Biodiversity of *Trichoderma* (Hypocreaceae) in southern Europe and Macaronesia. *Studies in Mycology* 80: 1–87. <https://doi.org/10.1016/j.simyco.2014.11.001>
- Jiang Y, Wang JL, Chen J, Mao LJ, Feng XX, Zhang CL, Lin FC (2016) *Trichoderma* biodiversity of agricultural fields in East China reveals a gradient distribution of species. *PLoS ONE* 11(8): e0160613. <https://doi.org/10.1371/journal.pone.0160613>
- Katoh K, Standley DM (2013) MAFFT Multiple sequence alignment software version 7: improvements in performance and usability. *Molecular Biology and Evolution* 30: 772–780. <https://doi.org/10.1093/molbev/mst010>
- Kopchinskiy A, Komoń M, Kubicek CP, Druzhinina IS (2005) TrichoBLAST: a multilocus database for *Trichoderma* and *Hypocrea* identifications. *Mycological Research* 109: 658–660. <https://doi.org/10.1017/S0953756205233397>
- Liu YJJ, Whelen S, Benjamin DH (1999) Phylogenetic relationships among ascomycetes: Evidence from an RNA polymerase II subunit. *Molecular Biology and Evolution* 16: 1799–1808. <https://doi.org/10.1093/oxfordjournals.molbev.a026092>
- Nylander JAA (2004) MrModeltest v2. Program distributed by the author. Evolutionary Biology Centre, Uppsala University. <https://github.com/nylander/MrModeltest2>

- Phookamsak R, Hyde KD, Jeewon R, Bhat DJ, Jones EBG, Maharachchikumbura SSN, Raspé O, Karunarathna SC, Wanasinghe DN, Hongsanan S, Doilom M, Tennakoon DS, Machado AR, Firmino AL, Ghosh A, Karunarathna A, Mešić A, Dutta AK, Thongbai B, Devadatha B, Norphanphoun C, Senwanna C, Wei D, Pem D, Ackah FK, Wang GN, Jiang HB, Madrid H, Lee HB, Goonasekara ID, Manawasinghe IS, Kušan I, Cano J, Gené J, Li J, Das K, Acharya K, Raj KNA, Latha KPD, Chethana KWT, He MQ, Dueñas M, Jadan M, Martín MP, Samarakoon MC, Dayarathne MC, Raza M, Park MS, Telleria MT, Chaiwan N, Matočec N, de Silva NI, Pereira OL, Singh PN, Manimohan P, Uniyal P, Shang QJ, Bhatt RP, Perera RH, Alvarenga RLM, Nogal-Prata S, Singh SK, Vadthananat S, Oh SY, Huang SK, Rana S, Konta S, Paloi S, Jayasiri SC, Jeon SJ, Mehmood T, Gibertoni TB, Nguyen TTT, Singh U, Thiyagaraja V, Sarma VV, Dong W, Yu XD, Lu YZ, Lim YW, Chen Y, Tkalčec Z, Zhang ZF, Luo ZL, Daranagama DA, Thambugala KM, Tibpromma S, Camporesi E, Bulgakov T, Dissanayake AJ, Senanayake IC, Dai DQ, Tang LZ, Khan S, Zhang H, Promptutha I, Cai L, Chomnunti P, Zhao RL, Lumyong S, Boonmee S, Wen TC, Mortimer PE, Xu J (2019) Fungal diversity notes 929–1036: taxonomic and phylogenetic contributions on genera and species of fungal taxa. *Fungal Diversity* 95: 1–273. <https://doi.org/10.1007/s13225-019-00421-w>
- Qiao M, Du X, Zhang Z, Xu JP, Yu ZF (2018) Three new species of soil-inhabiting *Trichoderma* from southwest China. *Mycokokeys*: 63–80. <https://doi.org/10.3897/mycokeys.44.30295>
- Qin WT, Zhuang WY (2016a) Four new species of *Trichoderma* with hyaline ascospores from central China. *Mycological Progress* 15: 811–825. <https://doi.org/10.1007/s11557-016-1211-y>
- Qin WT, Zhuang WY (2016b) Two new hyaline-ascospored species of *Trichoderma* and their phylogenetic positions. *Mycologia* 108: 205–214. <https://doi.org/10.3852/15-144>
- Qin WT, Zhuang WY (2017) Seven new species of *Trichoderma* (Hypocreales) in the Harzi-anum and Strictipile clades. *Phytotaxa* 305: 121–139. <https://doi.org/10.11646/phyto-taxa.305.3.1>
- Rambaut A (2012) FigTree v1. 4. Molecular evolution, phylogenetics and epidemiology. Edinburgh: University of Edinburgh, Institute of Evolutionary Biology.
- Ronquist F, Teslenko M, van der Mark P, Ayres DL, Darling A, Höhna S, Larget B, Liu L, Suchard MA, Huelsenbeck JP (2012) MrBayes 3.2: efficient Bayesian phylogenetic inference and model choice across a large model space. *Systematic Biology* 61: 539–542. <https://doi.org/10.1093/sysbio/sys029>
- Stamatakis A (2006) RAxML-VI-HPC: maximum likelihood-based phylogenetic analyses with thousands of taxa and mixed models. *Bioinformatics* 22: 2688–2690. <https://doi.org/10.1093/bioinformatics/btl446>
- Sun JZ, Liu XZ, Jeewon R, Li YL, Lin CG, Tian Q, Zhao Q, Xiao XP, Hyde KD, Nilthong S (2019a) Fifteen fungicolous Ascomycetes on edible and medicinal mushrooms in China and Thailand. *Asian Journal of Mycology* 2(1): 129–169. <https://doi.org/10.5943/ajom/2/1/7>
- Sun JZ, Liu XZ, McKenzie EH, Jeewon R, Liu JK, Zhang XL, Zhao Q, Hyde KD (2019b) Fungicolous fungi: terminology, diversity, distribution, evolution, and species checklist. *Fungal Diversity* 95(1): 337–430. <https://doi.org/10.1007/s13225-019-00422-9>

- Sun RY, Liu ZC, Fu KH, Fan LL, Chen J (2012) *Trichoderma* biodiversity in China. *Journal of Applied Genetics* 53: 343–354. <https://doi.org/10.1007/s13353-012-0093-1>
- Sun JZ, Pei YF, Li EW, Li W, Hyde KD, Yin WB, Liu XZ (2016) A new species of *Trichoderma hypoxylon* harbours abundant secondary metabolites. *Scientific Reports* 6, 37369. <https://doi.org/10.1038/srep37369>
- White T, Bruns T, Lee S, Taylor J (1990) Amplification and direct sequencing of fungal ribosomal RNA genes for phylogenetics In: Innis MA, Gelfand DH, Sninsky JJ, White TJ (Eds) *PCR protocols: a guide to methods and applications*, 315–322. <https://doi.org/10.1016/B978-0-12-372180-8.50042-1>
- Zhang WW, Zhang XL, Li K, Wang CS, Cai L, Zhuang WY, Xiang M, Liu XZ (2018) Introgression and gene family contraction drive the evolution of lifestyle and host shifts of hypocrealean fungi. *Mycology* 9: 176–188. <https://doi.org/10.1080/21501203.2018.1478333>
- Zhang YJ, Zhang S, Liu XZ, Wen HA, Wang M (2010) A simple method of genomic DNA extraction suitable for analysis of bulk fungal strains. *Letters in applied microbiology* 51(1): 114–118. <https://doi.org/10.1111/j.1472-765X.2010.02867.x>
- Zhu ZX, Zhuang WY (2015) *Trichoderma* (Hypocrea) species with green ascospores from China. *Persoonia* 34: 113–129. <https://doi.org/10.3767/003158515X686732>

## Supplementary material I

### Figure S1

Authors: Xin Gu, Rui Wang, Quan Sun, Bing Wu, Jing-Zu Sun

Data type: phylogenetic tree

Explanation note: Phylogenetic tree based on Maximum Likelihood analysis of ITS sequence dataset. *Trichoderma ceramicum*, *Trichoderma estonicum*, and *Trichoderma parastinicum* were chosen as the outgroup. Bootstrap Values higher than 70% from RAxML (BSML) (left) and Bayesian posterior probabilities greater than 0.95 (BYPP) (right) are given above the nodes. <sup>T</sup> indicates the type; <sup>ET</sup> indicates the ex-living type. Isolates obtained in this study are in red.

Copyright notice: This dataset is made available under the Open Database License (<http://opendatacommons.org/licenses/odbl/1.0/>). The Open Database License (ODbL) is a license agreement intended to allow users to freely share, modify, and use this Dataset while maintaining this same freedom for others, provided that the original source and author(s) are credited.

Link: <https://doi.org/10.3897/mycokeys.73.51424.suppl1>

## Supplementary material 2

### Figure S2

Authors: Xin Gu, Rui Wang, Quan Sun, Bing Wu, Jing-Zu Sun

Data type: phylogenetic tree

Explanation note: Phylogenetic tree based on Maximum Likelihood analysis of RPB2 sequence dataset. *Trichoderm ceramicum*, *Trichoderma estonicum*, and *Trichoderm parastinicum* were chosen as the outgroup. Bootstrap Values higher than 70% from RAxML (BSML) (left) and Bayesian posterior probabilities greater than 0.95 (BYPP) (right) are given above the nodes. <sup>T</sup> indicates the type; <sup>ET</sup> indicates the ex-living type. Isolates obtained in this study are in red

Copyright notice: This dataset is made available under the Open Database License (<http://opendatacommons.org/licenses/odbl/1.0/>). The Open Database License (ODbL) is a license agreement intended to allow users to freely share, modify, and use this Dataset while maintaining this same freedom for others, provided that the original source and author(s) are credited.

Link: <https://doi.org/10.3897/mycokeys.73.51424.suppl2>

## Supplementary material 3

### Figure S3

Authors: Xin Gu, Rui Wang, Quan Sun, Bing Wu, Jing-Zu Sun

Data type: phylogenetic tree

Explanation note: Phylogenetic tree based on Maximum Likelihood analysis of TEF1 $\alpha$  sequence dataset. *Trichoderm ceramicum* was chosen as the outgroup. Bootstrap Values higher than 70% from RAxML (BSML) (left) and Bayesian posterior probabilities greater than 0.95 (BYPP) (right) are given above the nodes. <sup>T</sup> indicates the type; <sup>ET</sup> indicates the ex-living type. Isolates obtained in this study are in red.

Copyright notice: This dataset is made available under the Open Database License (<http://opendatacommons.org/licenses/odbl/1.0/>). The Open Database License (ODbL) is a license agreement intended to allow users to freely share, modify, and use this Dataset while maintaining this same freedom for others, provided that the original source and author(s) are credited.

Link: <https://doi.org/10.3897/mycokeys.73.51424.suppl3>

# Three new species of *Conidiobolus sensu stricto* from plant debris in eastern China

Yong Nie<sup>1,2</sup>, Yue Cai<sup>3</sup>, Yang Gao<sup>4</sup>, De-Shui Yu<sup>1</sup>,  
Zi-Min Wang<sup>2</sup>, Xiao-Yong Liu<sup>5</sup>, Bo Huang<sup>1</sup>

**1** Anhui Provincial Key Laboratory for Microbial Pest Control, Anhui Agricultural University, Hefei 230036, China **2** School of Civil Engineering and Architecture, Anhui University of Technology, Ma'anshan 243002, China **3** Department of Biological and Environmental Engineering, Hefei University, Hefei 230601, China **4** Bioengineering and Technological Research Centre for Edible and Medicinal Fungi, Jiangxi Agricultural University, Nanchang, 330045, China **5** State Key Laboratory of Mycology, Institute of Microbiology, Chinese Academy of Sciences, Beijing 100101, China

Corresponding author: Bo Huang ([bhuang@ahau.edu.cn](mailto:bhuang@ahau.edu.cn)); Xiao-Yong Liu ([liuxiaoyong@im.ac.cn](mailto:liuxiaoyong@im.ac.cn))

Academic editor: C. Wurzbacher | Received 25 July 2020 | Accepted 23 September 2020 | Published 8 October 2020

**Citation:** Nie Y, Cai Y, Gao Y, Yu D-S, Wang Z-M, Liu X-Y, Huang B (2020) Three new species of *Conidiobolus sensu stricto* from plant debris in eastern China. MycoKeys 73: 133–149. <https://doi.org/10.3897/mycokeys.73.56905>

## Abstract

The genus *Conidiobolus* Bref. is widely distributed and the *Conidiobolus sensu lato* contained three other genera, *Capillidium*, *Microconidiobolus* and *Neoconidiobolus*. A molecular phylogeny based on the nuclear large subunit of rDNA (nuLSU), the mitochondrial small subunit of rDNA (mtSSU) and the translation elongation factor 1-alpha gene (TEF1) revealed three novel species within the clade of *Conidiobolus s.s.*, i.e. *C. bifurcatus sp. nov.*, *C. taihushanensis sp. nov.* and *C. variabilis sp. nov.* These three species were isolated from plant debris in eastern China. Morphologically, *C. bifurcatus sp. nov.* is characterised by its secondary conidiophores often branched at the tip to form two short stipes each bearing a secondary conidium. *C. taihushanensis sp. nov.* is different from the others in its straight apical mycelia and the production of 2–5 conidia. *C. variabilis sp. nov.* is distinctive because of its various shapes of primary conidia. All these three new taxa are illustrated herein with an update key to the species of the genus *Conidiobolus s.s.*

## Keywords

basal fungi, *Entomophthorales*, taxonomy, molecular phylogenetics, new species

## Introduction

The genus *Conidiobolus* Bref. (Ancylistaceae) was established to accommodate the type *C. utriculosus* Bref. and a second species *C. minor* Bref. (Brefeld 1884). This genus was characterised by simple conidiophores, globose to pyriform conidia and resting spores formed in the axis of the hypha (mostly as zygospores) (Humber 1997). Until 1968, a total of 41 species occurring saprotrophically in soil and plant debris had been assigned to this genus (Martin 1925, Couch 1939, Drechsler 1952, 1953a, b, 1954, 1955a, b, c, 1956, 1957a, b, c, 1960, 1961, 1962, 1965, Srinivasan and Thirumalachar 1961, 1962a, b, 1965, 1967, 1968a, b). In a review of these taxa with the numerical technique, 27 definitive species were recognised (King 1976a, b, 1977). On the basis of the shape of secondary conidia, Ben-Ze'ev and Kenneth (1982) classified the genus *Conidiobolus* into three subgenera, including *Capillidium* Ben-Ze'ev & Kenneth, *Conidiobolus* Brefeld and *Delacroixia* Tyrrell & Macleod. Until 2018, no remarkable taxonomic treatments had been made for this genus, although additional species were reported continuously (Bałazy et al. 1987, Waters and Callaghan 1989, Bałazy 1993, Tosi et al. 2004, Huang et al. 2007, Waingankar et al. 2008, Nie et al. 2012, 2016, 2017, 2018). Meanwhile, higher-rank molecular phylogenetic studies on entomophthoroid fungi suggested *Conidiobolus* to be polyphyletic (Jensen et al. 1998, Gryganskyi et al. 2013, Nie et al. 2020). Consequently, the three genera *Capillidium*, *Microconidiobolus* and *Neoconidiobolus* were separated from *Conidiobolus* sensu lato and *Conidiobolus* sensu stricto was characterised by microspores arising from conidia (Nie et al. 2020).

During the past decade, Bo Huang's research group have carried out a comprehensive study on the taxonomy of *Conidiobolus* sensu lato in China and proposed five new species, five Chinese new records and 23 new combinations (Wang et al. 2010a, b, Nie et al. 2012, 2016, 2017, 2018, 2020, Chen and Huang 2018). Recent collections by this research group in eastern China resulted in the discovery of three unique species within the *Conidiobolus* sensu stricto lineage, which are described and illustrated herein with a multi-locus molecular phylogeny on the nuclear large subunit of rDNA (nuLSU), the mitochondrial small subunit of rDNA (mtSSU) and the translation elongation factor 1-alpha gene (TEF1).

## Materials and methods

### Isolates and morphology

Plant debris was collected from Taihushan and Jilongshan National Forest Parks, Anhui Province, China and Laoshan National Forest Park, Jiangsu Province, China. Isolations were carried out using the canopy-plating approach (Drechsler 1952, King 1976a). A Petri dish with potato dextrose agar (PDA; potato 200 g, dextrose 20 g, agar 20 g, H<sub>2</sub>O 1000 ml) was inverted over the plant debris and incubated at 21 °C

for daily examining for one week. When entomophthoroid fungi on the PDA canopy were detected, they were quickly transferred to new PDA and 2% water agar (agar 20 g, H<sub>2</sub>O 1000 ml) plates for purification and description. Morphological features were measured with an Olympus BX51 research microscope for 35 primary conidia and conidiophores each and photographed by an Olympus DP25 microscope-camera system. The descriptions were made with the method of King (1976a). Cultures were deposited in the Research Center for Entomogenous Fungi of Anhui Agricultural University, Anhui Province, China (RCEF) and the China General Microbiological Culture Collection Center, Beijing, China (CGMCC). Dried cultures were deposited in the Herbarium Mycologicum Academiae Sinicae, Beijing, China (HMAS). In order to infer the phylogeny of the genus *Conidiobolus* s.s., a total of 21 ex-types of species in *Conidiobolus* s.l., serving as outgroup, were obtained from the American Type Culture Collection, Manassas, USA (ATCC).

### DNA extraction, PCR amplification and sequencing

Fungal biomass was collected from the plate surface and ground in liquid nitrogen with a pestle and mortar. Genomic DNA was extracted using the CTAB method (Watanabe et al. 2010). The extracted DNA was stored in 100 µl TE buffer (10 mM Tris-HCl, 1 mM EDTA, pH 8.0) at -20 °C. Universal primer pairs LR0R (5'-ACC CGC TGA ACT TAA GC-3') and LR5 (5'-TCC TGA GGG AAA CTT CG-3') (Vilgalys and Hester 1990), mtSSU1 (5'-GCW GCA GTG RGG AAT NTT GGR CAA T-3') and mtSSU2R (5'-GTR GAC TAM TSR GGT ATC TAA TC-3') (Zoller et al. 1999) and EF983 (5'-GCY CCY GGH CAY CGT GAY TTY AT-3') and EF1aZ-1R (5'-ACA TCW CCG ACA CCC TTG ATC TTG -3') (Nie et al. 2012) were used for the amplification of the partial region of nuLSU, mtSSU and TEF1, respectively. The PCR reactions followed those in Liu et al. (2005) and Nie et al. (2012, 2020). A 50 µl mixture contained 200 µM dNTPs each, 1 × Mg-free buffer, 2.5 mM MgCl<sub>2</sub>, 0.5 µM primers each, 50 ng genomic DNA and 2 U Taq polymerase (Super Pfx DNA Polymerase, Cowinbioscience Co. Ltd., Shanghai, China). The programme consisted of an initial denaturation at 100 °C for 5 min without Taq polymerase, an extra denaturation at 95 °C for 5 min after the Taq polymerase was added, then 34 cycles of 94 °C for 1 min plus 55/54/57 °C (nuLSU / mtSSU / TEF1) for 2 min plus 72 °C for 2 min and a final extension at 72 °C for 10 min. The amplification products were sequenced by Shanghai GeneCore BioTechnologies Co. Ltd. (Shanghai, China), with the same primers as used in relative PCR reactions. All sequences were assembled with BioEdit (Hall 1999) and deposited at GenBank (Table 1).

### Phylogenetic analyses

In addition to the sequences obtained in this paper, nuLSU, mtSSU and TEF1 sequences of 20 strains in *Conidiobolus* sensu stricto were downloaded from GenBank.

**Table 1.** The taxa used in phylogenetic analyses.

Species	Strains*	GenBank accession numbers			References
		nuLSU	EF-1 $\alpha$	mtSSU	
<i>Capillidium adiaereturum</i>	CGMCC 3.15888	MN061284	MN061481	MN061287	Nie et al. 2020
<i>Ca. lobatum</i>	ATCC 18153 (T)	JF816218	JF816233	MK301187	Nie et al. 2012, 2020
<b><i>Conidiobolus bifurcatus</i> sp. nov.</b>	<b>CGMCC 3.15889 (T)</b>	<b>MN061285</b>	<b>MN061482</b>	<b>MN061288</b>	This article
<i>C. brefeldianus</i>	ARSEF 452 (T)	EF392382	–	EF392495	Genbank
<i>C. chlamydosporus</i>	ATCC 12242 (T)	JF816212	JF816234	MK301178	Nie et al. 2012, 2020
<i>C. coronatus</i>	NRRL 28638	AY546691	DQ275337	–	Lutzoni et al. 2004
<i>C. coronatus</i>	RCEF 4518	JN131537	JN131543	–	Nie et al. 2016, 2018
<i>C. dabieshanensis</i>	CGMCC 3.15763 (T)	KY398125	KY402206	MK301180	Nie et al. 2017, 2020
<i>C. firmipilleus</i>	ARSEF 6384	JX242592	–	JX242632	Gryganskyi et al. 2012
<i>C. gonimodes</i>	ATCC 14445 (T)	JF816221	JF816226	MK301182	Nie et al. 2012, 2020
<i>C. humicolus</i>	ATCC 28849 (T)	JF816220	JF816231	MK301184	Nie et al. 2012, 2020
<i>C. incongruus</i>	NRRL 28636	AF113457	–	–	Voigt et al. 1999
<i>C. iuxtagenitus</i>	ARSEF 6378 (T)	KC788410	–	–	Gryganskyi et al. 2013
<i>C. kbandalensis</i>	ATCC 15162 (T)	KX686994	KY402204	MK301185	Nie et al. 2012, 2020
<i>C. lampraugus</i>	ARSEF 2338	DQ364206	–	DQ364226	Genbank
<i>C. lichenicolus</i>	ATCC 16200 (T)	JF816216	JF816232	MK301186	Nie et al. 2012, 2020
<i>C. macrosporus</i>	ATCC 16578 (T)	KY398124	KY402209	MK301188	Nie et al. 2017, 2020
<i>C. megalotocus</i>	ATCC 28854 (T)	MF616383	MF616385	MK301189	Nie et al. 2018, 2020
<i>C. mycophagus</i>	ATCC 16201 (T)	JX946694	JX946698	MK301190	Nie et al. 2018, 2020
<i>C. mycophilus</i>	ATCC 16199 (T)	KX686995	KY402205	MK301191	Nie et al. 2016, 2020
<i>C. parvus</i>	ATCC 14634 (T)	KX752051	KY402207	MK301192	Nie et al. 2016, 2020
<i>C. polyspermus</i>	ATCC 14444 (T)	MF616382	MF616384	MK301193	Nie et al. 2018, 2020
<i>C. polytocus</i>	ATCC 12244 (T)	JF816213	JF816227	MK301194	Nie et al. 2012, 2020
<b><i>C. taihusanensis</i> sp. nov.</b>	<b>CGMCC 3.16016 (T)</b>	<b>MT250086</b>	<b>MT274290</b>	<b>MT250088</b>	This article
<b><i>C. variabilis</i> sp. nov.</b>	<b>CGMCC 3.16015 (T)</b>	<b>MT250085</b>	<b>MT274289</b>	<b>MT250087</b>	This article
<i>Microconidiobolus nodosus</i>	ATCC 16577 (T)	JF816217	JF816235	MK333388	Nie et al. 2012, 2020
<i>M. terrestris</i>	ATCC 16198 (T)	KX752050	KY402208	MK301199	Nie et al. 2016, 2020
<i>Neoconidiobolus stromoides</i>	ATCC 15430 (T)	JF816219	JF816229	MK301198	Nie et al. 2012, 2020
<i>N. thromboides</i>	ATCC 12587 (T)	JF816214	JF816230	MK301200	Nie et al. 2012, 2020

\*ARSEF, ARS Entomopathogenic Fungus Collection (Ithaca, U.S.A.). ATCC, American Type Culture Collection (Manassas, U.S.A.). CGMCC, China General Microbiological Culture Collection Center (Beijing, China). NRRL, ARS Culture Collection (Peoria, U.S.A.). RCEF, Research Center for Entomogenous Fungi (Hefei, China). T = ex-type.

Three genera *Capillidium*, *Microconidiobolus* and *Neoconidiobolus*, each represented by two species, were selected as outgroups. The nuLSU, mtSSU and TEF1 sequences were aligned with Clustal X (Thompson et al. 1997) and deposited at TreeBase (submission ID 26063). Phylogenetic analyses with Bayesian Inference (BI), Maximum Parsimony (MP) and Maximum Likelihood (ML) were carried out according to Nie et al. (2018, 2020). BI phylogeny was estimated using MrBayes 3.1.2 (Ronquist and Huelsenbeck 2003). The best-fit model selected with the Akaike Information Criterion (AIC) in Modeltest 3.7 (Posada and Crandall 1998) was used to evaluate Posterior Probabilities (PP) and the critical value for the topological convergence diagnostic was set to 0.01 of the average standard deviation of split frequencies. Four Markov chains ran simultaneously from random starting trees for 0.5 million generations and trees were sampled every 100<sup>th</sup> generation. MP analyses were performed using a heuristic search with PAUP\* 4.0b10 (Swofford 2002). All characters were weighted and gaps were treated as missing data. Tree bisection-reconnection (TBR) was set as the branch swapping algo-

rithm. Branch robustness was estimated with bootstrapping 1,000 replicates (Felsenstein 1985). ML analyses were performed with the RAxML (Stamatakis 2006), implemented in raxmlGUI 1.5b1 (Silvestro and Michalak 2012). Branch reliabilities were determined by 1,000 ML rapid bootstrap replicates with the GTRGAMMA substitution model. Phylogenetic trees were checked and modified in FigTree 1.4 (Rambaut 2012).

## Results

### Phylogenetic analyses

The combined nucLSU+TEF1+mtSSU dataset was composed of 29 taxa representing 27 species and 1949 characters including 986 constant, 276 parsimony-uninformative and 687 parsimony-informative. The most parsimonious tree was generated with a tree length (TL) of 2716 steps, a consistency index (CI) of 0.5497, a homoplasy index (HI) of 0.4503, a retention index (RI) of 0.6191 and a rescaled consistency index (RC) of 0.3403. The best model applied in the BI analysis was GTR+I+G. The final average standard deviation of split frequencies was 0.0086 and the final likelihood value was -14423. The three phylograms resulted in similar topologies and the ML tree was presented along with MP/ML bootstrap and BI posterior probability values at relative branches (Fig. 1).

Three clades can be seen to form for the *Conidiobolus* s.s. The three species, described here, were located in clade I.

### Taxonomy

#### *Conidiobolus bifurcatus* B. Huang & Y. Nie, sp. nov.

Mycobank No: 831599

Facesoffungi: FoF 08142

Figure 2

**Typification.** CHINA, Jiangsu: Nanjing, Laoshan National Forest Park, 32°6'7"N, 118°36'17"E, from plant debris, 1 Dec 2018, *Y. Nie and Y. Gao* (holotype HMAS 248359, ex-holotype culture CGMCC 3.15889 = RCEF 6551, GenBank: nucLSU = MN061285; TEF1 = MN061482; mtSSU = MN061288).

**Etymology.** *bifurcatus* (Lat.), referring to secondary conidiophores often branched at the tip to form two short stipes, each bearing a secondary conidium.

**Ecology and distribution.** Plant debris in Jiangsu Province, China.

**Description.** Colonies on PDA at 21 °C for 3 d, opaque, white, reaching ca. 2 mm in diameter, with many small colonies around the periphery due to discharged conidia. Mycelia colourless, 8–11 µm wide, rarely branched and non-septate when young, often septate and distended to a width of 10–27 µm after 5 d. Primary conidiophores arising from the hyphal segments, colourless, 38–254 × 7.5–12 µm, unbranched and producing a single globose conidium, without widening upwards near the tip. Primary conidia for-

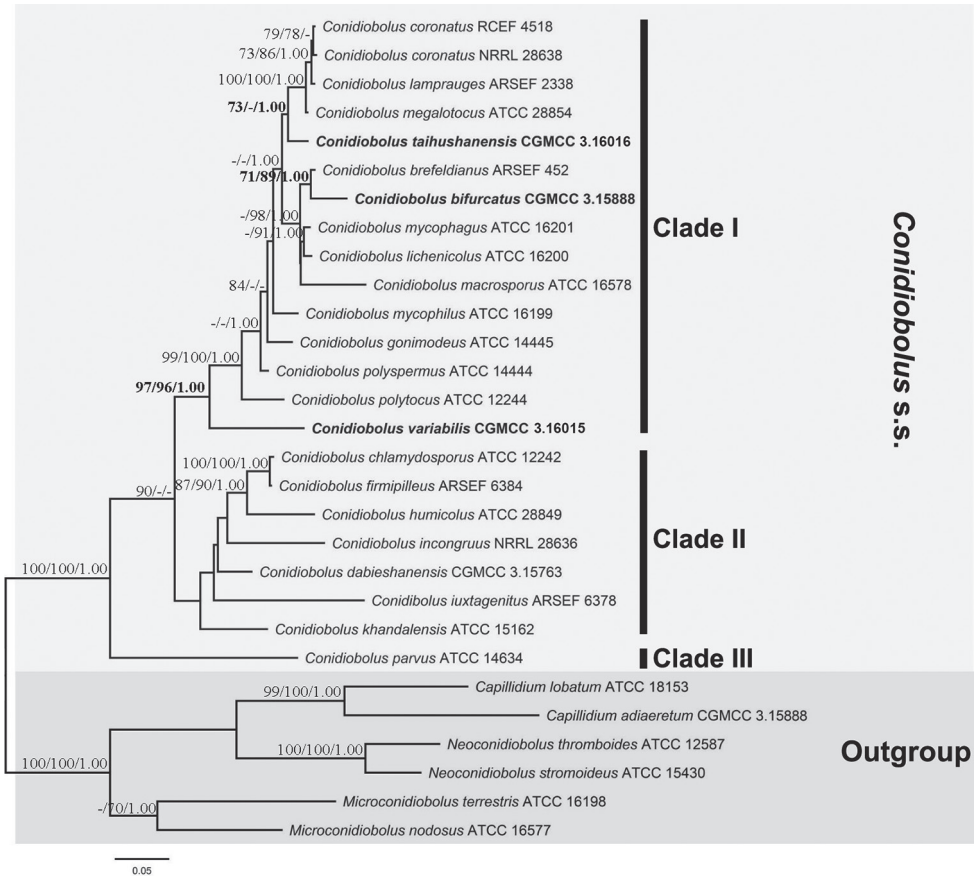


**Figure 1.** Phylogenetic tree of *Conidiobolus* s.s. reconstructed by maximum likelihood analyses of nucLSU, mtSSU and TEF1 sequences, with six *Conidiobolus* s.l. species as outgroups. Three new species of *Conidiobolus* are shown in bold. Maximum parsimony bootstrap values ( $\geq 70\%$ ) / Maximum likelihood bootstrap values ( $\geq 70\%$ ) / Bayesian posterior probabilities ( $\geq 0.95$ ) of each clade are indicated along branches. Scale bar indicates substitutions per site.

cibly discharged, globose to subglobose,  $2\text{--}40 \times 2\text{--}33 \mu\text{m}$ , with a papilla more or less tapering and pointed,  $7\text{--}11 \mu\text{m}$  wide at the base,  $3\text{--}12 \mu\text{m}$  long. Secondary conidiophores arising from the primary conidia, often branched almost at the tip, forming two short stipes each bearing a secondary conidium. Secondary conidia similar to, but smaller than the primary ones, mostly forcibly discharged, occasionally falling off and leaving a relic of the secondary conidiophores. On 2% water agar, microconidia produced readily, globose to ellipsoidal,  $7\text{--}12 \times 6\text{--}9 \mu\text{m}$ . Zygosporangia homothallic, usually formed between adjacent segments of the same hypha after an incubation of 5–7 d at 21 °C on PDA, smooth, mostly globose,  $25\text{--}40 \mu\text{m}$  in diameter, with a  $1.5\text{--}3 \mu\text{m}$  thick wall.

**Notes.** *Conidiobolus bifurcatus* sp. nov. is characterised by its secondary conidiophores, which are often bifurcated near the tip and bear a secondary conidium on each

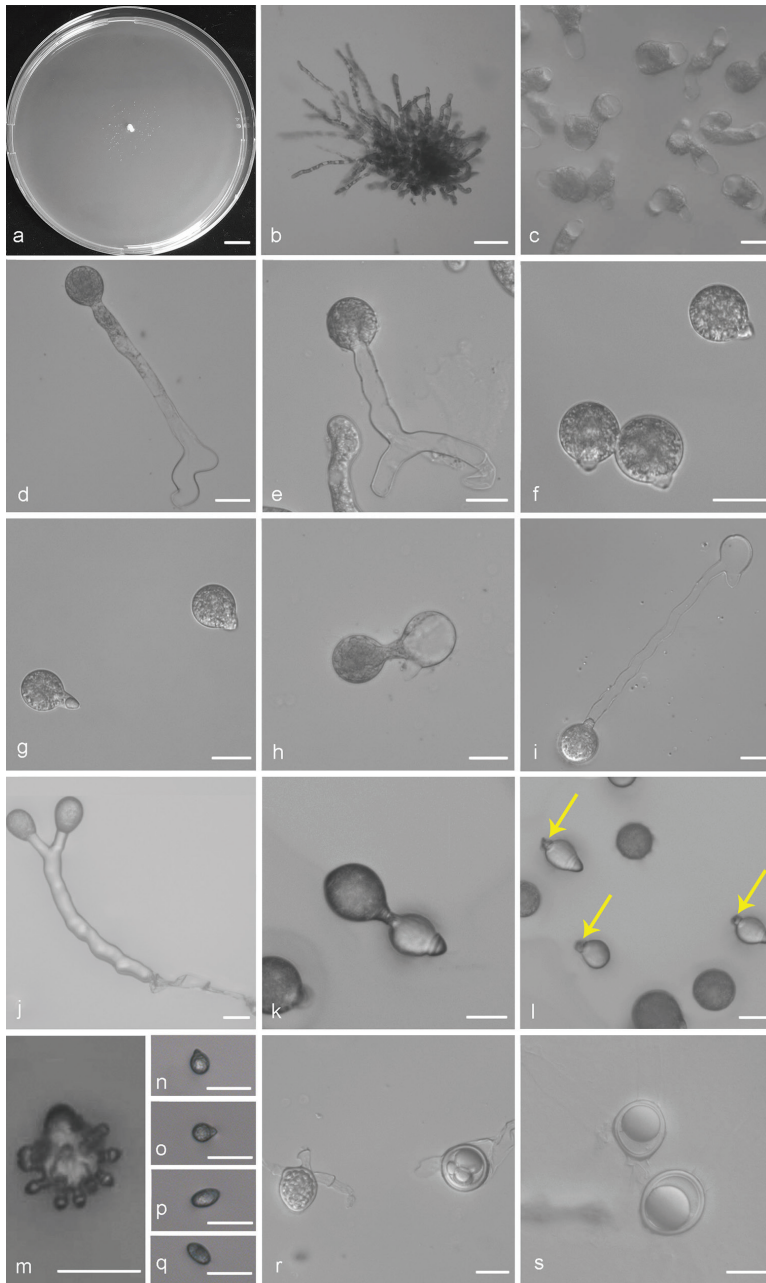


**Figure 2.** *Conidiobolus bifurcatus* sp. nov. **a** Colony on PDA after 3 d at 21 °C **b** mycelium **c** septate mycelium and distended segments **d**, **e** primary conidiophores bearing primary conidia **f**, **g** primary conidia **h**, **i** a single secondary conidium produced from primary conidia **j** two secondary conidia arising from a branched conidiophore **k** secondary conidia falling from primary conidia **l** the relic of secondary conidiophores on secondary conidia (arrows) **m** microconidia arising from a conidium **n**, **o** globose microconidia **p**, **q** ellipsoidal microconidia **r** zygospores formed between adjacent segments of the same hypha **s** zygospores. Scale bars: 10 mm (**a**); 100 µm (**b**); 20 µm (**c**–**s**).

stipe. Morphologically, it is allied to *Conidiobolus mycophilus* Srin. & Thirum., which has smaller primary conidia (Srinivasan and Thirumalachar 1965). It appears to be similar to *C. incongruus* Drechsler and *C. mycophagus* Srin. & Thirum. in the size of primary conidia and zygospores and the formation of microconidia, but different in its longer primary conidiophores (Drechsler 1960; Srinivasan and Thirumalachar 1965). However, it is distantly related to these two species in the molecular phylogenetic tree. Instead, it is phylogenetically closely related to *C. brefeldianus* Couch (Figure 1: MP 71/ML 89/BI 1.00), but morphologically distinct by its larger primary conidia and zygospores (Couch 1939).

***Conidiobolus taihushanensis* B. Huang & Y. Nie, sp. nov.**

MycoBank No: 835124

Facesoffungi: FoF 08143

Figure 3

**Typification.** CHINA, Anhui: Ma'anshan City, Hanshan County, Taihushan National Forest Park, 31°30'53"N, 118°2'49"E, from plant detritus, 12 Jan 2019, *Y. Nie and Y. Cai* (holotype HMAS 248724, ex-holotype culture CGMCC 3.16016 = RCEF 6559, GenBank: nuLSU = MT250086; TEF1 = MT274290; mtSSU = MT250088).

**Etymology.** *taihushanensis* (Lat.), referring to the region where the fungus was isolated.

**Ecology and distribution.** Plant debris in Anhui Province, China.

**Description.** Colonies on PDA at 21 °C after 3 d, white, reaching ca. 11–14 mm in diameter. Mycelia colourless, straight and unbranched when young, 8.5–12 µm wide; distended and non-contiguously segmented when old, 10–20 µm wide. Primary conidiophores arising from the older mycelia without an upward widening near the tip, colourless, 44–180 × 7–13 µm, usually unbranched and often producing a single globose primary conidium, at the initial growth stage 2–5 short branches bearing a primary conidium each. Primary conidia forcibly discharged, mostly subglobose, 27–42 × 19–32 µm, with tapering and pointed papilla, 4–10 × 8–12 µm. Secondary conidia arising from primary conidia, similar to, but smaller than the primary ones, forcibly discharged. On 2% water agar, microconidia not observed. Zygospores usually formed between adjacent segments of the same hypha after 5 d, 34–48 × 23–40 µm, with a 2–4 µm thick wall, ellipsoid and rich in content when young, smooth, mostly globose, subglobose to ovate when mature.

**Notes.** *Conidiobolus taihushanensis* sp. nov. is morphologically highly distinct with its straight apical mycelia and the production of 2–5 conidia from the hyphal body. *Conidiobolus taihushanensis* sp. nov. is similar to *C. polytocus* Drechsler in the structure of several short branches at the top of conidiophores, but the latter is distinguished by smaller primary conidia (12–25 × 14–29 µm) and slightly curved mycelia (Drechsler 1955c). *Conidiobolus taihushanensis* sp. nov. is related to *C. margaritatus* B. Huang, Humber & K.T. Hodge and *C. megalotocus* Drechsler by the size of primary conidia, but *C. margaritatus* forms a chain of undischarged repetitional conidia (Huang et al. 2007) and *C. megalotocus* lacks zygospores (Drechsler 1956). Phylogenetically, *C. taihushanensis* sp. nov. is closely related to *C. megalotocus* (Figure 1: MP 73/BI 1.00) and distantly related to *C. polytocus*, though no molecular data are available for *C. margaritatus*. Phylogenetically, *C. taihushanensis* sp.

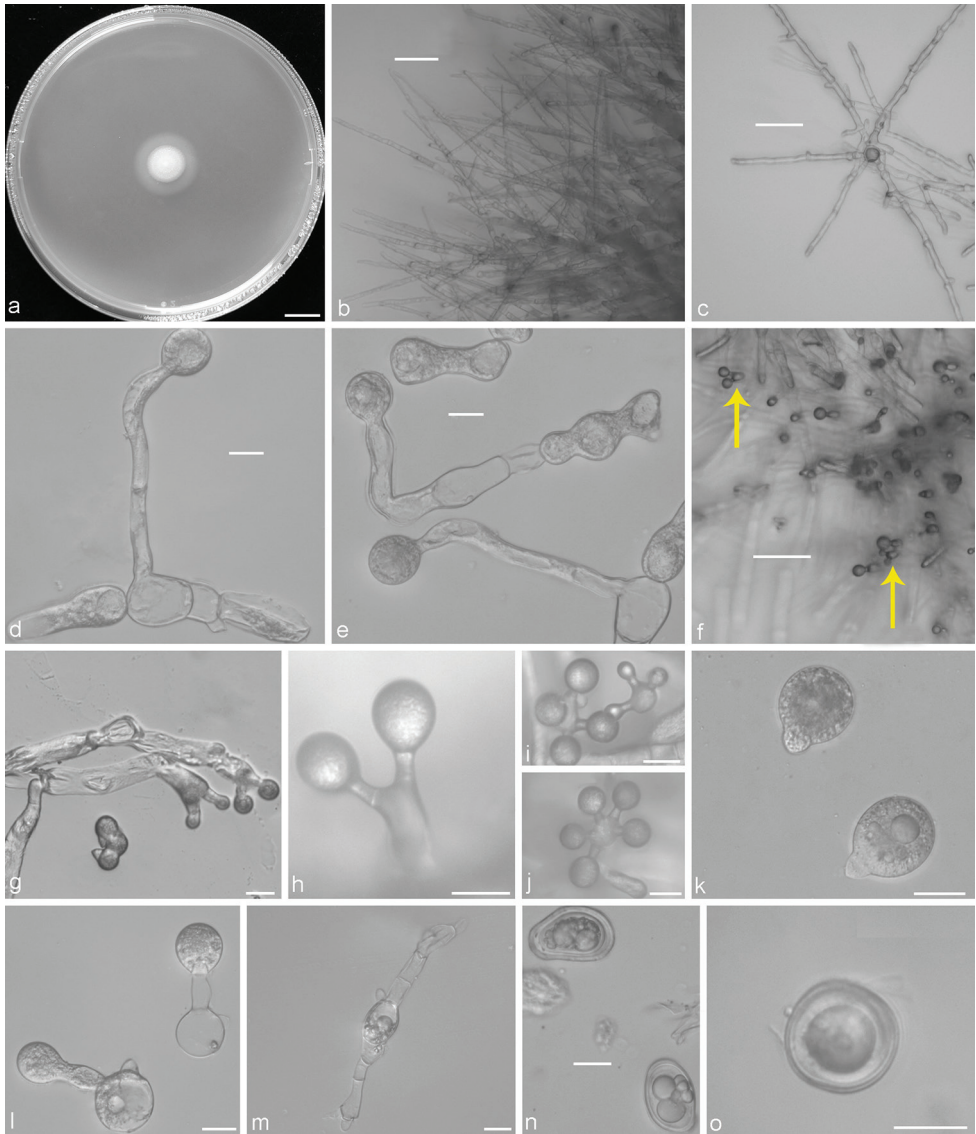


**Figure 3.** *Conidiobolus taihushanensis* sp. nov. **a** colony on PDA after 3 d at 21 °C **b** mycelia unbranched at the colony edge **c** young mycelia **d**, **e** primary conidiophores arising from mycelia segments **f** two branches germinated from hyphal bodies and each bearing a primary conidium (arrows) **g–j** two, three, four or five branches germinated from hyphal bodies and each bearing a primary conidium **k** globose to subglobose primary conidia **l** secondary conidia arising from primary conidia **m** zygospores formed between adjacent segments of the same hypha **n** young zygospores **o** mature zygospores. Scale bars: 10 mm(**a**); 100 µm (**b**, **c**, **f**); 20 µm (**d**, **e**, **g–o**).

nov. is also closely related to *C. lamprauges* Drechsler and *C. coronatus* Batko, but it differs from *C. lamprauges* by larger primary conidia (27–42 × 19–32 µm vs. 12.5–20 × 15–22 µm) and from *C. coronatus* by the absence of villose resting spores (Drechsler 1953a).

***Conidiobolus variabilis* B. Huang & Y. Nie, sp. nov.**

MycoBank No: 835125

Facesoffungi: FoF 08144

Figure 4

**Typification.** CHINA, Anhui: Ma'anshan City, Hexian County, Jilongshan National Forest Park, 31°48'1"N, 118°12'19"E, from plant debris, 23 Dec 2017, *Y. Nie* (holotype HMAS 248723, ex-holotype culture CGMCC 3.16015 (= RCEF 6540), GenBank: nuLSU = MT250085; TEF1 = MT274289; mtSSU = MT250087).

**Etymology.** *variabilis* (Lat.), referring to producing various shapes of primary conidia.

**Ecology and distribution.** Plant debris from Anhui Province, China.

**Description.** Colonies on PDA at 21 °C after 3 d white, reaching ca. 41–48 mm in diameter. Mycelia colourless, 6–11 µm wide, rarely branched at the colony edge. Primary conidiophores unbranched and producing a single globose conidium, colourless, 60–200 × 9–15 µm, without an upward widening near the tip. Primary conidia forcibly discharged, globose, subglobose, pyriform to obovoid, 31–55 × 25–40 µm, with tapering and pointed papilla, 3.5–9 × 8–13 µm. Secondary conidia arising from primary conidia, similar to, but smaller than primary ones, forcibly discharged. On 2% water agar, microconidia rarely observed, globose, subglobose to ellipsoidal, 10–12 × 9–14 µm. Resting spores not observed.

**Notes.** Considering the large size of primary conidia, *Conidiobolus variabilis* sp. nov. is allied to *C. coronatus* (Cost.) Batko (14.5–38.5 × 17–48.5 µm), *C. macrosporus* Srin. & Thirum. (38–45 × 48–54 µm) and *C. utriculosus* Brefeld (25–35 × 37.5–51 µm). It is distinguished from *C. coronatus* by its various shapes of primary conidia and the absence of villose spores. It differs from *C. macrosporus* by its longer primary conidiophores and the absence of resting spores (Batko 1964, Srinivasan and Thirumalachar 1967). It is differentiated from *C. utriculosus* by the shapes of primary conidia and the absence of zygosporangia. Phylogenetically, *C. variabilis* sp. nov. is basal in clade I and distantly related to *C. coronatus* and *C. macrosporus*.

## Discussion

The genus *Conidiobolus* has recently been divided into four lineages and one of them was treated as *Conidiobolus* sensu stricto on the basis of a synapomorph, namely microspores (Nie et al. 2020). The three new species *C. bifurcatus* sp. nov., *C. taihushanensis* sp. nov. and *C. variabilis* sp. nov. are located in the clade of *Conidiobolus* s.s. (Fig. 1). *Conidiobolus taihushanensis* sp. nov. was paraphyletic to *C. megalotocus* Drechsler, *C. lamprauges* Drechsler and *C. coronatus* (Cost.) Batko with a robust support of BI posterior probability of 1.00. *Conidiobolus bifurcatus* sp. nov. was a sister group to *C. brefeldianus*, which was supported by all three inferring methods (MP 71/ML 89/BI 1.00). *Conidiobolus variabilis* sp. nov. was basal in clade I with a relatively high confidence (MP 97/ML 96/BI 1.00). *Conidiobolus bifurcatus* sp. nov. and *C. variabilis* sp. nov.

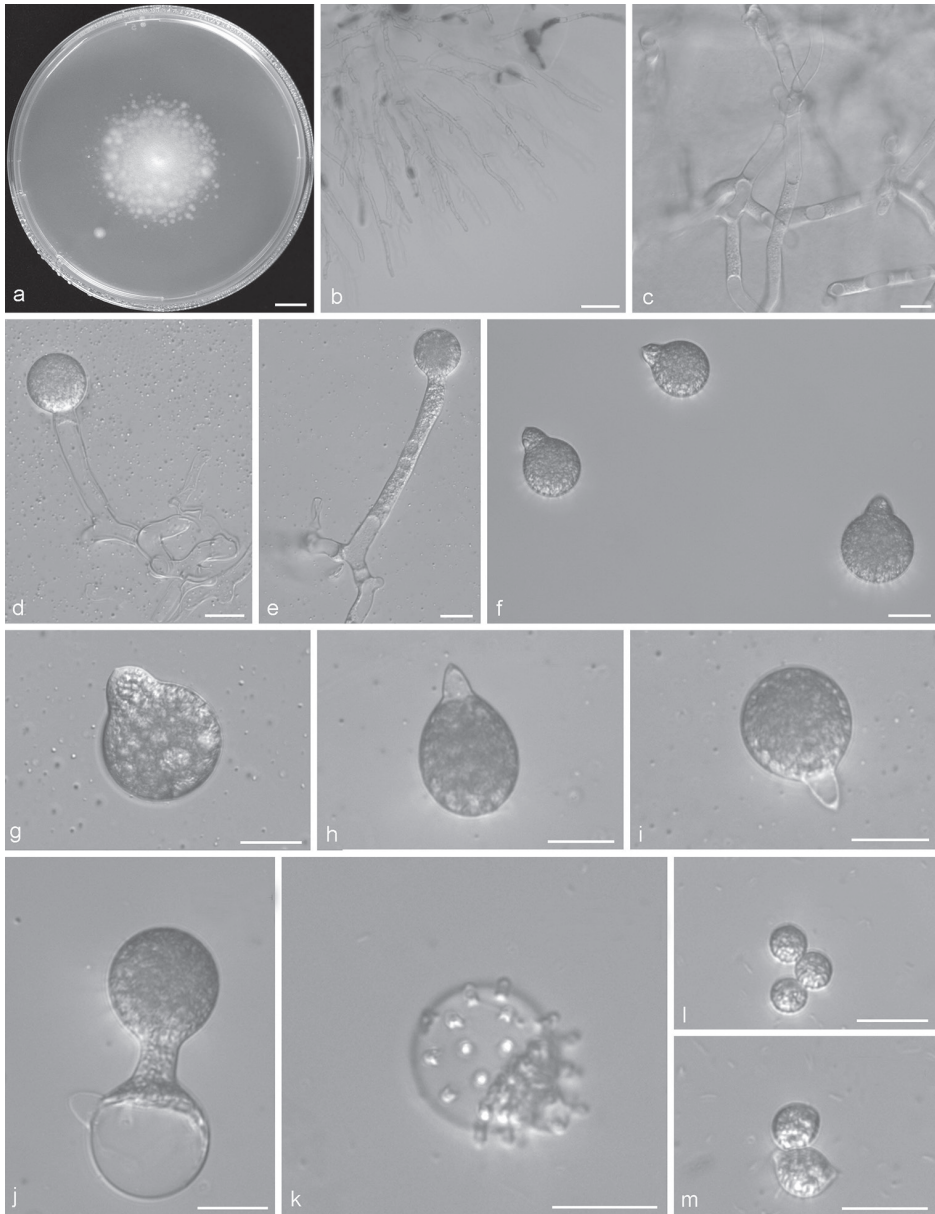


**Figure 4.** *Conidiobolus variabilis* sp. nov. **a** Colony on PDA after 3 d at 21 °C **b** mycelia rarely branched at the colony edge **c** mycelia **d, e** primary conidiophores bearing primary conidia **f–i** primary conidia with different shapes **j** secondary conidia arising from primary conidia **k** microconidia arising from conidia **l** globose microconidia **m** ellipsoidal microconidia. Scale bars: 10 mm (**a**); 100 µm (**b**); 20 µm (**c–m**).

morphologically produce microspores. However, *C. taihushanensis* sp. nov. lacks this synapomorph. Besides *C. taihushanensis* sp. nov., four other species in the *Conidiobolus* s.s., i.e. *C. dabieshanensis* Y. Nie & B. Huang, *C. iuxtagenitus* S.D. Waters & Calla-

ghan, *C. lamprauges* and *C. parvus* Drechsler were not reported to produce microspores either. This may be due to the need for particular conditions, such as growth temperature and nutritional supply. For example, the microspores of *C. khandalensis* Srin. & Thirum. were only observed on 2% water-agar at 16 °C (Nie et al. 2020).

Except microspores, species of the *Conidiobolus* s.s. clade are morphologically diverse, particularly the secondary conidia. For instance, *C. iuxtagenitus* produces single fusiform discharged secondary conidia (Waters and Callaghan 1989) and *C. margaritatus* forms a necklace-like chain of up to seven undischarged conidia (Huang et al. 2007). Although these special characteristics provide good identification, most members of this lineage are difficult to distinguish phenotypically. Sequence data of nuLSU and TEF1 have provided a better understanding of species circumscription or inter- and intraspecific variations (Nie et al. 2012). In this study, morphology and molecular data support *C. bifurcatus* sp. nov., *C. taihushanensis* sp. nov. and *C. variabilis* sp. nov. as new species in the *Conidiobolus* s.s. clade. Although the microspores of *C. taihushanensis* sp. nov. were not observed, its straight apical mycelium and the production of 2–5 conidia from the hyphal body make it easily distinguishable from other species of *Conidiobolus* s.s.

With the proposal of the three new species herein, 17 species are currently accepted in the genus *Conidiobolus* s.s. and only five were found distributed in China (King 1976a, b, 1977, Wang et al. 2010a, b, Nie et al. 2017, 2020). For updating, the key to all these 17 species are provided as follows.

### Key to the species of *Conidiobolus* s.s.

- |   |   |                                      |
|---|---|--------------------------------------|
| 1 | Villose resting spores produced .....   | <b><i>Conidiobolus coronatus</i></b> |
| – | Villose resting spores not produced.....  | <b>2</b>                             |
| 2 | Microspores produced.....   | <b>3</b>                             |
| – | Microspores not observed .....  | <b>4</b>                             |
| 3 | Two types of sexual reproduction, zygospores formed in axial alignment with one or both conjugating segments..... | <b>5</b>                             |
| – | One type of sexual reproduction, zygospores formed in one of the conjugating segments .....                       | <b>6</b>                             |
| 5 | Primary conidia larger, up to 51 µm .....   | <b><i>C. utriculosus</i></b>         |
| – | Primary conidia smaller, less than 36 µm .....  | <b><i>C. brefeldianus</i></b>        |
| 6 | 2–4 branches germinated at the top of primary conidiophores.....  | <b>7</b>                             |
| – | Unbranched at the top of conidiophores.....   | <b>8</b>                             |
| 7 | Only 2 primary conidia arising from 2 branches, larger, up to 44 µm .....   | <b><i>C. megalotocus</i></b>         |
| – | 2–4 primary conidia arising from 2–4 branches, smaller, less than 29 µm.....                                      | <b><i>C. polytocus</i></b>           |
| 8 | Secondary conidiophores branched.....   | <b>9</b>                             |
| – | Secondary conidiophores unbranched.....   | <b>10</b>                            |

- 9 Secondary conidiophores branched almost at the tip, primary conidia larger, up to 40  $\mu\text{m}$ ..... *C. bifurcatus* sp. nov.
- Secondary conidiophores branched at the tip or base, primary conidia smaller, less than 30  $\mu\text{m}$ ..... *C. mycophilus*
- 10 Primary conidia larger, up to 55  $\mu\text{m}$  ..... 11
- Primary conidia smaller, maximum not over 42  $\mu\text{m}$ ..... 12
- 11 Primary conidia globose to pyriform, zygospores globose, 26–40  $\mu\text{m}$ ..... *C. macrosporus*
- Primary conidia globose, subglobose, pyriform to obovoid, zygospores not observed ..... *C. variabilis* sp. nov.
- 12 Primary conidia smaller, less than 21  $\mu\text{m}$  ..... *C. kbandalensis*
- Primary conidia larger, more than 33  $\mu\text{m}$ ..... 13
- 13 Two types of resting spores produced: zygospores or chlamydospores..... *C. humicolus*
- One type of resting spores produced ..... 14
- 14 Only chlamydospores produced..... *C. firmipilleus*
- Only zygospores produced ..... 15
- 15 Primary conidiophores shorter, less than 80  $\mu\text{m}$ ..... *C. gonimodes*
- Primary conidiophores longer, more than 130  $\mu\text{m}$  ..... 16
- 16 Zygospores globose or elongate, larger, 15–40  $\times$  18–45  $\mu\text{m}$  ... *C. incongruus*
- Zygospores globose, smaller, 30–36  $\mu\text{m}$  ..... *C. mycophagus*
- 4 Fusiform secondary conidia produced, each zygospore in a position separated by a short, but relatively constant distance from a lateral conjugation outgrowth or beak..... *C. iuxtagenitus*
- Fusiform secondary conidia not produced, each zygospore in a position not separated by a short, but relatively constant distance from a lateral conjugation outgrowth or beak ..... 17
- 17 A chain of up to seven undischarged repetitional conidia produced ..... *C. margaritatus*
- No chains of undischarged repetitional conidia produced ..... 18
- 18 Primary conidiophores produced from cushion mycelia..... *C. lichenicolus*
- Primary conidiophores not produced from cushion mycelia..... 19
- 19 Apical mycelia straight, 2–5 conidia arising from hyphal body, no chlamydospores, zygospores produced..... *C. taihushanensis* sp. nov.
- Apical mycelia slightly curved, unbranched at the top of conidiophore, chlamydospores produced, no zygospores..... *C. dabieshanensis*

## Acknowledgements

This study was supported by the National Natural Science Foundation of China (Nos. 30770008, 31900008 and 31670019).

## References

- Bałazy S, Wiśniewski J, Kaczmarek S. (1987) Some noteworthy fungi occurring on mites. Bulletin of the Polish Academy of Sciences, Biological Sciences 35: 199–224.
- Bałazy S (1993) Entomophthorales. Flora of Poland (Flora Polska), Fungi (Mycota) 24:1–356. Polish Academy of Sciences, W. Szafer Institute of Botany, Kraków, Poland.
- Barko A (1964) Notes on entomophthoraceous fungi in Poland Entomophaga. Mémoires hors série. 2: 129–131.
- Ben-Ze'ev IS, Kenneth RG (1982) Features-criteria of taxonomic value in the *Entomophthorales*: I. A revision of the *Batkoan* classification. Mycotaxon 14: 393–455.
- Brefeld O (1884) *Conidiobolus utriculosus* und *minor*. Untersuchungen aus der Gesamtgebiete der Mykologie 6(2):35–78.
- Callaghan AA, Waters SD, Manning RJ (2000) Alternative repetitional conidia in *Conidiobolus adiaeretus*: development and germination. Mycological Research 104: 1270–1275. <https://doi.org/10.1017/S0953756200003063>
- Chen MJ, Huang B (2018) *Conidiobolus antarcticus*, a synonym of *C. osmodes*. Mycotaxon 133(4): 635–641. <https://doi.org/10.5248/133.635>
- Couch JN (1939) A new *Conidiobolus* with sexual reproduction. American Journal of Botany 26:119–130. <https://doi.org/10.1002/j.1537-2197.1939.tb12878.x>
- Drechsler C (1952) Widespread distribution of *Delacroixia coronata* and other saprophytic *Entomophthoraceae* in plant detritus. Science 115: 575–576. <https://doi.org/10.1126/science.115.2995.575>
- Drechsler C (1953a) Three new species of *Conidiobolus* isolated from leaf mold. Journal of the Washington Academy of Science 43(2): 29–34.
- Drechsler C (1953b) Two new species of *Conidiobolus* occurring in leaf mold. American Journal of Botany 40(3): 104–115. <https://doi.org/10.1002/j.1537-2197.1953.tb06458.x>
- Drechsler C (1954) Two species of *Conidiobolus* with minutely ridged zygosporangia. American Journal of Botany 41: 567–575. <https://doi.org/10.1002/j.1537-2197.1954.tb14380.x>
- Drechsler C (1955a) A small *Conidiobolus* with globose and with elongated secondary conidia. Journal of Washington Academy of Sciences 45(4): 114–117.
- Drechsler C (1955b) Three new species of *Conidiobolus* isolated from decaying plant detritus. American Journal of Botany 42(5): 437–443. <https://doi.org/10.1002/j.1537-2197.1955.tb11144.x>
- Drechsler C (1955c) Two new species of *Conidiobolus* that produce microconidia. American Journal of Botany 42(9): 793–802. <https://doi.org/10.1002/j.1537-2197.1955.tb10424.x>
- Drechsler C (1956) Two new species of *Conidiobolus*. American Journal of Botany 43(10): 778–787. <https://doi.org/10.1002/j.1537-2197.1956.tb11168.x>
- Drechsler C (1957a) Two small species of *Conidiobolus* forming lateral zygosporangia. Bulletin of the Torrey Botanical Club 84(4): 268–280. <https://doi.org/10.2307/2482673>
- Drechsler C (1957b) A new species of *Conidiobolus* with distended conidiophores. Sydowia Annales Mycologici 9: 189–192.
- Drechsler C (1957c) Two medium-sized species of *Conidiobolus* occurring in Colorado. Journal of Washington Academy of Sciences 47: 309–315.

- Drechsler C (1960) Two new species of *Conidiobolus* found in plant detritus. *American Journal of Botany* 47: 368–377. <https://doi.org/10.1002/j.1537-2197.1960.tb07138.x>
- Drechsler C (1961) Two species of *Conidiobolus* often forming zygospores adjacent to antheridium-like distentions. *Mycologia* 53(3): 278–303. <https://doi.org/10.2307/3756275>
- Drechsler C (1962) A small *Conidiobolus* with resting spores that germinate like zygospores. *Bulletin of the Torrey Botanical Club* 89(4): 233–240. <https://doi.org/10.2307/2483199>
- Drechsler C (1965) A robust *Conidiobolus* with zygospores containing granular parietal protoplasm. *Mycologia* 57(6): 913–926. <https://doi.org/10.2307/3756891>
- Felsenstein J (1985) Confidence limits on the bootstrap: an approach using the bootstrap. *Evolution* 38: 783–791. <https://doi.org/10.1111/j.1558-5646.1985.tb00420.x>
- Gryganskyi AP, Humber RA, Smith ME, Miadlikovska J, Wu S, Voigt K, Walther G, Anishchenko IM, Vilgalys R (2012) Molecular phylogeny of the *Entomophthoromycota*. *Molecular Phylogenetics and Evolution* 65: 682–694. <https://doi.org/10.1016/j.ympev.2012.07.026>
- Gryganskyi AP, Humber RA, Smith ME, Hodge K, Huang B, Voigt K, Vilgalys R (2013) Phylogenetic lineages in *Entomophthoromycota*. *Persoonia* 30: 94–105. <https://doi.org/10.3767/003158513X666330>
- Hall TA (1999) Bioedit: a user-friendly biological sequence alignment editor and analysis program for Windows 95/98/NT. *Nucleic Acids Symposium Series* 41: 95–98.
- Huang B, Humber RA, Hodge KT (2007) A new species of *Conidiobolus* from Great Smoky Mountains National Park. *Mycotaxon* 100: 227–233.
- Humber RA (1997) Fungi: identification. In: LA Lacey (Ed.) *Manual of Techniques in Insect Pathology*. London, Academic Press. <https://doi.org/10.1016/B978-012432555-5/50015-4>
- James TY, Letcher PM, Longcore JE, Mozley-Standridge SE, Porter D, Powell MJ, Griffith GW, Vilgalys R (2006) A molecular phylogeny of the flagellated fungi (*Chytridiomycota*) and description of a new phylum (*Blastocladiomycota*). *Mycologia* 98(6): 860–871. <https://doi.org/10.1080/15572536.2006.11832616>
- Jensen AB, Gargas A, Eilenberg J, Rosendahl S (1998) Relationships of the insect-pathogenic order *Entomophthorales* (*Zygomycota*, *Fungi*) based on phylogenetic analyses of nucleus small subunit ribosomal DNA sequences (SSU rDNA). *Fungal Genetics and Biology* 24(3): 325–334. <https://doi.org/10.1006/fgbi.1998.1063>
- King DS (1976a) Systematics of *Conidiobolus* (*Entomophthorales*) using numerical taxonomy I. Taxonomic considerations. *Canadian Journal of Botany* 54: 45–65. <https://doi.org/10.1139/b76-008>
- King DS (1976b) Systematics of *Conidiobolus* (*Entomophthorales*) using numerical taxonomy II. Taxonomic considerations. *Canadian Journal of Botany* 54: 1285–1296. <https://doi.org/10.1139/b76-141>
- King DS (1977) Systematics of *Conidiobolus* (*Entomophthorales*) using numerical taxonomy III. Descriptions of recognized species. *Canadian Journal of Botany* 55: 718–729. <https://doi.org/10.1139/b77-086>
- Liu M, Rombach MC, Humber RA, Hodge KT (2005) What's in a name? *Aschersonia insperata*: a new pleoanamorphic fungus with characteristics of *Aschersonia* and *Hirsutella*. *Mycologia* 97: 249–256. <https://doi.org/10.3852/mycologia.97.1.246>

- Lutzoni F, Kauff F, Cox CJ, McLaughlin D, Celio G, Dentinger B, Padamsee M, Hibbett DS, James TY, Baloch E, Grube M, Reeb V, Hofstetter V, Schoch C, Arnold AE, Miadlikowska J, Spatafora J, Johnson D, Hambleton S, Crockett M, Schoemaker R, Sun GH, Lücking R, Lumbsch HT, O'Donnell K, Binder M, Diederich P, Ertz D, Gueidan C, Hall B, Hansen K, Harris RC, Hosaka K, Lim YW, Liu Y, Matheny B, Nishida H, Pfister D, Rogers J, Rossman A, Schmitt I, Sipman H, Stone J, Sugiyama J, Yahr R, Vilgalys R (2004) Where are we in assembling the Fungal Tree of Life, classifying the fungi and understanding the evolution of their subcellular traits? *American Journal of Botany* 91(10): 1446–1480. <https://doi.org/10.3732/ajb.91.10.1446>
- Nie Y, Yu CZ, Liu XY, Huang B (2012) A new species of *Conidiobolus* (*Ancylistaceae*) from Anhui, China. *Mycotaxon* 120: 427–435. <https://doi.org/10.5248/120.427>
- Nie Y, Tang XX, Liu XY, Huang B (2016) *Conidiobolus stilbeus*, a new species with mycelial strand and two types of primary conidiophores. *Mycosphere* 7(6): 801–809. <https://doi.org/10.5943/mycosphere/7/6/11>
- Nie Y, Tang XX, Liu XY, Huang B (2017) A new species of *Conidiobolus* with chlamydospores from Dabie Mountains, eastern China. *Mycosphere* 8(7): 809–816. <https://doi.org/10.5943/mycosphere/8/7/1>
- Nie Y, Qin L, Yu DS, Liu XY, Huang B (2018) Two new species of *Conidiobolus* occurring in Anhui, China. *Mycological Progress* 17(10): 1203–1211. <https://doi.org/10.1007/s11557-018-1436-z>
- Nie Y, Yu DS, Wang CF, Liu XY, Huang B (2020) A taxonomic revision of the genus *Conidiobolus* (*Ancylistaceae*, *Entomophthorales*): four clades including three new genera. *Mycokokeys* 66: 55–81. <https://doi.org/10.3897/mycokeys.66.46575>
- Posada D, Crandall KA (1998) MODELTEST: testing the model of DNA substitution. *Bioinformatics* 14: 817–818. <https://doi.org/10.1093/bioinformatics/14.9.817>
- Rambaut A (2012) FigTree version 1.4.0. Available at <http://tree.bio.ed.ac.uk/software/figtree/>
- Ronquist F, Huelsenbeck JP (2003) MRBAYES 3: Bayesian phylogenetic inference under mixed models. *Bioinformatics* 19: 1572–1574. <https://doi.org/10.1093/bioinformatics/btg180>
- Silvestro D, Michalak I (2012) raxmlGUI: a graphical front-end for RAxML. *Organisms Diversity & Evolution* 12: 335–337. <https://doi.org/10.1007/s13127-011-0056-0>
- Srinivasan MC, Thirumalachar MJ (1961) Studies on species of *Conidiobolus* from India-I. Sydowia, *Annales Mycologici* 15: 237–241.
- Srinivasan MC, Thirumalachar MJ (1962a) Studies on species of *Conidiobolus* from India-II. Sydowia, *Annales Mycologici* 16: 60–66.
- Srinivasan MC, Thirumalachar MJ (1962b) Studies on species of *Conidiobolus* from India-III. *Mycologia* 54(6): 685–693. <https://doi.org/10.2307/3756504>
- Srinivasan MC, Thirumalachar MJ (1965) Studies on species of *Conidiobolus* from India-IV. Sydowia 19: 86–91.
- Srinivasan MC, Thirumalachar MJ (1967) Evaluation of taxonomic characters in the genus *Conidiobolus* with key to known species. *Mycologia* 59: 698–713. <https://doi.org/10.2307/3757098>
- Srinivasan MC, Thirumalachar MJ (1968a) Studies on species of *Conidiobolus* from India-V. *Mycopathologica et Mycologia Applicata* 36: 341–346. <https://doi.org/10.1007/BF02050380>

- Srinivasan MC, Thirumalachar MJ (1968b) Two new species of *Conidiobolus* from India. *Journal of the Mitchell Society* 84: 211–212.
- Stamatakis A (2006) RAxML-VI-HPC: maximum likelihoodbased phylogenetic analyses with thousands of taxa and mixed models. *Bioinformatics* 22: 2688–2690. <https://doi.org/10.1093/bioinformatics/btl446>
- Swofford DL (2002) PAUP\*: Phylogenetic analysis using parsimony (\*and other methods), Version 4.0b10. Sinauer Associates, Sunderland.
- Thompson JD, Gibson TJ, Plewniak F (1997) The Clustal-X windows interface: flexible strategies for multiple sequence alignment aided by quality analysis tools. *Nucleic Acids Research* 63: 215–228.
- Vaidya G, Lohman DJ, Meier R (2011) SequenceMatrix: concatenation software for the fast assembly of multi-gene datasets with character set and codon information. *Cladistics* 27(2): 171–180. <https://doi.org/10.1111/j.1096-0031.2010.00329.x>
- Vilgalys R, Hester M (1990) Rapid genetic identification and mapping of enzymatically amplified ribosomal DNA from several *Cryptococcus* species. *Journal of Bacteriology* 172: 4238–4246. <https://doi.org/10.1128/jb.172.8.4238-4246.1990>
- Voigt K, Cigelnik E, O'donnell K (1999) Phylogeny and PCR identification of clinically important zygomycetes based on Nuclear Ribosomal-DNA Sequence Data. *Journal of Clinical Microbiology* 37(12): 3957–3964. <https://doi.org/10.1128/JCM.37.12.3957-3964.1999>
- Waingankar VM, Singh SK, Srinivasan MC (2008) A new thermophilic species of *Conidiobolus* from India. *Mycopathologia* 165: 173–177. <https://doi.org/10.1007/s11046-007-9088-6>.
- Wang CF, Li KP, Huang B (2010a) A new record to China — *Conidiobolus iuxtagenitus*. *Journal of Fungal Research* 8: 12–14.
- Wang CF, Li KP, Liu YJ, Li ZZ, Huang B (2010b) Three new Chinese records of *Conidiobolus*. *Mycosystema* 29: 595–599.
- Watanabe M, Lee K, Goto K, Kumagai S, Sugita-Konishi Y, Hara-Kudo Y (2010) Rapid and effective DNA extraction method with bead grinding for a large amount of fungal DNA. *Journal of Food Protection* 73(6): 1077–1084. <https://doi.org/10.4315/0362-028X-73.6.1077>
- Waters SD, Callaghan AA (1989) *Conidiobolus iuxtagenitus*, a new species with discharge delongate repetitional conidia and conjugation tubes. *Mycological Research* 93: 223–226. [https://doi.org/10.1016/S0953-7562\(89\)80121-2](https://doi.org/10.1016/S0953-7562(89)80121-2)
- Zollera S, Scheidegger C, Sperisena C (1999) PCR primers for the amplification of mitochondrial small subunit ribosomal DNA of lichen-forming ascomycetes. *The Lichenologist* 31(5): 511–516. <https://doi.org/10.1006/lich.1999.0220>

